CHAPTER 4

KINETICS OF CHEMICAL REACTIONS IN IONIC AND NONIONIC MICROEMULSIONS.

4.1 Preview

In organic chemistry most reactions include bimolecular steps between ions and nonpolar molecules. For these reactions, it is often difficult to find appropriate solvents which dissolve both the polar and the nonpolar reactants. These reactions may either be carried out in two-phase media by adding phase transfer catalysts as well as the polar organic solvents such as halogenated hydrocarbons. Phase transfer catalysts as well as the polar organic solvents may cause problems since they are either toxic or hazardous or they are difficult to dispose off. Therefore microemulsions have been proposed as reaction media especially for industrial applications.[273]

Microemulsions belong to special type of surfactant assemblies in solution ccontaining nearly monodisperse micelles or oil solubilized micellar droplets, with sizes ranging from 10 to 100nm . They possess several advantages as reaction media. They provide a large interface between oil and water. The water content in the microemulsions can be varied within a large interval and phase separaton of the product is possible. The large interface helps in the faster reaction i.e., the reaction rate can be changed manifold and thus provides a higher yield when the microemulsion or micellar solutions serve as the reaction medium,[274,275] the rate enhancement may be attributed to the presence of microdroplet or micellar phase which create interfacial changes, excess interfacial area for substrate binding, decrease in the approachability barrier for similarly charged reactants. Through suitable control of size of droplets, rate acceleration can be controlled and acheived through variations in the composition of microemulsion components, i.e. oil, water, surfactant and cosurfactant. A suitable control of the size of the droplet, regulates the growth process of particle and polymer formations. We also

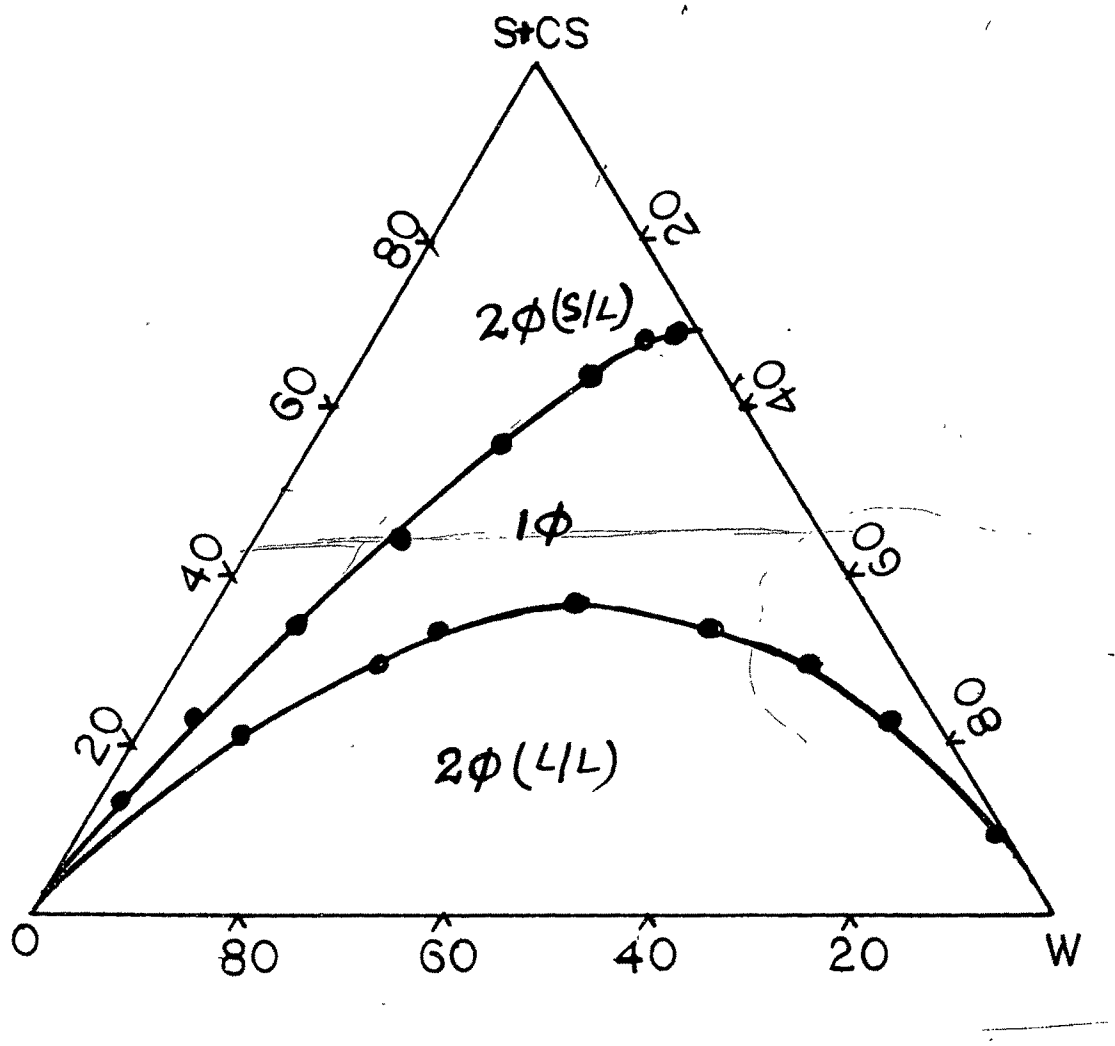

Fig.4.1 Pseudoternary phase diagram of cyclohexane / SDS + n-propanol/water at 40°C with 1:2 S to CS weight ratio.

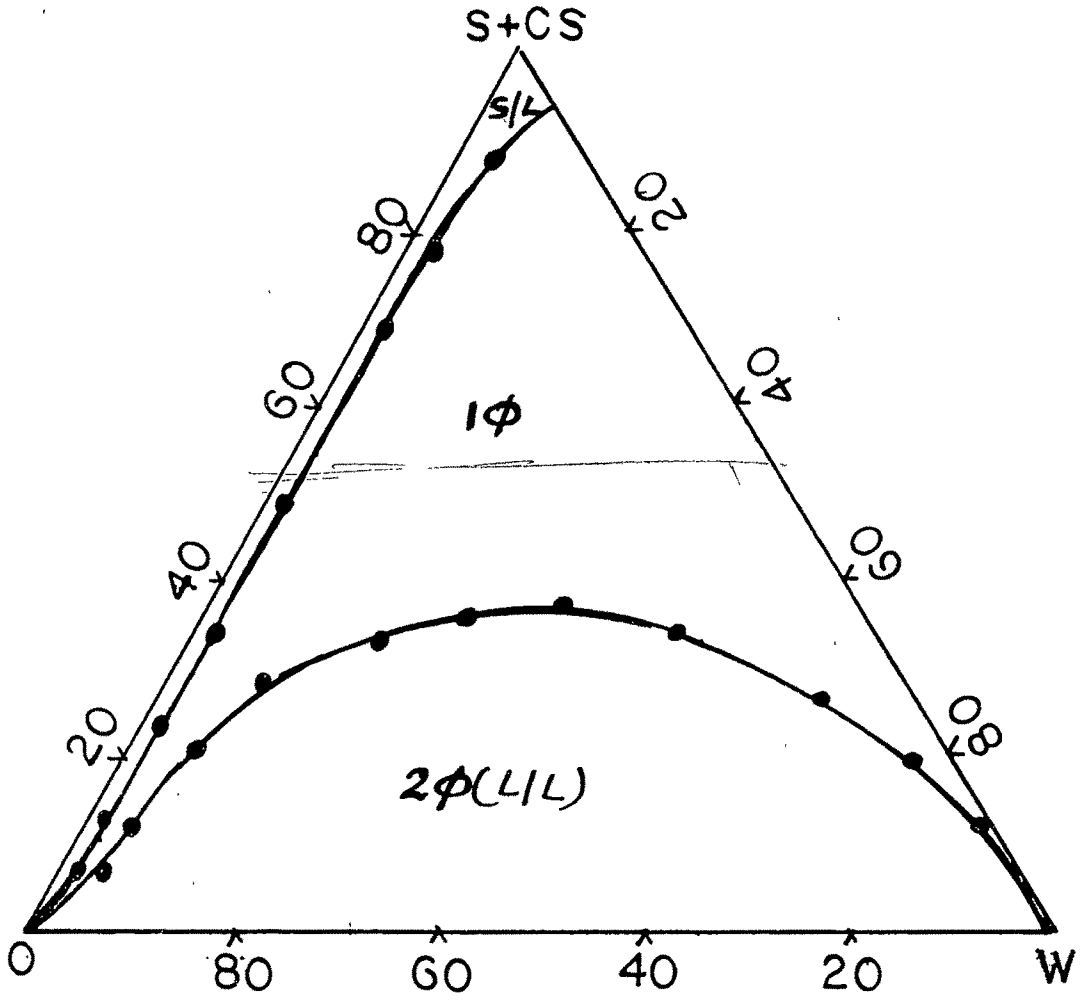

Fig.4.2 Pseudoternary phase diagram of cyclohexane/CTAB+n-propanol/water at 30°C with 1:2 S to CS weight ratio.

could prepare some polymers like polyvinyl acetate and polyvinyl Pyrrolidone in SDS microemulsion made of Benzene / SDS / Water system.[276] It also serves as a potential media for promoting compartmentalized, enzymatic, catalytic and encapsulation reactions. Enzymes can be solubilized in the polar core of W/O microemulsions with the added advantage of the enzymes being dispersed in a form rather than an enzyme cluster. Isotropic and thermodynamic stability of the microemulsion are exploited by scientists to study the various chemical reactions using microemulsions as the medium. We have studied the reactions in SDS, CTAB and TX100 microemulsions. Phase diagrams with different compositions are shown in fig. 4.1 & 2. For the phase diagram of TX100 systems see Chapter 3 (Fig. 3.1)

Microemulsion is considered to be microhetrogeneous having dispersed oil droplets in water or water droplets in oil. The size of the droplets are generally similar though variability has been observed. These microdroplets can be considered as micro reactors[8,204,274] where certain chemical reactions may take place within the very small domain provided by the droplet. The presence of the droplets can enhance or retard chemical reaction rates from the rates observed in conventional media by large factors. They can solubilize a large number of very different compounds both polar and nonpolar. They possess large internal interface and form spontaneously due to its thermodynamical stability .The reactants are, generally, added to the microemulsion in trace amounts in order to prevent perturbations of the structure of microemulsion. The reaction may occur either in microphases or at the interface. When the two reactants are hydrophilic, they can react together only in the water droplet phase and when a hydrophilic substrate reacts with a hydrophobic reagent, the reaction must necessarily occur at the interface of the droplet with the bulk phase. The catalytic effect of micro emulsion is explained in term of electrostatic interaction between the surfactant and the substrate, droplet size and the change on the reactants.

There are two fundamental reasons for studying the chemical reactions in microemulsions. These are :

1. Microemulsions mimic the biological reactions occuring at the cellular level.
2. The promising future opened to physical chemistry by microemulsions within the field of food science and industry.

The scheme[2.277] for the formation of the products in microemulsion can be represented as :

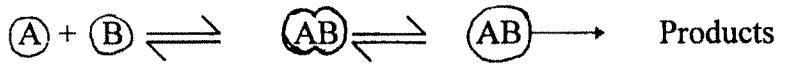

This represents the chemical reaction between A and B where A & B are water soluble reactants initially confined within seperate micro droplets. The microdroplets are in continuous Brownian motion. A certain fraction of the droplet collisions result in the formation of a transient dimer species by a short lived fusion process. The fused dimer is very short lived and decomposes to product. When they are mixed up, intermixing of the contents happen or it is assumed that A moved into the droplet containing B. The interfacial rigidity of the interface controls the rate of coalescence and exchange of contents in the droplets. A relatively rigid interface decreases the rate of coalescence and hence may lead to a decrease in the rate. On the other hand, a substantially fluid interface in the microemulsion may enhance the rate of reaction. Thus by controlling the structure of the interface one can change the reaction kinetics in microemulsions by orders of magnitude.[278]

4.2 Experimental Procedure

We have studied three model reactions in microemulsions.

1. Oxidation of potassium iodide by potassium persulphate.
2. Hydrolysis of methylacetate.
3. Iodination of acetone.

The reactions were carried out in SDS,CTAB and TX100 microemulsions. Cyclohexane, water and n-propanol being other components. In SDS and CTAB microemulsions, the reactions were carried out along the monophasic region with 42.5 % S composition by weight and changing oil-water composition ratio. The oil-water compositions were 5/52.5, 10/47.5, 15/42.5, 20/37.5, 25/32.5, 30/27.5 ,35/22.5, 40/17.5. ie. (o/w= 0.0952, 0.2105, 0.353, 0.5333, 0.7692, 1.0909, 1.5556. 2.2857 respectively).

The reactions in TX100 were carried out along 55% S composition by weight and changing oil-water compositions of 1/44,5/40, 10/35, 15/30 (o/w= 0.0227, 0.125, 0.2857 respectively). In all these cases, the reactions were also studied without any oil ie. 42.5%S and 57.5% W for SDS & CTAB microemulsion and 55% S and 45% W for TX100 microemulsions.

All these reactions were studied kinetically. Oxidation of potassium iodide was studied spectrophotometrically using a UV 240 Shimadzu spectrophotometer. The reaction concentration of KI and $K_2S_2O_8$ used was 5.10^{-2} & 5.10^{-4} M respectively. Aqueous KI and $K_2S_2O_8$ microemulsions with above compositions were prepared separately for each compositon of oil & water. 2ml of KI microemulsion was thermostated in the cuvette, having a constant temperature water circulation from a thermostated bath. $K_2S_2O_8$ microemulsion was also thermostated separately at the same temperature. After attaining the temperature, 1 ml of $K_2S_2O_8$ microemulsion was added to the cuvette containing KI microemulsion, mixed up well and the increasing absorbance due to the formation of I_2 was noted at λmax 360 nm, at regular time intervals. The mixing ratio was always kept 2:1 (v/v) for KI and $K_2S_2O_8$ microemulsion. In CTAB microemulsion, the reaction was carried out using a spectronic 20 (Bausch & Lomlb) colorimeter following the above procedures and the same compositions of KI and $K_2S_2O_8$. In TX100 microemulsion, the composition of KI and $K_2S_2O_8$ was kept 1.10^{-2} & 1.10^{-4} M respectively. The reaction was studied at different temperatures from 25°C to

45°C. The reaction was studied only in the monophasic region with various oil-water ratio.

Methyl acetate hydrolysis was studied by the titration method. Concentration of methyl acetate was 5.6 × 10^{-3} M in the reaction medium. Acidic microemulsions was prepared with 0.1N aqeous HCl and 7ml of this solution was thermostated at the required temperature. Methyl acetate was also thermostated separately and 2ml was added to the acidic microemulsions and mixed well and allowed to react together. 1ml of the reaction solution was withdrawn at regular intervals of time and the reaction was stopped immediately by adding to the ice cold water and the unreacted HCl was determined by titrating against standard NaOH. The infinite titre value was taken by keeping the reaction solution overnight. The reaction was carried out along the monophasic region with 42.5 % S by weight and changing oil-water composition of 5/52.5, 20/37.5, 40/17.5 for SDS and CTAB microemulsion and with 5% W and changing surfactant to oil composition of 32.5/62.5, 42.5, 52.5 & 55/40 for CTAB and TX100 microemulsion. The reaction was studied at 35,40, and 45°C. The solution remained a 1ϕ microemulsion throughout the study.

The iodination of acetone was carried out in aqueous NaOH medium. Microemulsion was prepared with aqueous NaOH by replacing water. Iodine was dissolved in it and the concentration was determined by titrating against a standard $Na_2S_2O_3$ solution using a standard $K_2Cr_2O_7$ solution.The concentration of the iodine was kept 6.47 x 10^{-4} M for SDS microemulsion^{-3} and 1.3 x 10^{-3} M for TX100 microemulsion. The reaction was followed spectrophotometrically. The I_2 microemulsions was thermostated in the cuvette which was jacketed to a water circulation through a thermostated waterbath. After the attainment of the required temperature, 0.1ml acetone was added to the reaction cuvette with stirring and the decrease in absorbance due to the disappearance of I_2 was recorded and the reaction was carried out at different temperatures from 25 to 45°C. The reaction studied along the monophasic region of 42.5% S by weight for SDS and changing

oil-water composition of 5/52.5, 10/47.5,15/42.5, 20/37.5,25/32.5, 30/27.5, 35/22.5,40/17.5 and 55% S by weight for TX100 and changing oil-water ratio of 1/44,5/40, 10/35, 15/30, 20/25, 25/20, 30/15, 35/10, 40/5. The reaction was studied at 30,35,40 &45°C.

4.3 Results and Discussion

a. Oxidation of potassium iodide by potassium persulphate.

The oxidation of iodide by persulphate proceeds by the following mechanism.[146]

$$S_2O_8^{2-} \longrightarrow 2SO_4^{2-}$$

$$S_2O_8^{2-} + 2I^- \underset{}{\overset{Ko}{\rightleftharpoons}} I^- + IS_2O_8^{3-} + M \overset{k}{\longrightarrow} P$$

$$MIS_2O_8^{3-} + I^- \overset{Km}{\rightleftharpoons} P + M$$

Where $P = 2SO_4^{2-} + I_2$; M = Microemulsion droplet.

The reaction folows a second order kinetics, first order with respect to each reactant as found in conventional aqueous solution.[279-281] The concentration of potassium iodide was taken in excess so that the first order kinetics followed.

If we assume that the initial concentration of potassium persulphate is 'a' and no I_2 was present, and after a time t, 'x' is the amount of I_2 formed, then the concentration of $K_2S_2O_8$ unreacted is (a-x).

First order rate constant for the decomposition of potasium persulphate is calculated assuming the rate of formation of I_2 is equivalent to the rate of decomposition of $S_2O_8^{2-}$. So the rate of formation of I_2 can be written as[229]

$$\frac{dx}{dt} = k(a-x)$$

Integrating with limits t=1 & t=2.

$$\int \frac{dx}{a-x} = \int k\,dt$$

$$-\ln (a-x)\Big]_1^2 = kt\Big]_1^2$$

$$-\ln (a-x_2) + \ln (a-x_1) = k (t_2-t_1)$$

$$k (t_2-t_1) = \ln \left(\frac{a-x_1}{a-x_2}\right) \qquad \text{.....(1)}$$

k is the first order rate constant and x_1 and x_2 are the concentration of I_2 formed at time t_1 & t_2 respectively. If a_o and b_o are the initial concentrations of $K_2S_2O_8$ and KI respectively and if x is the amount of $K_2S_2O_8$ that has disappeared in time t and bo is the amount of KI reacted in time t , the amount of potassium persulphate and potassium iodide remaining at time t are (a_o-x) & (b_o-x) respectively. Then the rate of disappearance of $K_2S_2O_8$ is equal to the rate of disappearance of KI and is therefore given by[229]

$$\frac{dx}{dt} = k (a_o-x) (b_o-x), \text{ assuming } a_o \text{ \& } b_o \text{ are different.}$$

Integrating,

$$\int \frac{dx}{(a_o-x) (b_o-x)} = \int k\,dt$$

$$kt = \frac{1}{(a_o-b_o)} \ln \frac{b_o (a_o-x)}{a_o (b_o-x)} \qquad \text{.....(2)}$$

where 'k' is the second order rate constant

First order rate constant for the decomposition of potassium persulphate is calculated assuming the rate of formation of I_2 is equivalent to the rate of decomposition of $S_2O_8^{2-}$ using the equation 1. Fig 4.3 (a-i) shows the plot of

$$\ln \left(\frac{a-x_1}{a-x} \right) \text{ vs } (t_2-t_1), \text{ for SDS system,}$$

a straight line graph passing through the origin is obtained. Slope of the line gives the first order rate constant for the reaction in SDS, CTAB and TX100 microemulsions at different temperatures and for varying oil-water ratios. The structure of microemulsion changes as the oil-water ratio changes and it can alter the rate of reaction also. The result is summarized in Table 4.1. The rate of reaction is much higher in SDS microemulsion than that in pure aqueous system. The k value for this reaction in water is 4.8×10^{-3} l mol^{-1} sec^{-1} at 25°C[143,145] The reaction is found to be faster than the system which does not contain any oil also. ie. the system which contains surfactant and water. It is clear from the Table 4.1 that the rate of reaction increases with increasing temperature and it also increases with decreasing water content. The rate enhancement can happen because of various factors. Microemulsion is microscopically heterogeneous due to the formation of microdroplets and they are assumed to have a large internal droplet/water interface. The different reactants solubilized in the microemulsion may meet at this microscopic interface and hence the reaction rate is enhanced.

Distribution of reactants in large number of microdroplets cause the dilution of the reactants in the aqueous core of the droplets due to the hydrophilic nature of the reactants and hence the reaction is slowed down when the water content increases.[8,144, 204,284] The local concentration of the reactant increases gradually as the oil - water ratio increases. Basically, the reactants are water soluble and they reside either in the water droplets or at the L interface. So the

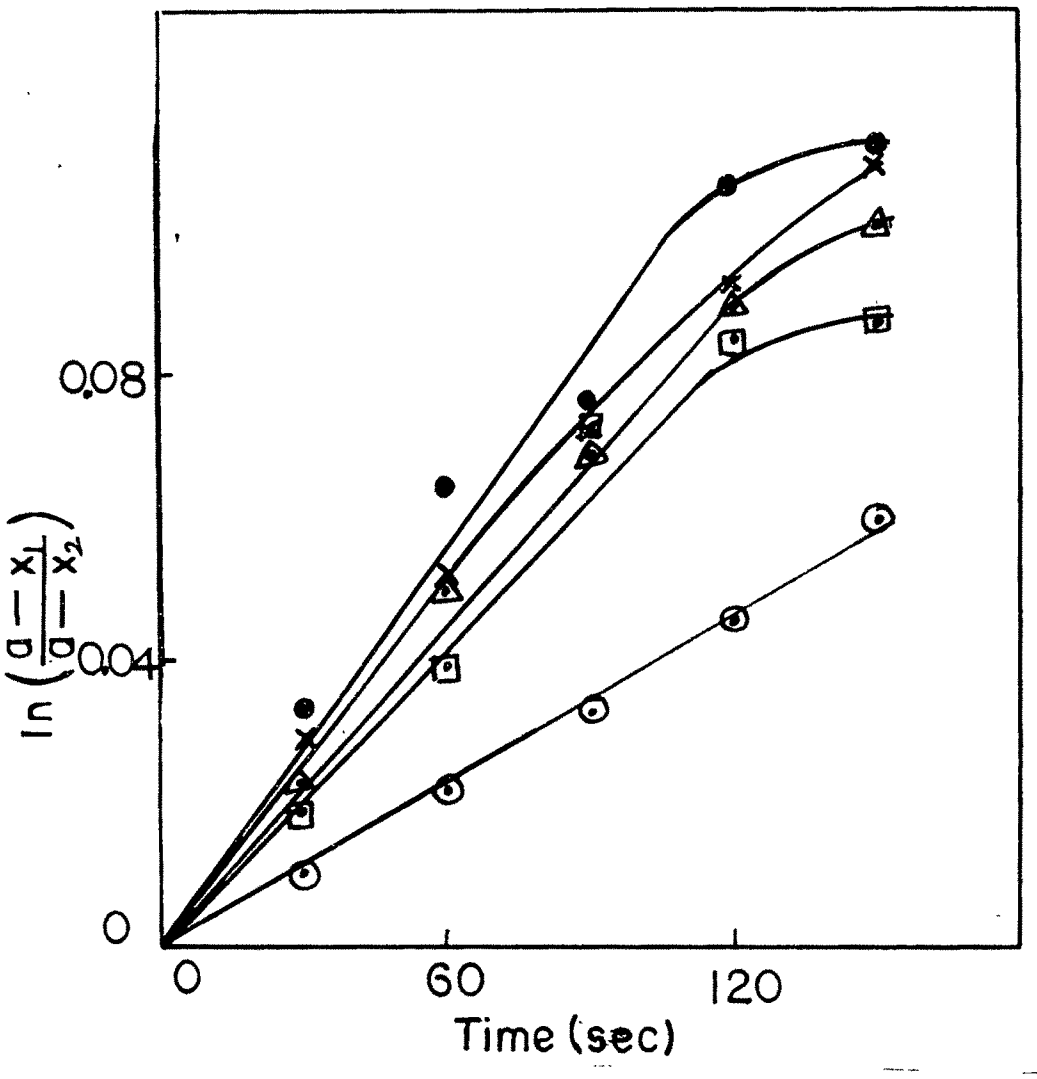

Fig.4.3a Plot of $\ln \frac{(a-x_1)}{(a-x_2)}$ vs time for $KI+K_2S_2O_8$ reaction in SDS microemulsion system with o/w= 5/52.5

⊙ 25°C; ⊡ 30°C; △ 35°C; × 40°C; ● 45°C

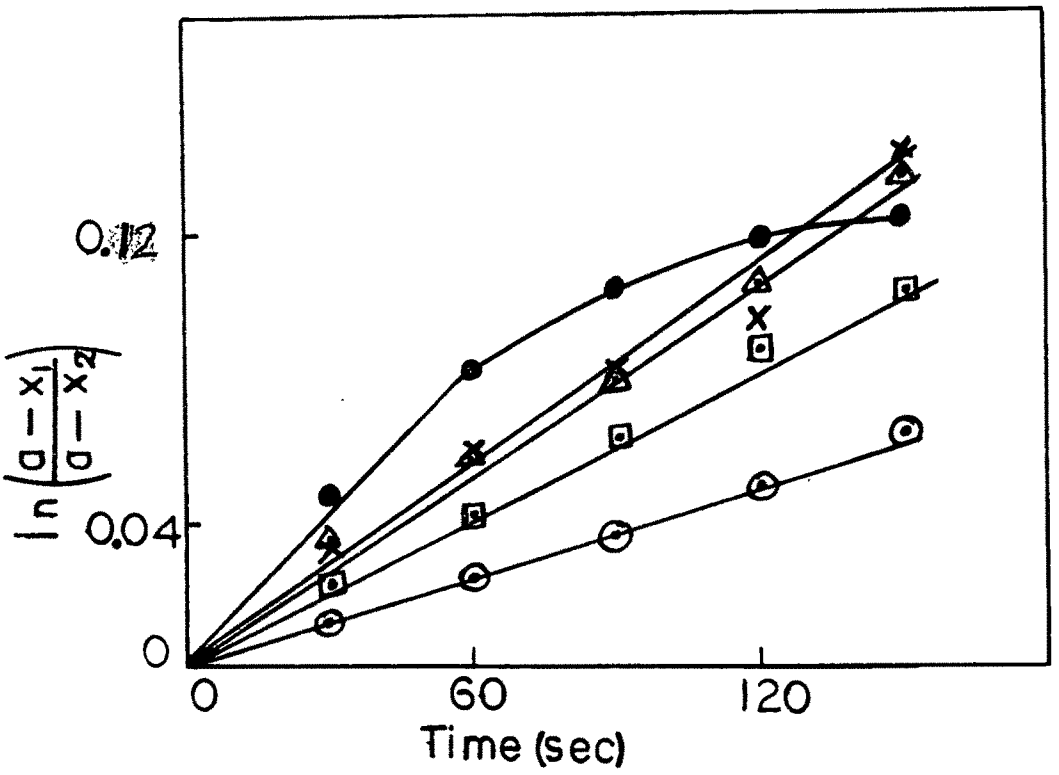

Fig.4.3b Plot of $\ln \frac{(a-x_1)}{(a-x_2)}$ vs time for $KI+K_2S_2O_8$ reaction in SDS microemulsion system with o/w=10/47.5. Symbols are the same as in Fig.4.3a.

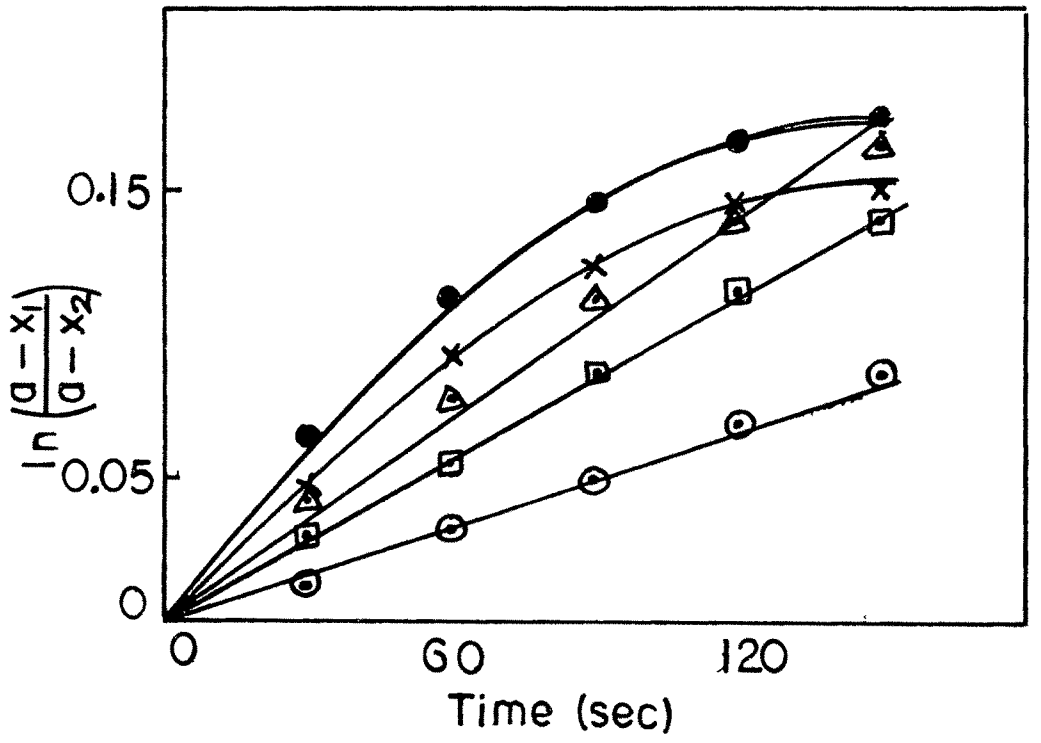

Fig.4.3c Plot of ln $\frac{(a-x_1)}{(a-x_2)}$ vs time for $KI+K_2S_2O_8$ reaction in SDS microemulsion system with o/w=15/42.5. Symbols are the same as in Fig.4.3a.

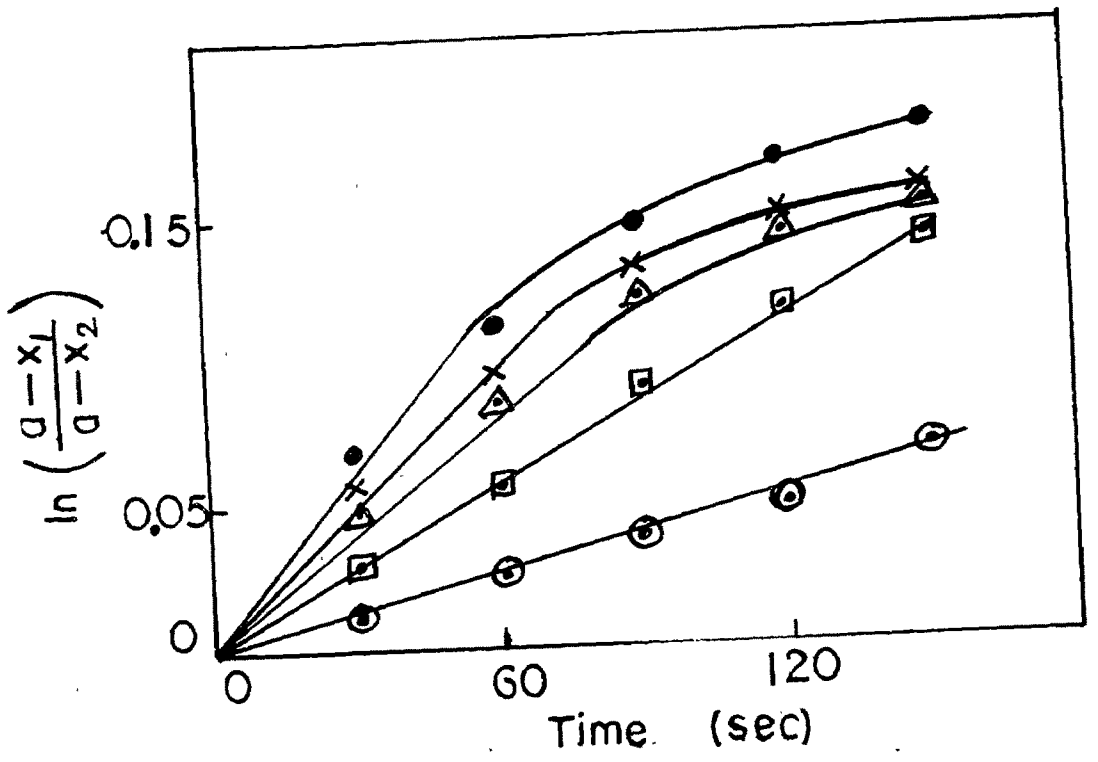

Fig.4.3d Plot of ln $\frac{(a-x_1)}{(a-x_2)}$ vs time for $KI+K_2S_2O_8$ reaction in SDS microemulsion system with o/w=20/37.5. Symbols are the same as in Fig.4.3a.

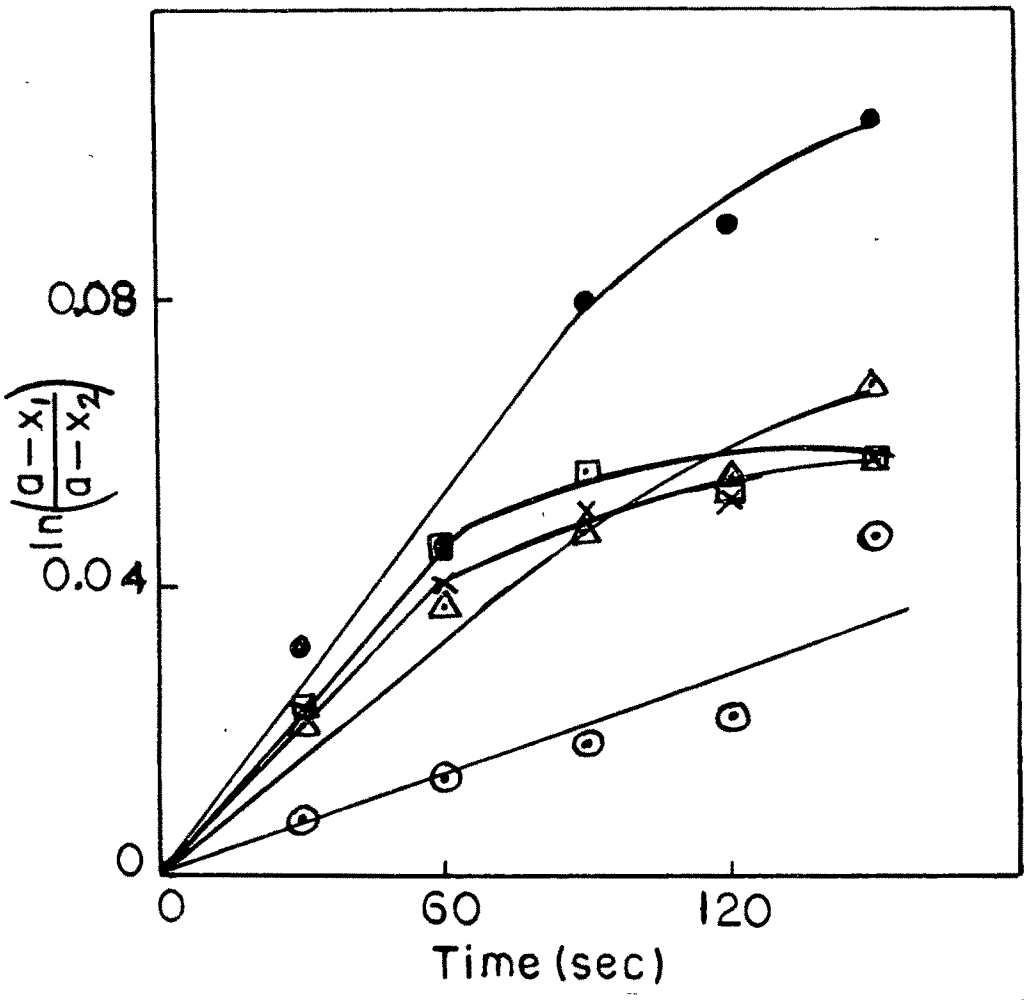

Fig.4.3e Plot of $\ln \frac{(a-x_1)}{(a-x_2)}$ vs time for $KI+K_2S_2O_8$ reaction in SDS microemulsion system with o/w=25/32.5. Symbols are the same as in Fig.4.3a.

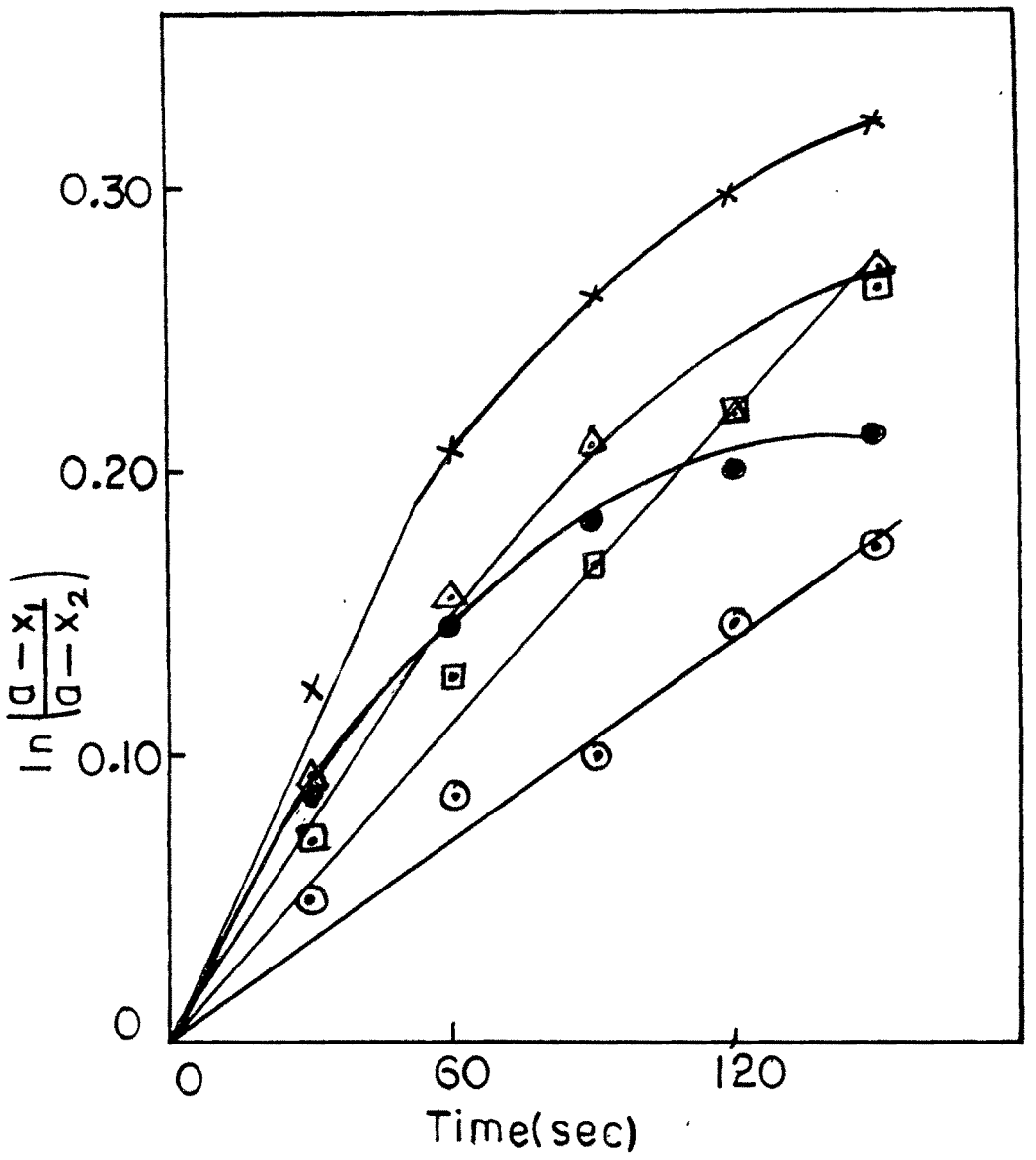

Fig.4.3f Plot of $\ln \frac{(a-x_1)}{(a-x_2)}$ vs time for $KI+K_2S_2O_8$ reaction in SDS microemulsion system with o/w=30/27.5. Symbols are the same as in Fig.4.3a.

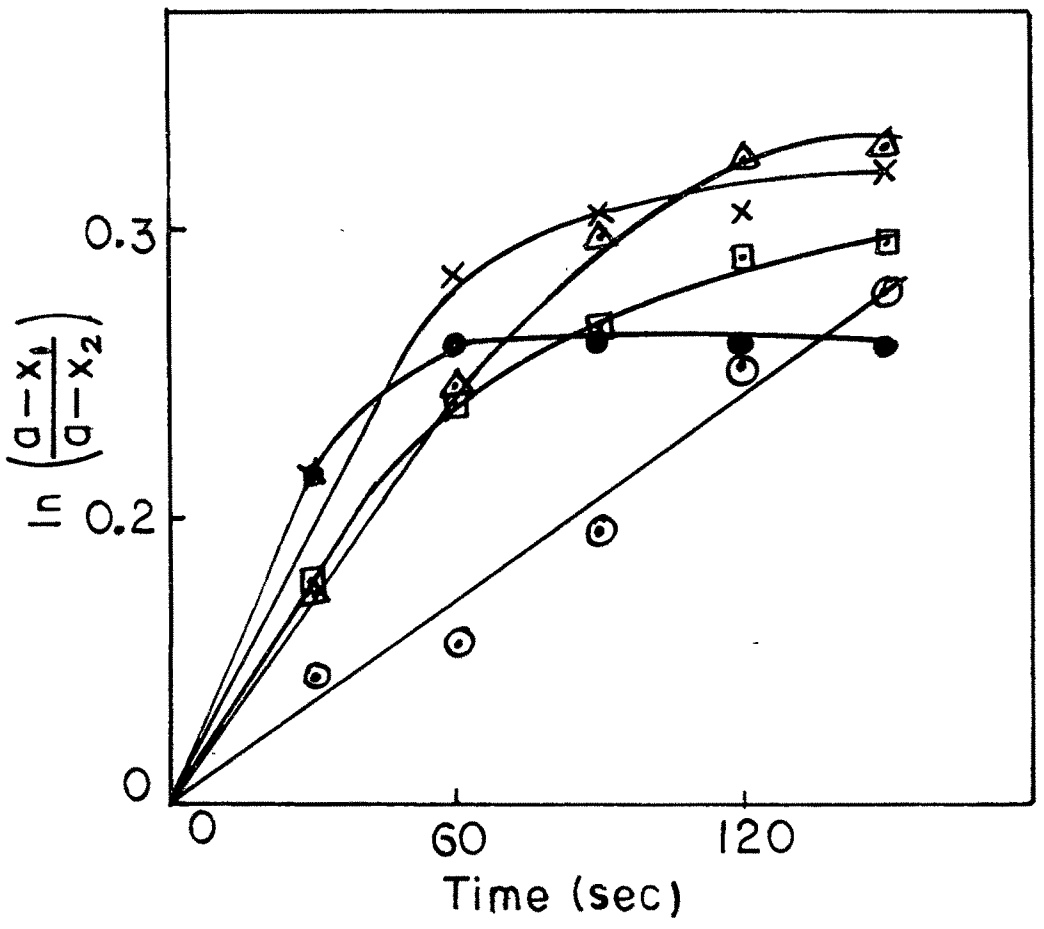

Fig.4.3g Plot of $\ln \frac{(a-x_1)}{(a-x_2)}$ vs time for $KI+K_2S_2O_8$ reaction in SDS microemulsion system with o/w=35/22.5. Symbols are the same as in Fig.4.3a.

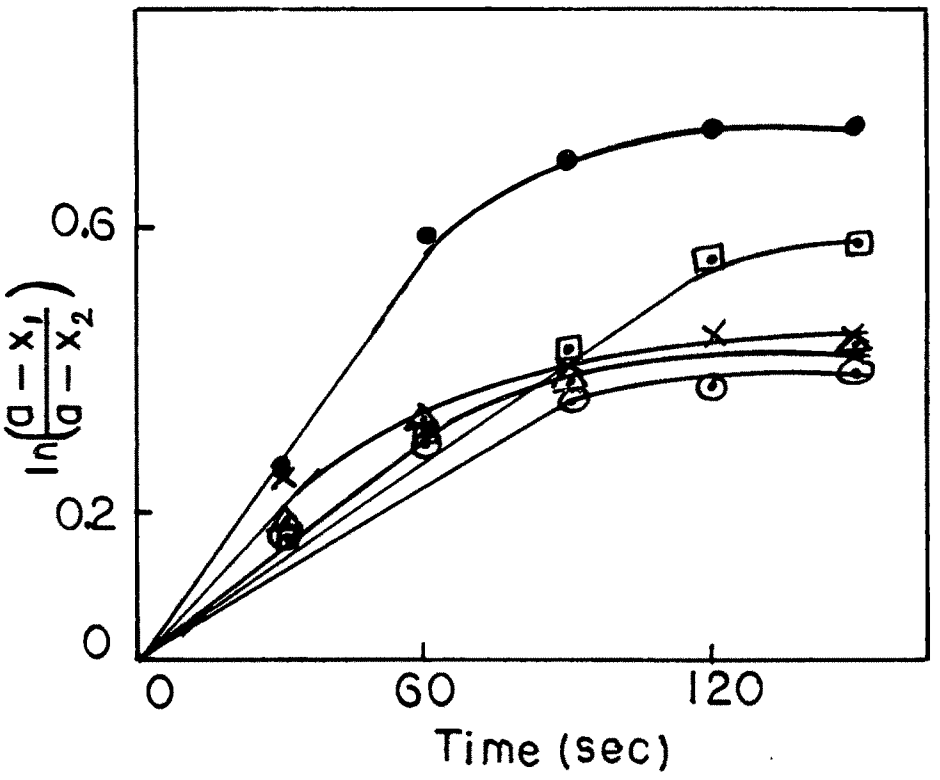

Fig.4.3h Plot of $\ln \frac{(a-x_1)}{(a-x_2)}$ vs time for $KI+K_2S_2O_8$ reaction in SDS microemulsion system with o/w=40/47.5. Symbols are the same as in Fig.4.3a.

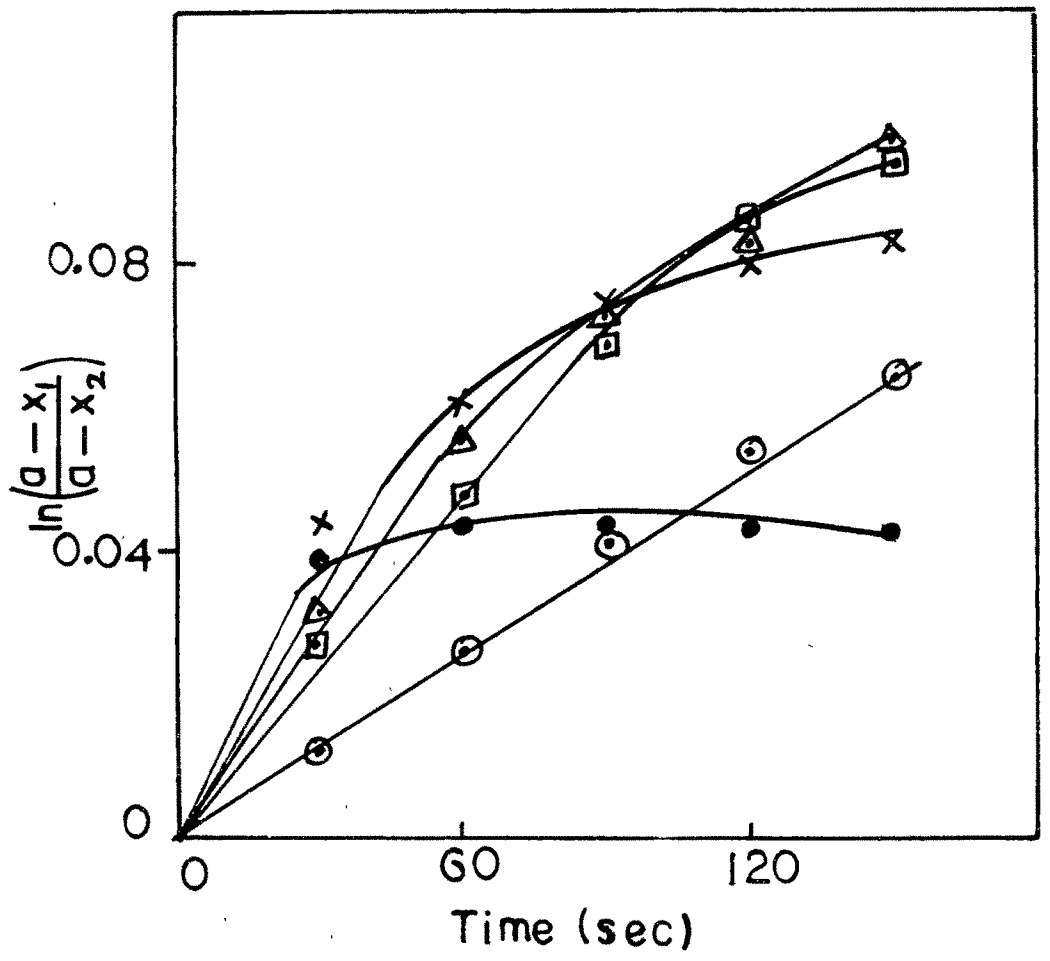

Fig.4.3i Plot of $\ln \frac{(a-x_1)}{(a-x_2)}$ vs time for $KI+K_2S_2O_8$ reaction in SDS system with no oil. s/w=42.5/57.5. Symbols are the same as in Fig.4.3a.

Table 4.1 **Pseudofirst order rate constant k (sec^{-1}) for the decomposition of $S_2O_8^{2-}$ in SDS microemulsion SDS concentration = 42.5%.**

O/W	Temperature (°C)				
	25	30	35	40	45
5/52.5	3.92×10^{-4}	7.41×10^{-4}	7.41×10^{-4}	8.33×10^{-4}	9.52×10^{-4}
10/47.5	4.94×10^{-4}	7.02×10^{-4}	8.89×10^{-4}	9.52×10^{-4}	1.33×10^{-4}
15/42.5	5.05×10^{-4}	9.80×10^{-4}	1.11×10^{-3}	1.39×10^{-3}	1.85×10^{-3}
20/37.5	4.94×10^{-4}	1.00×10^{-3}	1.32×10^{-3}	1.42×10^{-3}	1.85×10^{-3}
25/32.5	4.94×10^{-4}	1.03×10^{-3}	1.48×10^{-3}	1.48×10^{-3}	1.90×10^{-3}
30/27.5	1.11×10^{-3}	1.85×10^{-3}	2.38×10^{-3}	4.17×10^{-3}	4.17×10^{-3}
35/22.5	2.38×10^{-3}	4.17×10^{-3}	5.56×10^{-3}	6.67×10^{-3}	8.33×10^{-3}
40/17.5	3.92×10^{-3}	4.44×10^{-3}	5.13×10^{-3}	6.67×10^{-3}	8.33×10^{-3}
S/W= 42.5/57.5	3.92×10^{-4}	7.14×10^{-4}	7.41×10^{-4}	8.33×10^{-4}	8.33×10^{-4}
W (100%)	8.40×10^{-5}	1.46×10^{-4}	1.86×10^{-4}	1.82×10^{-4}	2.28×10^{-4}

solubilization site also affect the rate of reaction. That is , the size and aggregation number also affect the rate of reaction.

It has been reported earlier that the rate of reaction increases with decrease in molar ratio, ie. W=$[H_2O]/[S]$. M. L. Moya et al[8,204] has explained the decrease in reaction rate with increase in water by considering the decrease in water activity.This could be due to the interaction between water molecules and the SDS molecules. The step of the reaction studied will be the contact of the reactants to form the activated complex. In this step, some water molecules pass through from the solvation sphere of the reactants to the bulk. The overall process may be written as :[143]

$$(I^-)_{solv} + (S_2O_8^{2-})_{solv} \longleftrightarrow (I^-, S_2O_8^{2-})^{\#}_{solv} + nH_2O$$

In agreement with the transition state theory, the observed rate constant would be,[285]

$$k_{obs} = k_o \frac{\gamma_{I^-} \cdot \gamma_{S_2O_8^{2-}}}{\gamma^{\#}} \cdot \frac{1}{a^n_{H_2O}} \qquad .....(3)$$

where γ is the activity coefficient.

According to this expression, a decrease in the water activity a_{H_2O} would bring about an increase in the reaction rate. They have reported earlier that the water activity in different organic phase / AOT / Water system diminishes with diminishing W. This decrease of a_{H_2O} would be due to the interaction between water molecules and the charged heads of the AOT molecules as well as with the sodium counter ions present in the water pools.

We assume that the the cyclohexane does not influence a_{H_2O} values qualitatively and only slightly influence the values quantitatively. It is possible to extrapolate the results for our system in a qualitative way. Thus we can rationalize the increase observed in the reaction rate when the w values decrease on the basis of a decrease in the water activity in the system.

The positive kinetic salt effect for reactions between ions of the same sign was interpreted as a consequence of the greater destabilization of the initial state compared with that of the transition state, caused by the electrolytes present in the reaction media. In other words, the increase in the reaction rate has its origin in the increase of the effective concentration of the reactants, because a part of the water present in the reaction medium of reaction is involved in the hydration of the background electrolyte.[8,146,204,286-287] In this sense, we can interpret the positive kinetic effects of decresing W in the same way that we can with the positive salt effects, as a consequence of the greater destabilization of the initial state compared with that of the transition state, because a part of the water present in the media of reaction is involved in the hydration of the polar interior of the micelle.

When the temperature is increased, the rate of coalescence of droplets are higher and the thermal effects induce the instability of the associated complex due to competitive desorption of substrates from the interface.[146] The instability of the intermediate is removed through the fast formation of a stable product. Bisal et al[288] have discussed the temperature effect on the structural properties of microemulson, pointing out that the number of droplets increases upon increasing temperature and the droplet radius decreases. A temperature increase reduces the interfacial tension between oil and water. The dispersion of water in oil is thus favoured by increasiing the number of smaller sized droplets and hence higher interfacial area and an increase in rate constant also. The rate enhancement is much higher in SDS than in AOT system was reported earlier and this is true for our SDS system also with reaction studied at different oil-water ratio.

Fig 4.4(a-i) shows the first order kinetic plot for the oxidation of iodide by persulphate in cyclohexane / CTAB+n-propanol / water.

$$\ln \left(\frac{a-x_1}{a-x_2}\right) \text{ versus } (t_2-t_1)$$

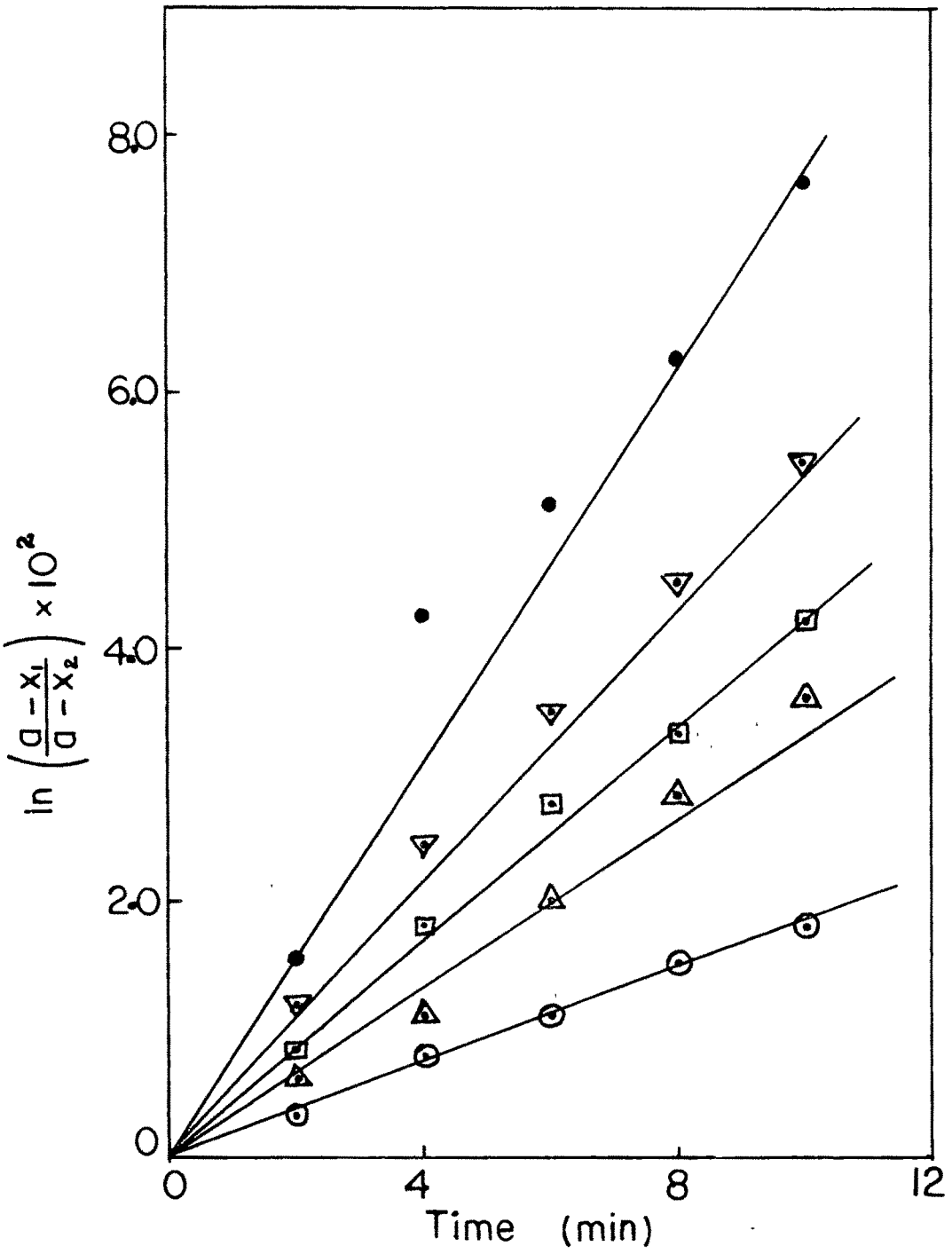

Fig.4.4a Plot of $\ln \frac{(a-x_1)}{(a-x_2)}$ -------- vs time for $KI+K_2S_2O_8$ reaction in CTAB microemulsion system with o/w=5/52. ⊙ 25°C; △ 30°C; ⊡ 35°C; ▽ 40°C; ● 45°C

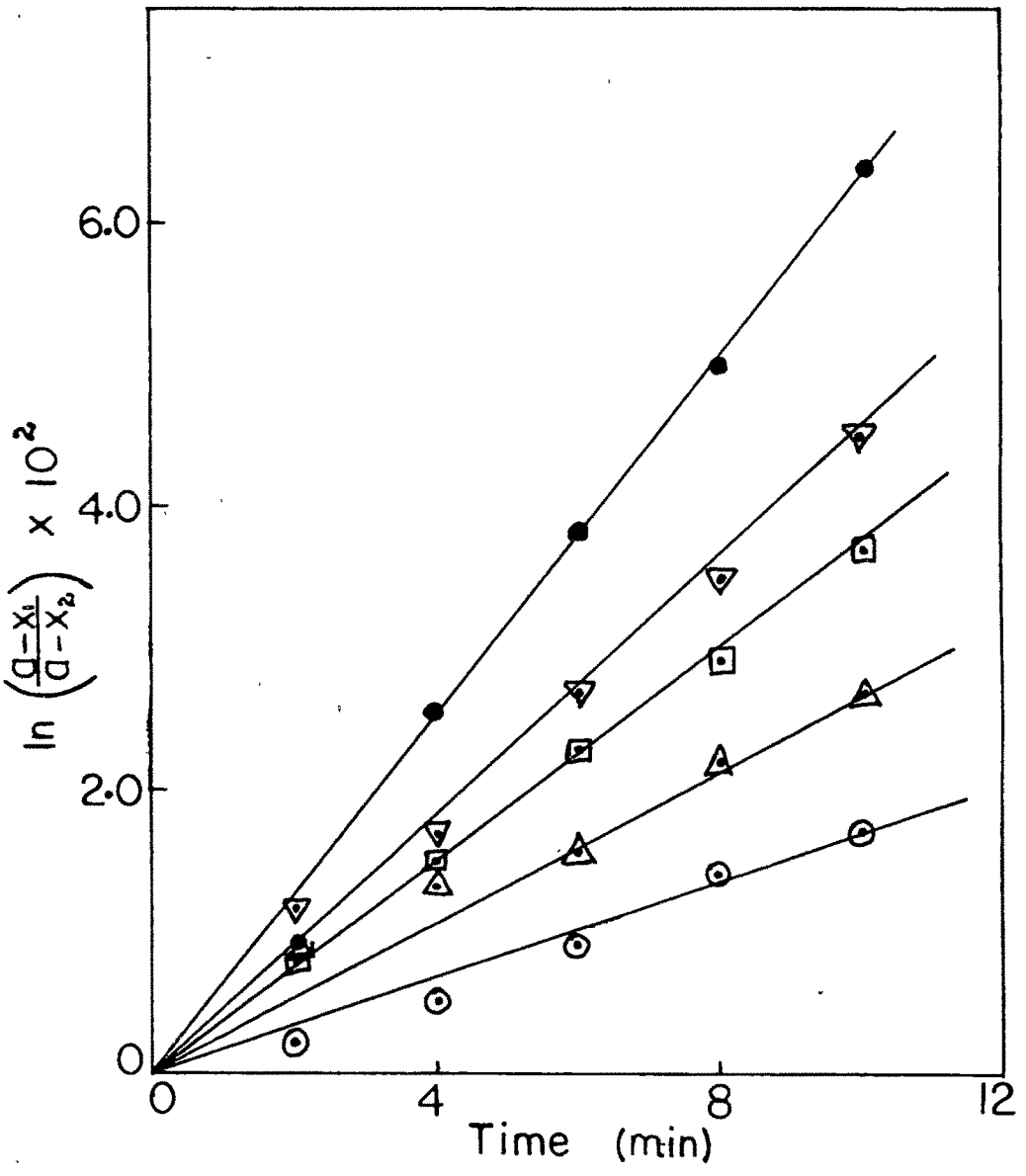

Fig.4.4b Plot of $\ln \frac{(a-x1)}{(a-x2)}$ vs time for $KI+K_2S_2O_8$ reaction in CTAB microemulsion system with o/w=10/47.5. Symbols are the same as in Fig. 4.4a.

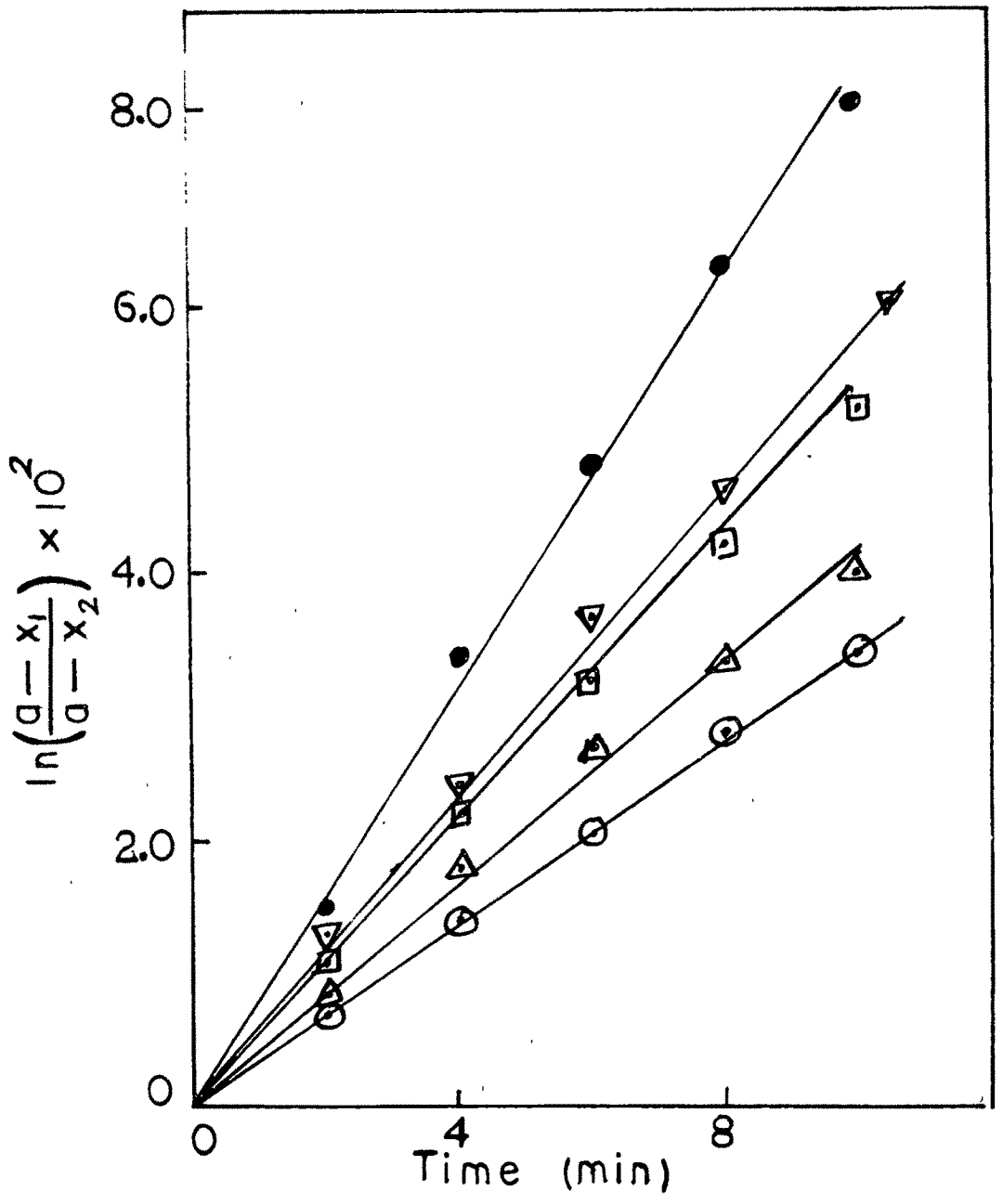

Fig.4.4c Plot of $\ln \frac{(a-x_1)}{(a-x_2)}$ vs time for $KI+K_2S_2O_8$ reaction in CTAB microemulsion system with o/w=15/42.5. Symbols are the same as in Fig. 4.4a.

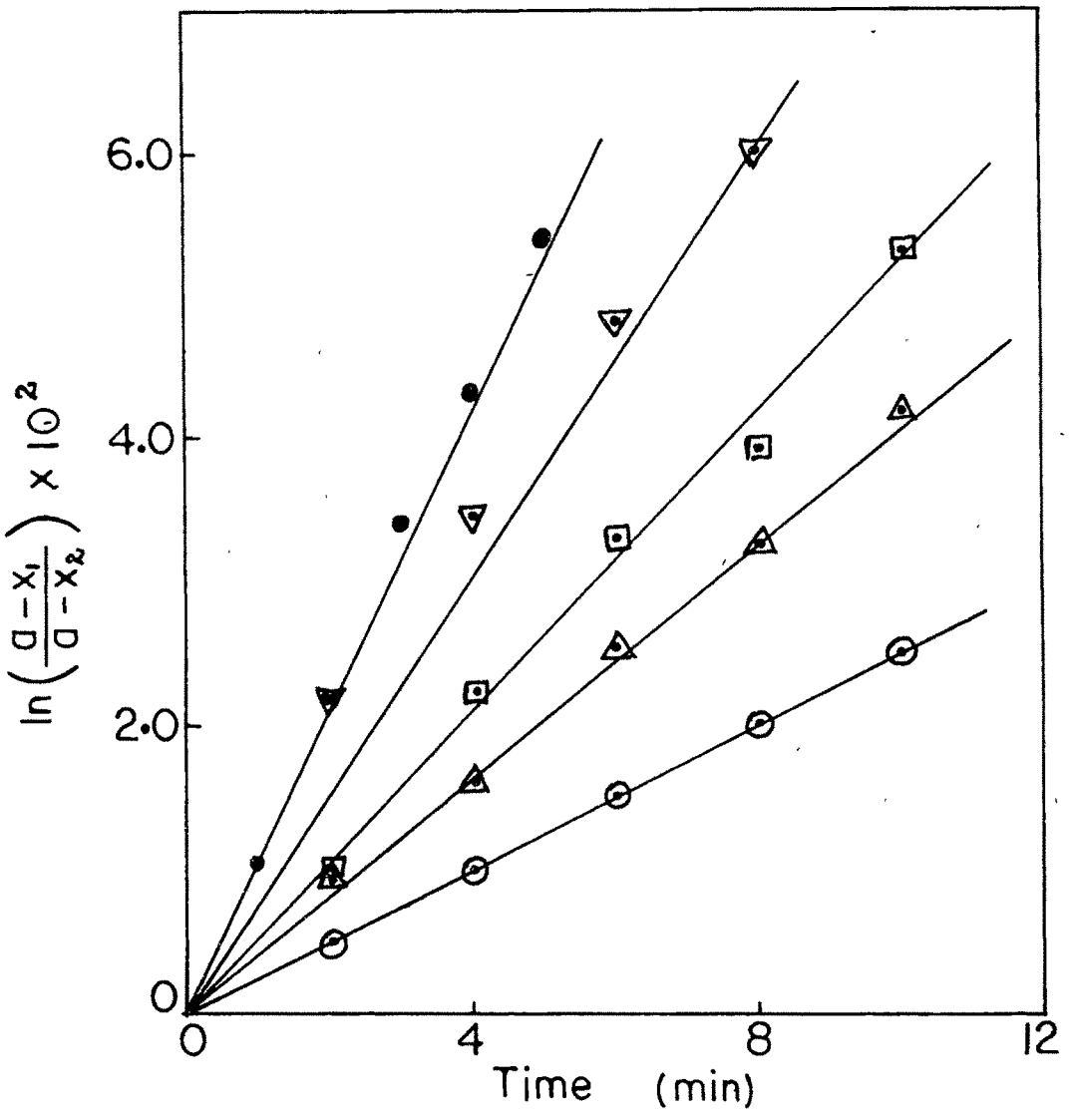

Fig.4.4d Plot of $\ln \frac{(a-x_1)}{(a-x_2)}$ vs time for $KI+K_2S_2O_8$ reaction in CTAB microemulsion system with o/w=20/37.5. Symbols are the same as in Fig.4.4a.

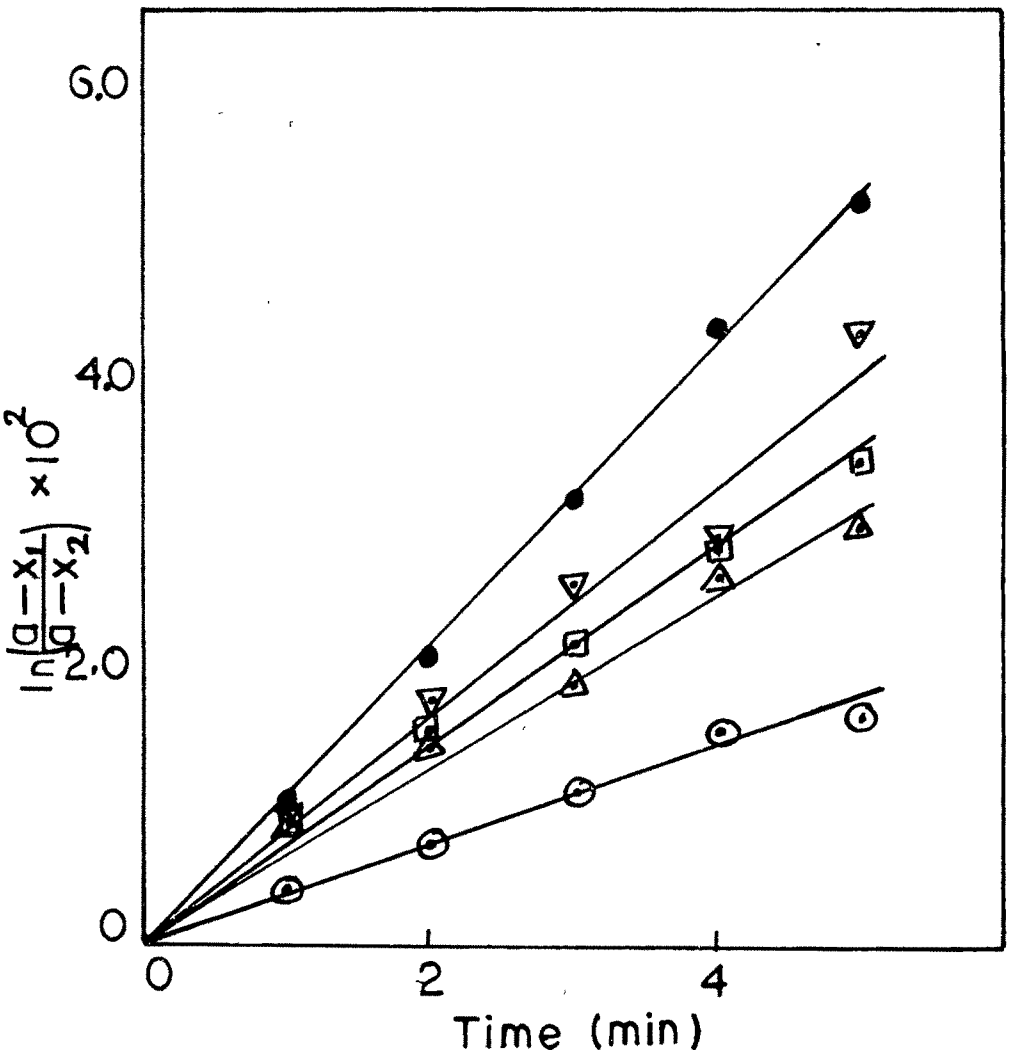

Fig.4.4e Plot of $\ln \frac{(a-x_1)}{(a-x_2)}$ vs time for $KI+K_2S_2O_8$ reaction in CTAB microemulsion system with o/w=25/32.5. Symbols are the same as in Fig.4.4a.

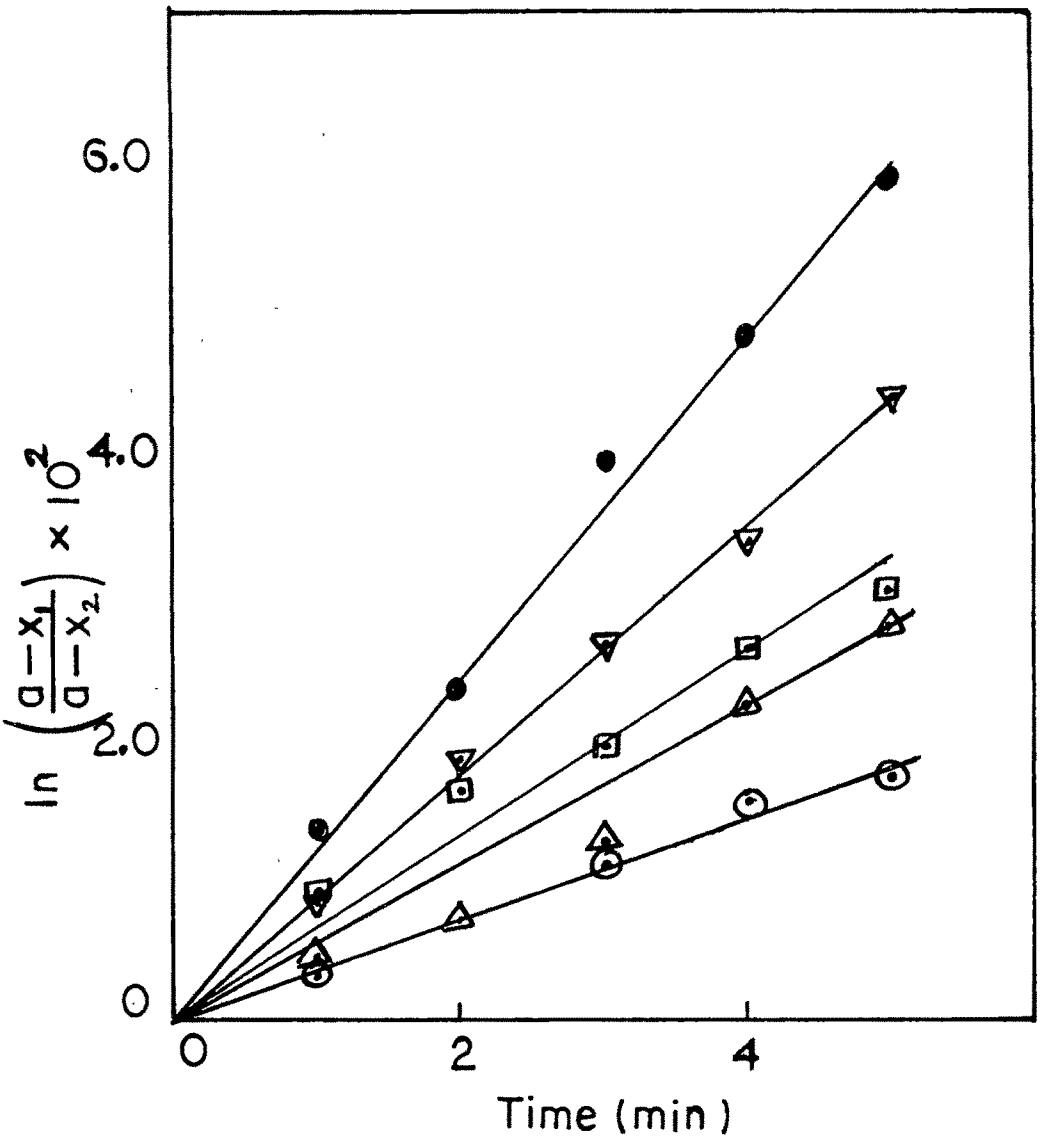

Fig.4.4f Plot of $\ln \frac{(a-x_1)}{(a-x_2)}$ -------- vs time for $KI+K_2S_2O_8$ reaction in CTAB microemulsion system with o/w=30/27.5. Symbols are the same as in Fig.4.4a.

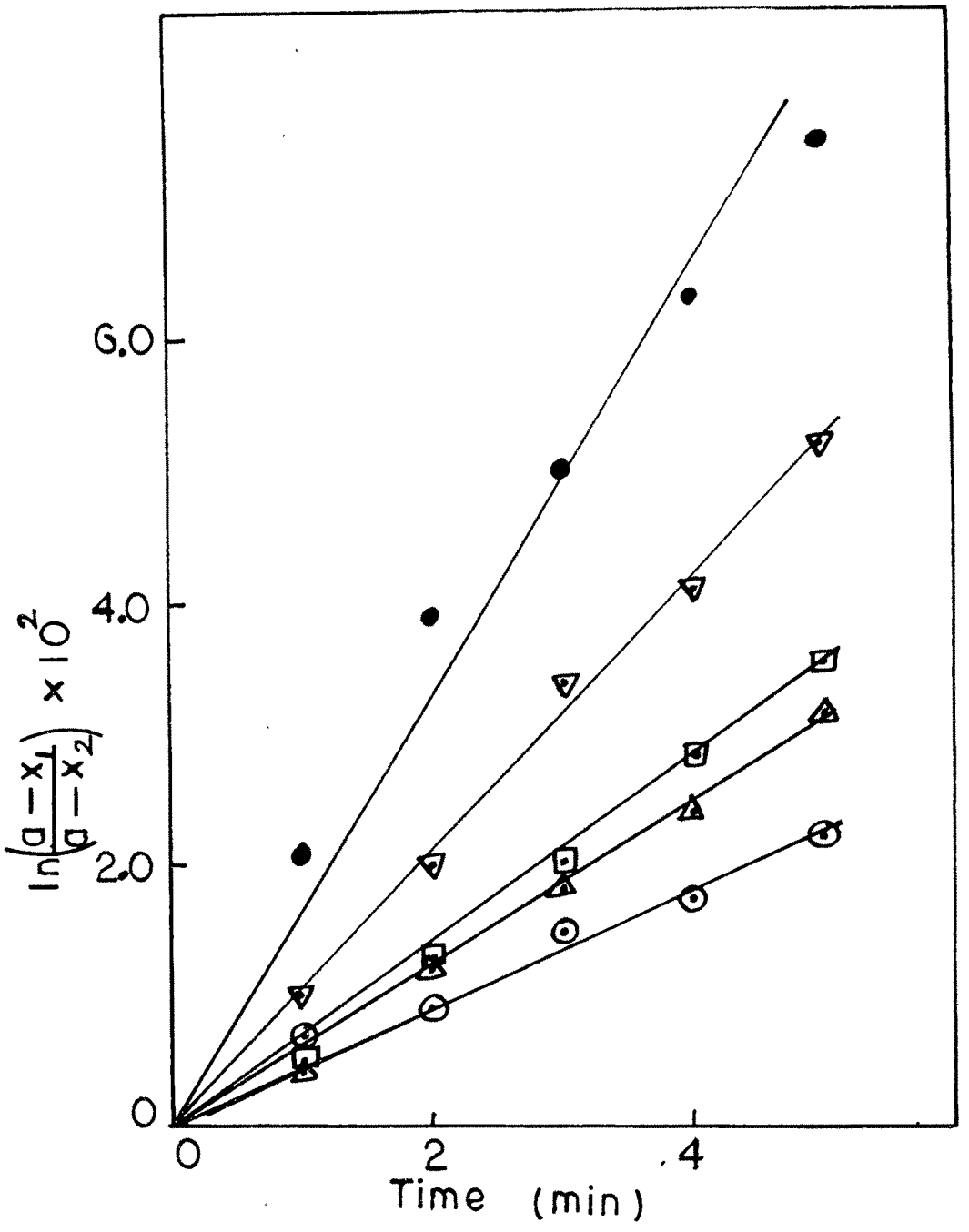

Fig.4.4g Plot of $\ln \frac{(a-x_1)}{(a-x_2)}$ -------- vs time for $KI+K_2S_2O_8$ reaction in CTAB microemulsion system with o/w=35/22.5. Symbols are the same as in Fig.4.4a.

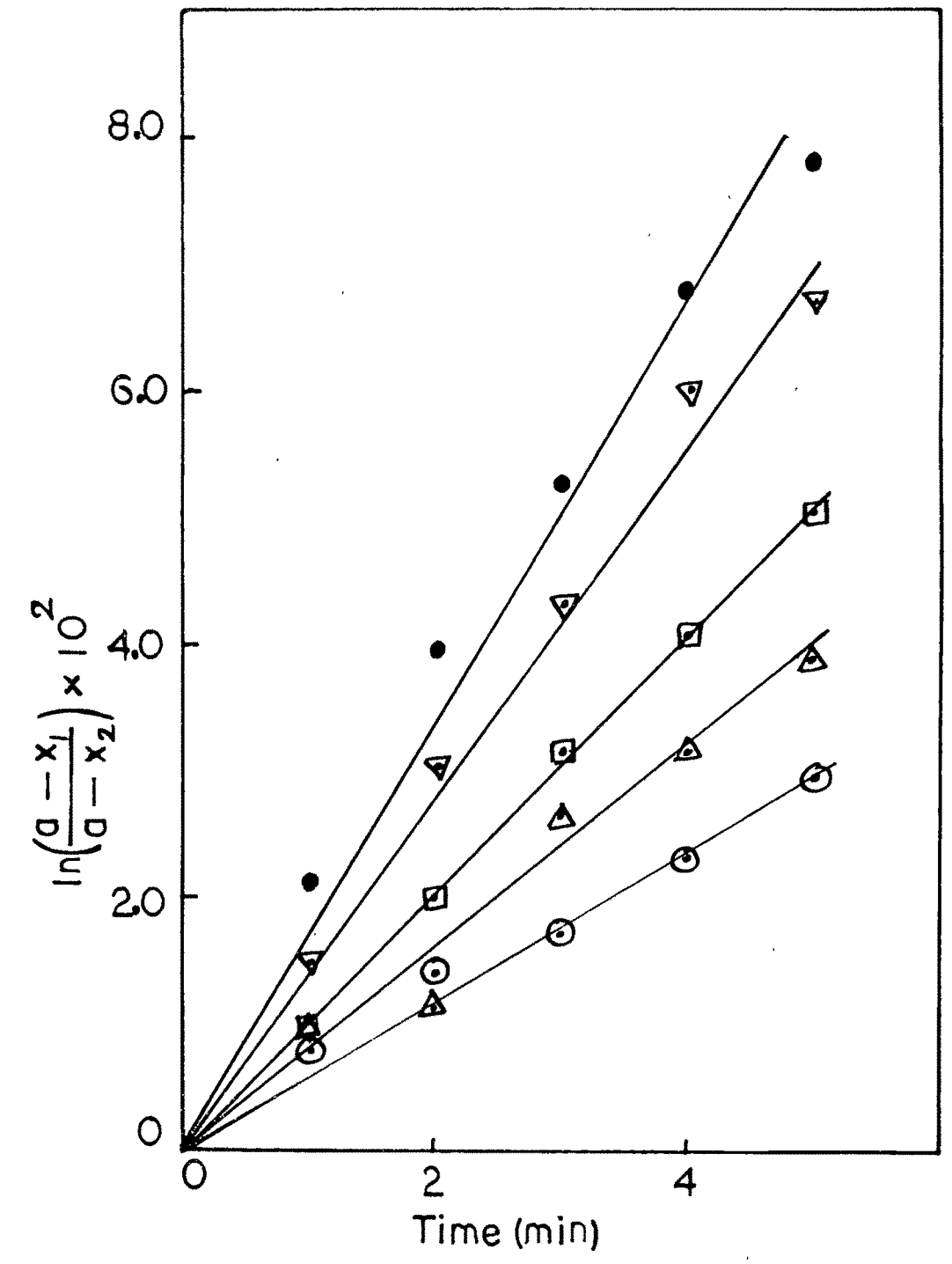

Fig.4.4h Plot of $\ln \frac{(a-x_1)}{(a-x_2)}$ -------- vs time for $KI+K_2S_2O_8$ reaction in CTAB microemulsion system with o/w=40/17.5. Symbols are the same as in Fig.4.4a.

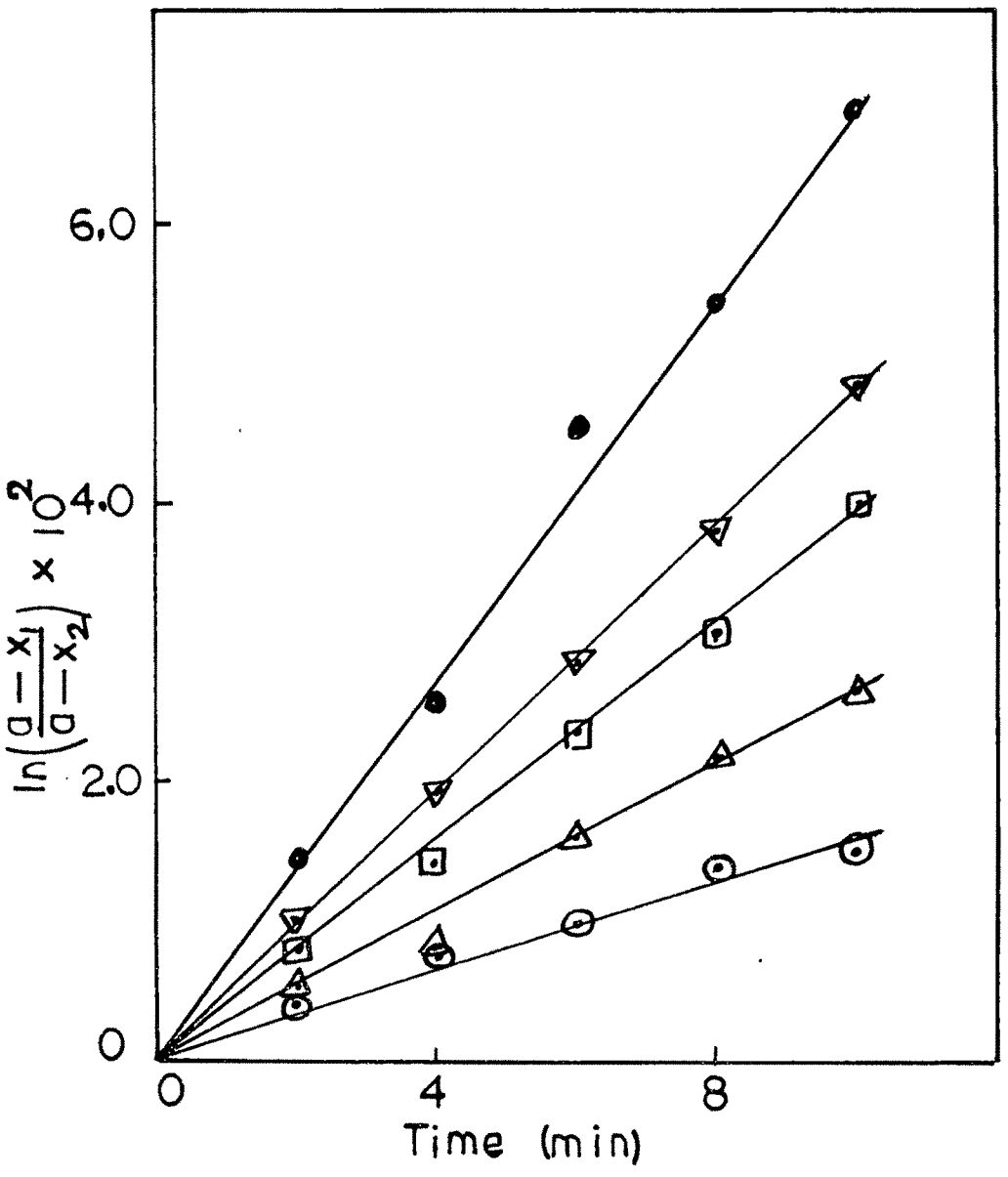

Fig.4.4i Plot of $\ln \frac{(a-x_1)}{(a-x_2)}$ vs time for $KI+K_2S_2O_8$ reaction in CTAB system with no oil s/w=42.5/57.5. Symbols are the same as in Fig.4.4a.

Table 4.2 **Pseudofirst order rate constant k(sec^{-1}) for the decomposition of $S_2O_8^{2-}$ in CTAB microemulsion CTAB concentration = 42.5.**

O/W	Temperature (^{0}C)				
	25	30	35	40	45
5/52.5	2.25×10^{-5}	3.79×10^{-5}	6.41×10^{-5}	8.33×10^{-5}	1.04×10^{-4}
10/47.5	3.08×10^{-5}	4.39×10^{-5}	6.41×10^{-5}	8.33×10^{-5}	1.04×10^{-4}
15/42.5	5.21×10^{-5}	6.41×10^{-5}	8.33×10^{-5}	9.26×10^{-5}	1.19×10^{-4}
20/37.5	4.60×10^{-5}	6.40×10^{-5}	8.33×10^{-5}	1.19×10^{-4}	1.67×10^{-4}
25/32.5	5.56×10^{-5}	9.80×10^{-5}	1.11×10^{-4}	1.28×10^{-4}	1.67×10^{-4}
30/27.5	5.59×10^{-5}	9.26×10^{-5}	1.11×10^{-4}	1.52×10^{-4}	2.08×10^{-4}
35/22.5	7.57×10^{-5}	1.04×10^{-4}	1.19×10^{-4}	1.67×10^{-4}	2.78×10^{-4}
40/17.5	9.88×10^{-5}	1.28×10^{-4}	1.67×10^{-4}	2.08×10^{-4}	2.78×10^{-4}
S/W = 42.5/57.5	2.69×10^{-5}	4.63×10^{-5}	6.41×10^{-5}	7.58×10^{-5}	1.04×10^{-4}

is plotted. Initial concentration are same as for the SDS system. Slope of the line gives the rate constant and it has been plotted at different temperatures and changing oil-water ratios. The result is summarized in Table 4.2. The rate of reaction is lower in comparison to that in water. The rate in SDS microemulsions is higher though. Unpublished work obtained by F. Sanchez et al[143] supports this result. The temperature effect shows the expected trend. The rate increases with increasing temperature . Even with decreasing oil-water ratios, the rate constant decreases.

We expected a rate enhancement in CTAB microemulsion because of the large interfacial area provided by the formation of microdroplets. However we observed a rate inhibition (Table 4.2) which can be explained in terms of electrostatic interaction. Gomez - Herrera et al[8,204] explained the rate enhancement in AOT microemulsion by the repulsive interaction of anionic reactants and the negatively charged heads of the AOT molecules which would increase the local reactant concentration and this would favour the approach of reactants and thus the reaction rate is increased.[8,143,204] This we have extrapolated to our SDS microemulsions system also. This electrostatic interaction is in agreement with the large decrease observed in the reaction rate of the process I^- $+S_2O_8^{2-}$ in microemulsion, with respect to aqueous media. When we exchange the anionic surfactant with a cationic one. The electrostatic interaction between the positively charged head of the CTAB molecule and the anionic reactants would decrease the local concentration of reactants and it offers an approachability barrier to the reactants and hence the reaction is low down.[143]

The rate increasing with decreasing water content is the result of mainly three factors.[8,143,144,204] The first one is the dilution of the reactants in the aqueous phase when the water content increases and the second factor might be related to the structural changes produced in the microemulsion system by changing the water fraction. The size and number of microdroplets are expected to be different for diferent water fraction. The rate increase with decrease in water fraction is

also explained by considering the decrease in water activity due to the interaction between water molecules and the surfactant.

As we have noticed for SDS system, the rate of reaction increases with increase in temperature. The rate of coalescence of droplets is higher and the thermal effects induce instability of associated complex due to competitive desorption of substrate from the interface. The instability of the intermediate is removed through the fast formation of a stable product. According to Bisal et al,[288] the number of droplets increases upon increasing the temperature and the droplet radius decreases by the formation of the large number of smaller sized droplets providing large interfacial area and hence an increase in rate constant with increasing temperature.

Kinetically, we have studied the effect of TX100 stabilized microemulsion on the oxidation of iodide by persulphate also. Fig. 4.5 (a-e) & Table 4.3 show the k values for the first order reaction at different temperatures and with changing oil-water ratios. Oil-water ratios are 0.0227, 0.125, 0.2857, 0.5. Like CTAB microemulsion, TX100 microemulsion also retards the reaction. Potassium iodide and potassium persulphate are soluble in water and the reaction in TX100 containing microemulsions are in o/w systems. Due to the presence of oil (where KI & K_2 S_2O_8 are not soluble) it was expected that the local concentration would increase & hence the reaction rate. However, the reaction rate was found to decrease in these systems. The reason probably lies in the fact that the polyoxyethylene group is highly hydrated and I^- & $S_2O_8^{2-}$ get embeded in those hydration spheres. Such highly swollen surfactant molecules make the approachability of the two ions to each other difficult and hence the reaction rate is lower. However, increase in oil concentration and hence low hydration force the ions to come together and to increase the rate of reaction. With decreasing amount of water, the rate increases as in the case of ionic surfactants which was observed earlier[143,284] due to the increase in local concentration of the reactants.

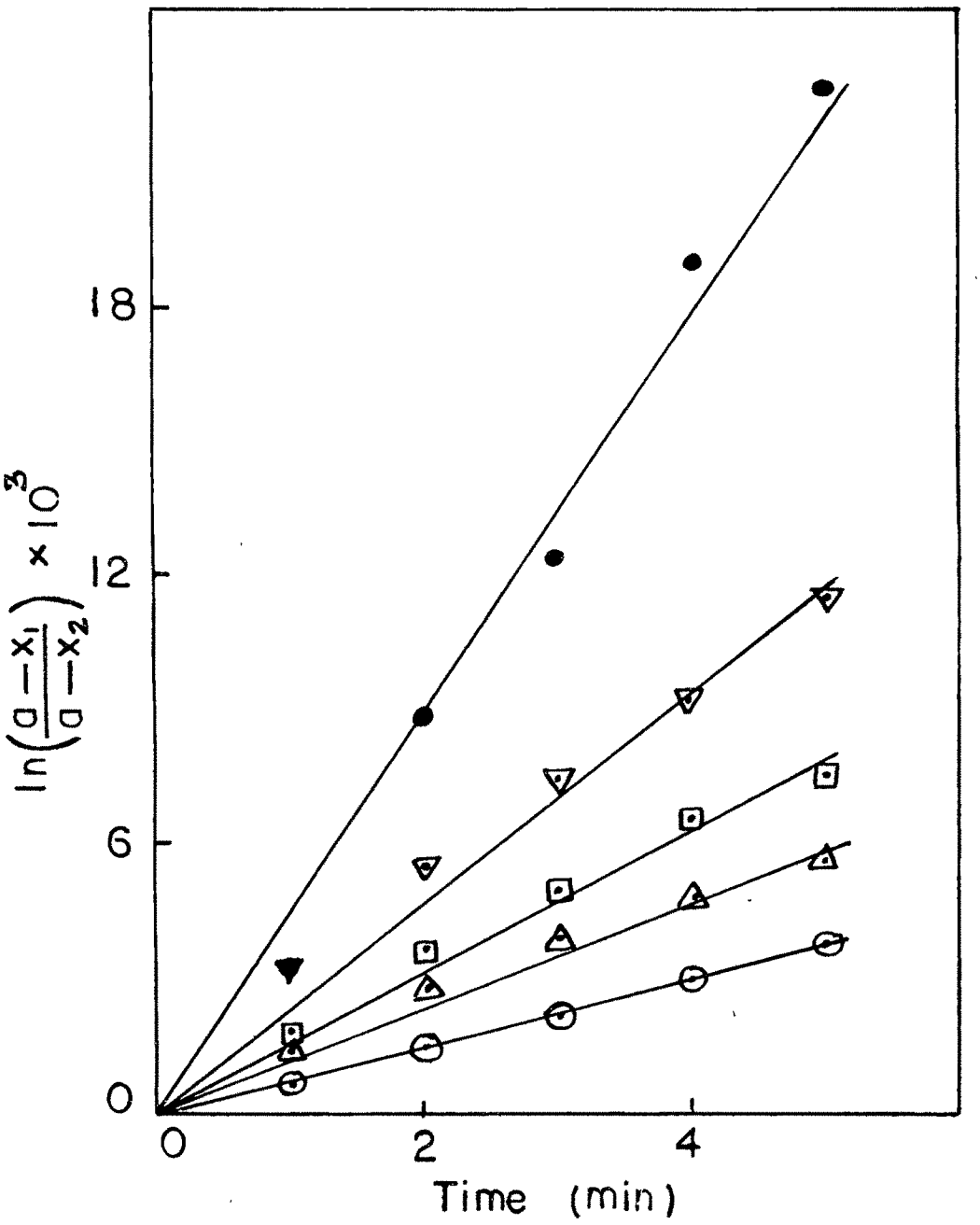

Fig.4.5a Plot of $\ln \frac{(a-x_1)}{(a-x_2)}$ -------- vs time for $KI+K_2S_2O_8$ reaction in TX100 microemulsion system with o/w=1/44.

⊙ 25°C; △ 30°C; ⊡ 35°C; ▽ 40°C; ● 45°C

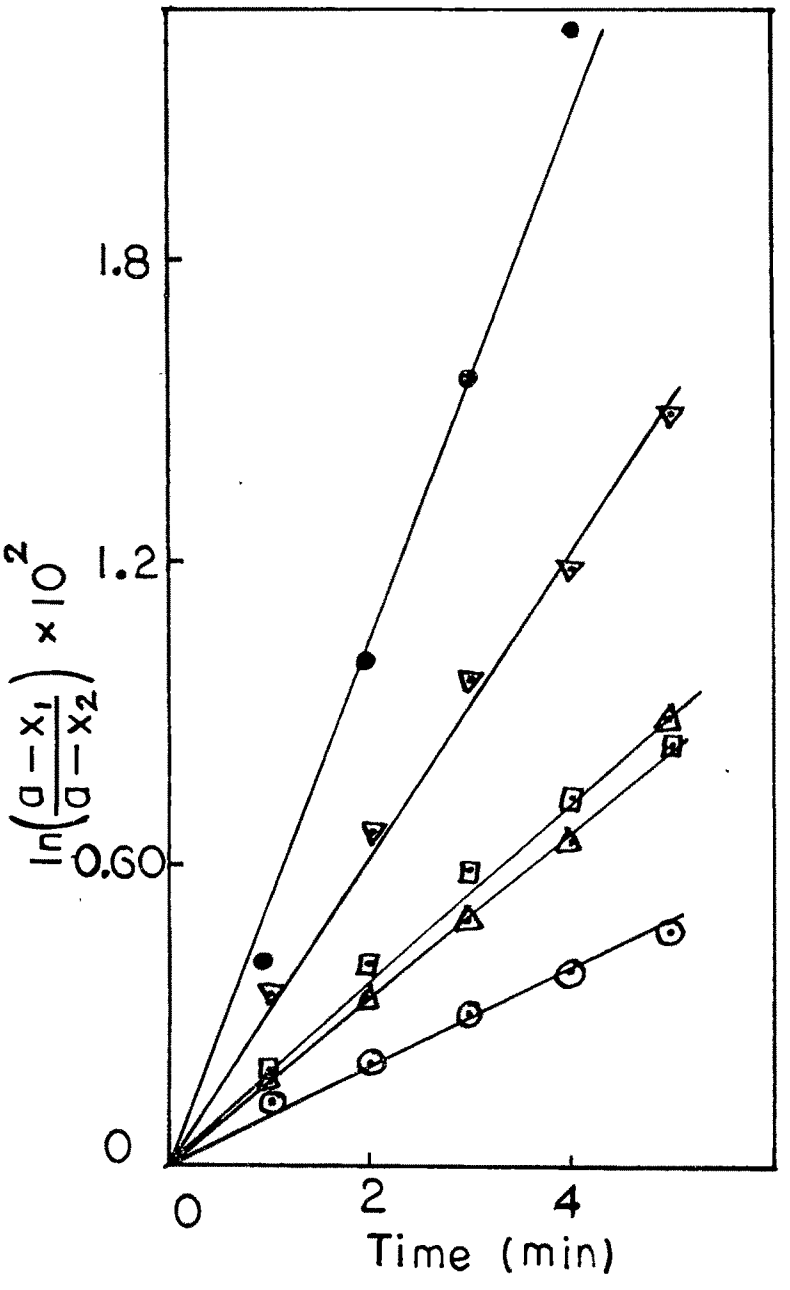

Fig.4.5b Plot of $\ln \frac{(a-x_1)}{(a-x_2)}$ ------- vs time for $KI+K_2S_2O_8$ reaction in TX100 microemulsion system with o/w=5/40. Symbols are the same as in Fig.4.5a.

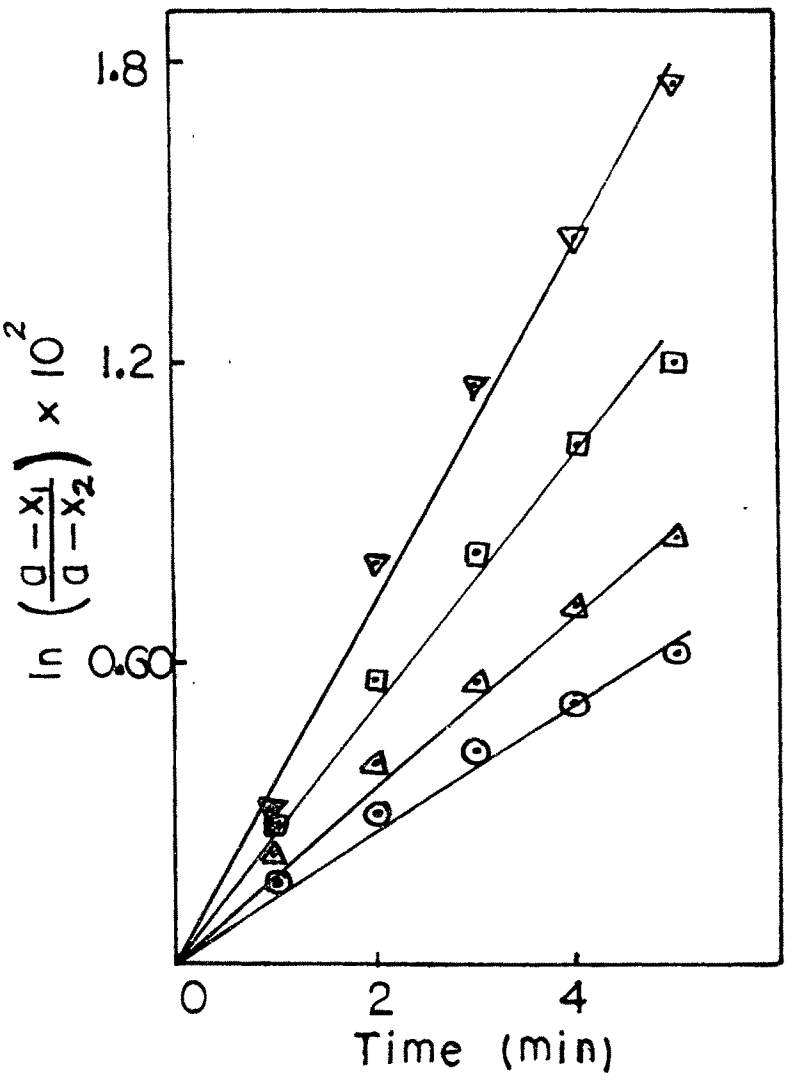

Fig.4.5c Plot of $\ln \frac{(a-x_1)}{(a-x_2)}$ vs time for $KI+K_2S_2O_8$ reaction in TX100 microemulsion system with o/w=10/35. Symbols are the same as in Fig.4.5a.

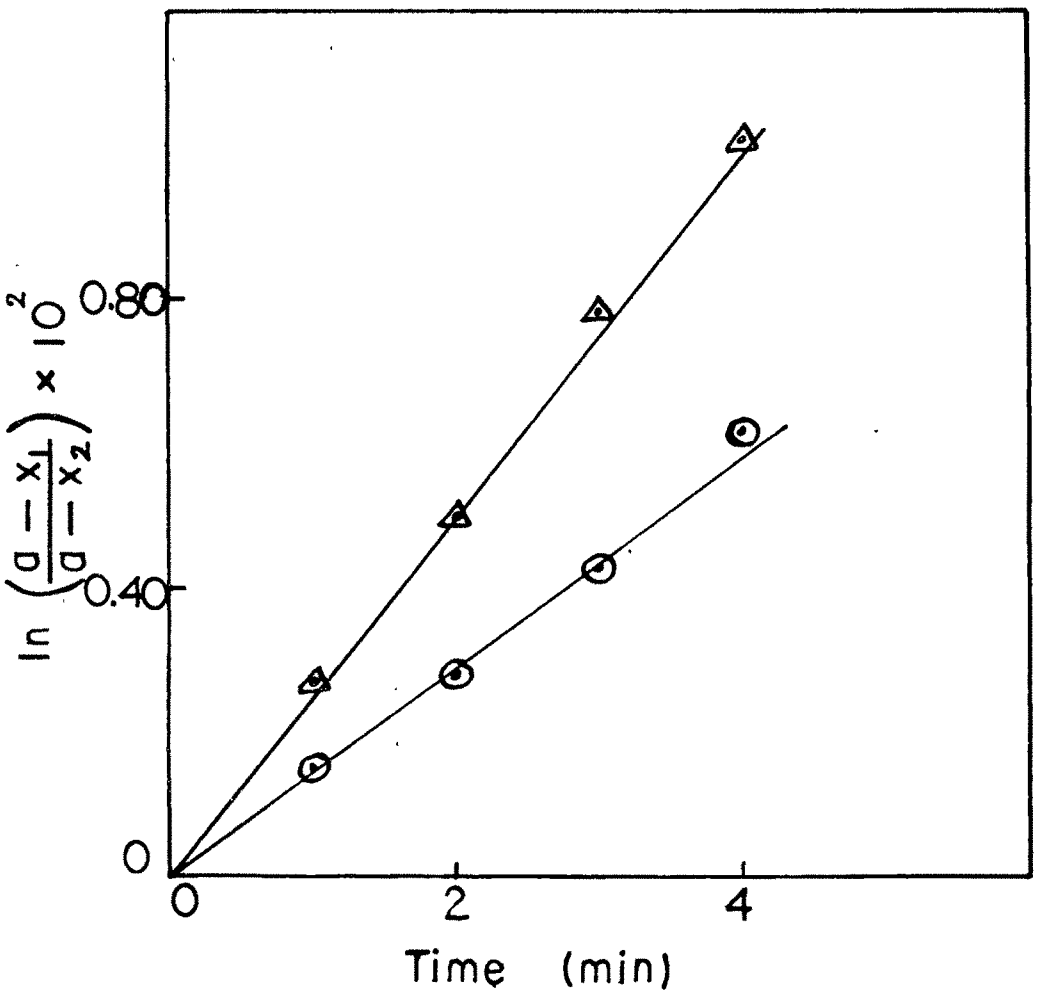

Fig.4.5d Plot of $\ln \frac{(a-x_1)}{(a-x_2)}$ -------- vs time for $KI+K_2S_2O_8$ reaction in TX100 microemulsion system with o/w=15/30. Symbols are the same as in Fig.4.5a.

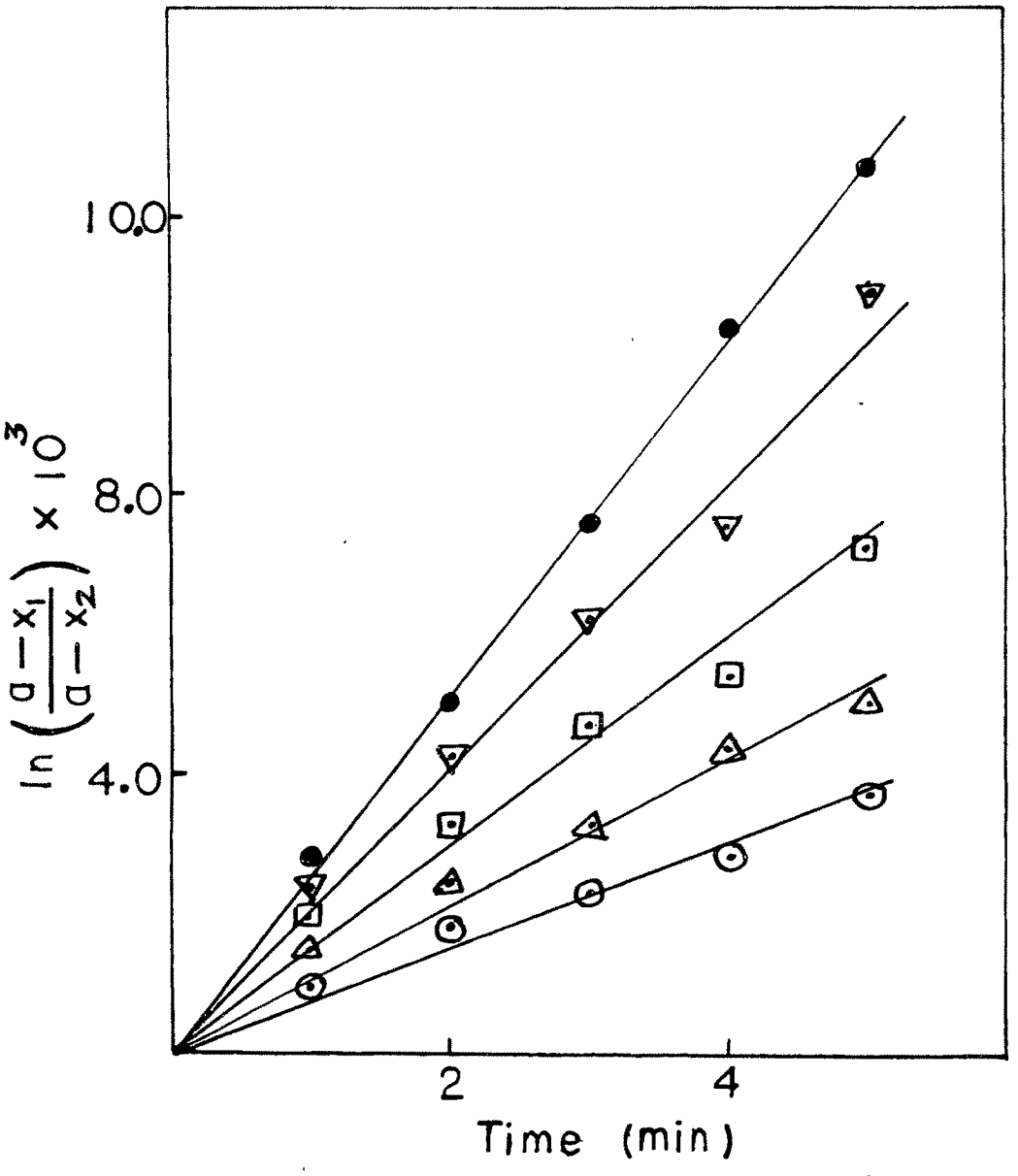

Fig.4.5e Plot of $\ln \frac{(a-x_1)}{(a-x_2)}$ -------- vs time for $KI+K_2S_2O_8$ reaction in TX100 system with no oil s/w=55/45. Symbols are the same as in Fig.4.5a.

Table 4.3 **Pseudofirst order rate constant k(sec^{-1}) for the decomposition of $S_2O_8^{2-}$ in TX100 microemulsion. TX100 concentration = 55%.**

O/W	Temperature (^0C)				
	25	30	35	40	45
1/44	1.25×10^{-5}	1.92×10^{-5}	2.5×10^{-5}	3.57×10^{-5}	6.25×10^{-5}
5/40	1.59×10^{-5}	2.78×10^{-5}	3.03×10^{-5}	5.56×10^{-5}	8.33×10^{-5}
10/35	2.08×10^{-5}	2.78×10^{-5}	4.17×10^{-5}	5.56×10^{-5}	-
15/30	2.56×10^{-5}	4.17×10^{-5}	-	-	-
S/W = 55/45	1.19×10^{-5}	1.67×10^{-5}	2.38×10^{-5}	3.33×10^{-5}	4.17×10^{-5}

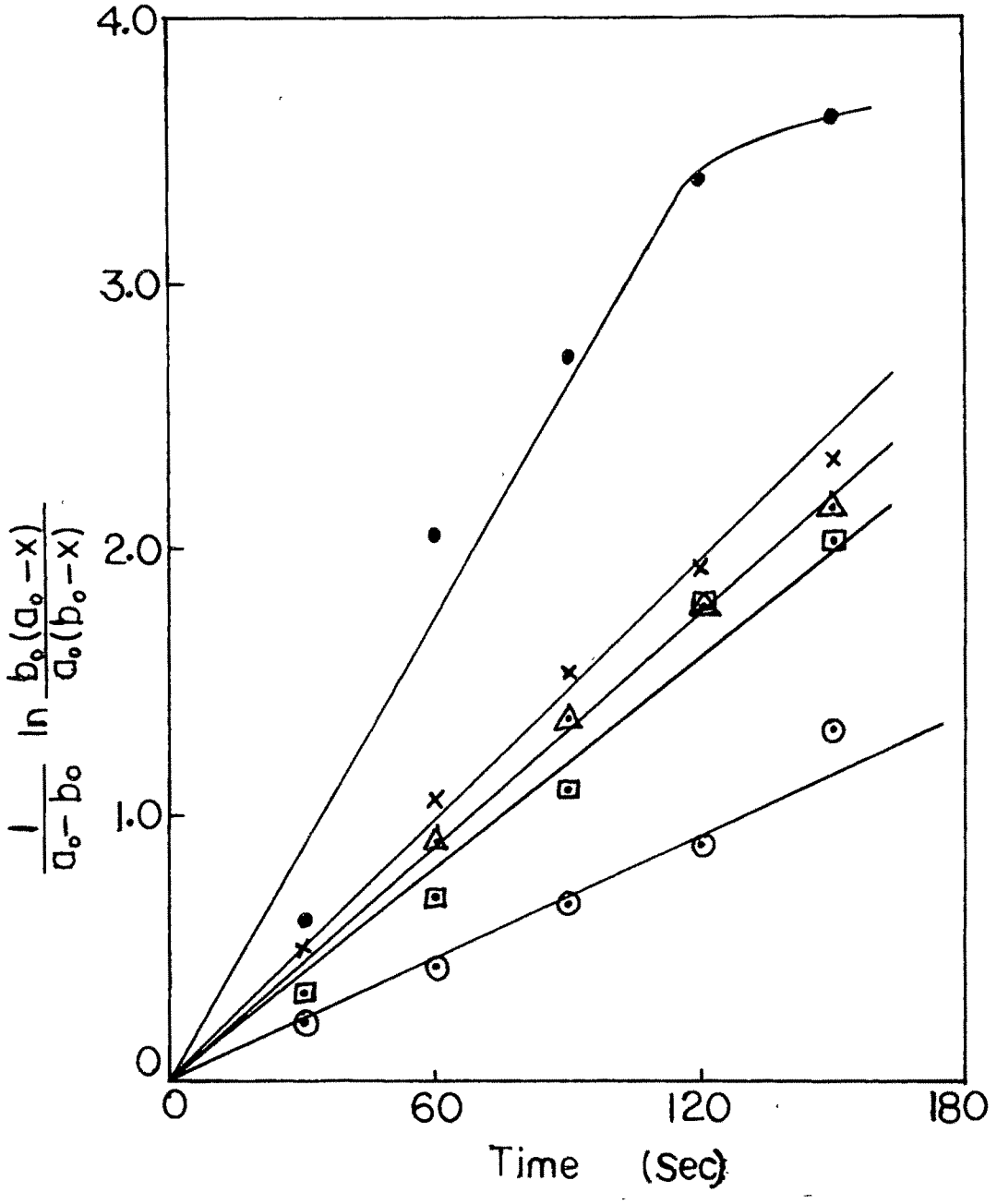

Fig.4.6a Plot of $\frac{1}{a_o - b_o} \ln \frac{b_o (a_o - x)}{a_o (b_o - x)}$ vs time for $KI+K_2S_2O_8$ reaction in SDS microemulsion system with o/w=5/52.5.

⊙ 25°C; ⊡ 30°C; △ 35°C; × 40°C; ● 45°C

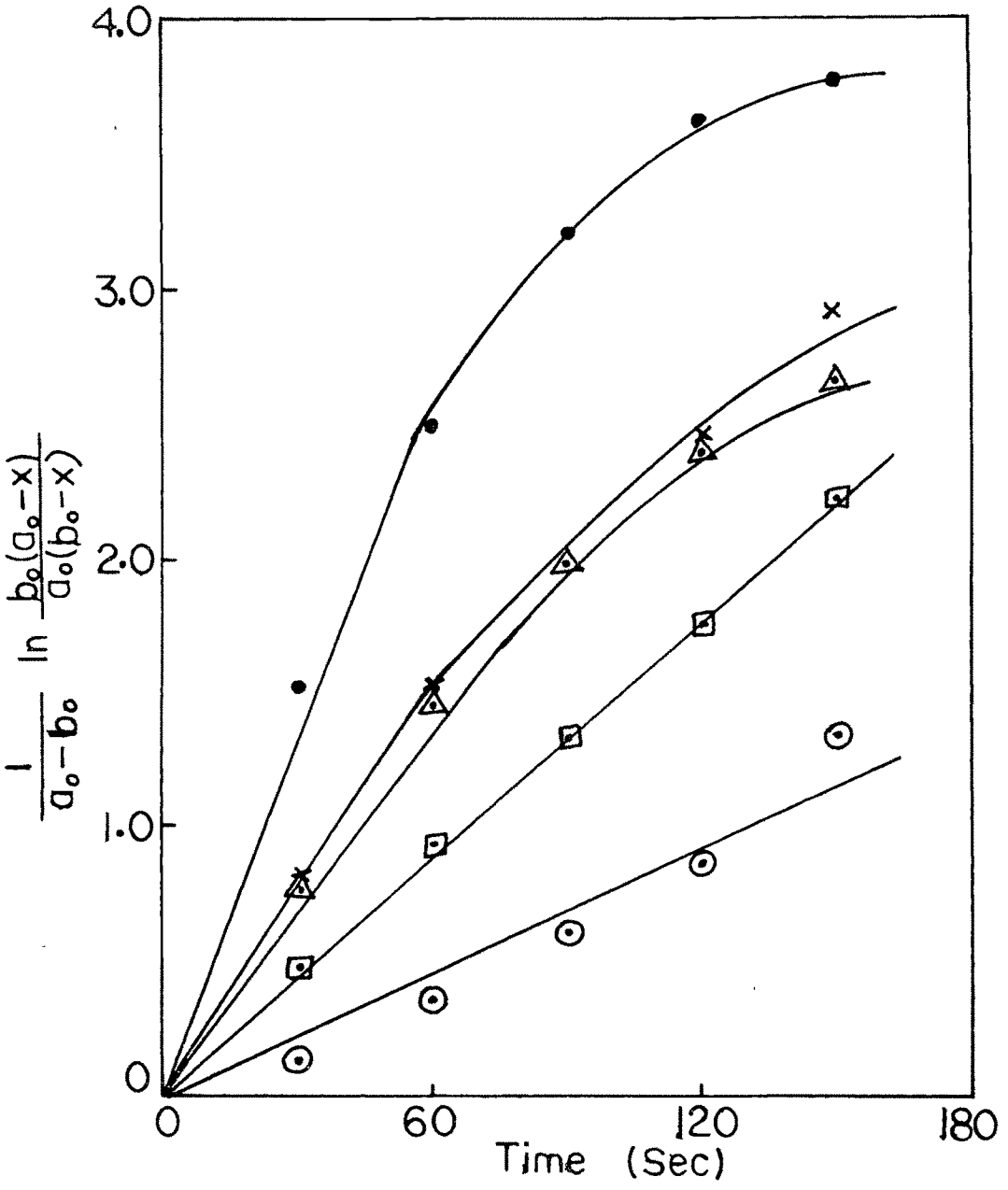

Fig.4.6b Plot of $\frac{1}{a_o-b_o} \ln \frac{b_o(a_o-x)}{a_o(b_o-x)}$ vs time for $KI+K_2S_2O_8$ reaction in SDS microemulsion system with o/w=10/47.5. Symbols are the same as in Fig.4.6a.

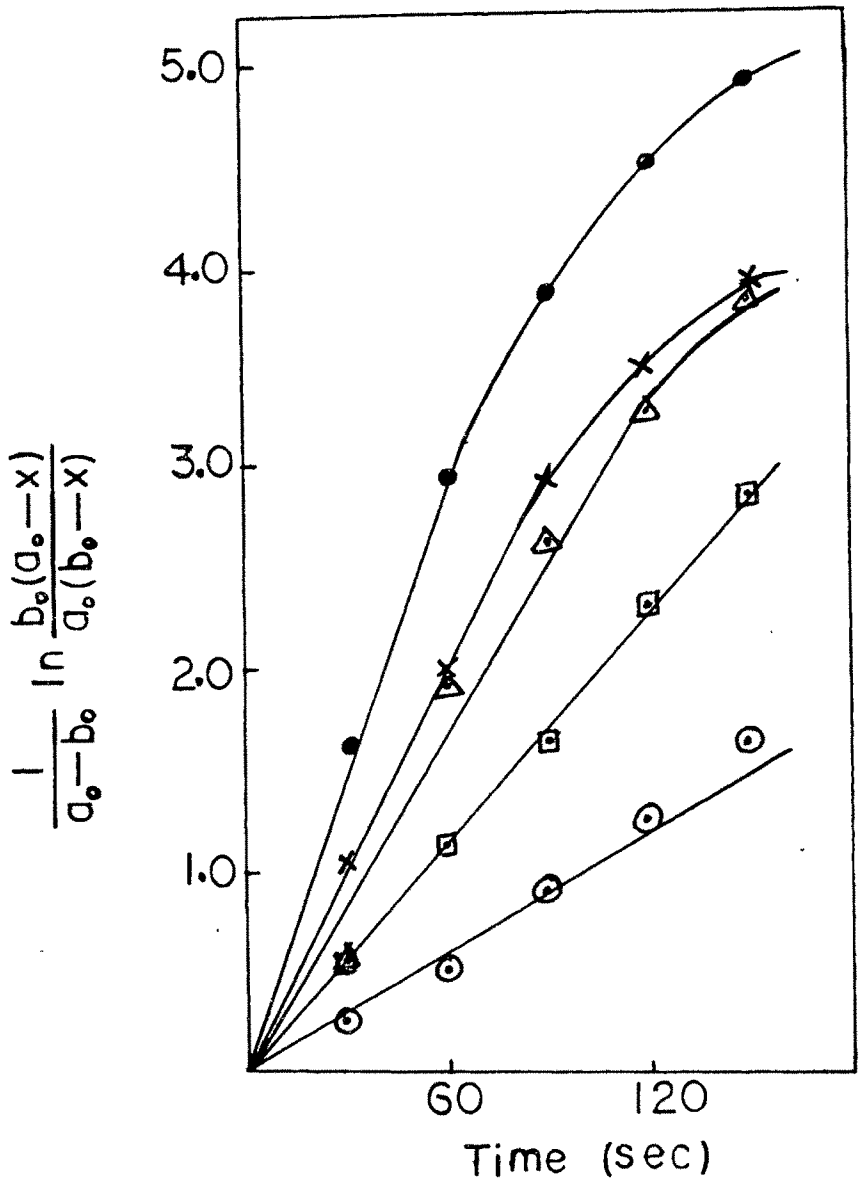

Fig.4.6c Plot of $\frac{1}{a_o-b_o} \ln \frac{b_o(a_o-x)}{a_o(b_o-x)}$ vs time for $KI+K_2S_2O_8$ reaction in SDS microemulsion system with o/w=15/42.5. Symbols are the same as in Fig.4.6a.

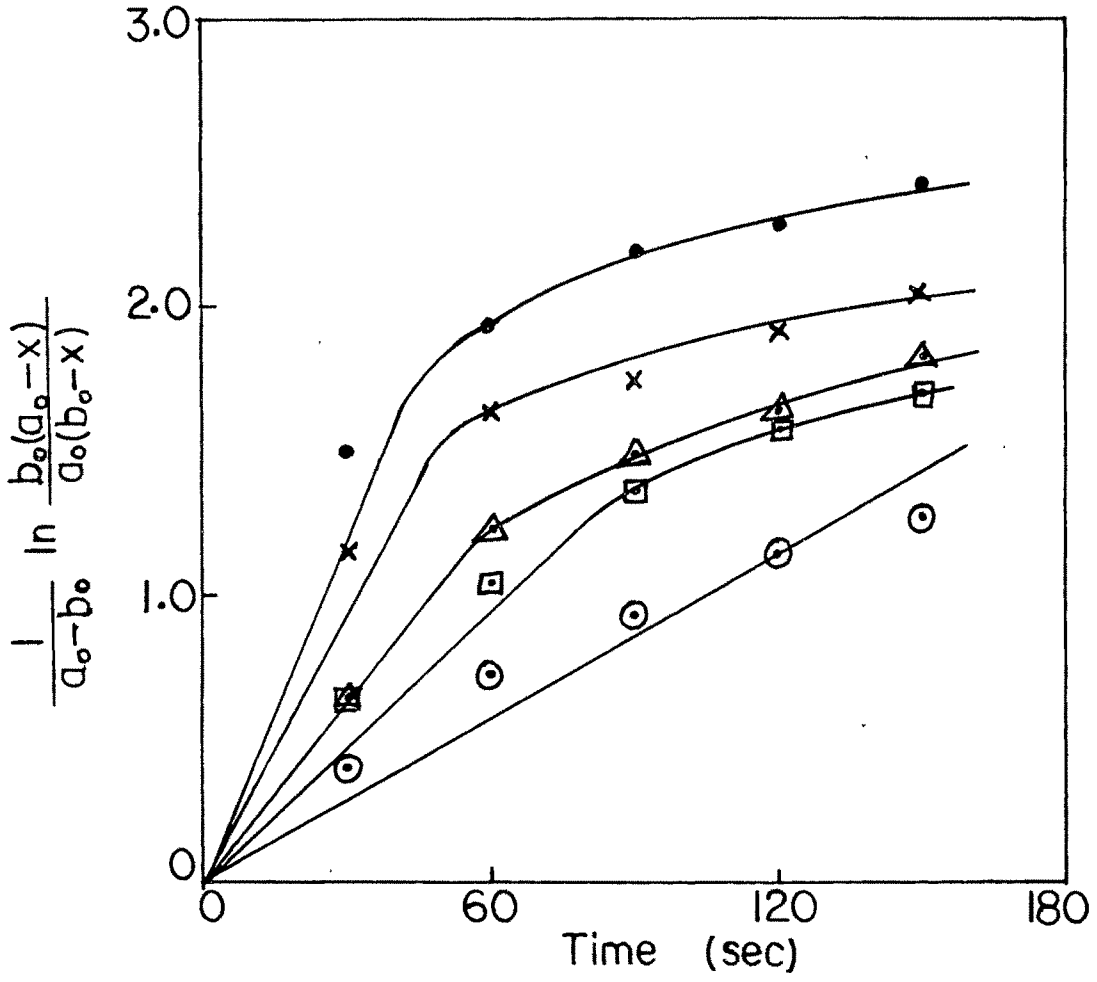

Fig.4.6d Plot of $\frac{1}{a_o-b_o} \ln \frac{b_o(a_o-x)}{a_o(b_o-x)}$ vs time for $KI+K_2S_2O_8$ reaction in SDS microemulsion system with o/w=20/37.5. Symbols are the same as in Fig.4.6a.

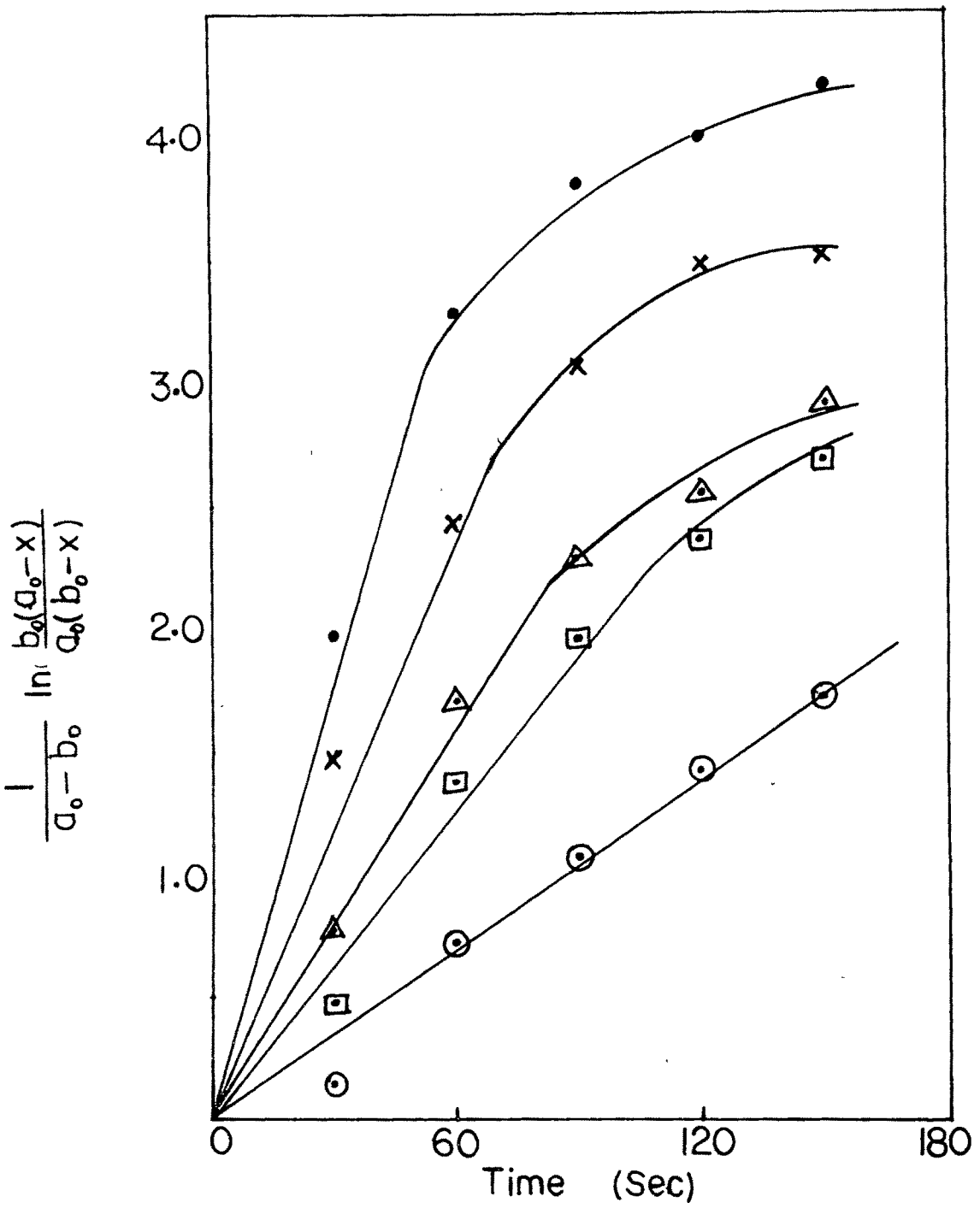

Fig.4.6e Plot of $\frac{1}{a_o-b_o} \ln \frac{b_o(a_o-x)}{a_o(b_o-x)}$ vs time for $KI+K_2S_2O_8$ reaction in SDS microemulsion system with o/w=25/32.5. Symbols are the same as in Fig.4.6a.

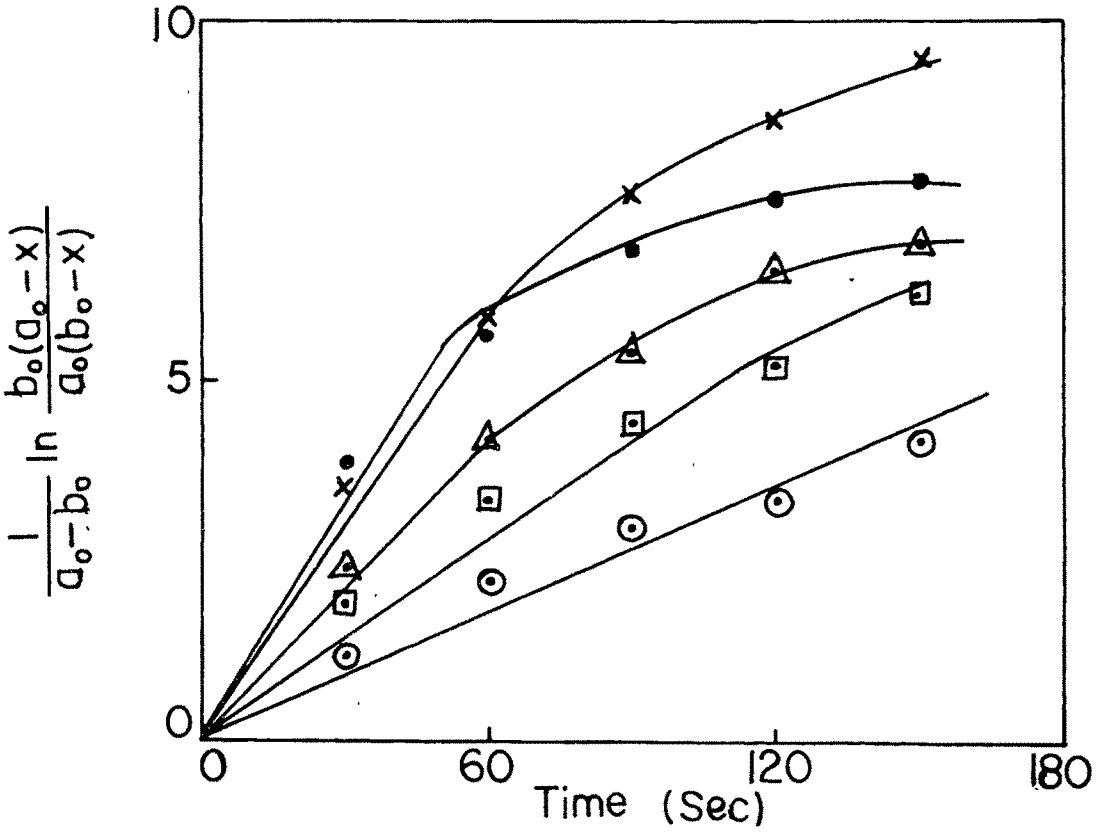

Fig.4.6f Plot of $\frac{1}{a_o-b_o} \ln \frac{b_o(a_o-x)}{a_o(b_o-x)}$ vs time for $KI+K_2S_2O_8$ reaction in SDS microemulsion system with o/w=25/32.5. Symbols are the same as in Fig.4.6a.

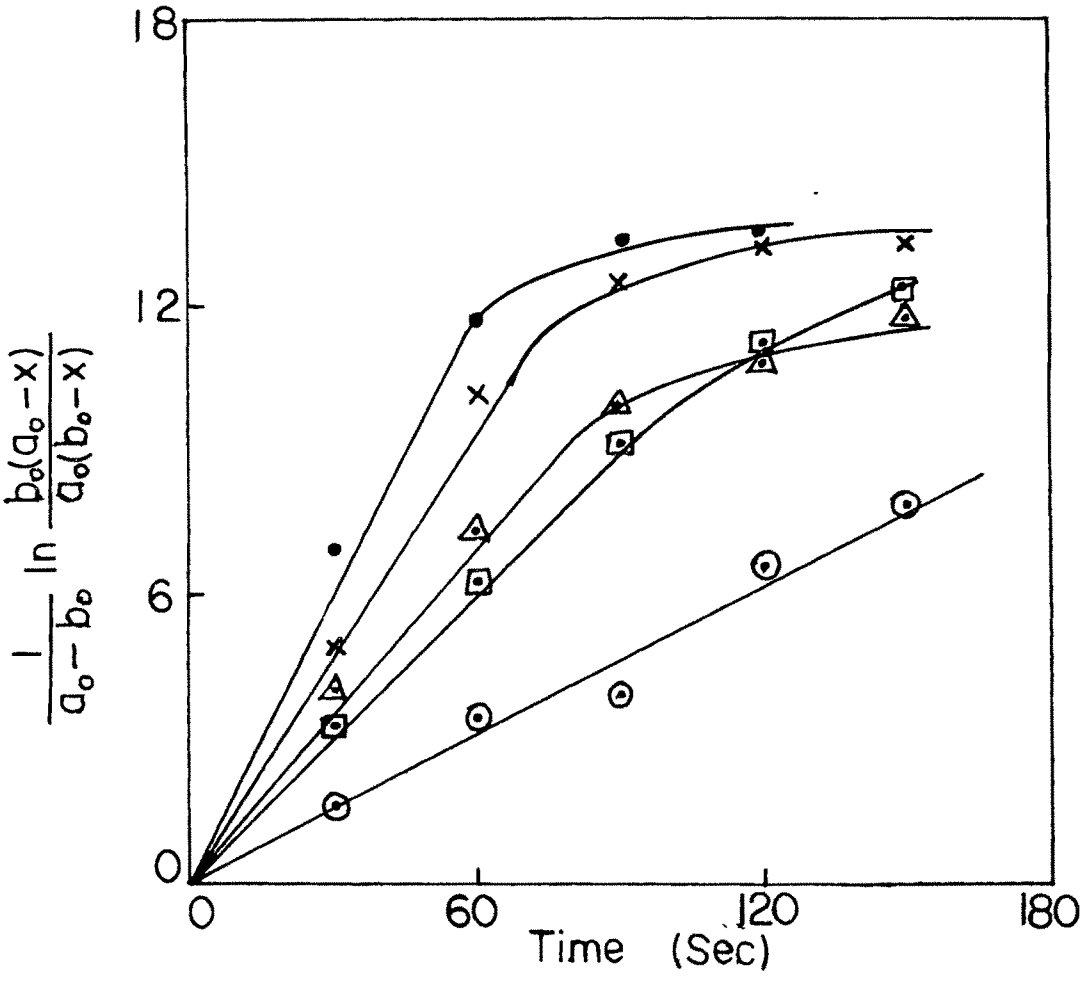

Fig.4.6g Plot of $\frac{1}{a_o-b_o} \ln \frac{b_o(a_o-x)}{a_o(b_o-x)}$ vs time for $KI+K_2S_2O_8$ reaction in SDS microemulsion system with o/w=30/27.5. Symbols are the same as in Fig.4.6a.

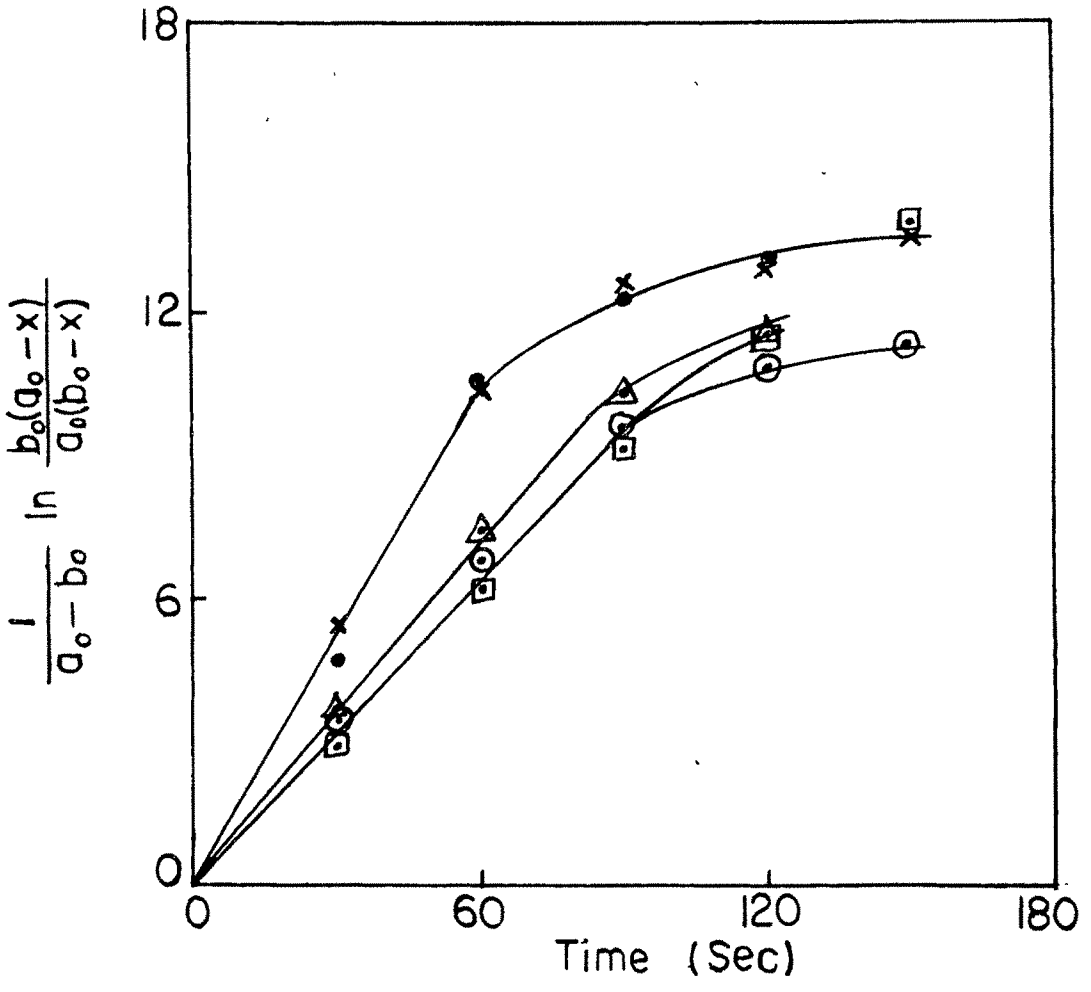

Fig.4.6h Plot of $\frac{1}{a_o-b_o} \ln \frac{b_o(a_o-x)}{a_o(b_o-x)}$ vs time for $KI+K_2S_2O_8$ reaction in SDS microemulsion system with o/w=40/17.5. Symbols are the same as in Fig.4.6a.

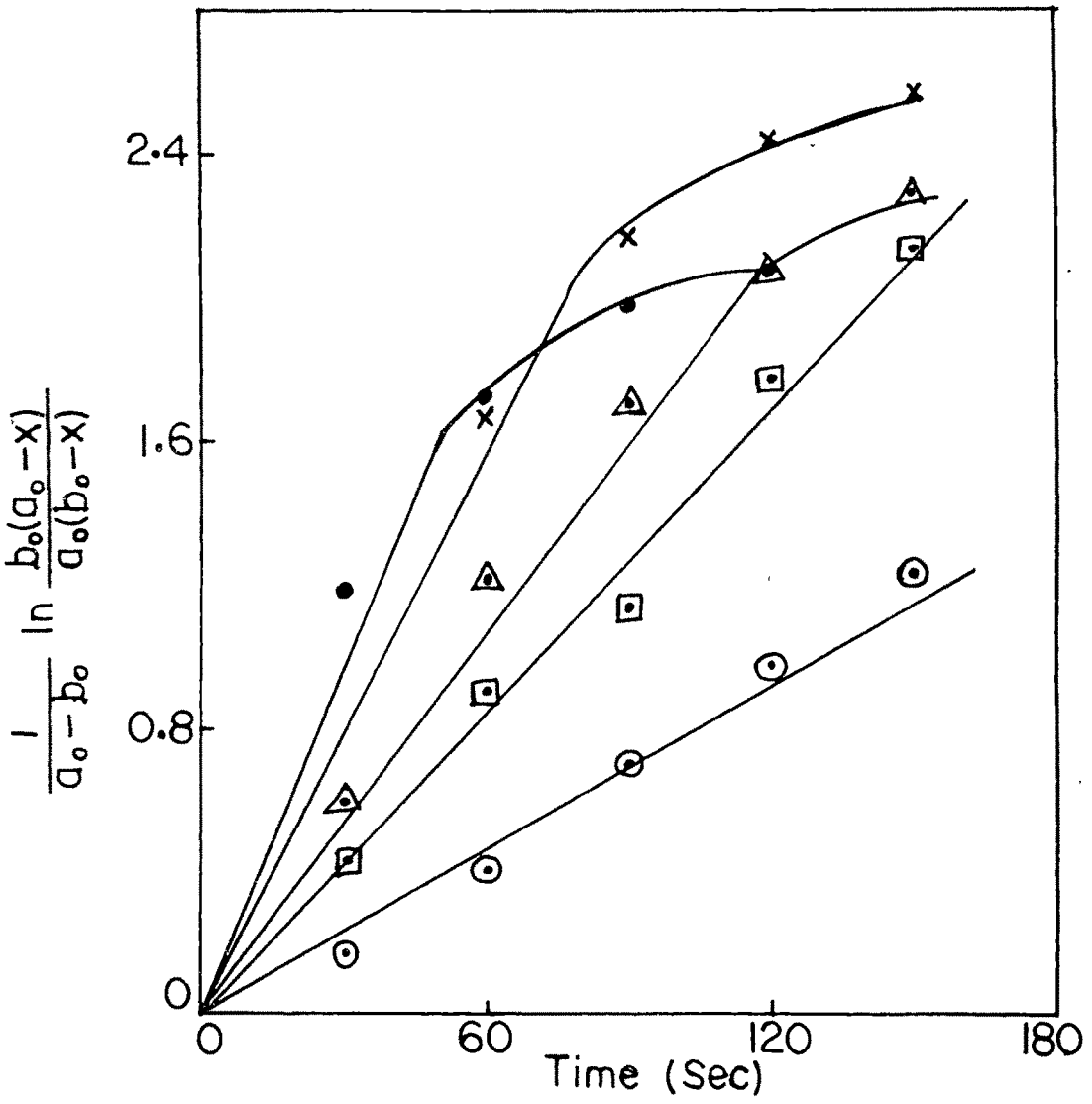

Fig.4.6i Plot of $\frac{1}{a_o - b_o} \ln \frac{b_o(a_o - x)}{a_o(b_o - x)}$ vs time for $KI+K_2S_2O_8$ reaction in SDS microemulsion system with o/w=45/57.5. Symbols are the same as in Fig.4.6a.

Table 4.4 **The second order rate constant k($lmol^{-1}$ sec^{-1}) of $KI+K_2S_2O_8$ in SDS microemulsion. SDS concentration = 42.5%**

O/W	Temperature (^0C)				
	25	30	35	40	45
5/52.5	7.90×10^{-3}	1.38×10^{-2}	1.52×10^{-2}	1.67×10^{-2}	3.33×10^{-2}
10/47.5	7.94×10^{-3}	1.39×10^{-2}	2.08×10^{-2}	2.38×10^{-2}	4.17×10^{-2}
15/42.5	9.80×10^{-3}	1.67×10^{-2}	2.08×10^{-2}	3.33×10^{-2}	4.17×10^{-2}
20/37.5	9.80×10^{-3}	1.67×10^{-2}	2.08×10^{-2}	3.33×10^{-2}	4.17×10^{-2}
25/32.5	1.12×10^{-2}	2.08×10^{-2}	2.38×10^{-2}	3.33×10^{-2}	5.56×10^{-2}
30/27.5	3.03×10^{-2}	4.44×10^{-2}	7.40×10^{-2}	9.52×10^{-2}	1.11×10^{-1}
35/22.5	5.26×10^{-2}	1.00×10^{-1}	1.11×10^{-1}	1.67×10^{-1}	2.00×10^{-1}
40/17.5	1.00×10^{-1}	1.00×10^{-1}	1.25×10^{-1}	1.67×10^{-1}	1.67×10^{-1}
S/W = 42.5/57.5	7.40×10^{-3}	1.33×10^{-2}	1.67×10^{-2}	2.2×10^{-2}	2.67×10^{-2}
W (100%)	4.80×10^{-3}	9.16×10^{-3}	1.41×10^{-2}	1.79×10^{-2}	2.24×10^{-2}

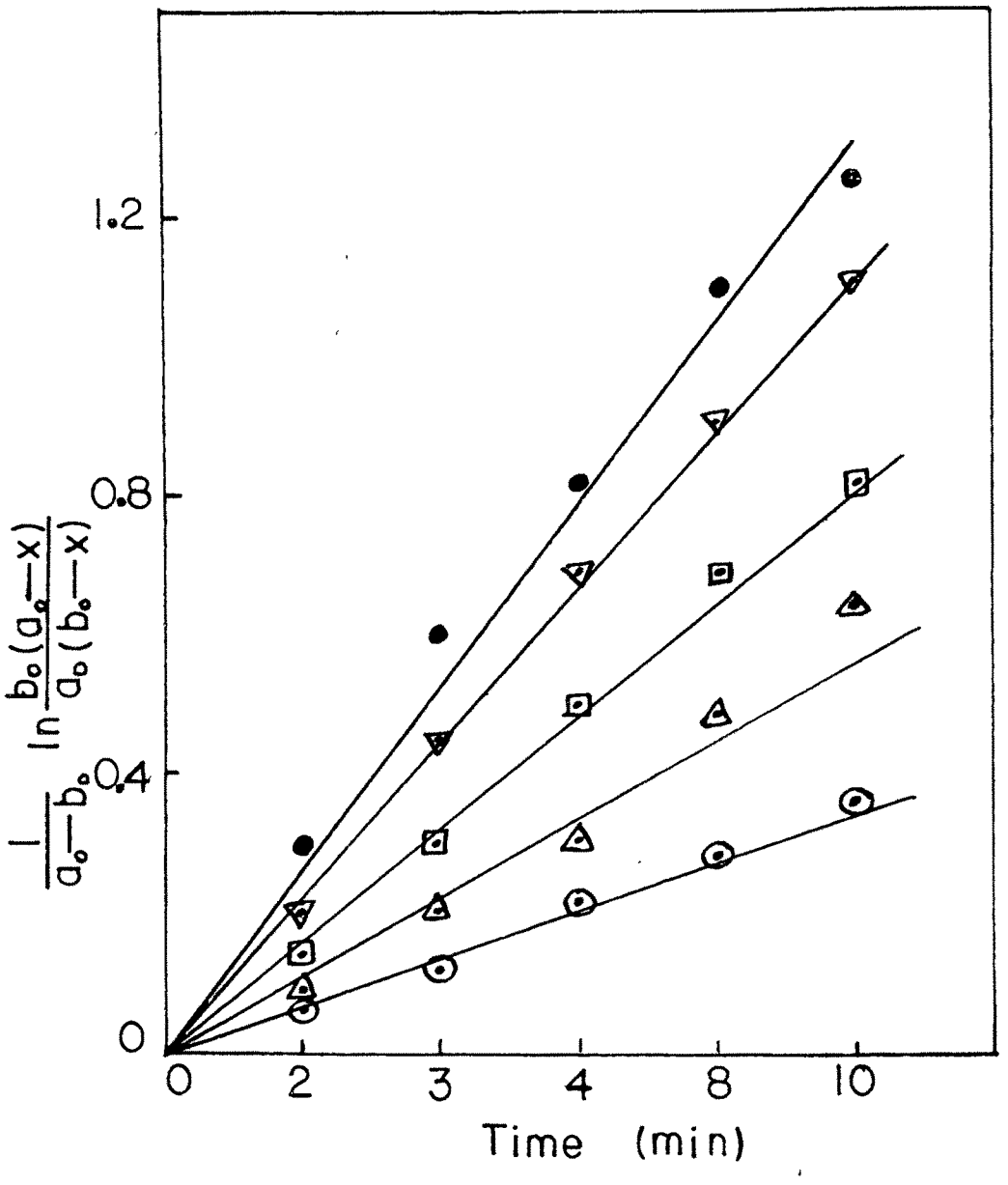

Fig.4.7a Plot of $\frac{1}{a_o-b_o} \ln \frac{b_o(a_o-x)}{a_o(b_o-x)}$ vs time for $KI+K_2S_2O_8$ reaction in CTAB microemulsion system o/w=5/52.5.

⊙ 25°C; △ 30°C; ⊡ 35°C; ▽ 40°C; ● 45°C

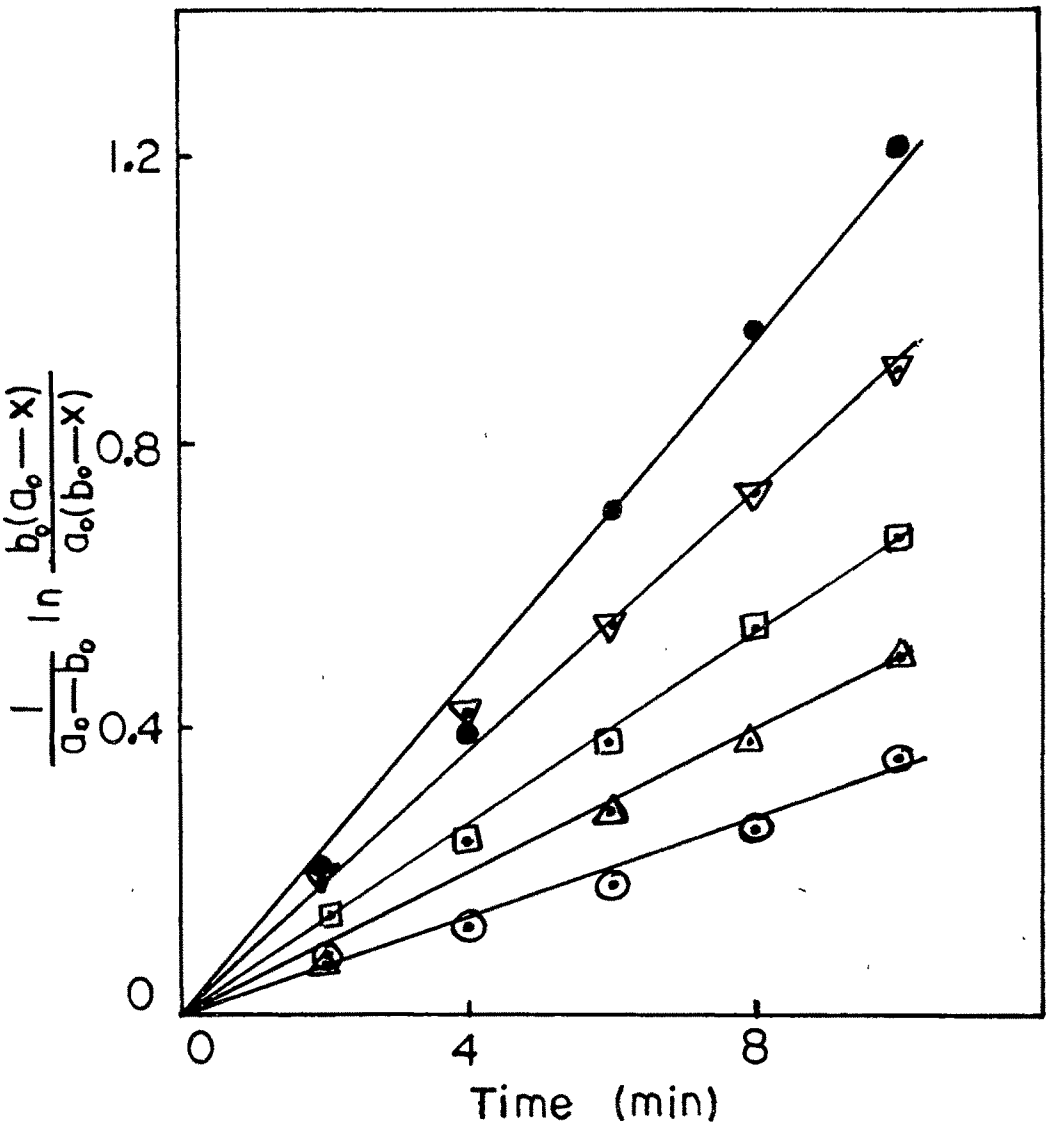

Fig.4.7b Plot of $\frac{1}{a_o-b_o} \ln \frac{b_o(a_o-x)}{a_o(b_o-x)}$ vs time for $KI+K_2S_2O_8$ reaction in CTAB microemulsion system with o/w=10/47.5. Symbols are the same as in Fig.4.7a.

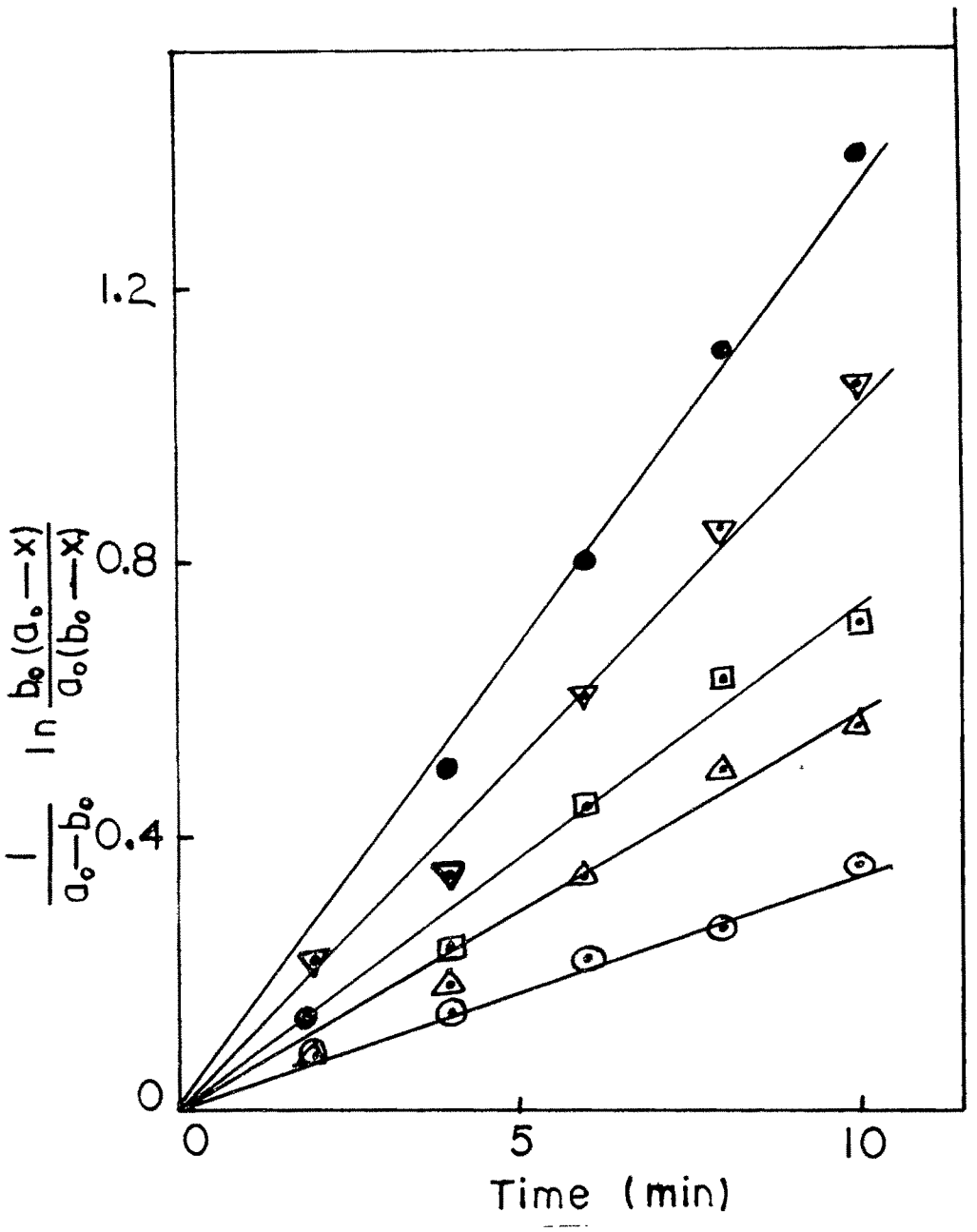

Fig.4.7c Plot of $\frac{1}{a_o-b_o} \ln \frac{b_o(a_o-x)}{a_o(b_o-x)}$ vs time for $KI+K_2S_2O_8$ reaction in CTAB microemulsion system with o/w=15/42.5. Symbols are the same as in Fig.4.7a.

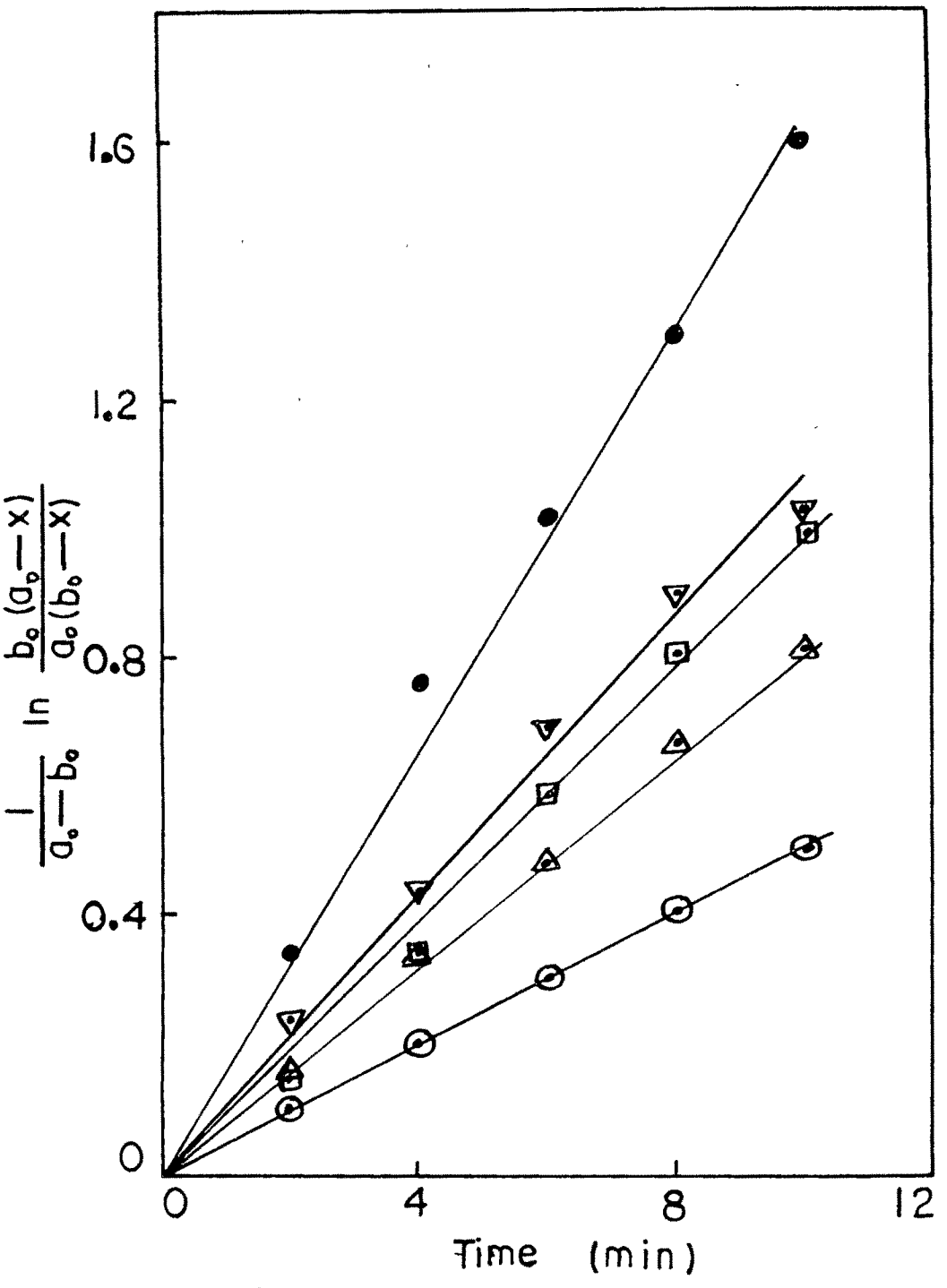

Fig.4.7d Plot of $\frac{1}{a_o-b_o} \ln \frac{b_o(a_o-x)}{a_o(b_o-x)}$ vs time for $KI+K_2S_2O_8$ reaction in CTAB microemulsion system with o/w=20/37.5. Symbols are the same as in Fig.4.7a.

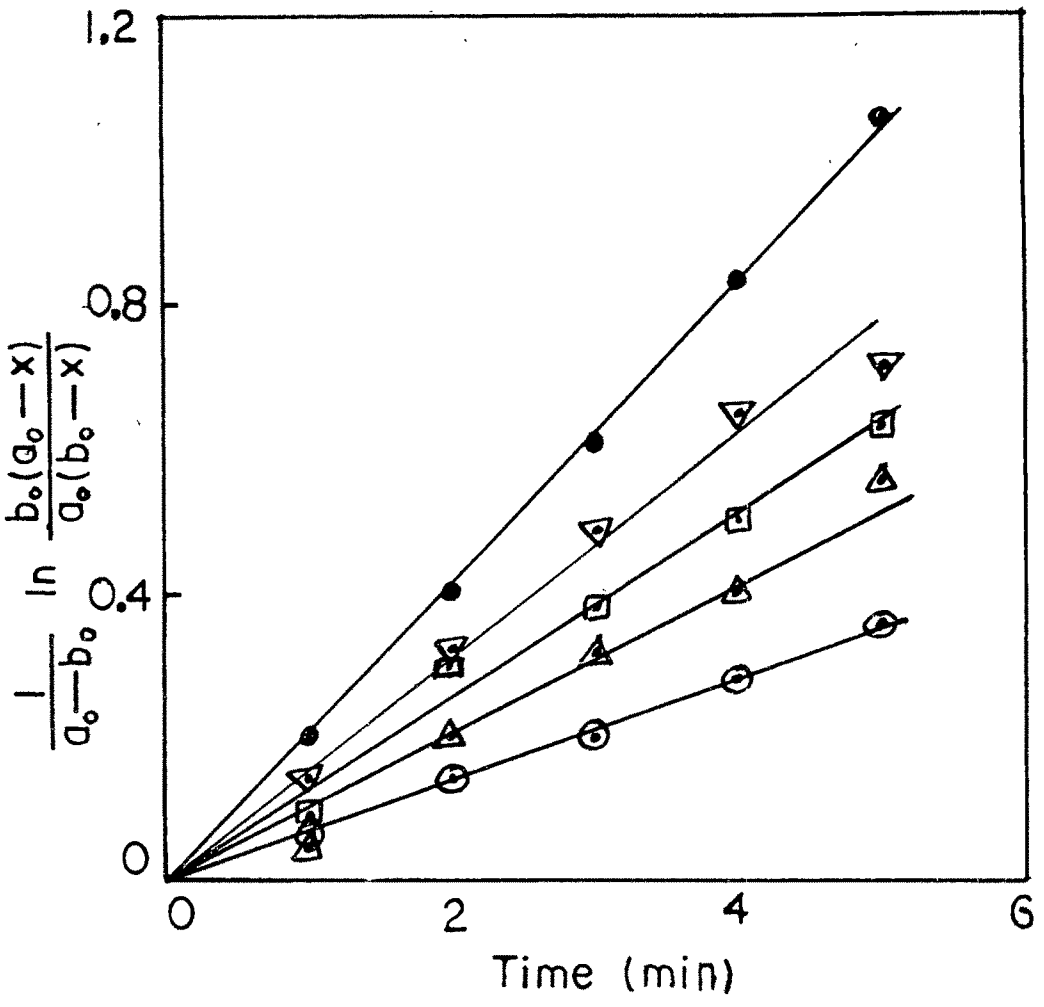

Fig.4.7e Plot of $\frac{1}{a_o-b_o} \ln \frac{b_o(a_o-x)}{a_o(b_o-x)}$ vs time for $KI+K_2S_2O_8$ reaction in CTAB microemulsion system with o/w=25/32.5. Symbols are the same as in Fig.4.7a.

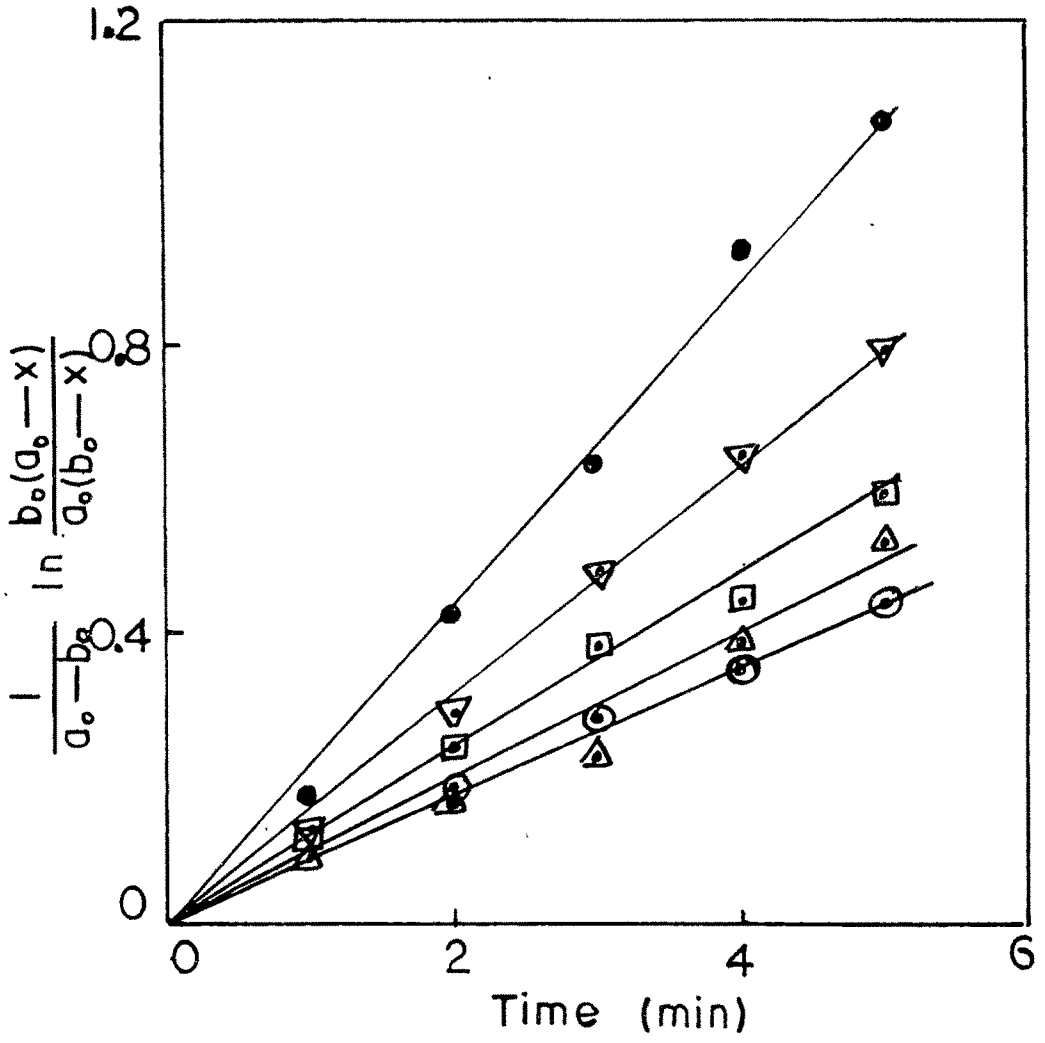

Fig.4.7f Plot of $\frac{1}{a_o-b_o} \ln \frac{b_o(a_o-x)}{a_o(b_o-x)}$ vs time for $KI+K_2S_2O_8$ reaction in CTAB microemulsion system with o/w=30/27.5. Symbols are the same as in Fig.4.7a.

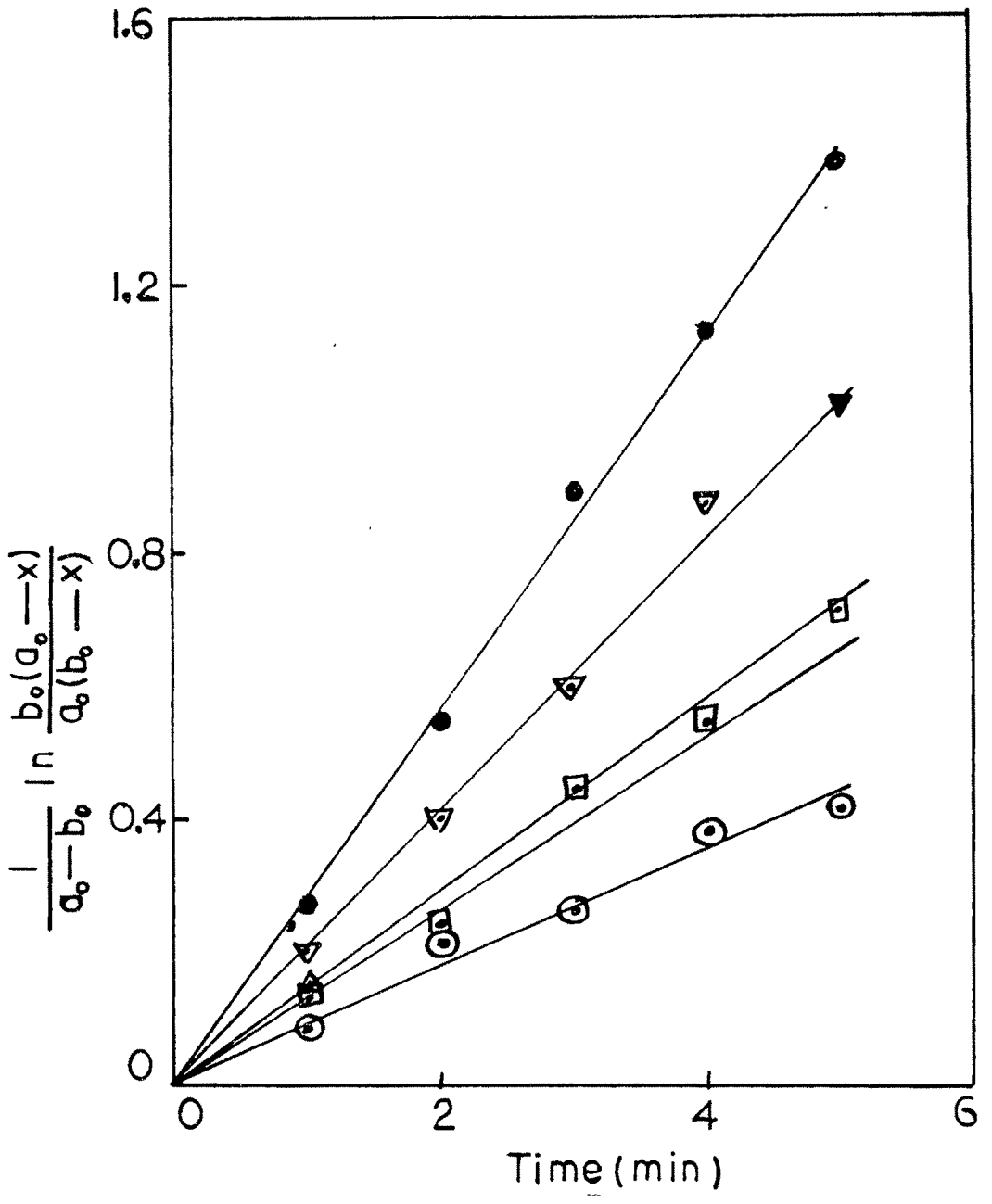

Fig.4.7g Plot of $\frac{1}{a_0-b_0} \ln \frac{b_0(a_0-x)}{a_0(b_0-x)}$ vs time for $KI+K_2S_2O_8$ reaction in CTAB microemulsion system with o/w=35/22.5. Symbols are the same as in Fig.4.7a.

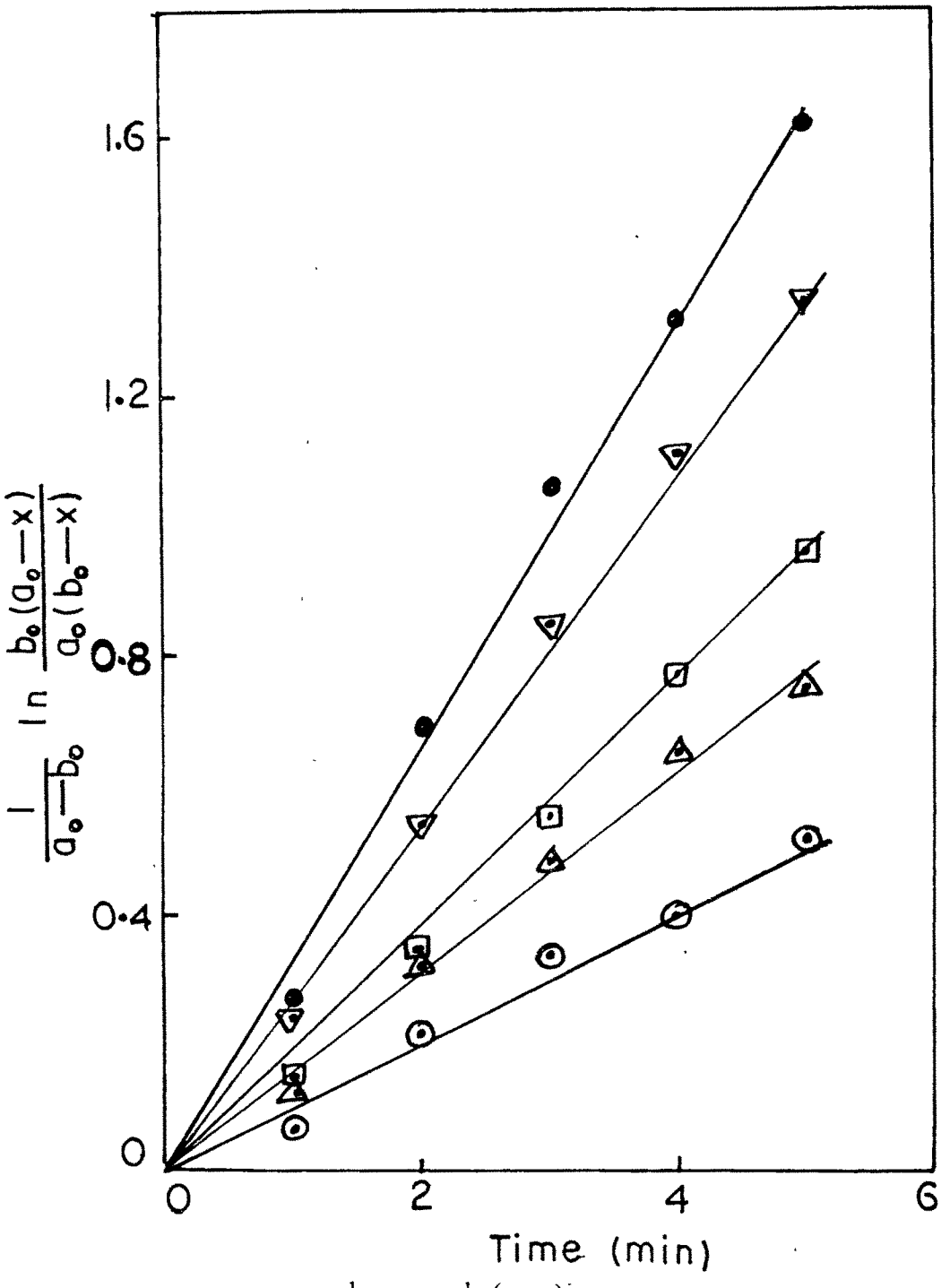

Fig.4.7h Plot of $\frac{1}{a_o - b_o} \ln \frac{b_o(a_o - x)}{a_o(b_o - x)}$ vs time for $KI+K_2S_2O_8$ reaction in CTAB microemulsion system with o/w=40/17.5. Symbols are the same as in Fig.4.7a.

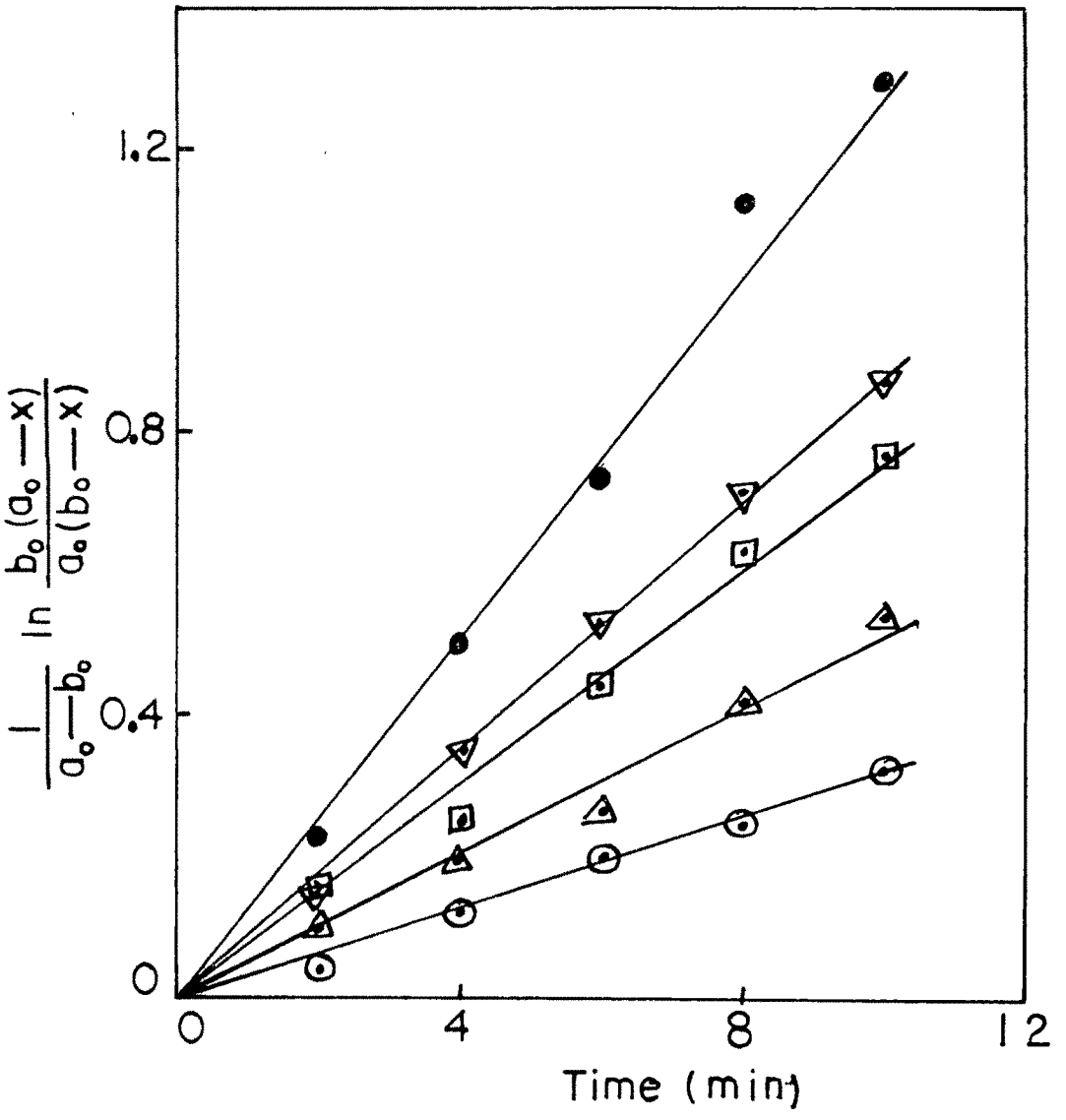

Fig.4.7i Plot of $\frac{1}{a_o-b_o} \ln \frac{b_o(a_o-x)}{a_o(b_o-x)}$ vs time for $KI+K_2S_2O_8$ reaction in CTAB microemulsion system with o/w=42.5/57.5. Symbols are the same as in Fig.4.7a.

Table 4.5 **The second order rate constant k($lmol^{-1}$ sec^{-1}) of $KI+K_2S_2O_8$ in CTAB microemulsion CTAB concentration = 42.5%**

O/W	Temperature (^0C)				
	25	30	35	40	45
5/52.5	5.75×10^{-4}	8.77×10^{-4}	1.19×10^{-3}	1.67×10^{-3}	1.85×10^{-3}
10/47.5	5.75×10^{-4}	8.33×10^{-4}	1.11×10^{-3}	1.52×10^{-3}	1.85×10^{-3}
15/42.5	5.95×10^{-4}	9.80×10^{-4}	1.19×10^{-3}	1.67×10^{-3}	2.08×10^{-3}
20/37.5	8.33×10^{-4}	1.28×10^{-3}	1.67×10^{-3}	1.85×10^{-3}	2.47×10^{-3}
25/32.5	1.19×10^{-3}	1.75×10^{-3}	1.96×10^{-3}	2.38×10^{-3}	3.33×10^{-3}
30/27.5	1.52×10^{-3}	1.67×10^{-3}	1.96×10^{-3}	2.56×10^{-3}	3.70×10^{-3}
35/22.5	1.45×10^{-3}	2.08×10^{-3}	2.56×10^{-3}	3.70×10^{-3}	4.17×10^{-3}
40/17.5	1.59×10^{-3}	2.56×10^{-3}	3.03×10^{-3}	3.33×10^{-3}	5.56×10^{-3}
S/W = 42.5/57.5	5.38×10^{-4}	8.33×10^{-4}	1.28×10^{-3}	1.38×10^{-3}	2.08×10^{-3}

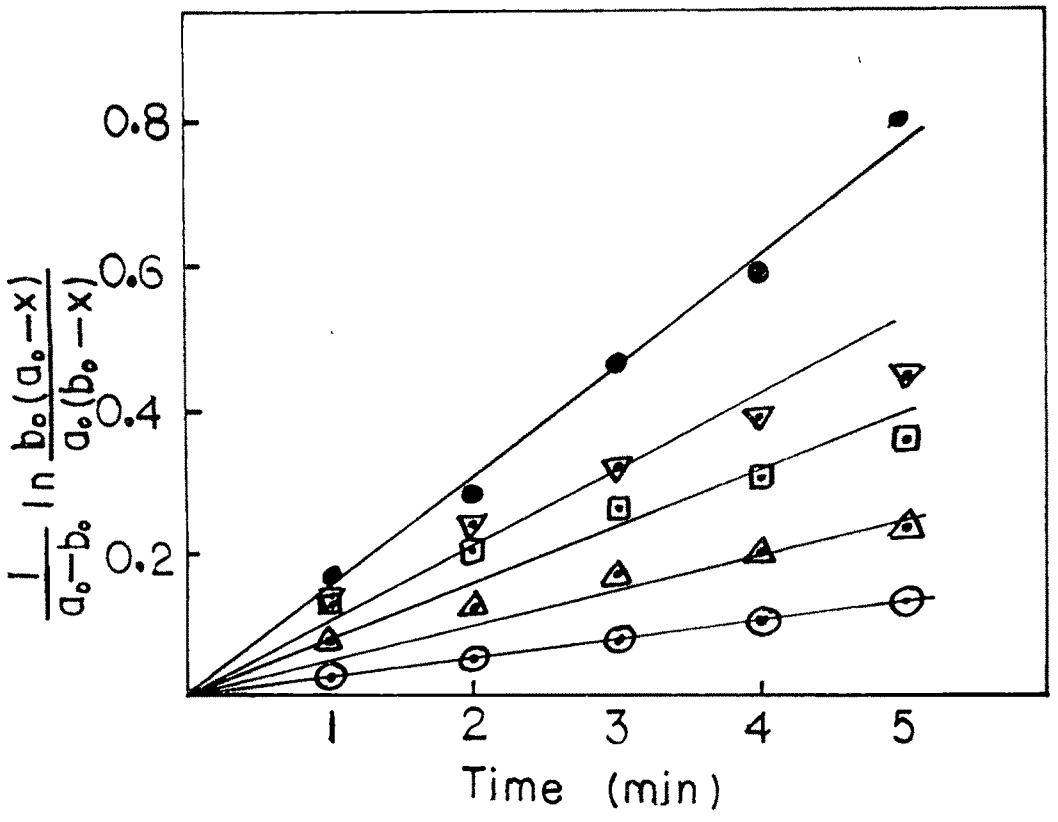

Fig.4.8a Plot of $\frac{1}{a_o-b_o} \ln \frac{b_o(a_o-x)}{a_o(b_o-x)}$ vs time for $KI+K_2S_2O_8$ reaction in TX100 microemulsion system with o/w=1/44.

⊙ 25°C; △ 30°C; ⊡ 35°C; ▽ 40°C; ● 45°C

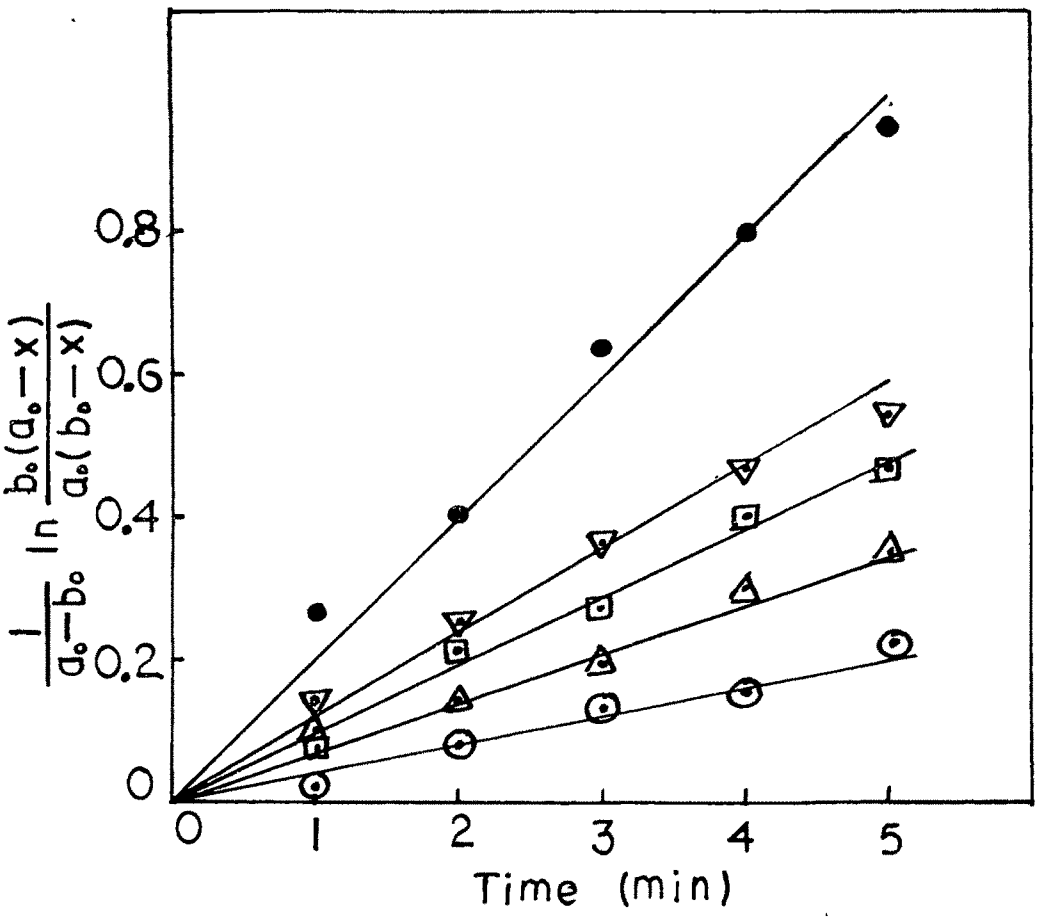

Fig.4.8b Plot of $\frac{1}{a_o-b_o} \ln \frac{b_o(a_o-x)}{a_o(b_o-x)}$ vs time for $KI+K_2S_2O_8$ reaction in TX100 microemulsion system with o/w=5/40. Symbols are the same as in Fig.4.8a.

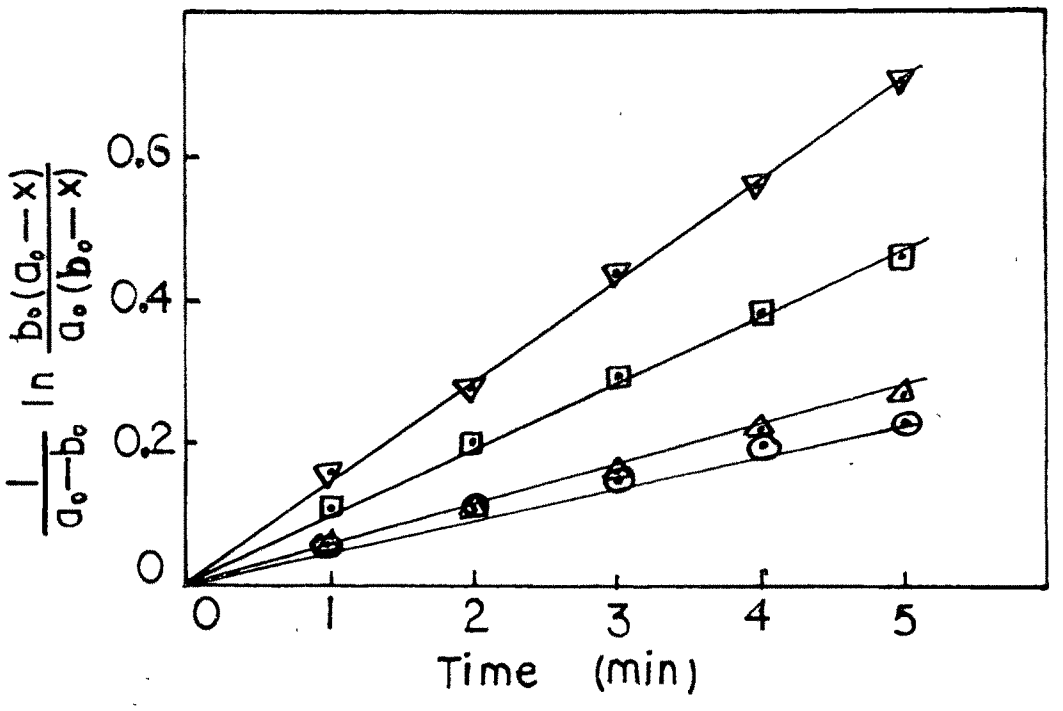

Fig.4.8c Plot of $\frac{1}{a_o-b_o} \ln \frac{b_o(a_o-x)}{a_o(b_o-x)}$ vs time for $KI+K_2S_2O_8$ reaction in TX100 microemulsion system with o/w=10/35. Symbols are the same as in Fig.4.8a.

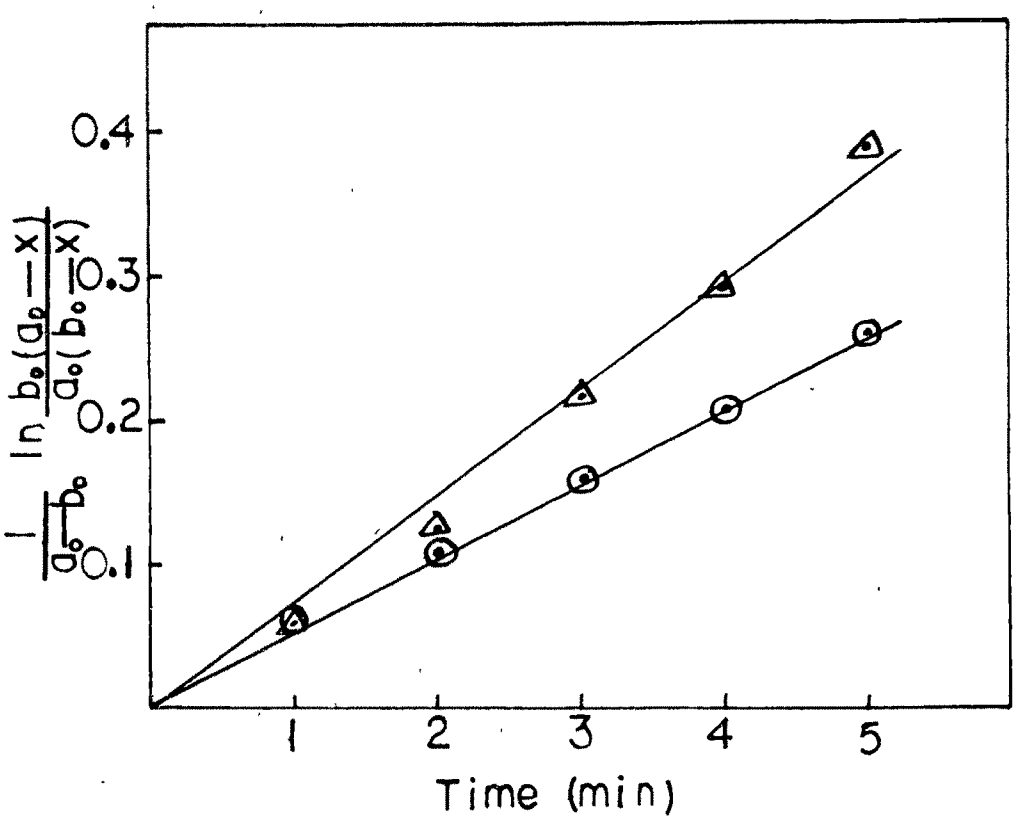

Fig.4.8d Plot of $\frac{1}{a_o-b_o} \ln \frac{b_o(a_o-x)}{a_o(b_o-x)}$ vs time for $KI+K_2S_2O_8$ reaction in TX100 microemulsion system with o/w=15/30. Symbols are the same as in Fig.4.8a.

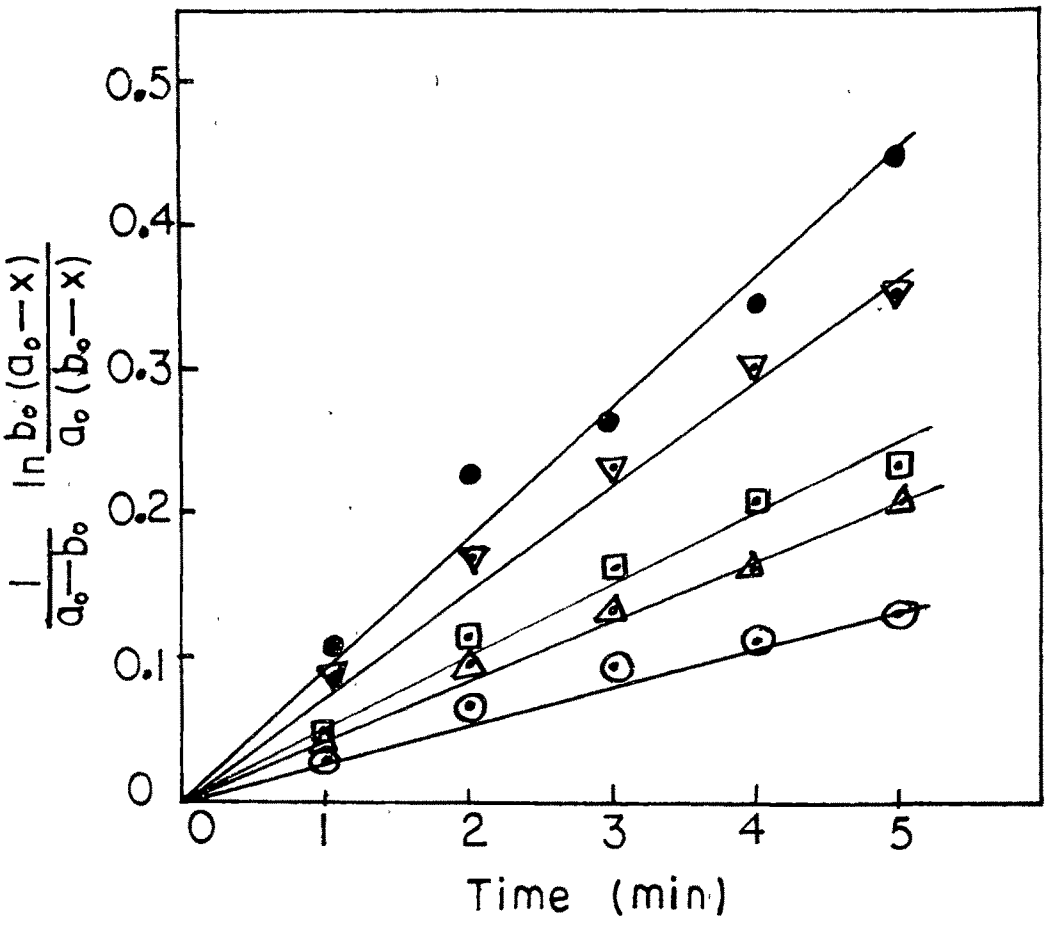

Fig.4.8e Plot of $\frac{1}{a_o-b_o} \ln \frac{b_o(a_o-x)}{a_o(b_o-x)}$ vs time for $KI+K_2S_2O_8$ reaction in TX100 microemulsion system with no oil s/w=55/45. Symbols are the same as in Fig.4.8a.

see p 174

Table 4.6a **The second order rate constant k($lmol^{-1}$ sec^{-1})] of $KI+K_2S_2O_8$ in TX100 microemulsion. TX100 concentration=55%**

O/W	Temperature (^0C)				
	25	30	35	40	45
1/44	4.27×10^{-4}	7.93×10^{-4}	1.28×10^{-3}	1.85×10^{-3}	2.38×10^{-3}
5/40	6.67×10^{-4}	8.77×10^{-4}	1.52×10^{-3}	1.85×10^{-3}	2.78×10^{-3}
10/35	7.93×10^{-4}	1.04×10^{-3}	1.67×10^{-3}	2.38×10^{-3}	-
15/30	8.33×10^{-4}	1.28×10^{-3}	- -	-	-
S/W = 55/45	4.5×10^{-4}	6.95×10^{-4}	8.33×10^{-4}	1.19×10^{-3}	1.52×10^{-3}

With increase of temperature, the rate of reaction between potassium iodide and potassium persulphate increases in nonionic microemulsion which was observed in systems with ionic surfactant stabilized microemulsions. This happens because of the increase in the number of microdroplets[288] and hence the interfacial area and also due to the higher thermal instability of the associated complex.[146]

Fig. 4.6 (a-i) shows the plots for the second order rate constant for the oxidation of iodide by persulphate in SDS microemulsion.

$$\frac{1}{a_o - b_o} \ln \frac{b_o (a_o - x)}{a_o (b_o - x)}$$ is plotted against time.

A straight line graph passing through the origin is obtained. The slope of the line gives the rate constant 'k' & it has been computed at various temperatures & changing oil-water ratios. The result is sumarized in Table 4.4. The rate of reaction is much higher than that in pure aqueous system. The k value for this reaction in water is 4.8×10^{-3} $lmol^{-1}$ sec^{-1} at 25°C. The reaction is found to be faster than the system which does not contain any oil. It is clear from the table that the rate of reaction increases with increasing temperature & it also increases with decreasing water content like the first order reaction rate constant in this system. The second order rate constant for the oxidation of potassium iodide by persulphate in cyclohexane/SDS + n-propanol (1:2) / water at lower water composition fall in the range of the values that had been reported in n-hexanol/SDS/water at lower water composition by Valaulikar[145]. However Gomez-Herrera et al[143] studied the same reaction in n-heptane/AOT/Water system at much lower concentration of AOT (0.16 mol Kg^{-1}) & found the reaction rate almost 30 times faster.

The second order rate constants for the oxidation of iodide by persulphate in CTAB & TX100 microemulsion were also computed. Fig.4.7(a-i) & Fig.4.8(a-e) show the plots in CTAB & TX100 microemulsions respectively. Table-4.5 & 4.6a sumarize the result in CTAB & TX100 systems. It is clear from the above table that the second order reaction is enhanced in SDS, retarded in CTAB and TX100

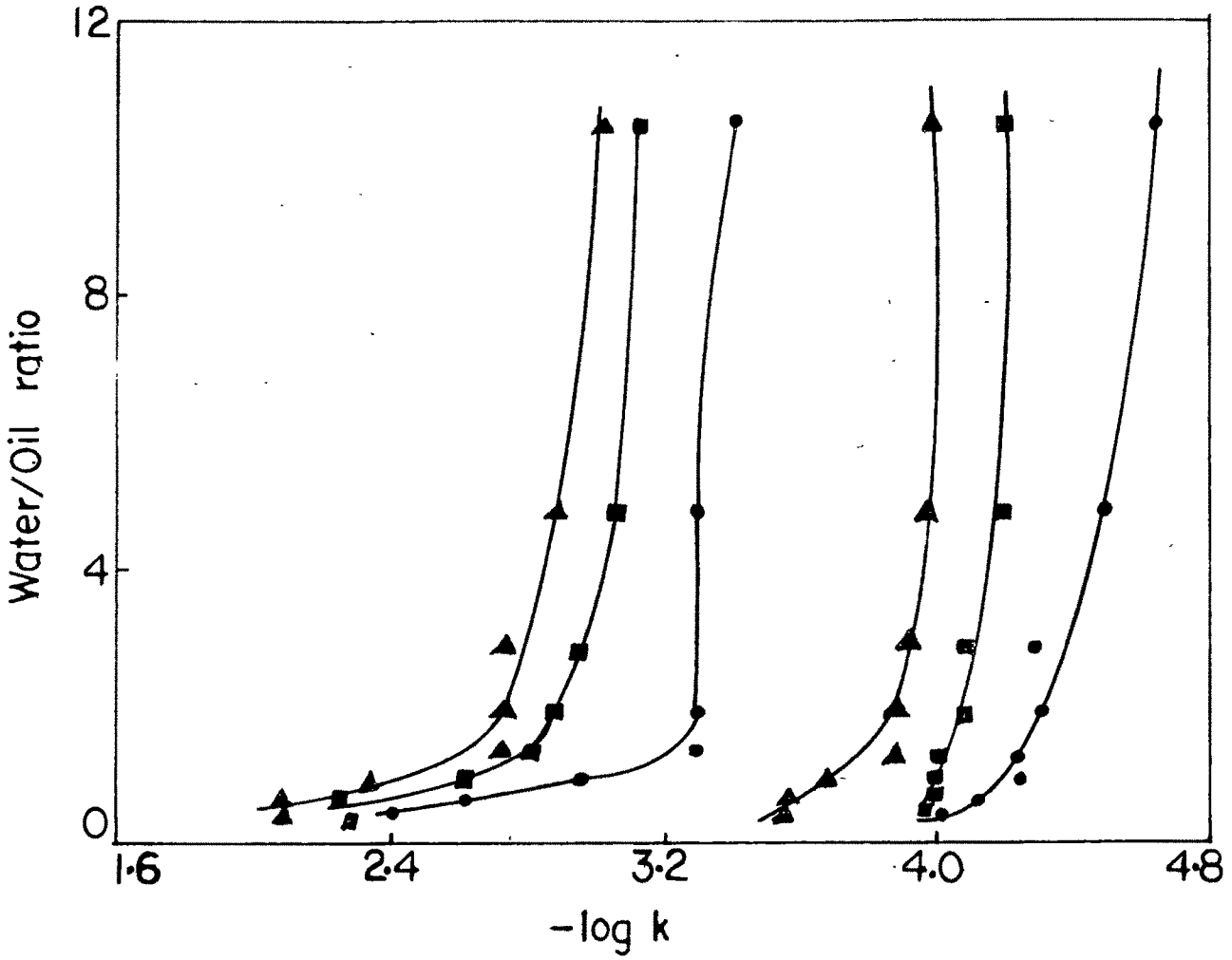

Fig.4.9a Plot of log k (I order) vs w/o ratio for KI+$K_2S_2O_8$ in SDS (left) & CTAB (right) microemulsion system.●25°C; ■ 35°C; ▲ 45°C;

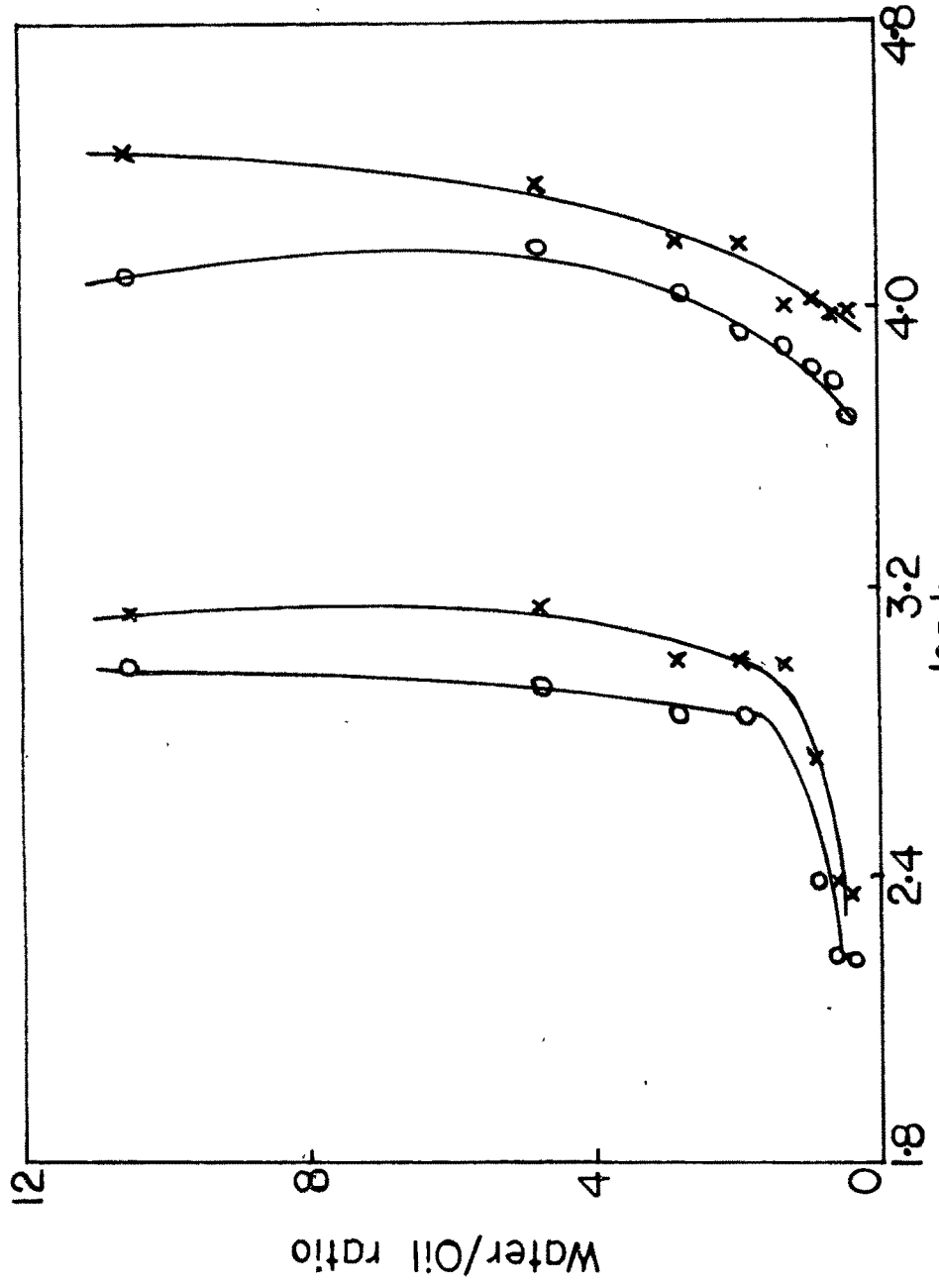

Fig.4.9a Plot of log k (I order) vs w/o ratio for $KI+K_2S_2O_8$ in SDS (left) & CTAB (right) microemulsion system. × 30°C; ○ 40°C

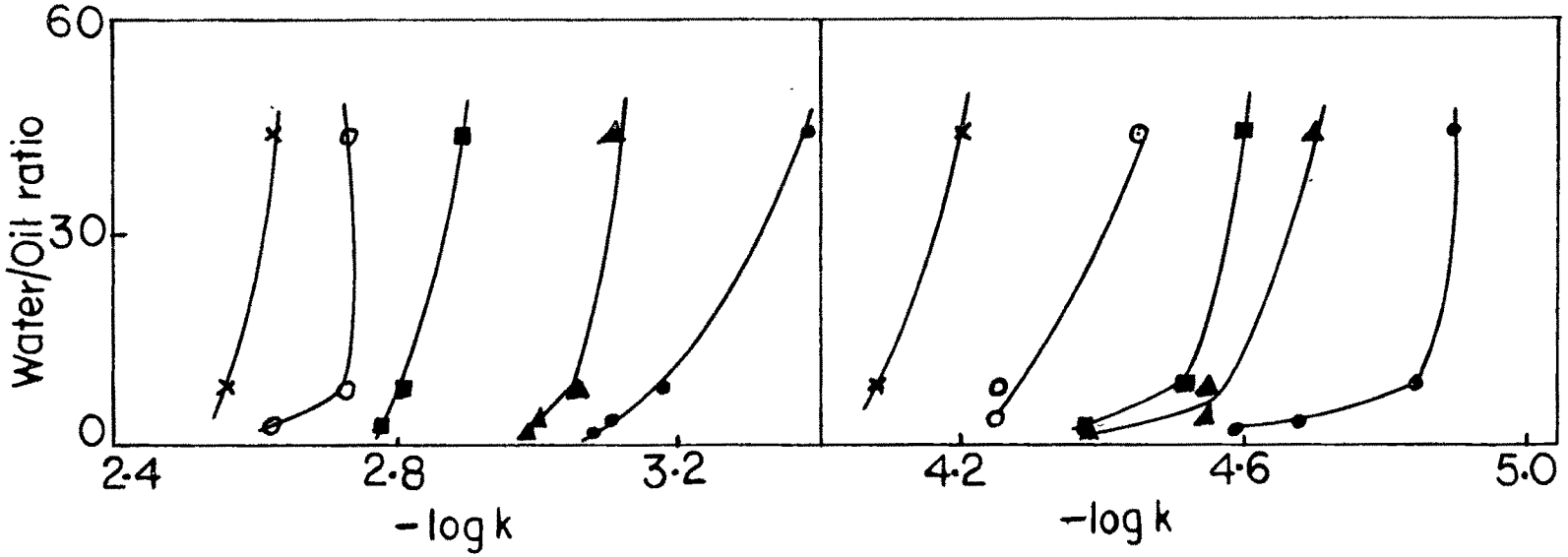

Fig.4.9b Plot of log k vs w/o ratio for KI+$K_2S_2O_8$ in TX100 for I order (right) II order (left).● 25°C; ▲ 30°C; ■ 35°C; O 40°C; × 45°C

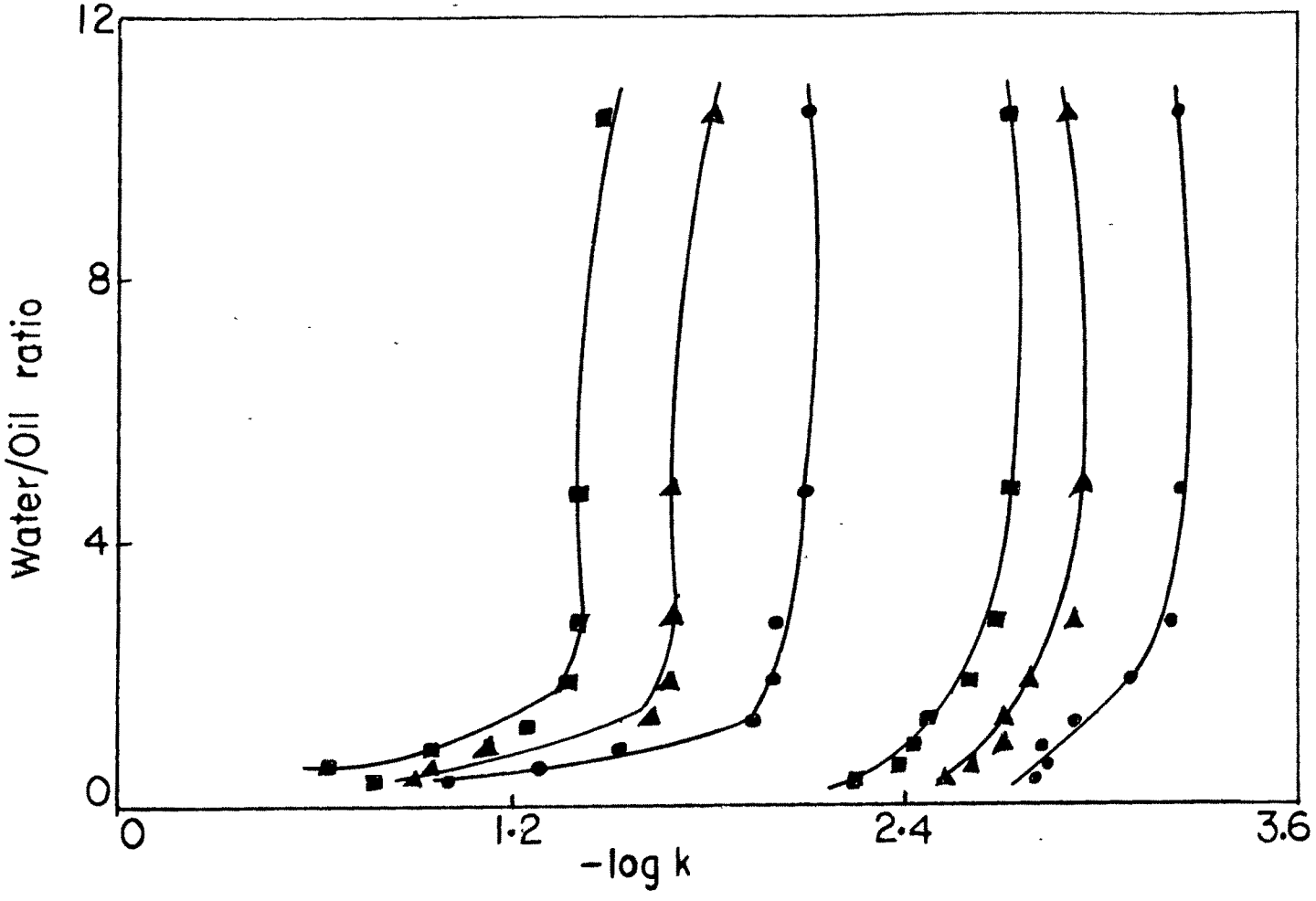

Fig.4.9c Plot of log k (II order) vs w/o ratio for KI+$K_2S_2O_8$ in SDS (left) & CTAB (right) microemulsion systems. ● 25°C; ▲ 35°C; ■ 45°C;

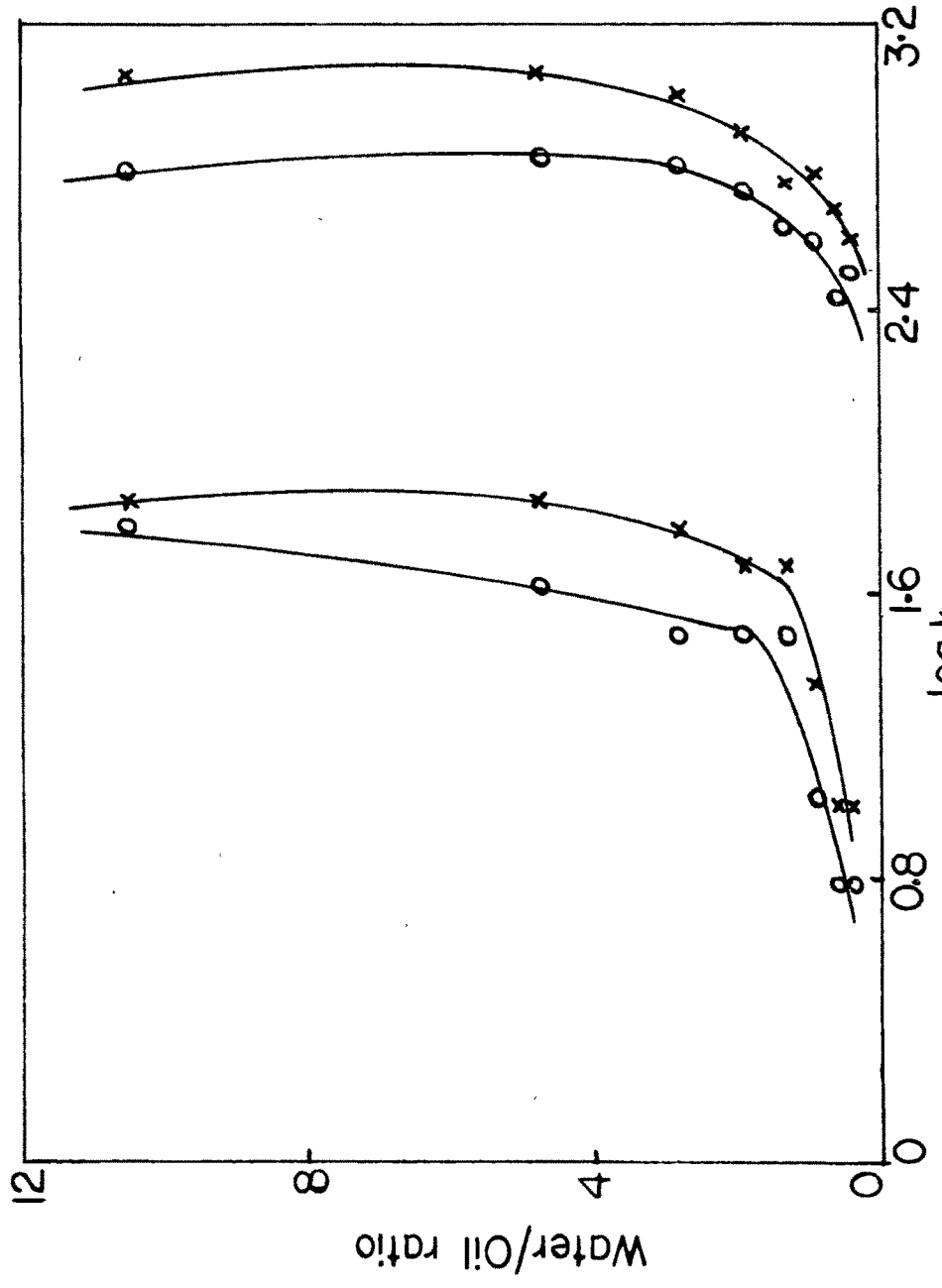

Fig.4.9c Plot of log k (II order) vs w/o ratio for KI+$K_2S_2O_8$ in SDS (left) & CTAB (right) microemulsion systems. × 30°C; ○ 40°C;

microemulsion systems. The second order rate of reaction increases with decreasing water content and increasing temperature. The reason is well understood from the earlier discussion as explained by the electrostatic interaction of hydrophilic heads of surfactant molecules and the hydrophilic anionic reactants. The magnitude of second order rate constant is much higher than the pseudo first order rate constant. With decreasing amount of water, the rate increases due to the increase in local concentration of the reactants. With increase of temperature, the rate of reaction between potassium iodide and potassium persulphate increases due to increase in the number of microdroplets and the interfacial area and also due to the higher thermal instability of the associated complex.

Figs 4.9 (a-c) show the effect of W/O ratio on the rate constant. W/O ratio is plotted against log k values. Log k values increase with decreasing W/O ratio. At lower W/O ratio, the reaction rate is high and we can assume a very high reaction rate when no water is present; but theoretically, this is impossible because no reaction takes place as the reactants are hydrophilic in nature and does not dissolve in the organic medium.

The kinetic activation energy (Ea) is determined from the rate constant (k) at different temperatures using the Arrhenius equation.[289]

$$k = A.e^{-Ea/RT} \qquad \text{.....(3)}$$

where 'R is gas constant, A-Arrhenius factor, T-Kelvin temperature. By plotting log k versus T^{-1} a straight line was obtained from the slope of which the activation energy Ea was computed. The activation energy was determined by miltiplying slope with -2.303R.

Table 4.6(b-d) summarizes the kinetic activation energy obtained from the temperature dependence of the rate constant. All the Ea values are positive. The positive activation energy values indicate that an energy barrier of this magnitude must be crossed during the passage of the reactants to the products. This indicates that the surfactant interface is reasonably rigid and offers a high potential

Table 4.6b **Activation energy ($kJmol^{-1}$) for the second order reaction of $KI+K_2S_2O_8(Ea_1)$ and the pseudofirst order decomposition of $S_2O_8^{2-}(Ea_2)$ in SDS microemulsion.**

O/W	Ea_1	Ea_2
5/52.5	54.7	36.5
10/47.5	54.7	36.5
15/42.5	54.7	34.8
20/37.5	54.7	31.9
25/32.5	54.7	31.9
30/27.5	47.9	30.6
35/22.5	47.9	30.6
40/17.5	38.3	30.6
S/W = 42.5/57.5	54.7	38.3
W (100%)	58.5	51.8

Table 4.6c **Activation energy ($kJmol^{-1}$) for the second order reaction of $KI+K_2S_2O_8(Ea_3)$ and the pseudofirst order decomposition of $S_2O_8^{2-}(Ea_4)$ in CTAB microemulsion.**

O/W	Ea_3	Ea_4
5/52.5	47.9	66.6
10/47.5	47.9	52.8
15/42.5	45.1	52.8
20/37.5	45.1	51.1
25/32.5	45.1	45.1
30/27.5	45.6	45.1
35/22.5	42.6	45.1
40/17.5	42.6	42.6
S/W = 42.5/52.5	42.55	38.3

Table 4.6d **Activation energy (Ea) in kJmol^{-1} for the second order reaction of KI+$K_2S_2O_8$ (Ea_5) and the pseudofirst order decomposition of $S_2O_8^{2-}$ (Ea_6) in TX100 microemulsion.**

O/W	Ea_5	Ea_6
1/44	58.91	58.91
5/40	54.71	58.91
10/35	51.06	54.71
S/W = 55/45	58.91	63.82

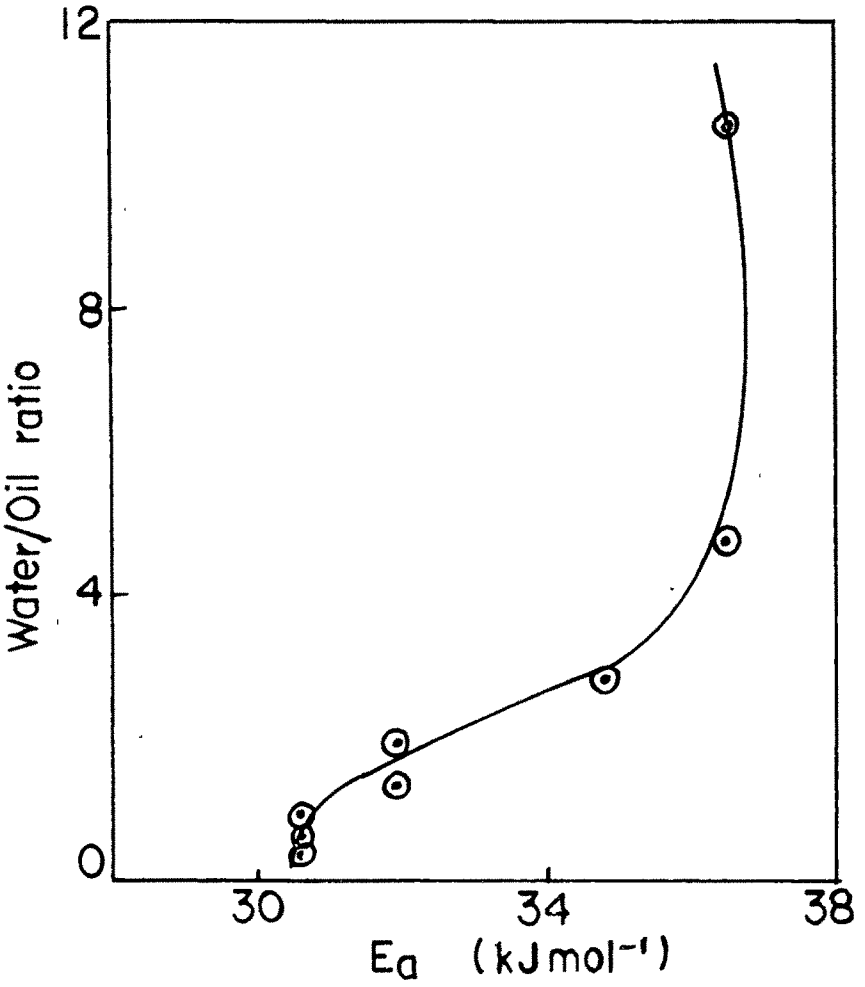

Fig.4.10a Plot of w/o ratio vs Ea(I order) for KI+$K_2S_2O_8$ in SDS microemulsion system.

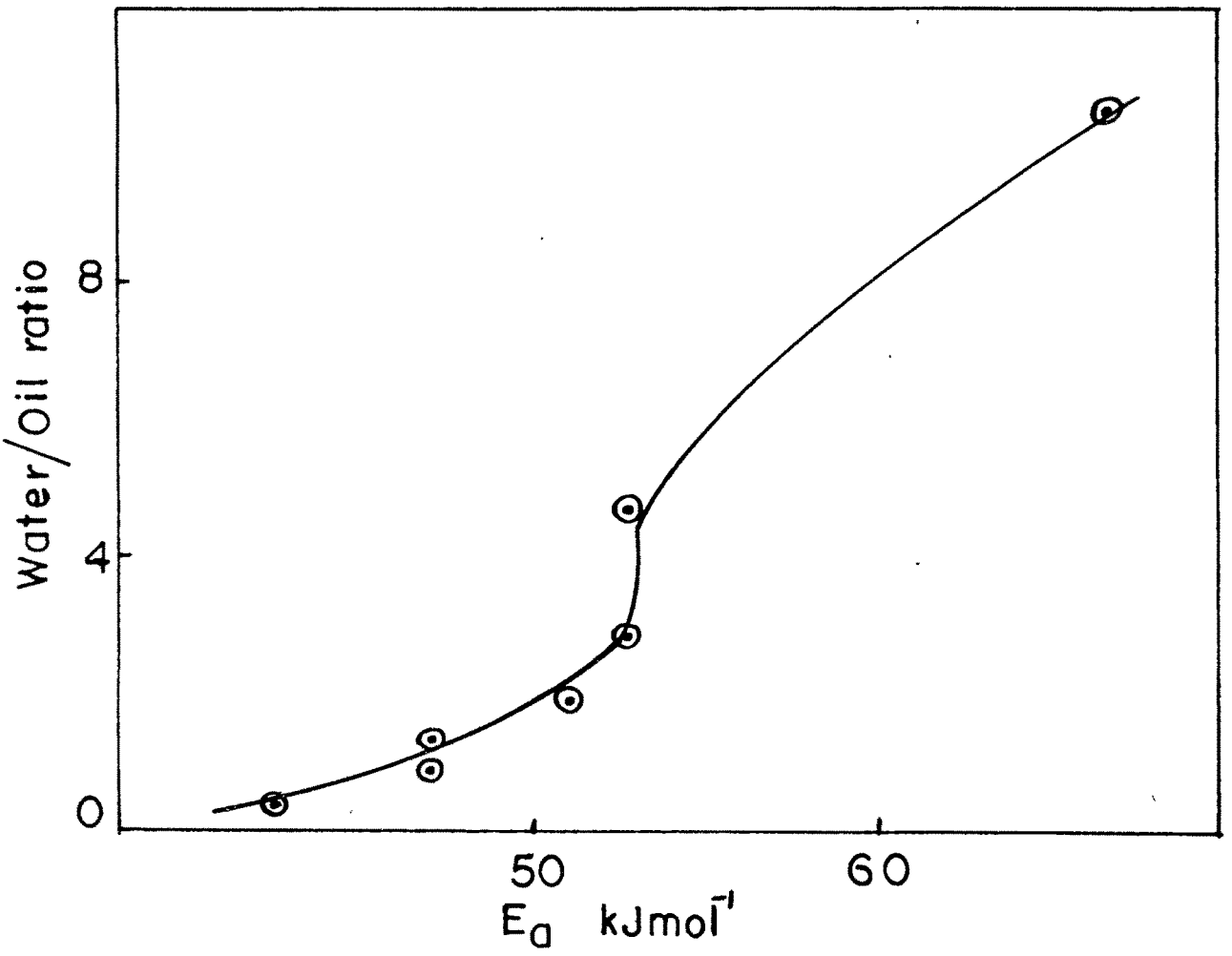

Fig.4.10b Plot of w/o ratio vs Ea (I order) for $KI+K_2S_2O_8$ in CTAB microemulsion system.

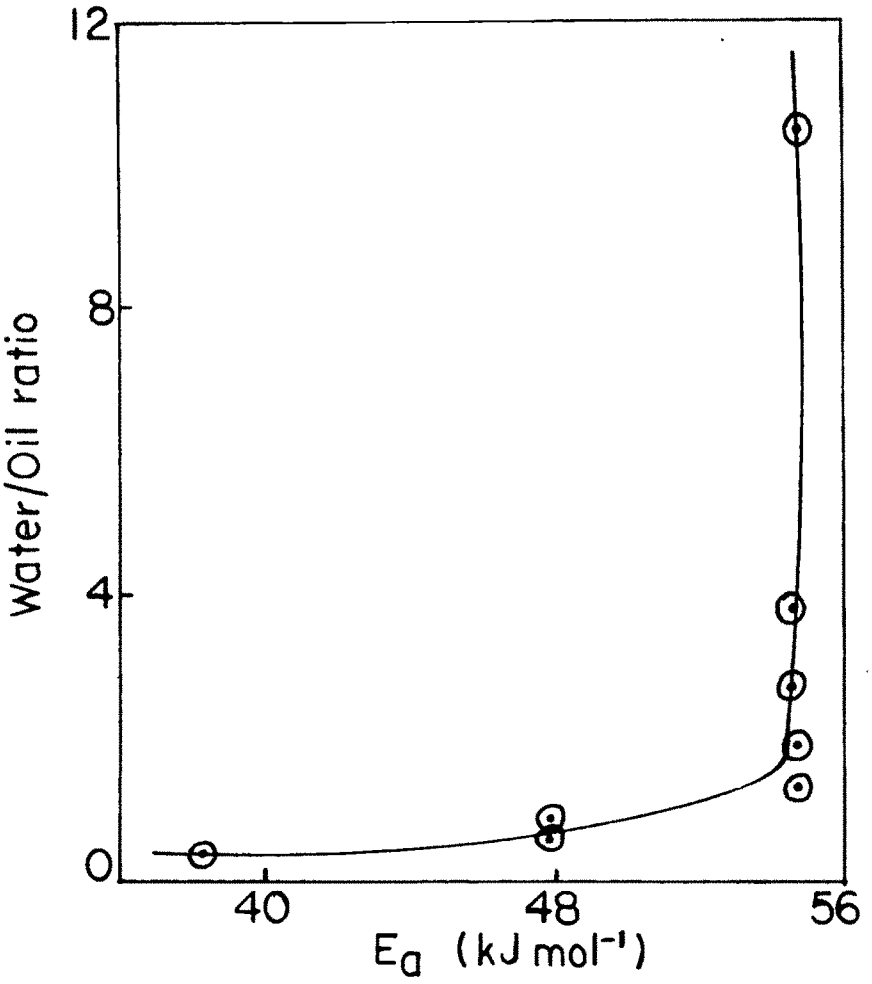

Fig.4.10c Plot of w/o ratio vs Ea(II order) for KI+$K_2S_2O_8$ in SDS microemulsion system.

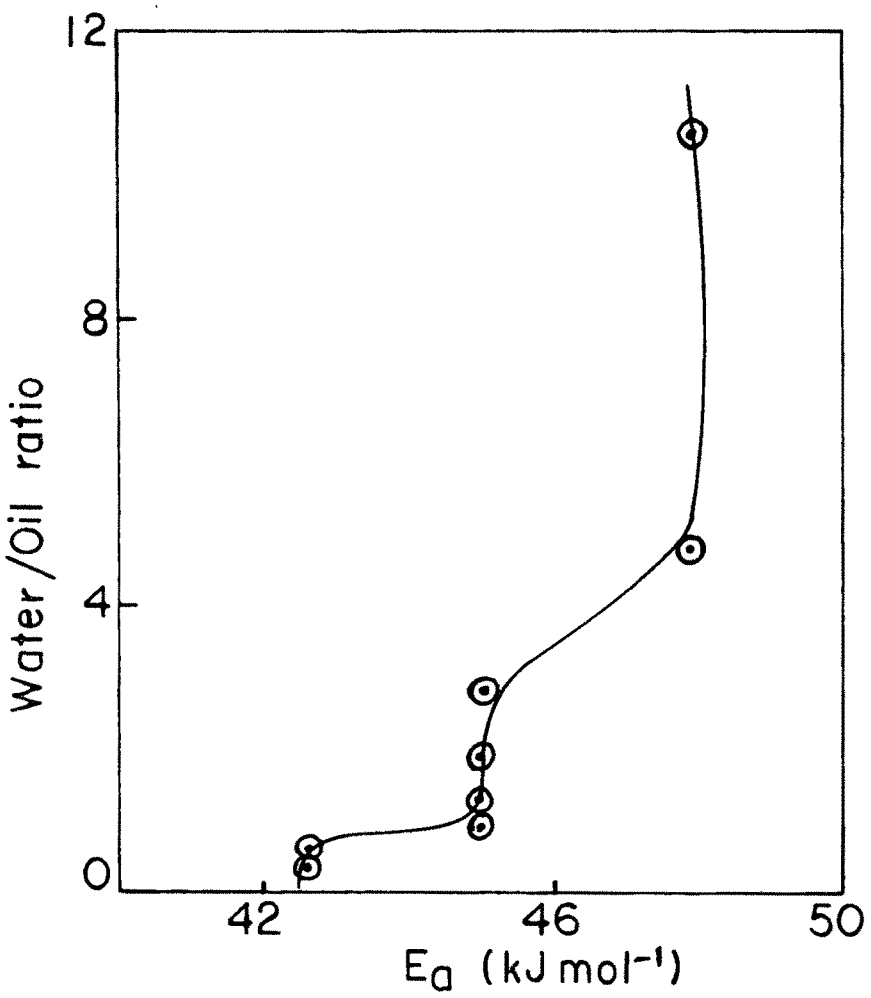

Fig.4.10d Plot of w/o ratio vs Ea(II order) for KI+$K_2S_2O_8$ in CTAB microemulsion system.

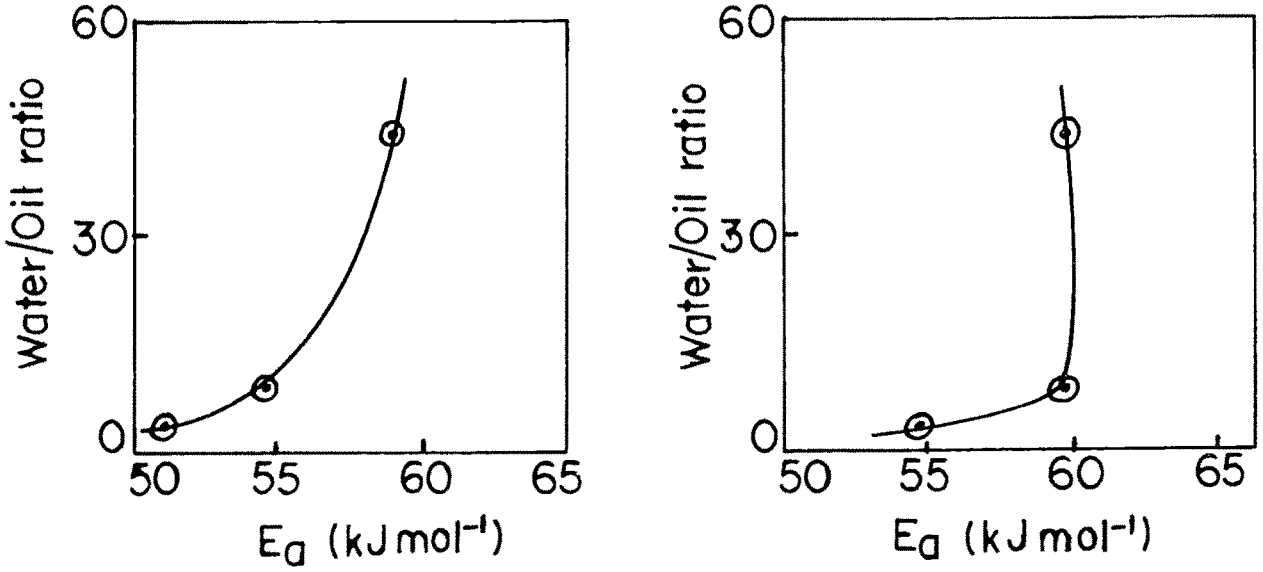

Fig.4.10e Plot of w/o ratio vs Ea I order (right) & II order (left) for $KI+K_2S_2O_8$ in TX100 microemulsion system.

energy though it is less than that of pure aqueous system to form the products. The activation energy shows a decreasing trend with decreasing water content as expected from the 'k' values. The effect of W/O ratio on Ea values are plotted in graph Fig. 4.10 (a-e). It shows that Ea values decrease with decreasing W/O ratio i.e. the Ea value is directly proportional to the water content as the rate constant increases with decreasing water content due to the increase in the local concentration of the reactants. We assume that the reaction follows a first order kinetics as the Ea Due values show the proper dependency on the rate constant.

b. Hydrolysis of Methyl acetate

Kinetically, we have studied the acid catalyzed methyl acetate hydrolysis , ie. CH_3 COOCH3+H_2O --> $CH_3COOH+CH_3OH$ in all the three microemulsion systems formed from SDS, CTAB and TX100. The reaction follows the following mechanism.[290]

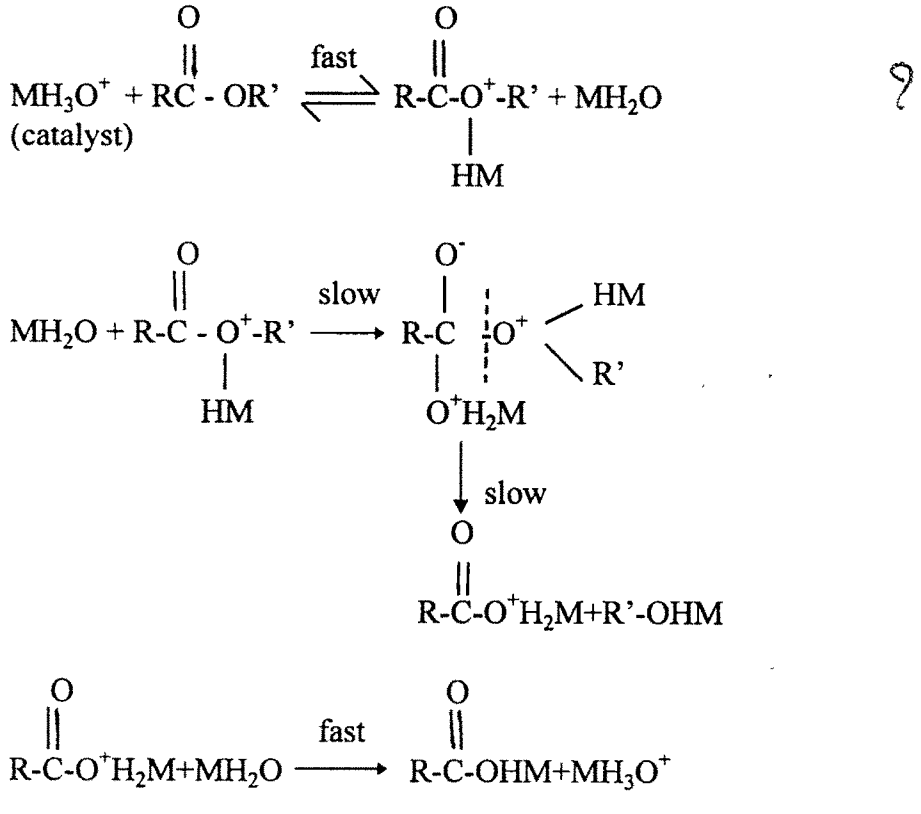

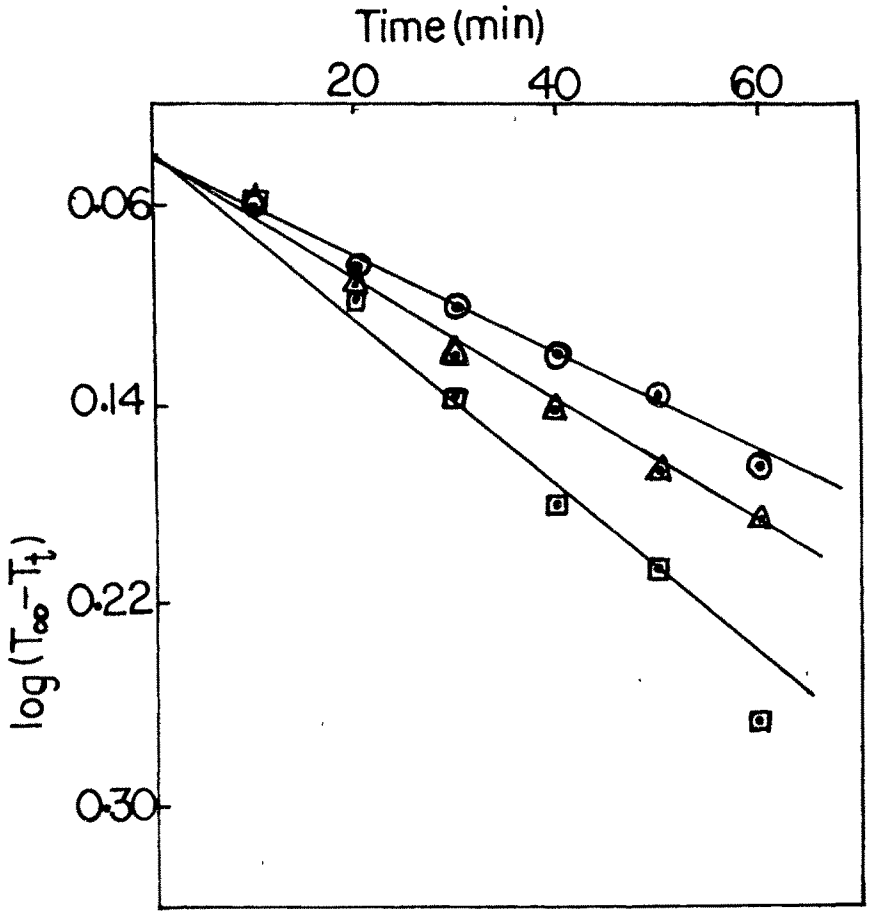

Fig.4.11a Hydrolysis of methyl acetate in SDS microemulsion system with o/w = 5/52.5
⊙ 35°C; △ 40°C; ⊡ 45°C

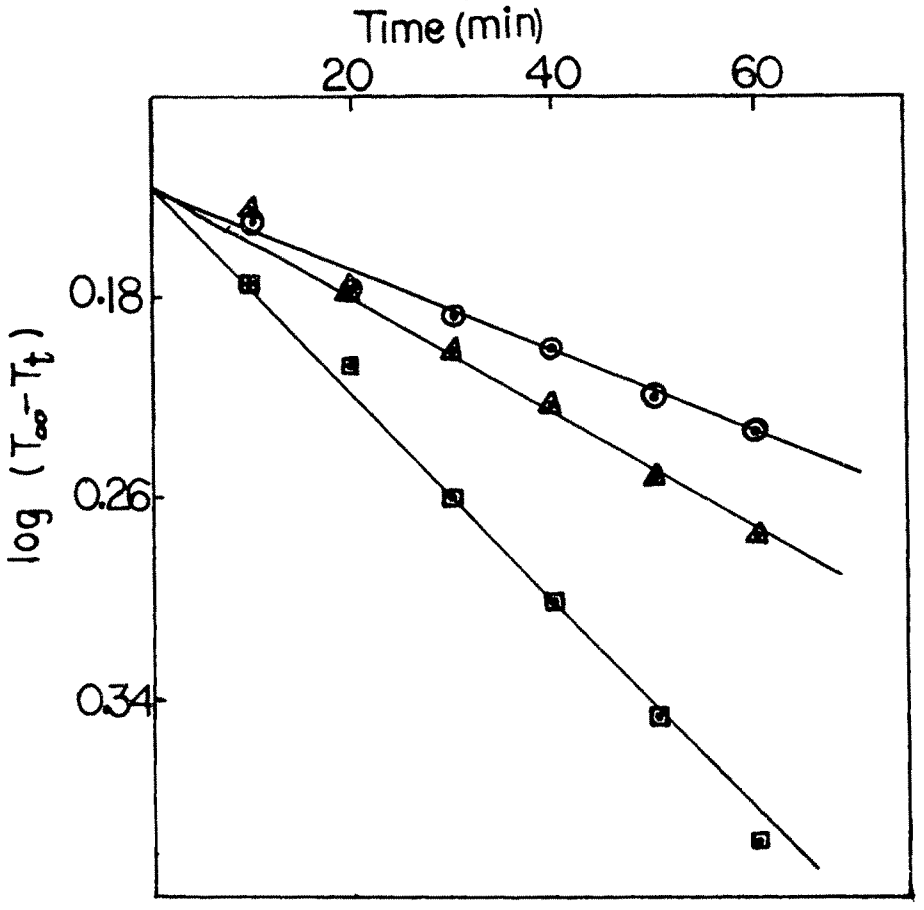

Fig.4.11b Hydrolysis of methyl acetate in SDS microemulsion system with o/w = 20/37.5. Symbols are the same as in Fig.4.11a.

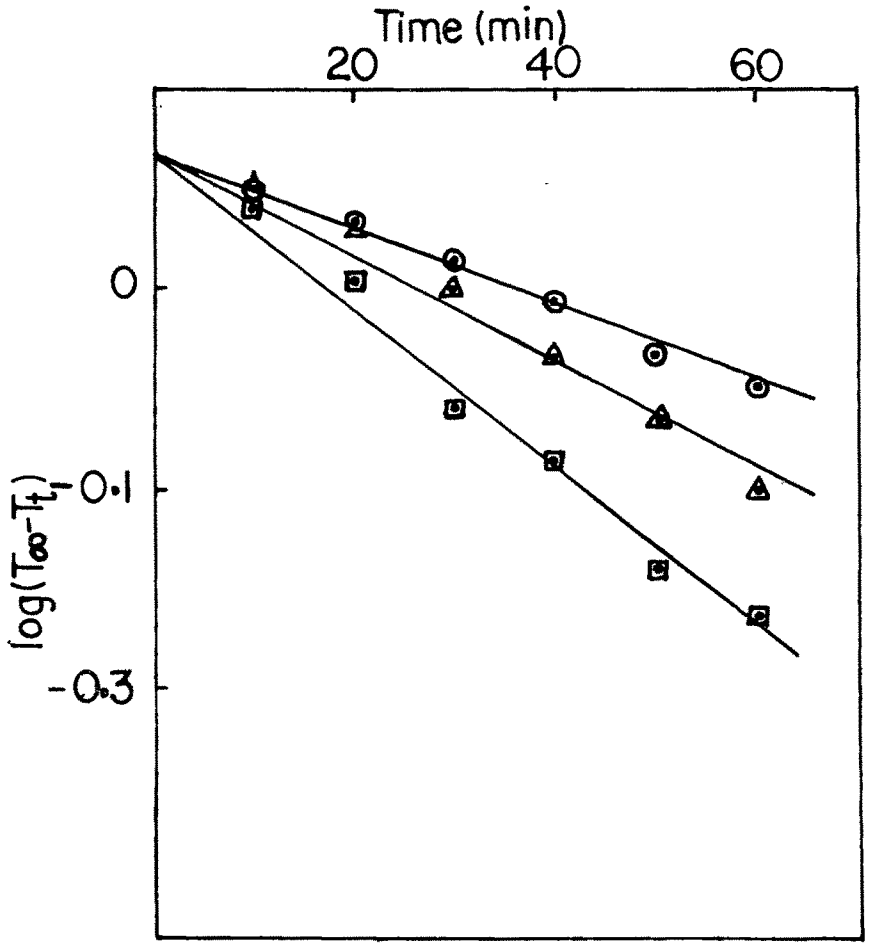

Fig.4.11c Hydrolysis of methyl acetate in SDS microemulsion system with o/w = 40/17.5. Symbols are the same as in Fig.4.11a.

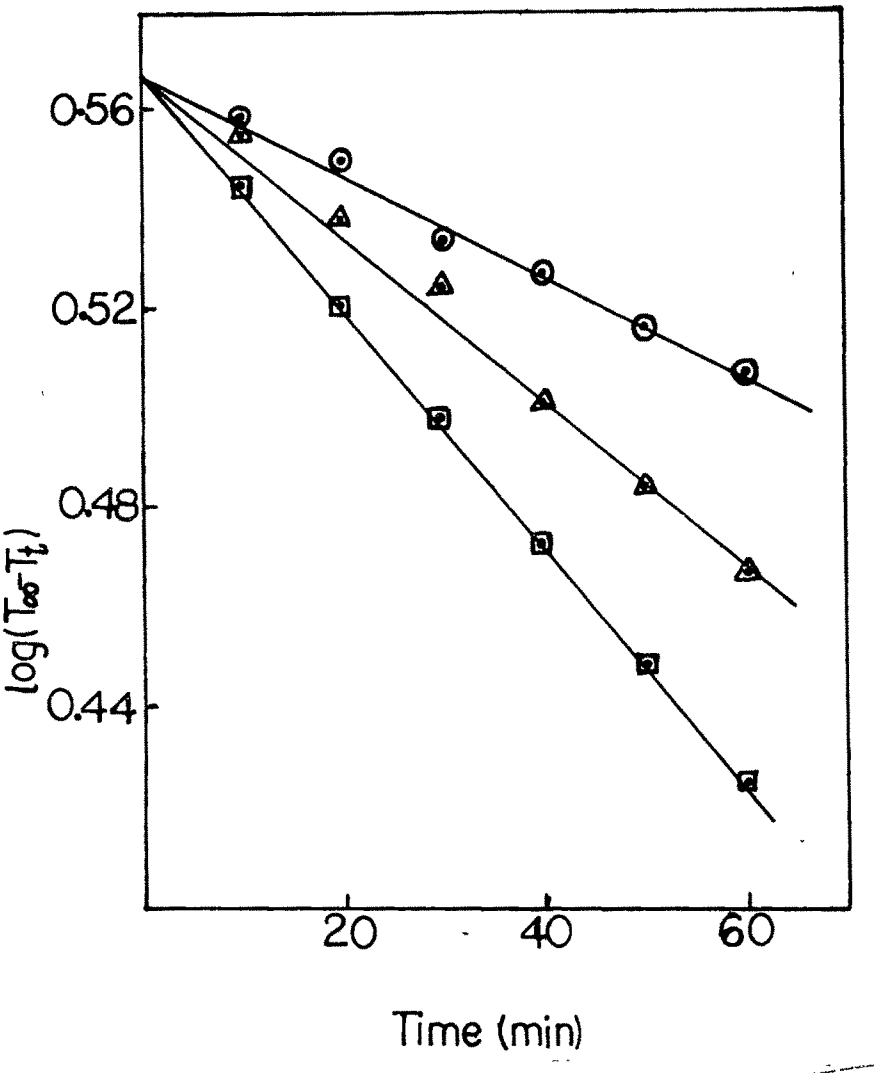

Fig.4.11d Hydrolysis of methyl acetate in SDS microemulsion system with no oil. s/w = 42.5/57.5. Symbols are the same as in Fig.4.11a.

Table 4.7 **Pseudofirst order rate constant k in min^{-1} for the methyl acetate hydrolysis in SDS and CTAB microemulsion. Surfactant concentration = 42.5%.**

O/W	(a) O/SDS + P/W			(b) O/CTAB + P/W		
	Temperature (^{0}C)					
	35	40	45	35	40	45
5/52.5	4.38×10^{-3}	5.42×10^{-3}	7.68×10^{-3}	2.19×10^{-3}	3.54×10^{-3}	5.12×10^{-3}
20/37.5	4.19×10^{-3}	5.42×10^{-3}	9.7×10^{-3}	2.88×10^{-3}	4.61×10^{-3}	6.58×10^{-3}
40/17.5	8.23×10^{-3}	1.21×10^{-2}	1.92×10^{-2}	5.76×10^{-3}	7.68×10^{-3}	1.15×10^{-2}
S/W = 42.5/57.5	2.30×10^{-3}	3.84×10^{-3}	6.58×10^{-3}	2.30×10^{-3}	3.54×10^{-3}	5.12×10^{-3}
H_2O (100%)	2.09×10^{-3}	2.88×10^{-3}	4.61×10^{-3}	-	-	-

For a pseudofirst order reaction,[229]

$$kt = 2.303 \log \frac{a}{a-x}, \qquad \text{.....(4)}$$

where a is the initial concentration and (a-x) is the concentration at any time t, The above equation can be written as ;

$$kt = 2.303 \log \frac{T_\infty - T_o}{T_\infty - T_t}$$

where T_∞ is the final titre value, T_o is the initial titre value and T_t is the titre value at any time t.

$$\frac{kt}{2.303} = \log (T_\infty - T_o) - \log (T_\infty - T_t)$$

$$\log (T_\infty - T_t) = \log (T_\infty - T_o) - \frac{kt}{2.303}$$

The rate constant is determined from log $(T_\infty - T_t)$ versus t (time) plot. The rate constant is obtained from the relation k= (-slope ×2.303). Fig. 4.11(a-d) shows the plot for the pseudofirst order reaction in SDS system. The reaction is carried out at different temperature and changing oil-water ratios where o/w are 5/52.5, 20/37.5, & 40/17.5. The result is summarized in table 4.7a. It is clear from the table that the reaction is enhanced slightly, almost 2-9 times faster than in the pure aqueous system. Due to the electrostatic attraction of anionic surfactant, there is a higher local concentration of protons at the interface. The reaction rate is directly proportional to $[H^+]$ and this could be a measure of hydrogen ion activity. It was repoted earlier[292] also that the rate constant increases with inreasing dielectric constant of the medium used. On acidification, the H^+ may neutralise some residual negative charge of SDS microemulsion interface or displace Na^+

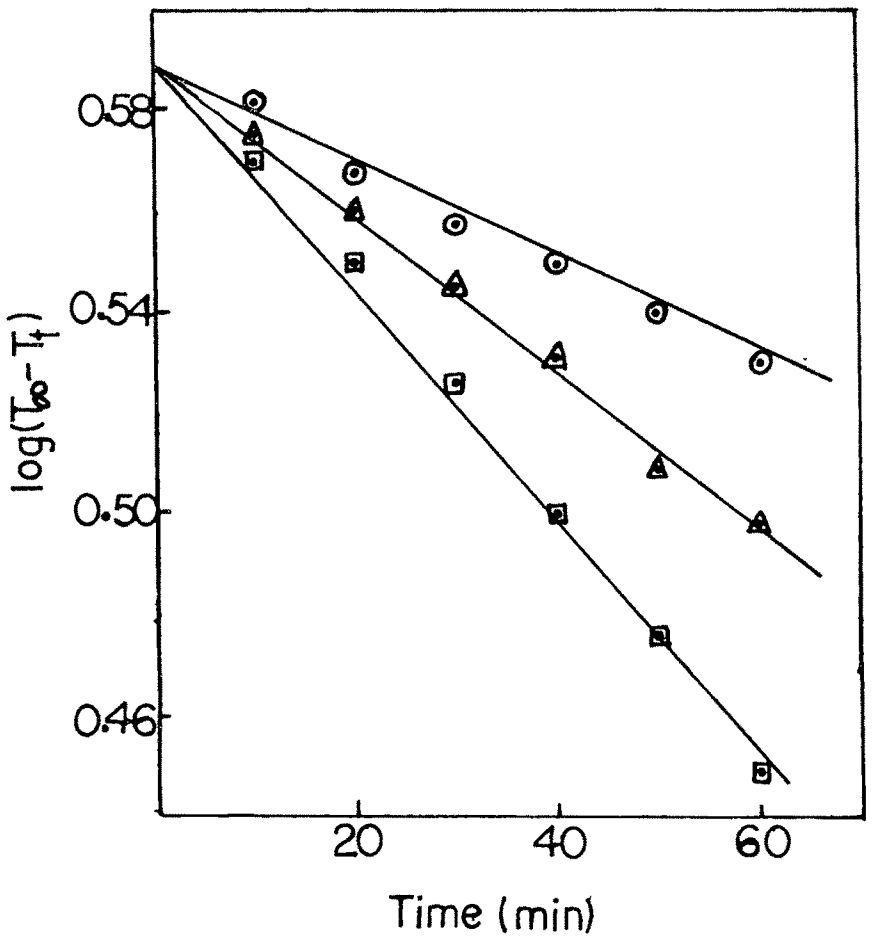

Fig.4.12a Hydrolysis of methyl acetate in CTAB microemulsion system with o/w = 5/52.5. ⊙ 35°C; △ 40°C; ⊡ 45°C

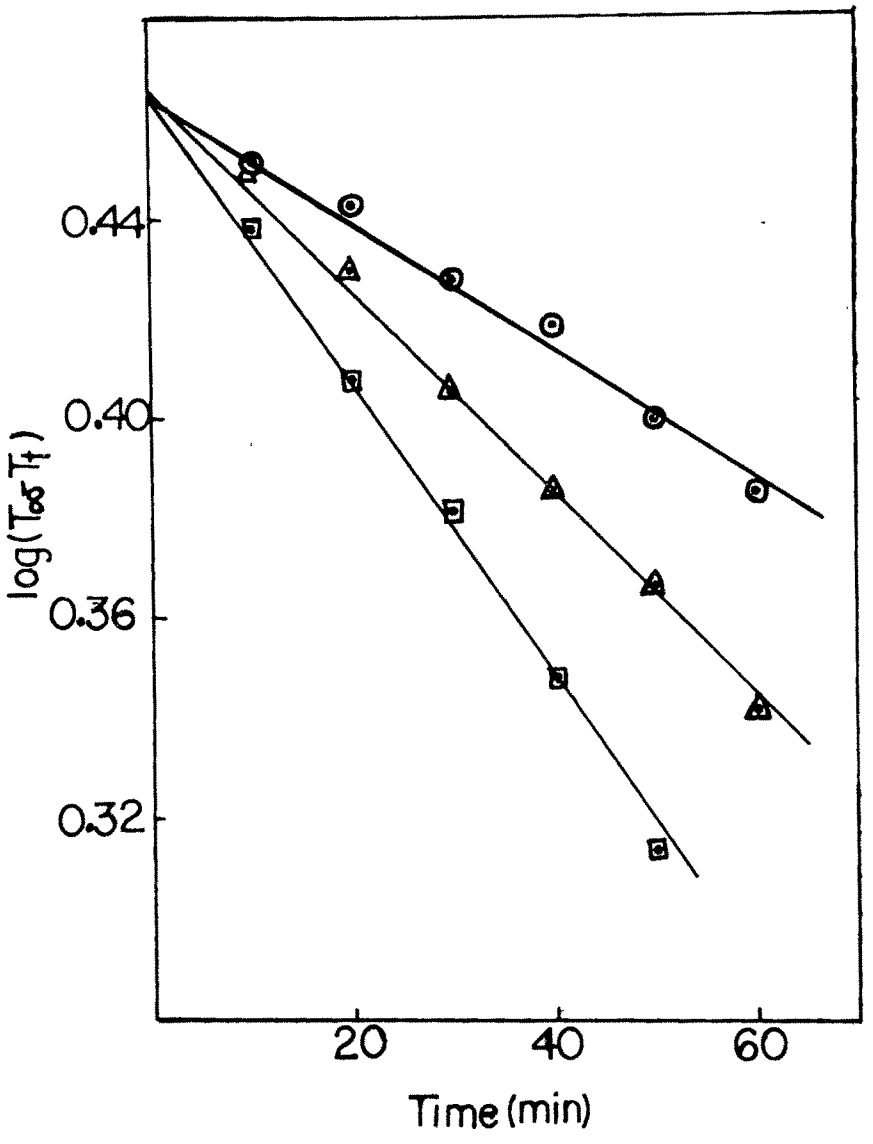

Fig.4.12b Hydrolysis of methyl acetate in CTAB microemulsion system with o/w = 20/37.5. Symbols are the same as in Fig.4.12a.

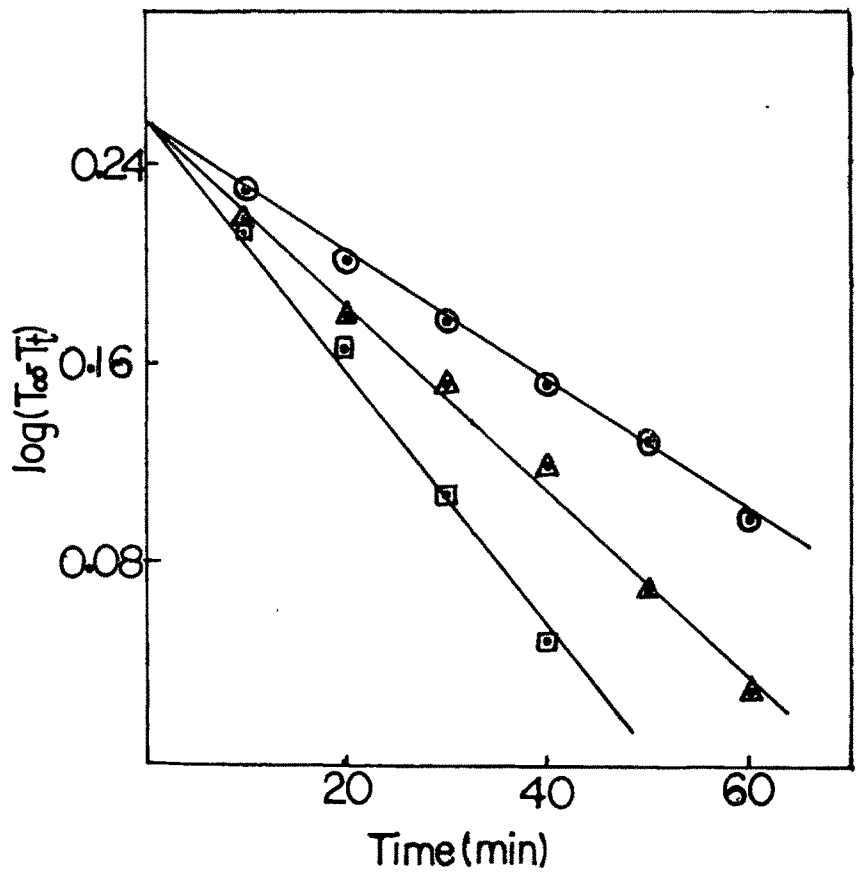

Fig.4.12c Hydrolysis of methyl acetate in CTAB microemulsion system with o/w = 40/17.5. Symbols are the same as in Fig.4.12a.

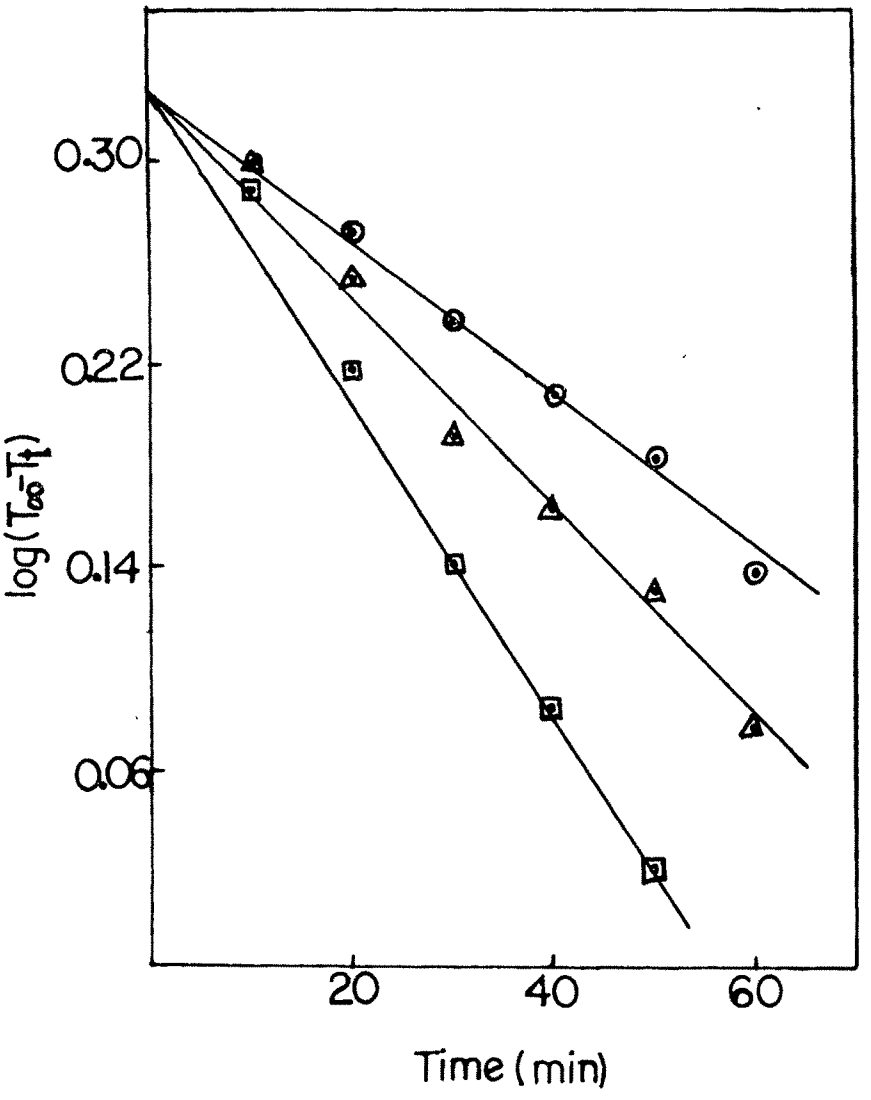

Fig.4.12d Hydrolysis of methyl acetate in CTAB microemulsion system with no oil. s/w = 42.5/57.5. Symbols are the same as in Fig.4.12a.

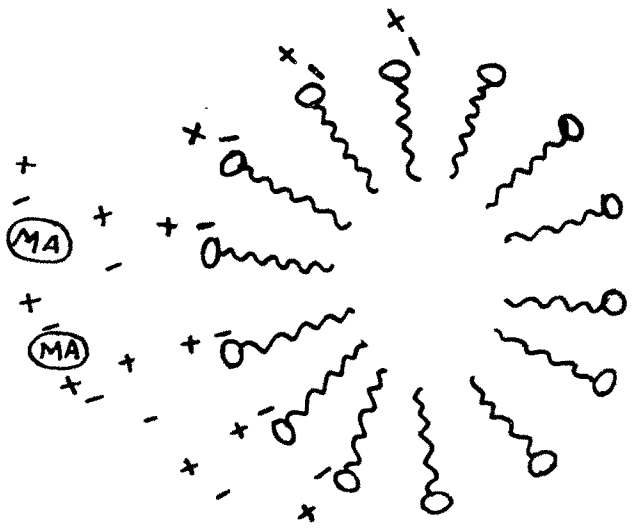

Fig.4.13 Pictorial representation of stern layer.

from the counter ion layers of SDS microemulsion. Hence the probability of hydrogen ion concentration at the interface is more than that in bulk water itself.[147, 291-293]

The plots for the pseudo first order methyl acetate hydrolysis in CTAB microemulsion is shown by plotting $\log(T_\infty - T_t)$ versus time in Fig.4.12(a-d) and the result is summarized in Table 4.7 b.The reaction is carried out with changing oil-water composition of 5/52.5, 20/37.5, 40/17.5 and changing S/O composition of 32.5/62.5, 42.5/52.5 & 55/45. The rate constant is higher than the pure aqueous system but the magnitude is less than that for SDS system.[147] This is due to the electrostatic attraction; anionic surfactant, SDS preferentially hold more H^+ ions than the cationic surfactant due to adsorption of the substrates in the Stern layer : Fig. 4.13 and hence higher of charge density of the H^+ ions.[147] Methyl acetate can be preferentially solubilized or adsorbed in the Stern layer of the interface. In CTAB microemulsion, the repulsive interaction of hydrophilic head of CTAB molecule will be dominating over the attractive interaction. So the local concentration of H^+ is more at SDS microemulsion. Similar results are reported for ethyl acetate hydrolysis in micellar medium of SDS and CTAB.[147]

It was reported earlier the effect of micellar solutions of sodium laurate and n-dodecyl trimethyl ammonium bromide on the rate of alkaline hydrolysis of p-nitrophenyl acetate, mono p-nitro phenyl dodecanedioate and p-nitro phenyl octanoate by Menger and Portnoy.[294] It was evident for these esters that anionic micelles retard and cationic micelles enhance the rate of hydrolysis. This has been reported for sulphate esters also. The rate of alkaline hydrolysis of aliphatic esters in anionic and cationic micelles have been found to retard by other researchers also.[295]

We have made a comparative study of this reaction in CTAB and TX100 microemulsion with constant (5%) water composition and 32.5/62.5, 42.5/52.5 & 55/40 surfactant to oil ratio. (Fig. 4.14 (a-f)). It has been observed that there is rate enhancement in both the systems and the magnitude is little higher for CTAB

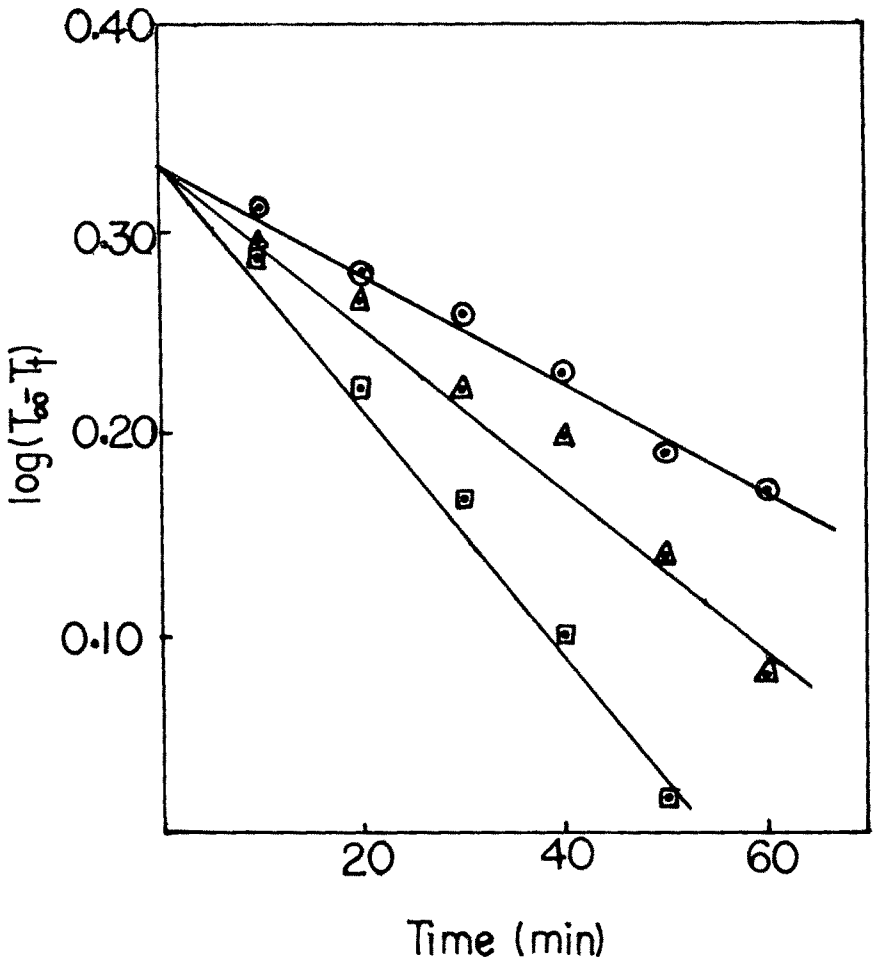

Fig.4.14a Hydrolysis of methyl acetate in CTAB microemulsion system with s/o = 32.5/62.5. ⊙ 35°C; △ 40°C; ⊡ 45°C

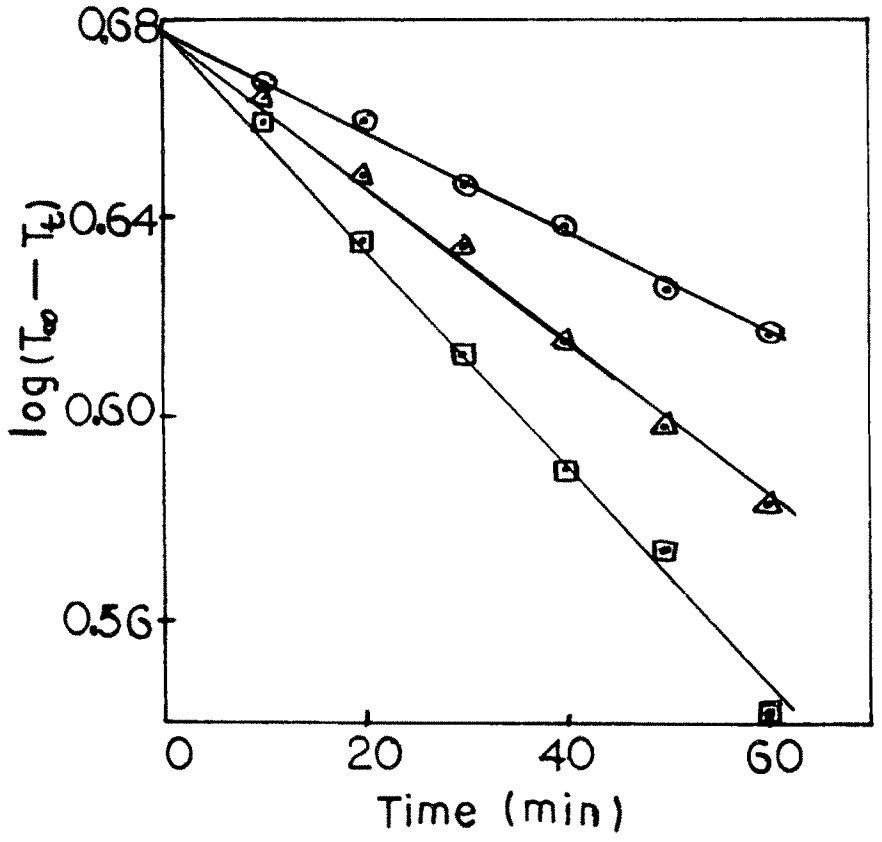

Fig.4.14b Hydrolysis of methyl acetate in CTAB microemulsion system with s/o=42.5/57.5. Symbols are the same as in Fig.4.14a.

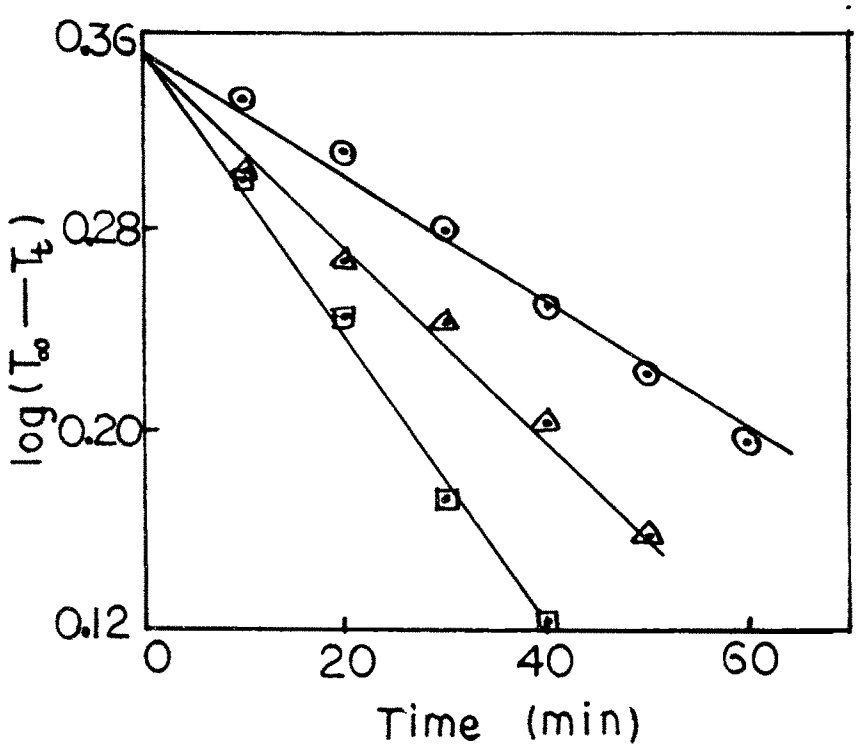

Fig.4.14c Hydrolysis of methyl acetate in CTAB microemulsion system with s/o=55/40. Symbols are the same as in Fig.4.14a.

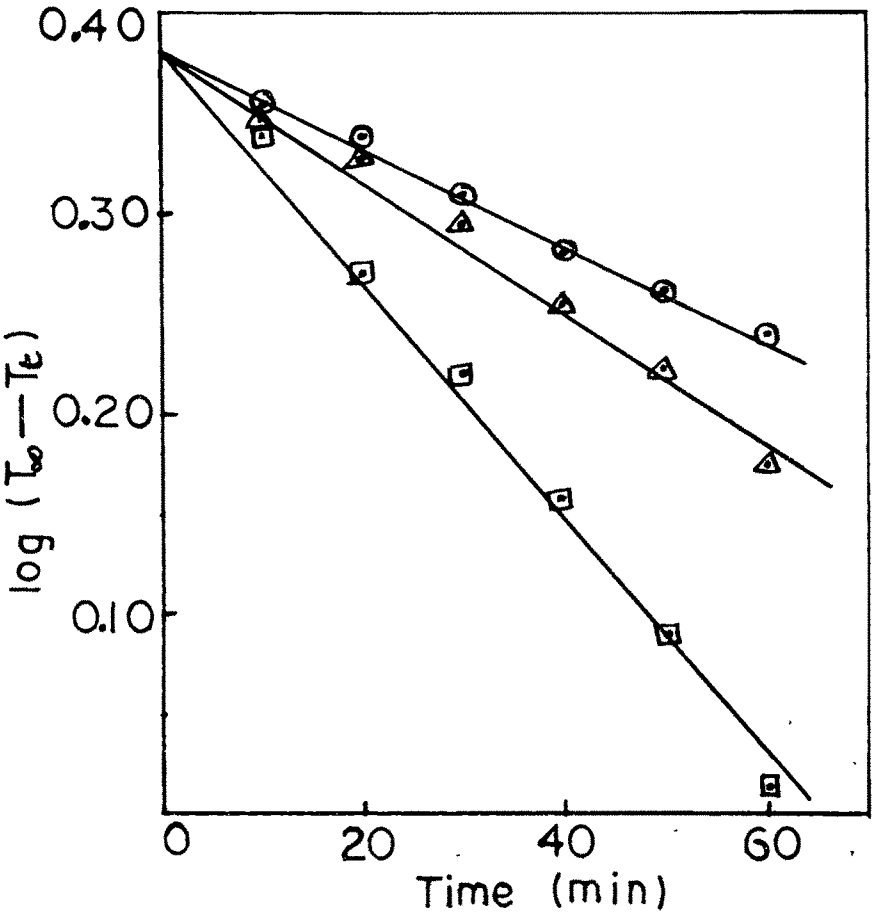

Fig.4.14d Hydrolysis of methyl acetate in TX100 microemulsion system with s/o=32.5/62.5. Symbols are the same as in Fig.4.14a.

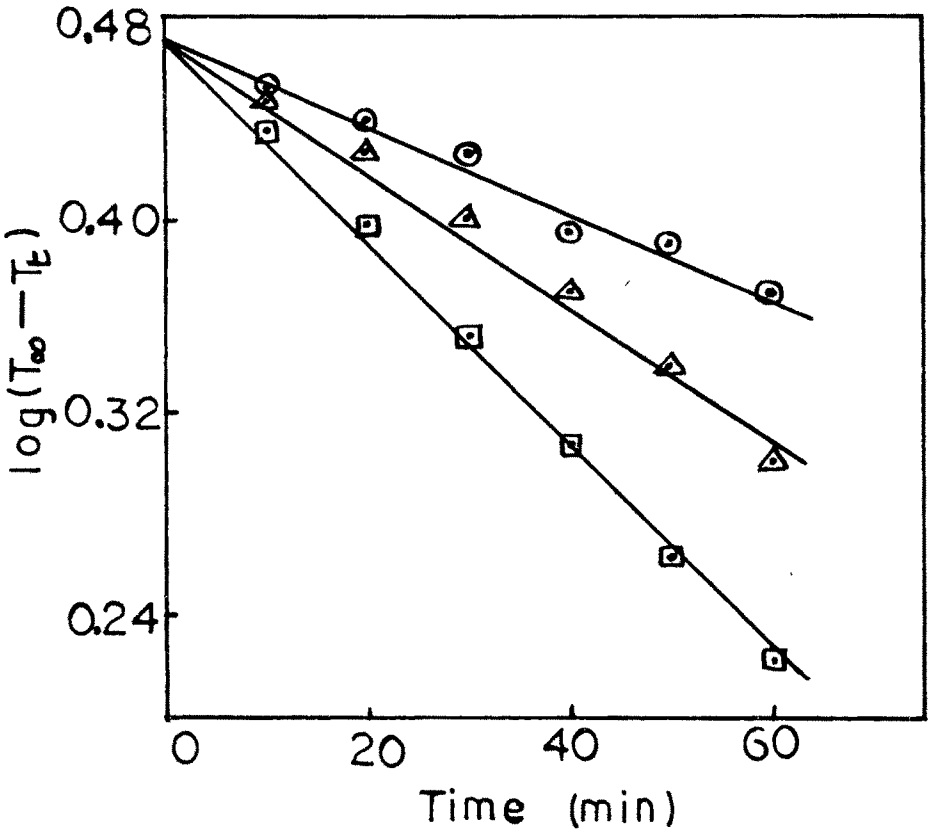

Fig.4.14e Hydrolysis of methyl acetate in TX100 microemulsion system with s/o=42.5/57.5. Symbols are the same as in Fig.4.14a.

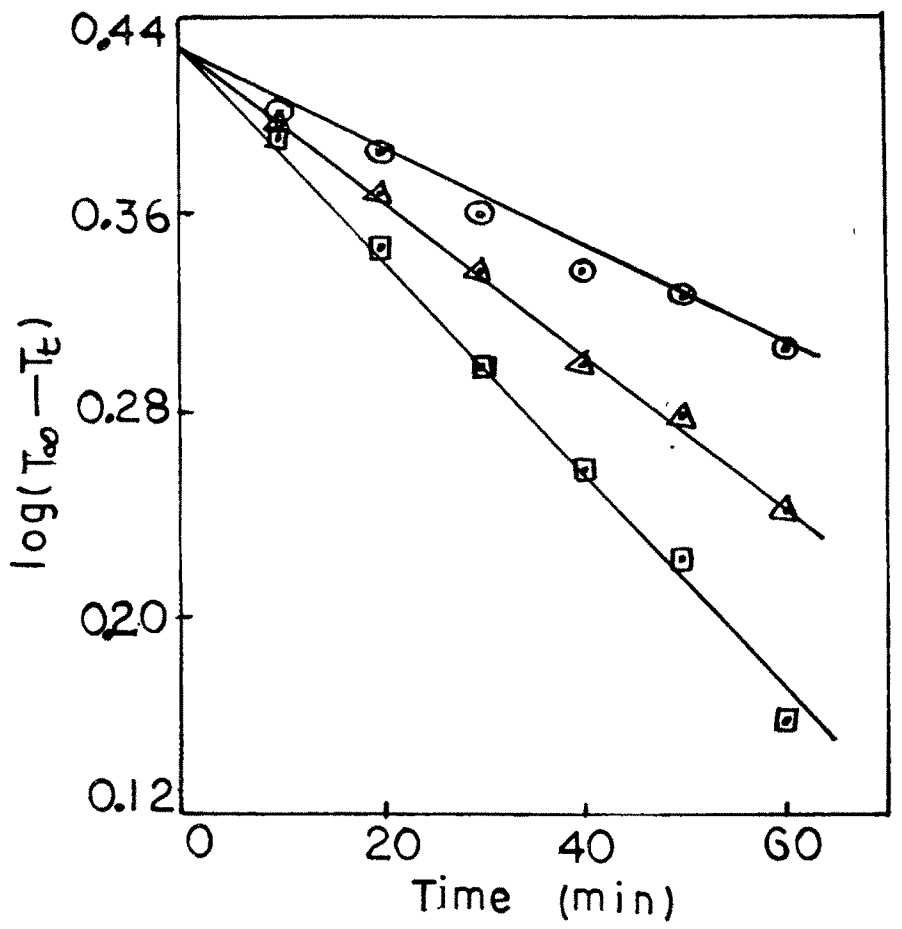

Fig.4.14f Hydrolysis of methyl acetate in CTAB microemulsion system with s/o=55/40. Symbols are the same as in Fig.4.14a.

Table 4.8 **Pseudofirst order rate constant k in min^{-1} for the methyl acetate hydrolysis in CTAB and TX100 microemulsion. Water concentration = 5%.**

S/O	(a) O/CTAB + P/W			(b) O/TX100 + P/W		
	Temperature (^{0}C)					
	35	40	45	35	40	45
32.5/62.5	6.06×10^{-3}	9.20×10^{-3}	1.44×10^{-2}	5.62×10^{-3}	7.68×10^{-3}	1.28×10^{-2}
42.5/52.5	6.82×10^{-3}	9.20×10^{-3}	1.42×10^{-2}	4.61×10^{-3}	7.68×10^{-3}	1.02×10^{-2}
55/40	5.76×10^{-3}	8.37×10^{-3}	1.15×10^{-2}	5.12×10^{-3}	7.68×10^{-3}	1.02×10^{-2}

system, (Table 4.8). With a particular composition, the rate of hydrolysis increases with increasing temperature. It may be due to the large interface provided by the small microdroplets as the interfacial tension reduced by increasing the temperature. Also, the higher temperature induces higher thermal instability of the intermediate complex. As the surfactant composition increases from 40% to 52.5 & 62.5 %, the rate constant almost remains a constant showing that percentage composition of surfactant hardly affects the rate of hydrolysis of methyl acetate in CTAB and TX100 microemulsion systems at constant water composition of 5 %.

In the case of SDS microemulsion, the presence of H^+ in the Stern layer is expected and the helps in catalyzing the reaction. However in case of CTAB microemulsion, the concentration of H^+ in the Stern layer will be much lower because of the presence of the counter ion (Br^- ion) and therefore the reaction rate is expected to be slower. In TX100 microemulsion system, the surfactant molecule is neutral and therefore the presence of H^+ as catalyst is less perceptable because of the absence of the ionic Stern layer. This therefore results in lower reaction rate. But microheterogenity of the system increases the reaction rate to a higher value than that in water. For CTAB microemulsion, there is an interaction between the hydrophilic head and H^+ and due to the presence of Br^-ions, the H^+ ions are not really away from the reaction site.[291,296]

Hydrolysis of esters in the micellar solutions of ionic and nonionic surfactants[296] is well studied in the literature. Nonionic surfactants either decrease the rate or have no significant effect on the rate of hydrolysis of carboxylic esters. The ester is probably solubilized at the micelle-water interface. The transition state for alkaline hydrolysis of the ester linkage carries a negative charge due to the oncoming OH^-;[297]

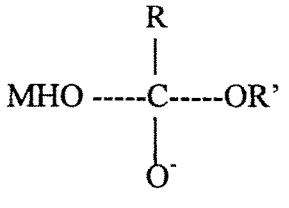

and this charge can be stabilized by the adjacent positive charges of the hydrophilic heads of cationic micelles and destabilized by the adjacent negative charges in anionic micelles.In addition, the concentration of OH^- at the micelle - water interface is increased by the multiple positive charges on the cationic micells and decreased by the multiple negative charges on the anionic micelles. Both of these effects may account for the enhancement and diminution of reaction rates in the respective cases.

The increase in the rate of acid catalyzed hydrolysis of esters in microemulsion media can be explained in a similar fashion as being due to stabilization of the positively charged transition state or to concentration of H^+ at the reaction site by the negatively charged hydrophilic head groups.

In all these three cases, the rate constant increases with decreasing water composition[143,144,282] due to the higher charge density of H^+ at the reaction site. The rate constant also increases with increasing temperature. As the temperature increases, more microdroplets are formed due to decrease in interfacial tension. This small microdroplets offers higher interfacial area for the reaction to take place and the rate is higher. Higher temperature also offer higher thermal instability to the transition state and the reaction takes place at a faster rate. Changing surfactant composition for CTAB and TX100 microemulsions have little or no significant effect on the rate of hydrolysis of methyl acetate.

A plot of W/O ratio versus log k (Fig 4.15a 4.15b) for SDS & CTAB at constant surfactant composition of 42.5% shows that the rate constant increases with decreasing W/O ratio ie. with decreasing water content. Fig 4.15b shows the S/O Ratio versus log k; log k values remain almost a constant when the water composition not changed (5%).

Table 4.9 summarizes the kinetic activation energy values of methyl acetate hydrolysis in SDS, CTAB and TX100 microemulsion system. All these values are positive and less than the Ea in pure aqueous system and the system which does not contain any oil also. The less activation energy value in microemulsion

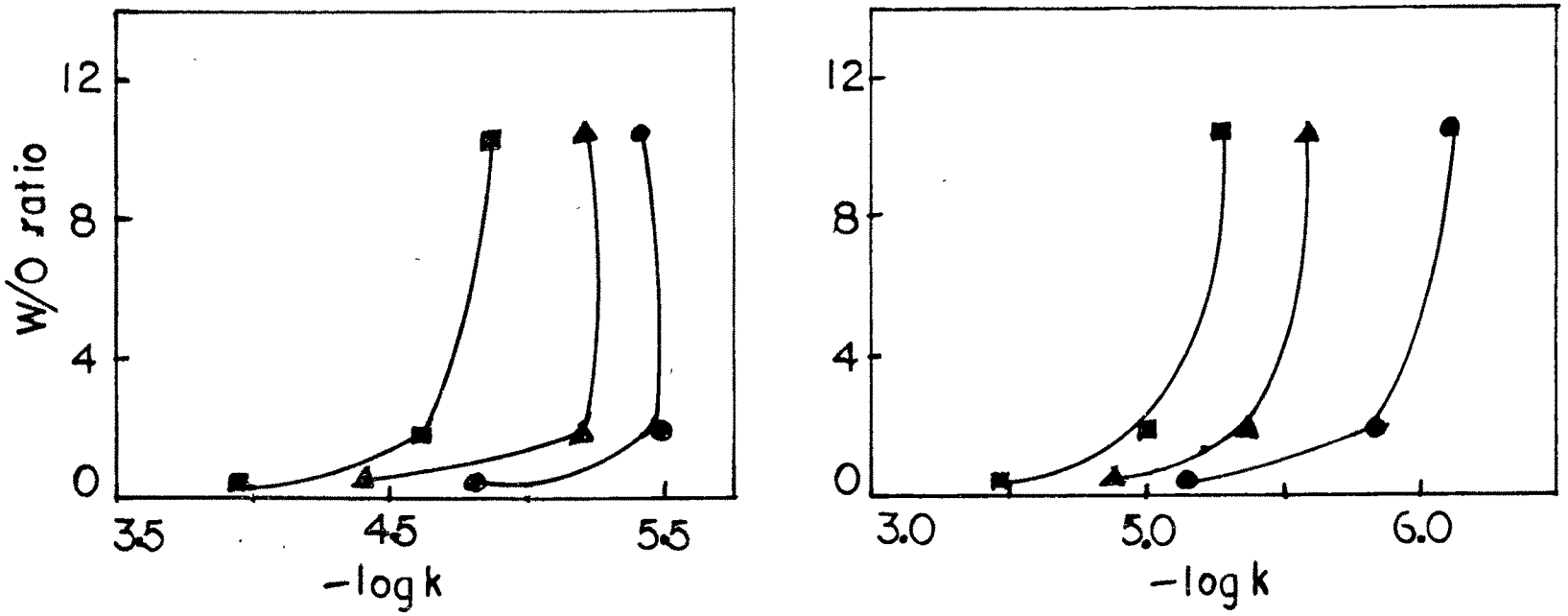

Fig.4.15a Plot of log k vs w/o ratio for the hydrolysis of methyl acetate in SDS (left) & CTAB (right) microemulsion system. ● 35°C; ▲ 40°C; ■ 45°C

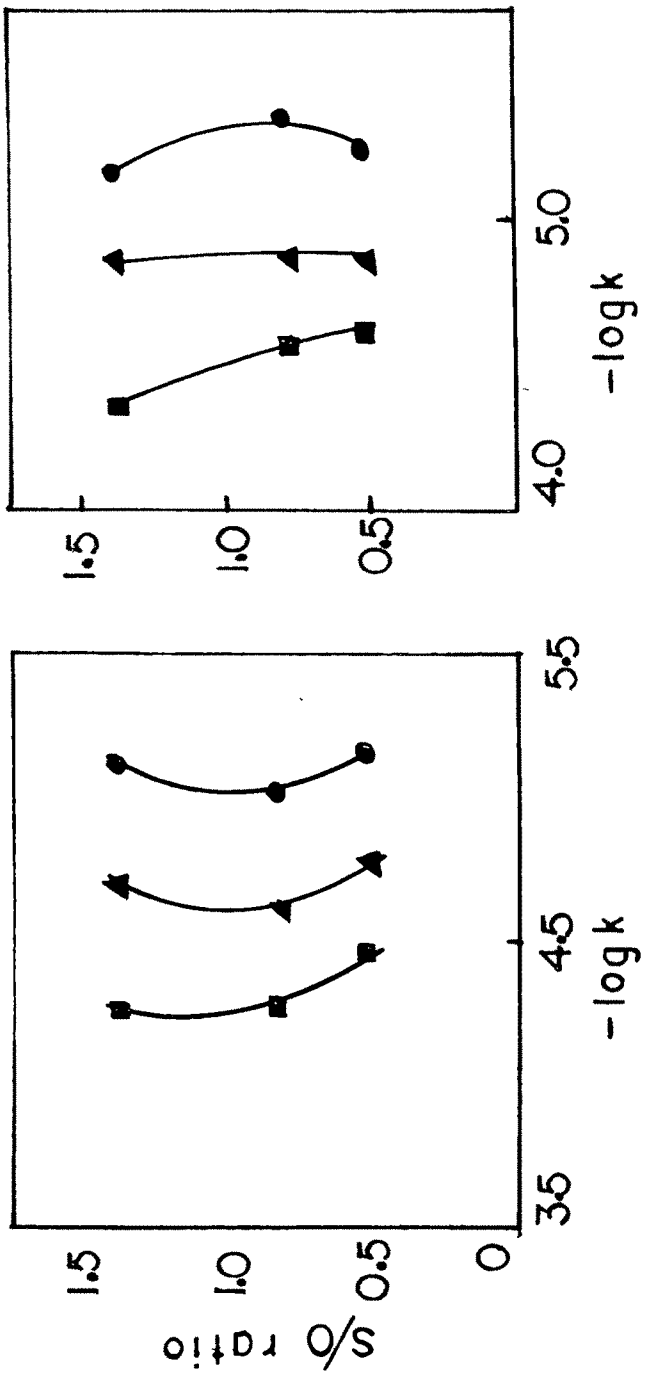

Fig.4.15b Plot of log k vs s/o ratio for hydrolysis of methyl acetate in CTAB (left) and TX100 (right) microemulsion system. ● 35°C; ▲ 40°C; ■ 45°C

Table 4.9a **Activation energy (Ea) in $kJmol^{-1}$ for the pseudofirst order methylacetate hydrolysis in SDS (Ea_7) and CTAB (Ea_8) microemulsion**

O/W	Ea_7	Ea_8
5/52.5	54.7	58.9
20/37.5	54.7	54.7
40/17.5	51.1	54.7
S/W = 42.5/57.5	58.9	58.9
W (100%)	64.4	-

Table 4.9b **Activation energy (Ea) in $_{j}Jmol^{-1}$ for the pseudofirst order methylacetate hydrolysis in CTAB (Ea_9) and TX100 (Ea_{10}) microemulsion.**

S/O	Ea_9	Ea_{10}
32.5/62.5	54.71	58.91
42.5/52.5	54.71	58.91
55/40	54.71	58.91

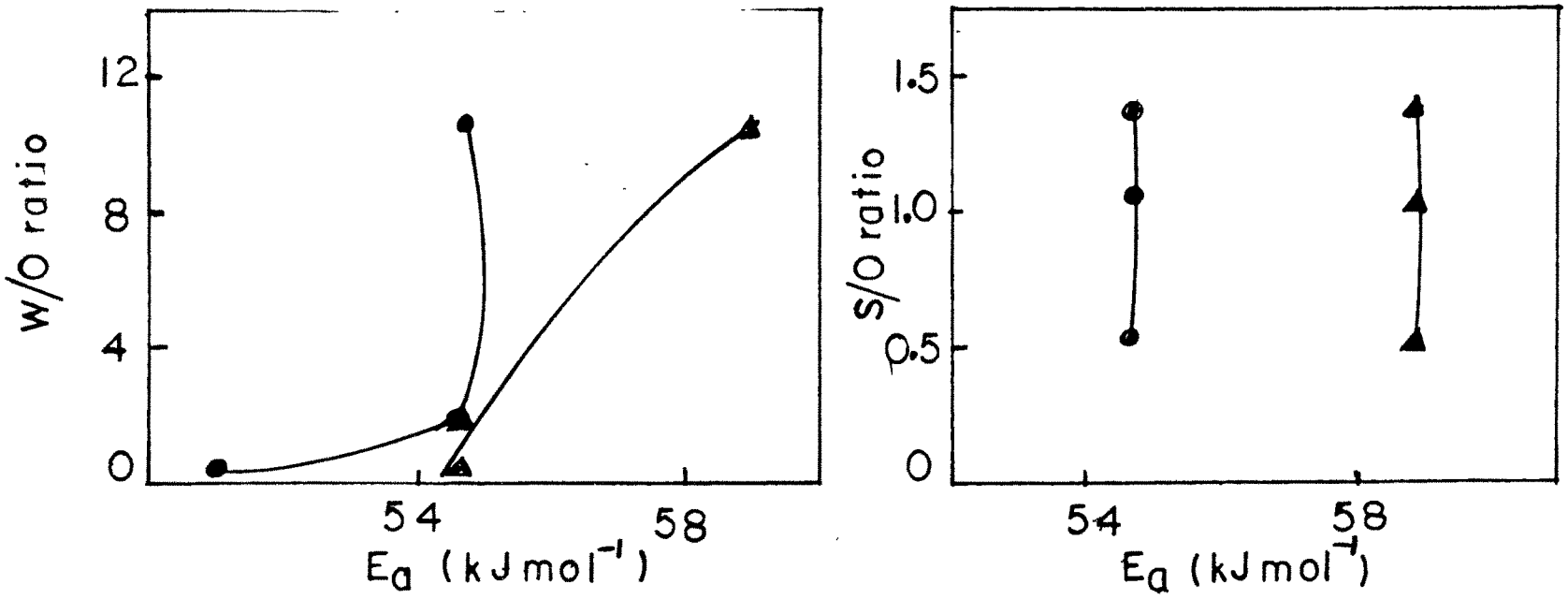

Fig.4.16 Plot of Ea vs w/o ratio for hydrolysis of methyl acetate in SDS, CTAB & TX100 microemulsion system.
left →● O/SDS +P/W; ▲ O/CTAB + P/W; with changing o/w ratio

Right→●O/CTAB+P/W;▲ O/TX100 + P/W with changing s/o ratio

corresponds to the fact that the reaction is faster in microemulsion medium. The activation energy is higher in TX100 system compared with the ionic systems formed by SDS and CTAB. With constant water composition (5%) and changing surfactant-oil ratio for CTAB and TX100 system, the activation energy remains a constant as the rate constant is not affected or little affected by increasing the surfactant concentration.

W/O ratio versus Ea values in SDS and CTAB system show that (Fig 4.16 activation energy is lower at lower water content as supported by the rate constant values. For constant water fraction 5% and changing S/O ratio, the activation energy remains a constant, showing that the rate of reaction is dependent of the water concentration rather than the surfactant concentration.

c. Iodination of acetone

Kinetically, we have studied the iodination of acetone in SDS and TX100 microemulsion systems. Mechanism of the reaction in microemulsion is represented as[298]

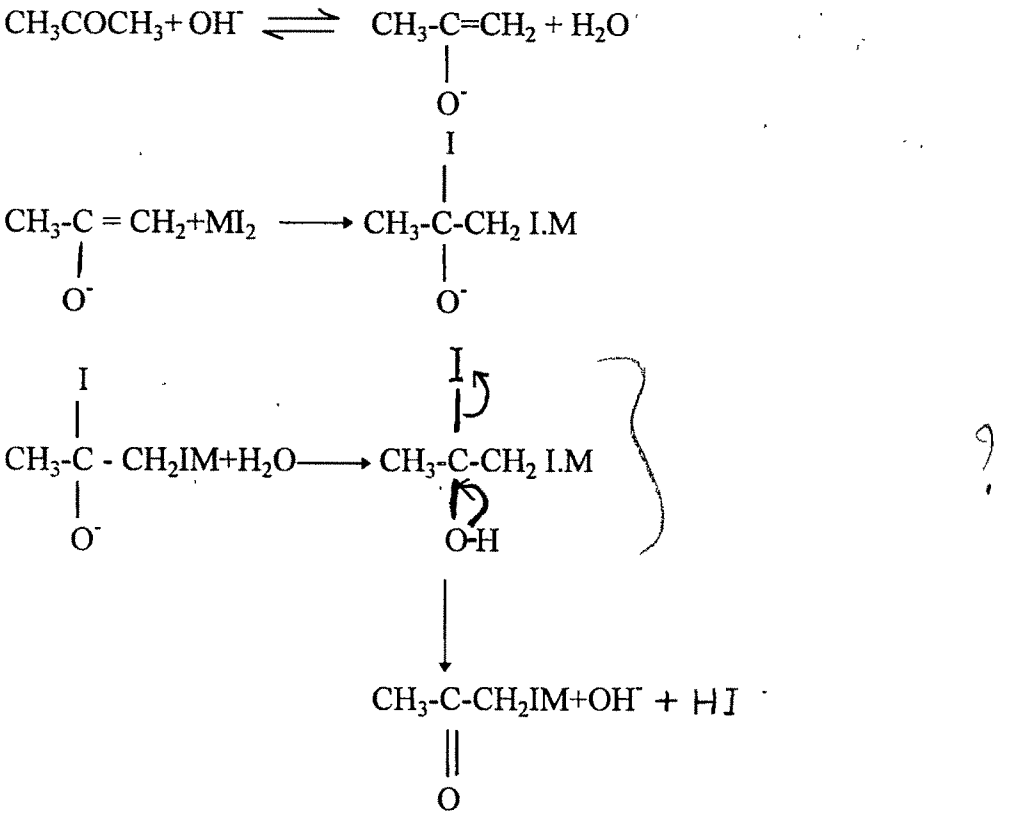

Figs 4.17 (a-i) & 4.18 (a-i) show

$$\frac{1}{a_o-b_o} \ln \frac{b_o(a_o-x)}{a_o(b_o-x)}$$ versus time plot

for second order kinetics for SDS and TX100 systems respectively. The reaction is studied at different temperatures from 25 to 45°C and with changing oil-water ratios at 42.5%S composition. Table 4.10 & 4.11 summarize the result. They show that the rate is enhanced in microemulsion system. The reason is manyfold. Investigation of the microstructure of microemulsion show that these systems are heterogeneous on a microscopic scale. They consist of microscopic domains of water and oil separated by a monolayer of amphiphile molecules. Different reactants solubilized in the microemulsion may meet and react at this microscopic interface. Microemulsions contain large internal interfaces compared to heterogeneous media and therefore high reaction rates may be expected.

Both iodine and acetone dissolve in water and cyclohexane and it is partitioned between the polar and nonpolar phase. But NaOH dissolve in the aqueous phase and the reaction takes place in the alkaline condition. So we assume that the reaction does not occur in the oil phase but in the aqueous phase.[8,204,299,300] Fig 4.19 & 4.20 show the plots. Table 4.12 & 4.13 show the rate constant by applying the partition coefficient. The partition coefficient of iodine between water and cyclohexane was determined and found to be 78.22 at room temperature[301] (~30°C). The partition coefficient for acetone between water and cyclohexane[302] was also determined and the value was 2.56 at ~30°C. The magnitude of rate constant is higher than the condition where we don't consider the partition of reactants between oil and water. The local concentration of the reactants are considered to be higher and hence the rate is higher.

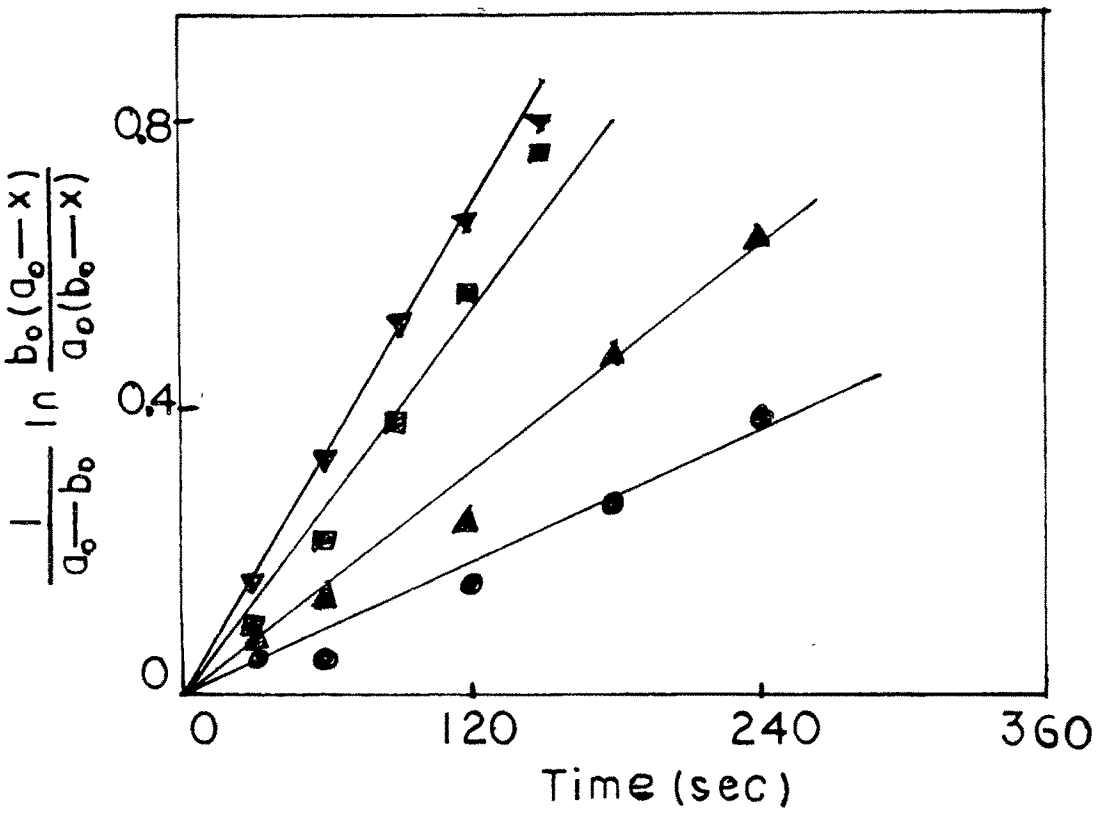

Fig.4.17a Plot of $\frac{1}{a_o-b_o} \ln \frac{b_o(a_o-x)}{a_o(b_o-x)}$ vs time for the iodination of acetone in SDS microemulsion system with o/w=5/52.5.

● 30°C; ▲ 35°C; ■ 40°C; ▼ 45°C

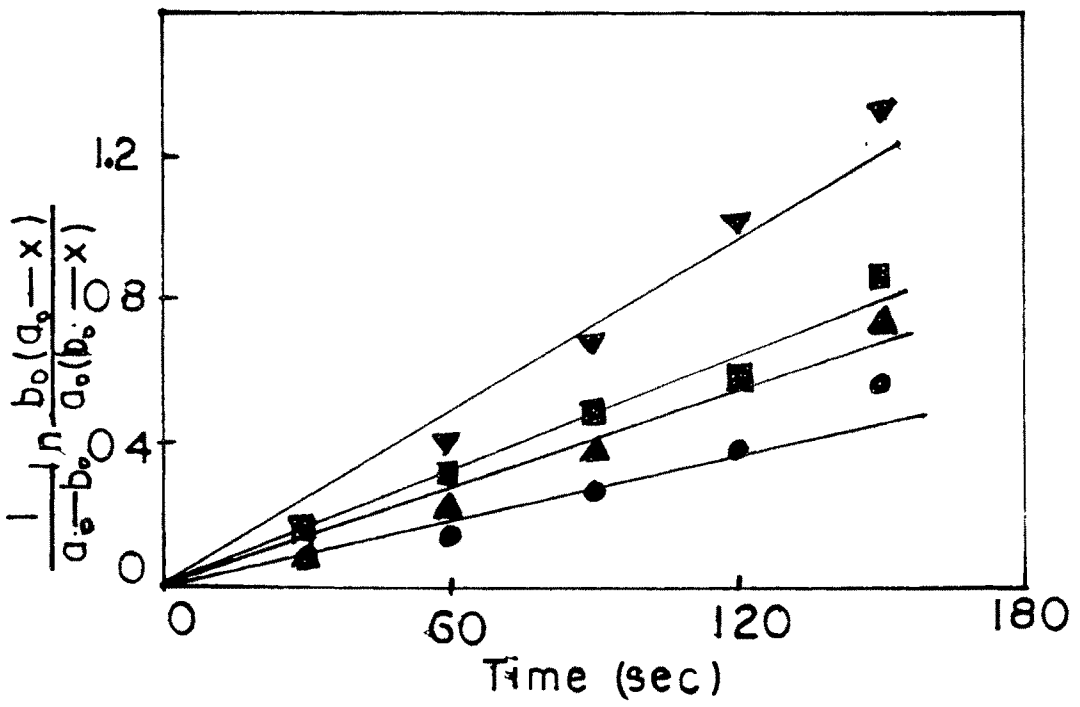

Fig.4.17b Plot of $\frac{1}{a_o-b_o} \ln \frac{b_o(a_o-x)}{a_o(b_o-x)}$ vs time for the iodination of acetone in SDS microemulsion system with o/w=10/47.5. Symbols are the same as in Fig.4.17a.

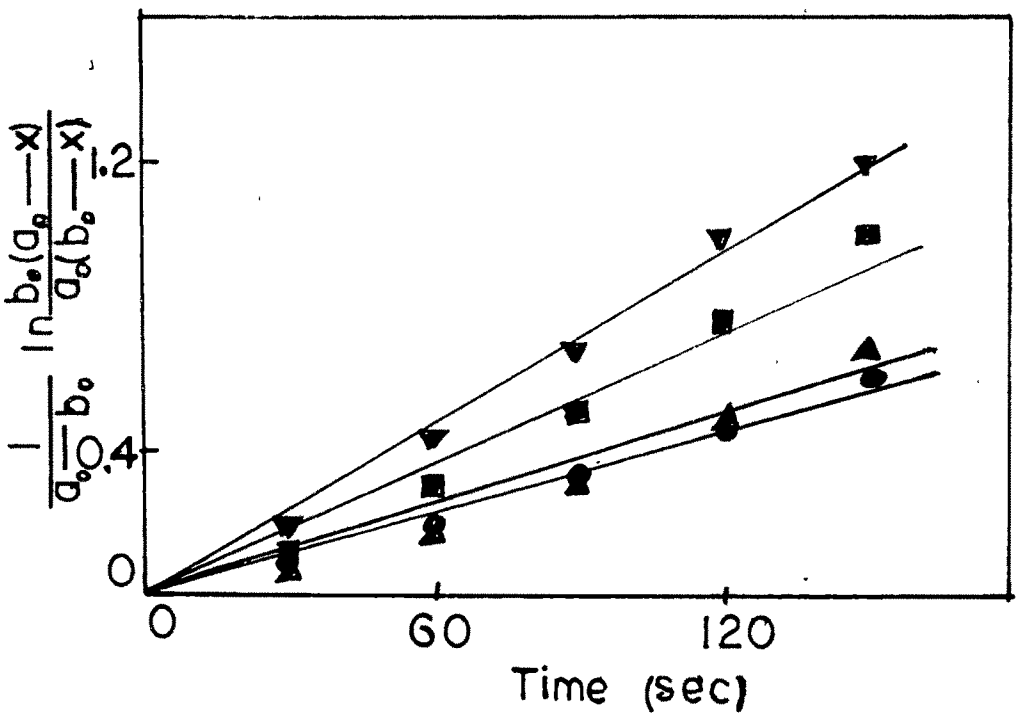

Fig.4.17c Plot of $\frac{1}{a_o-b_o} \ln \frac{b_o(a_o-x)}{a_o(b_o-x)}$ vs time for the iodination of acetone in SDS microemulsion system with o/w=15/42.5. Symbols are the same as in Fig.4.17a.

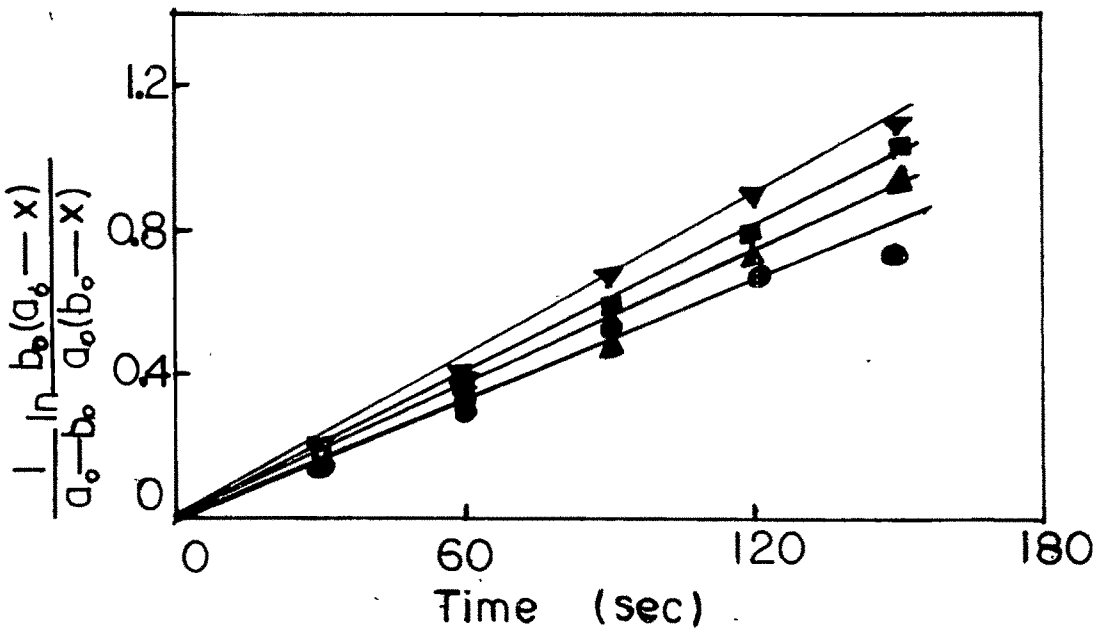

Fig.4.17d Plot of $\frac{1}{a_o-b_o} \ln \frac{b_o(a_o-x)}{a_o(b_o-x)}$ vs time for the iodination of acetone in SDS microemulsion system with o/w=20/37.5. Symbols are the same as in Fig.4.17a.

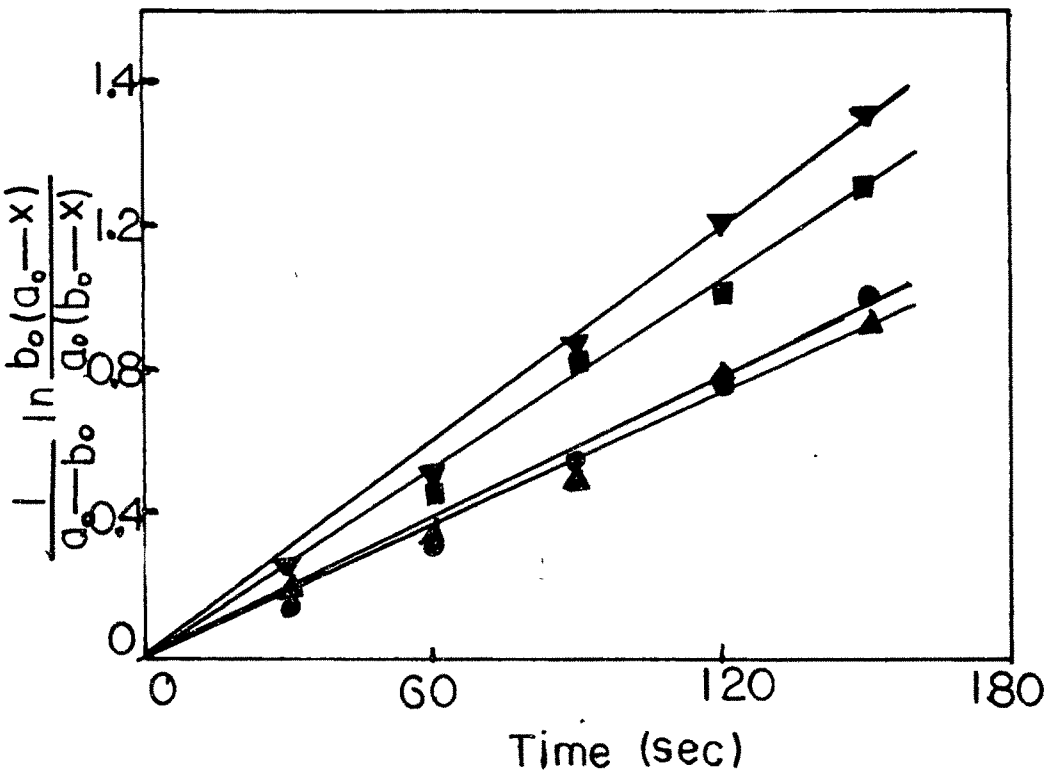

Fig.4.17e Plot of $\frac{1}{a_o-b_o} \ln \frac{b_o(a_o-x)}{a_o(b_o-x)}$ vs time for the iodination of acetone in SDS microemulsion system with o/w=25/32.5. Symbols are the same as in Fig.4.17a.

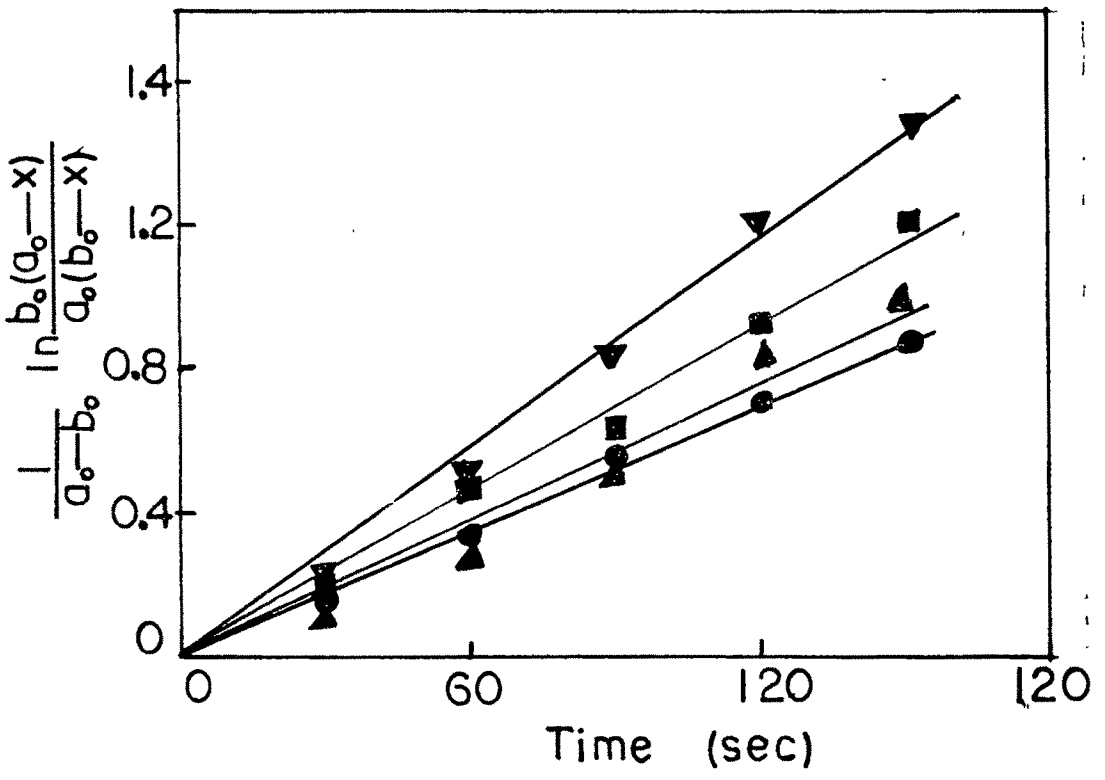

Fig.4.17f Plot of $\frac{1}{a_o-b_o} \ln \frac{b_o(a_o-x)}{a_o(b_o-x)}$ vs time for the iodination of acetone in SDS microemulsion system with o/w=30/27.5. Symbols are the same as in Fig.4.17a.

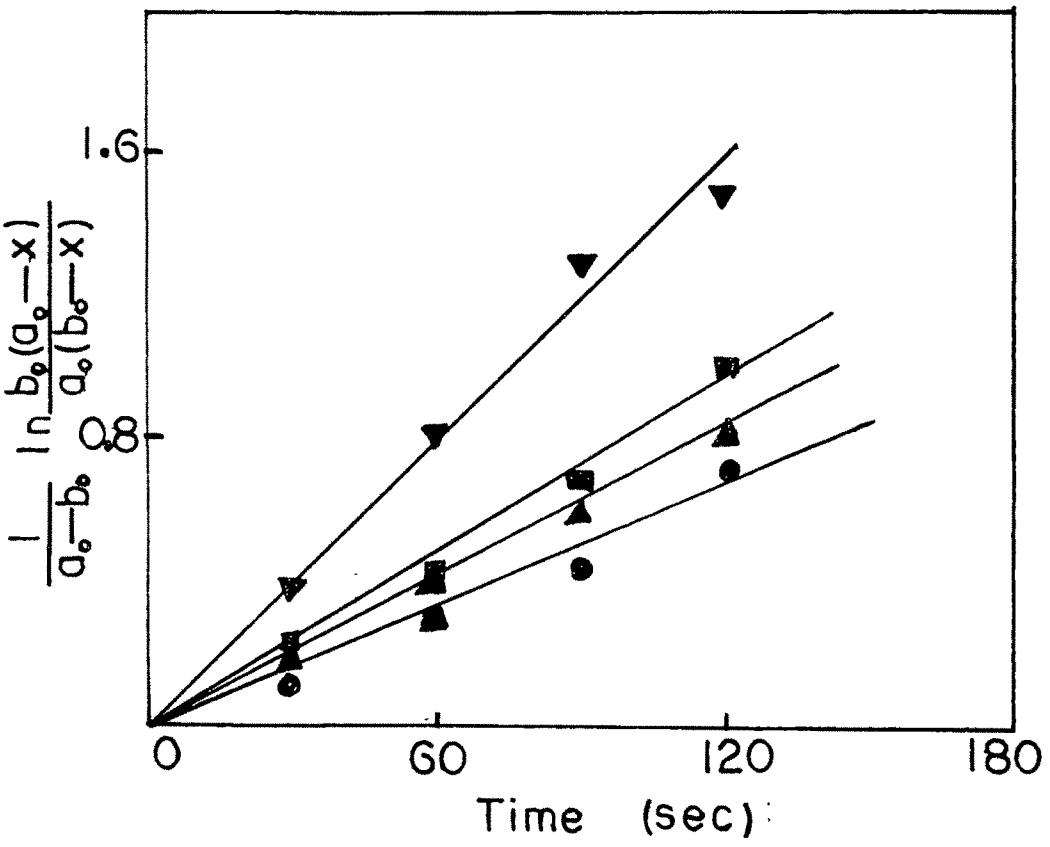

Fig.4.17g Plot of $\frac{1}{a_o-b_o} \ln \frac{b_o(a_o-x)}{a_o(b_o-x)}$ vs time for the iodination of acetone in SDS microemulsion system with o/w=35/22.5. Symbols are the same as in Fig.4.17a.

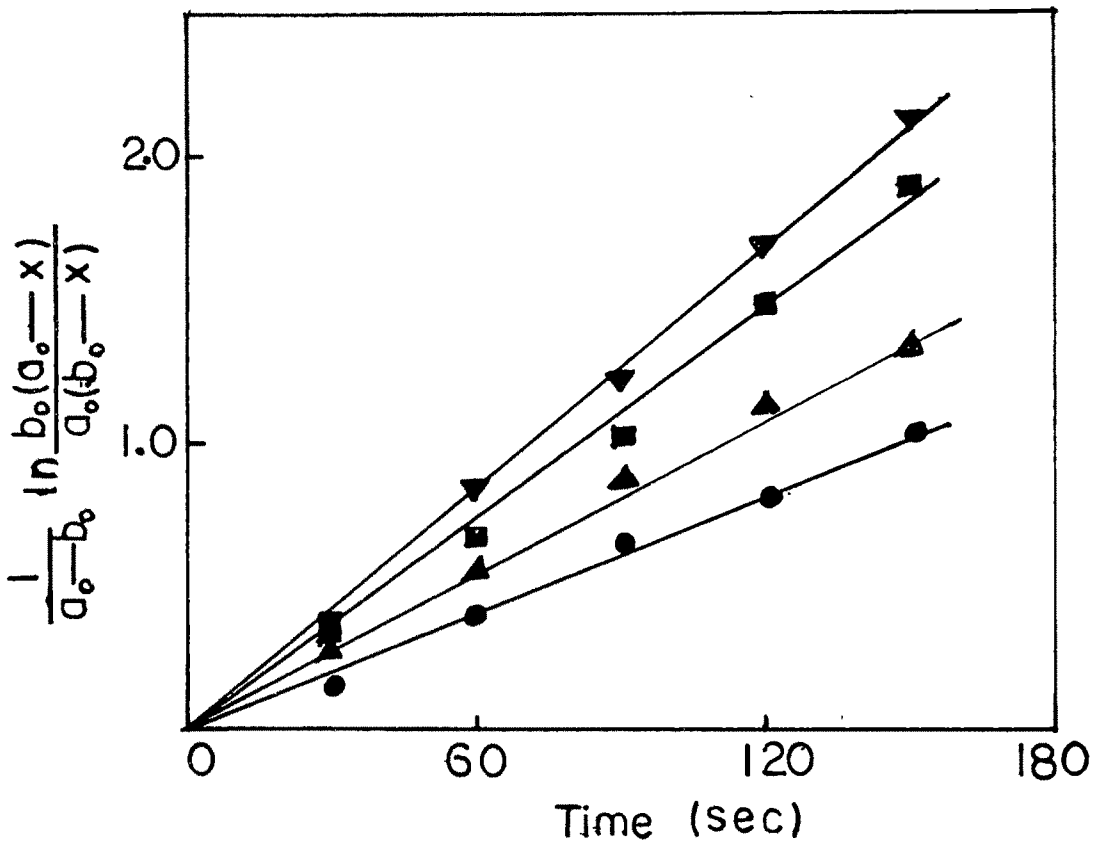

Fig.4.17h Plot of $\frac{1}{a_o-b_o} \ln \frac{b_o(a_o-x)}{a_o(b_o-x)}$ vs time for the iodination of acetone in SDS microemulsion system with o/w=40/17.5. Symbols are the same as in Fig.4.17a.

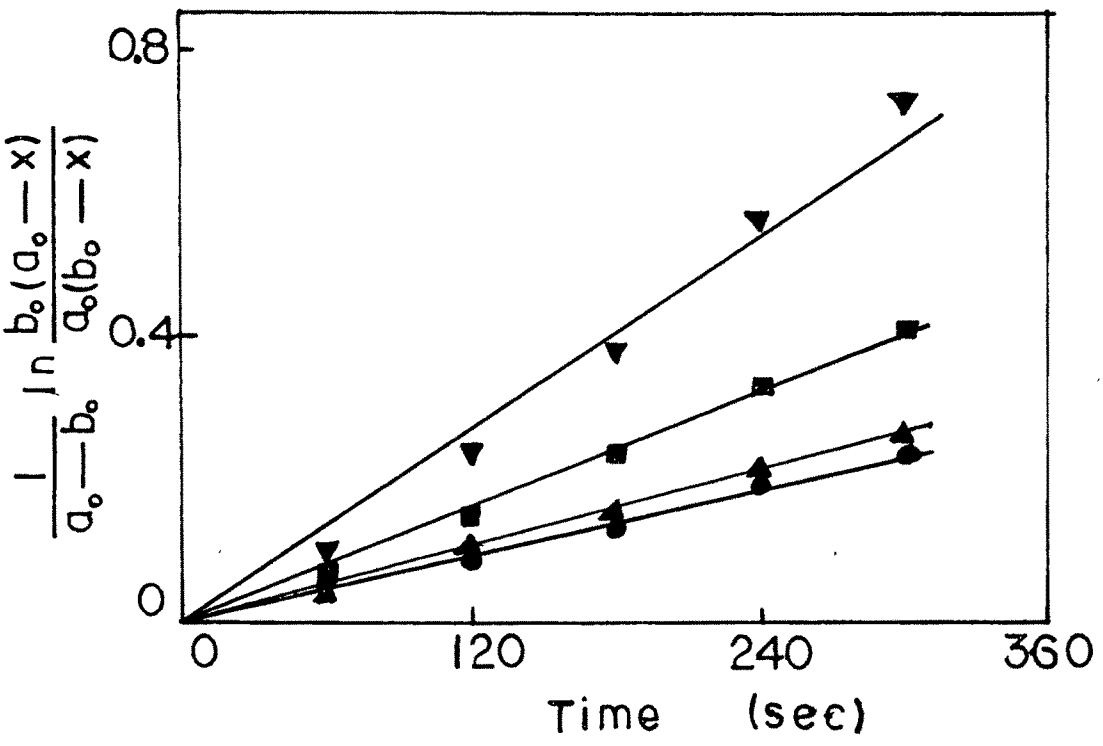

Fig.4.17i Plot of $\frac{1}{a_o - b_o} \ln \frac{b_o(a_o - x)}{a_o(b_o - x)}$ vs time for the iodination of acetone in SDS microemulsion system with no oil s/w=42.5/57.5. Symbols are the same as in Fig.4.17a.

Table 4.10 Second order rate constant k in $lmol^{-1}$ sec^{-1} for the iodination of acetone in SDS microemulsion. SDS concentration = 42.5%

O/W	Temperature ^0C			
	30	35	40	45
5/52.5	1.43×10^{-3}	2.09×10^{-3}	5.34×10^{-3}	5.65×10^{-3}
10/47.5	3.03×10^{-3}	4.44×10^{-3}	5.13×10^{-3}	8.33×10^{-3}
15/42.5	5.29×10^{-3}	5.41×10^{-3}	7.83×10^{-3}	8.41×10^{-3}
20/37.5	5.13×10^{-3}	6.06×10^{-3}	6.67×10^{-3}	1.07×10^{-2}
25/32.5	6.87×10^{-3}	7.60×10^{-3}	1.08×10^{-3}	1.06×10^{-2}
30/27.5	7.66×10^{-3}	8.04×10^{-3}	9.39×10^{-3}	1.21×10^{-2}
35/22.5	8.43×10^{-3}	9.02×10^{-3}	9.87×10^{-3}	1.23×10^{-2}
40/17.5	8.95×10^{-3}	9.82×10^{-3}	1.68×10^{-2}	1.31×10^{-2}
S/W=42.5/57.5	7.25×10^{-4}	1.84×10^{-3}	2.89×10^{-3}	5.43×10^{-3}
W (100%)	1.92×10^{-4}	2.77×10^{-4}	3.33×10^{-4}	4.8×10^{-4}

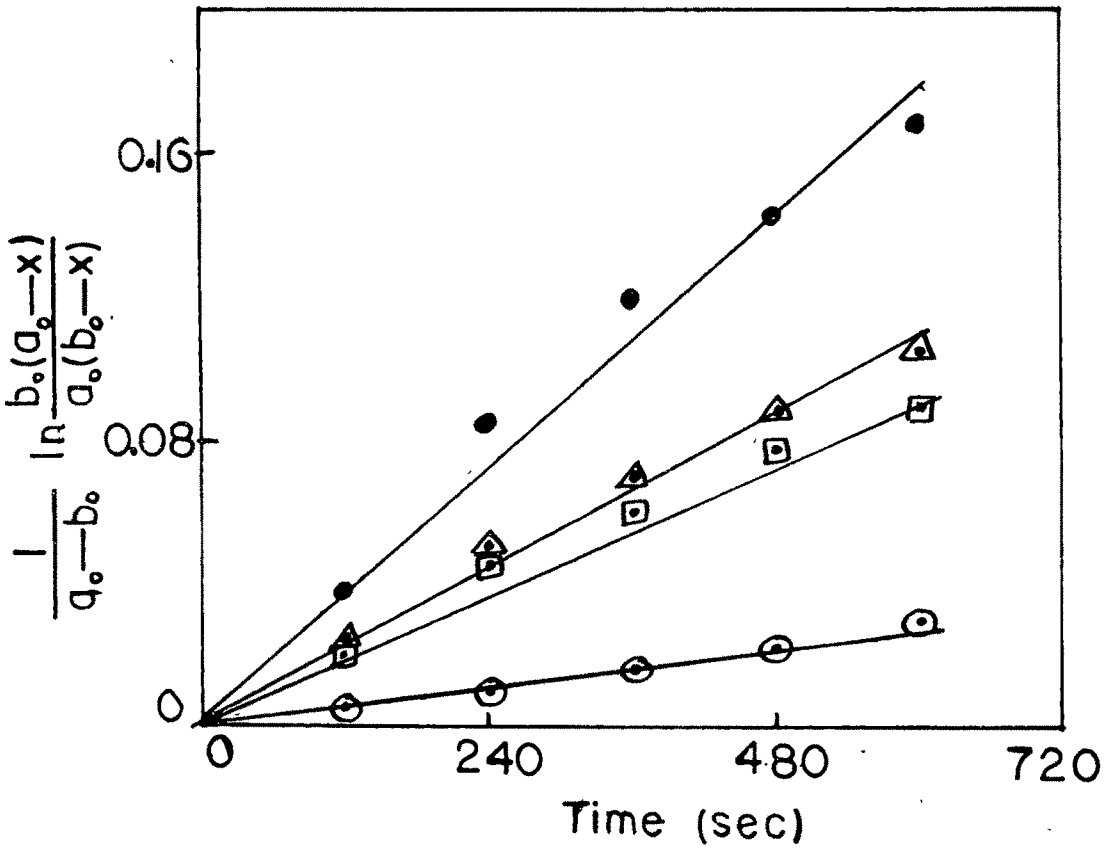

Fig.4.18a Plot of $\frac{1}{a_0-b_0} \ln \frac{b_0(a_0-x)}{a_0(b_0-x)}$ vs time for the iodination of acetone in TX100 microemulsion system with o/w=1/44.

⊙ 30°C; ⊡ 35°C; △ 40°C; ● 45°C

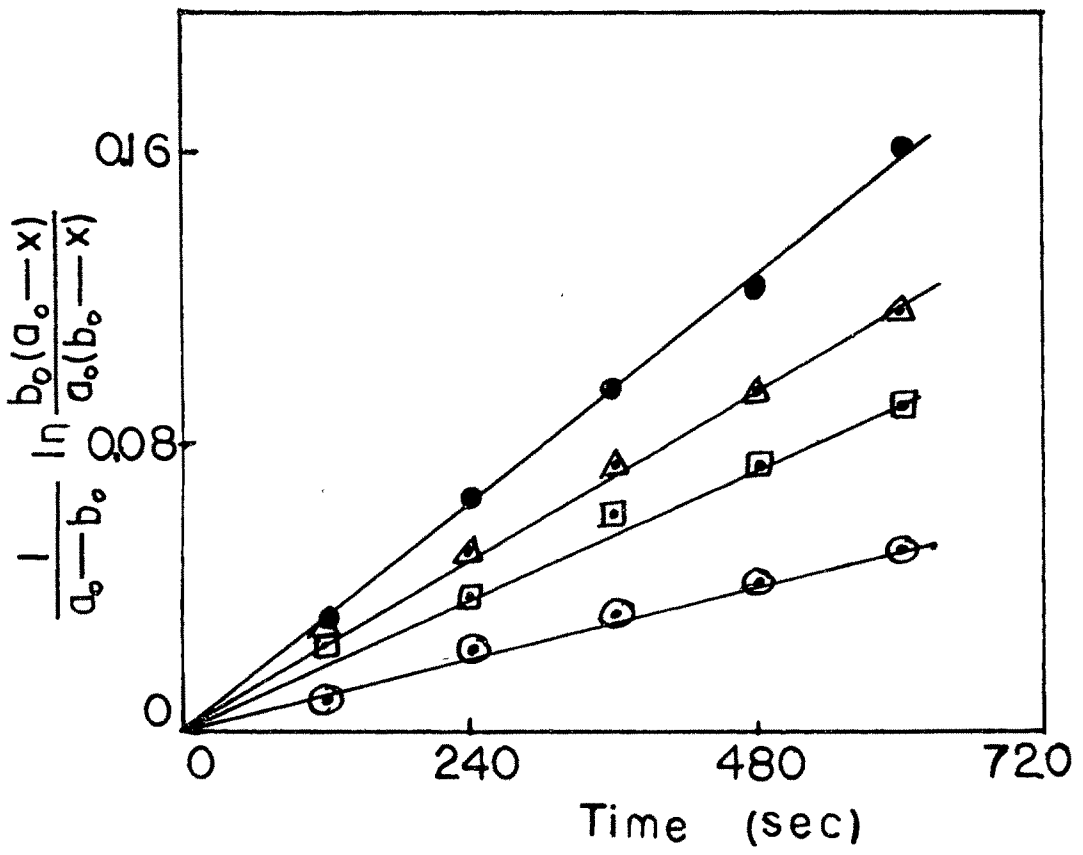

Fig.4.18b Plot of $\frac{1}{a_0-b_0} \ln \frac{b_0(a_0-x)}{a_0(b_0-x)}$ vs time for the iodination of acetone in TX100 microemulsion system with o/w=5/40. Symbols are the same as in Fig.4.18a.

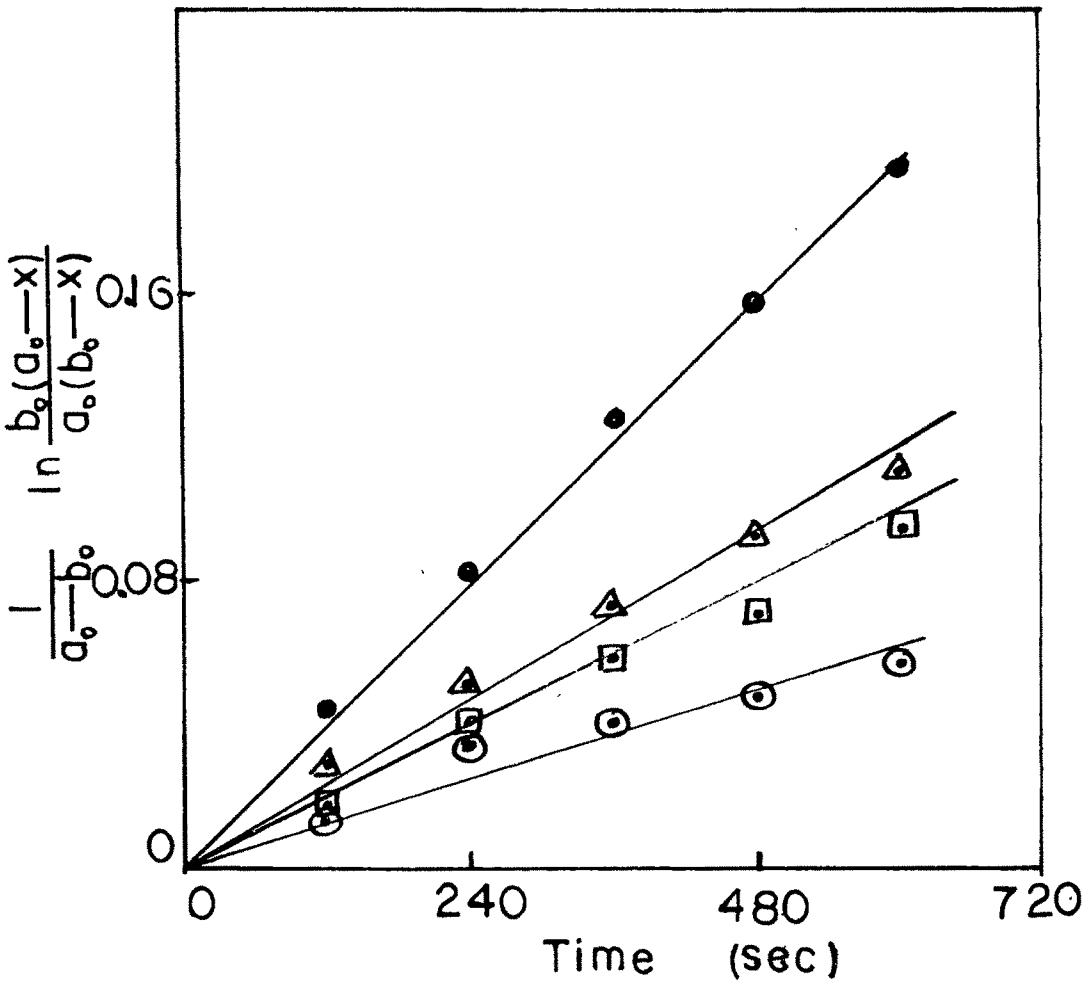

Fig.4.18c Plot of $\frac{1}{a_o-b_o} \ln \frac{b_o(a_o-x)}{a_o(b_o-x)}$ vs time for the iodination of acetone in TX100 microemulsion system with o/w=10/35. Symbols are the same as in Fig.4.18a.

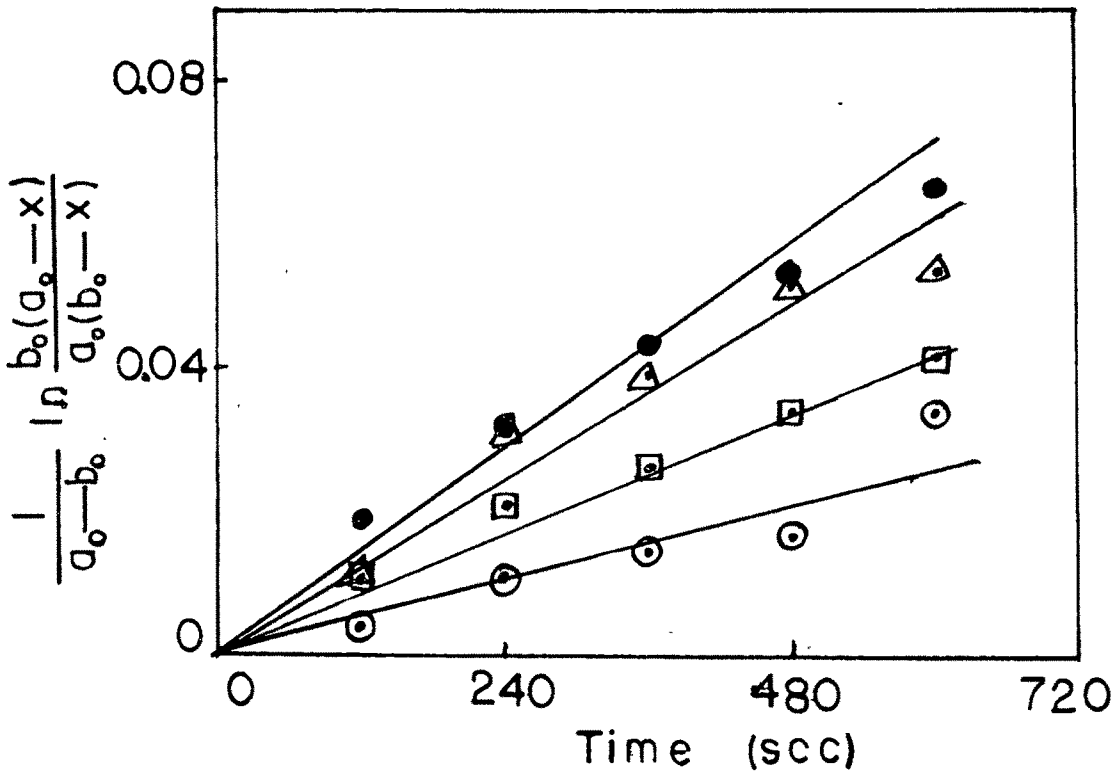

Fig.4.18d Plot of $\frac{1}{a_o-b_o} \ln \frac{b_o(a_o-x)}{a_o(b_o-x)}$ vs time for the iodination of acetone in TX100 microemulsion system with o/w=15/30. Symbols are the same as in Fig.4.18a.

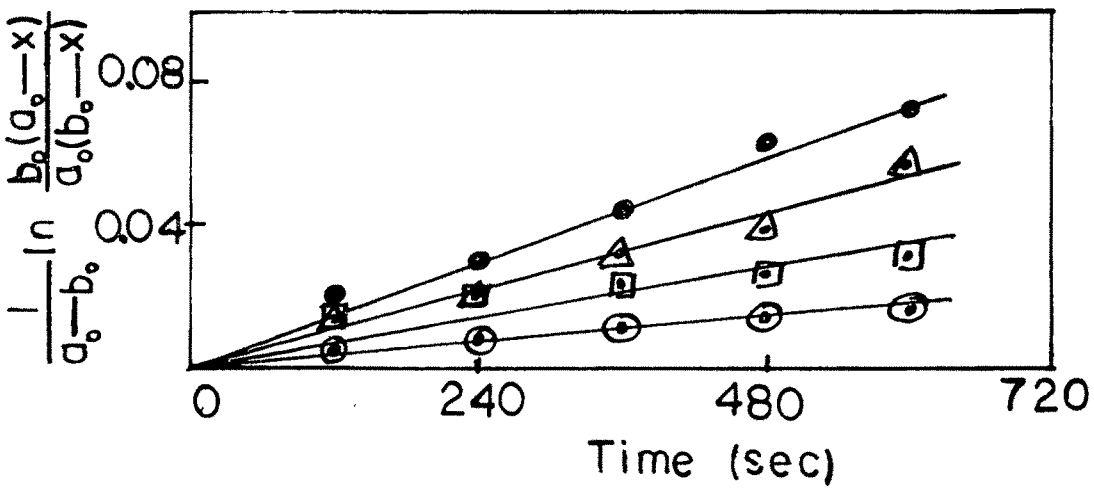

Fig.4.18e Plot of $\frac{1}{a_o-b_o} \ln \frac{b_o(a_o-x)}{a_o(b_o-x)}$ vs time for the iodination of acetone in TX100 microemulsion system with o/w=20/35. Symbols are the same as in Fig.4.18a.

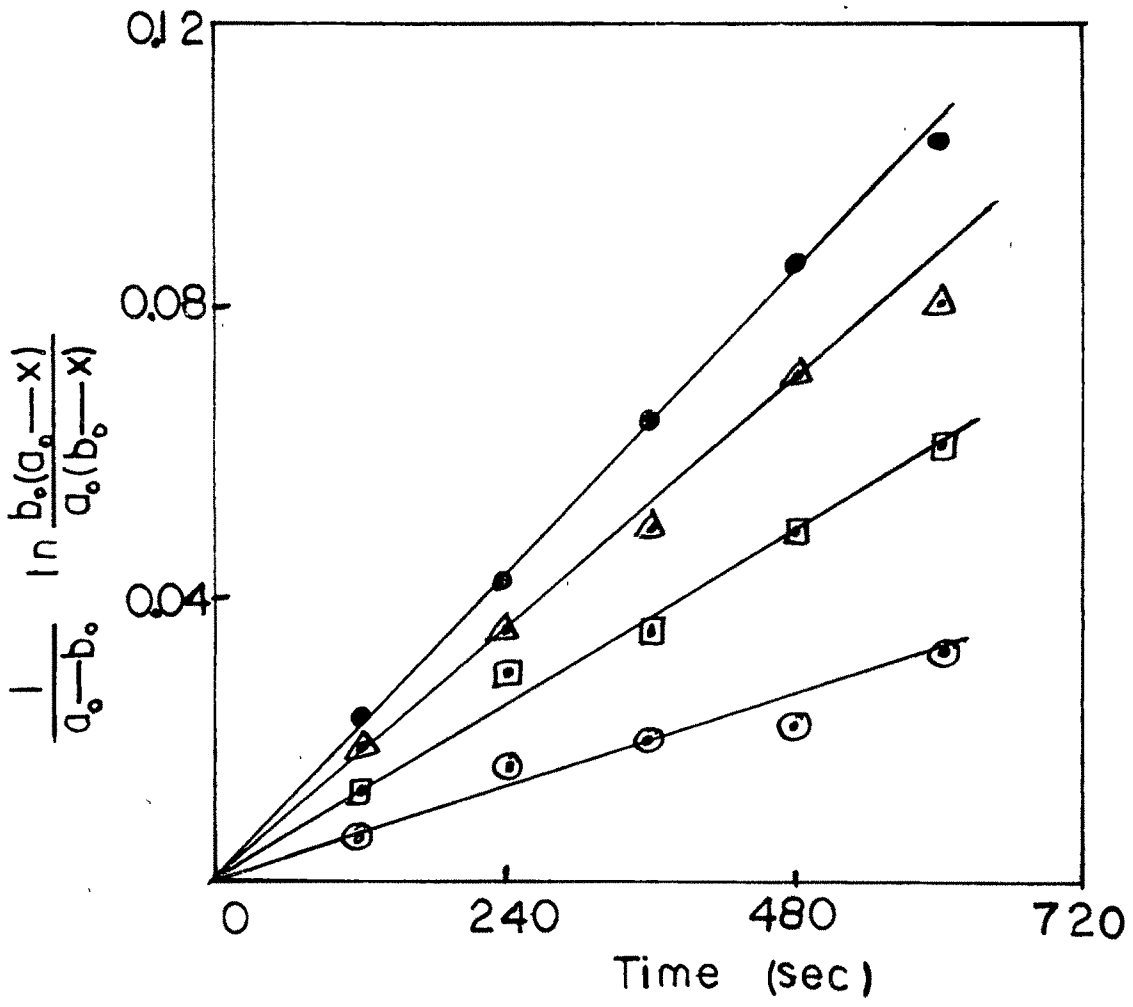

Fig.4.18f Plot of $\frac{1}{a_o-b_o} \ln \frac{b_o(a_o-x)}{a_o(b_o-x)}$ vs time for the iodination of acetone in TX100 microemulsion system with o/w=25/20. Symbols are the same as in Fig.4.18a.

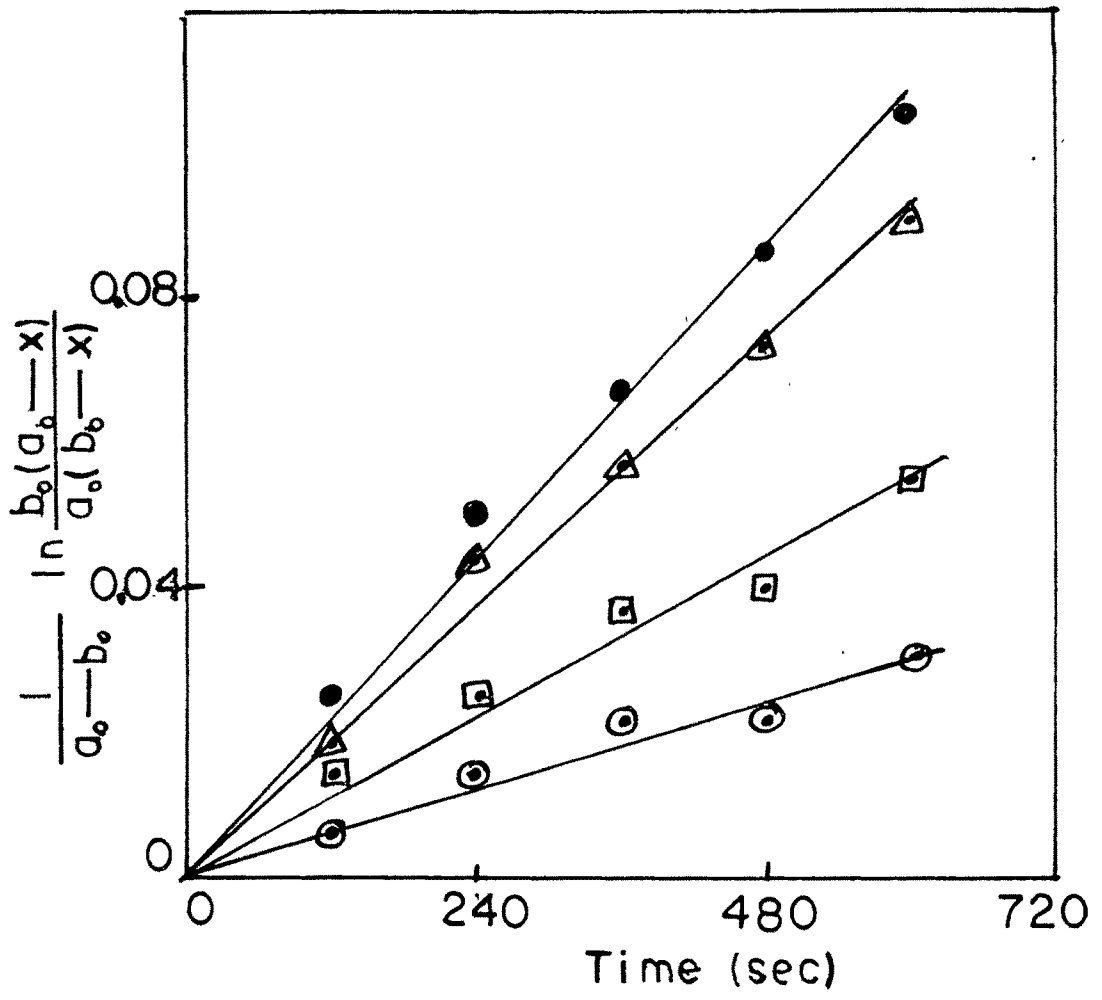

Fig.4.18g Plot of $\frac{1}{a_o-b_o} \ln \frac{b_o(a_o-x)}{a_o(b_o-x)}$ vs time for the iodination of acetone in TX100 microemulsion system with o/w=30/15. Symbols are the same as in Fig.4.18a.

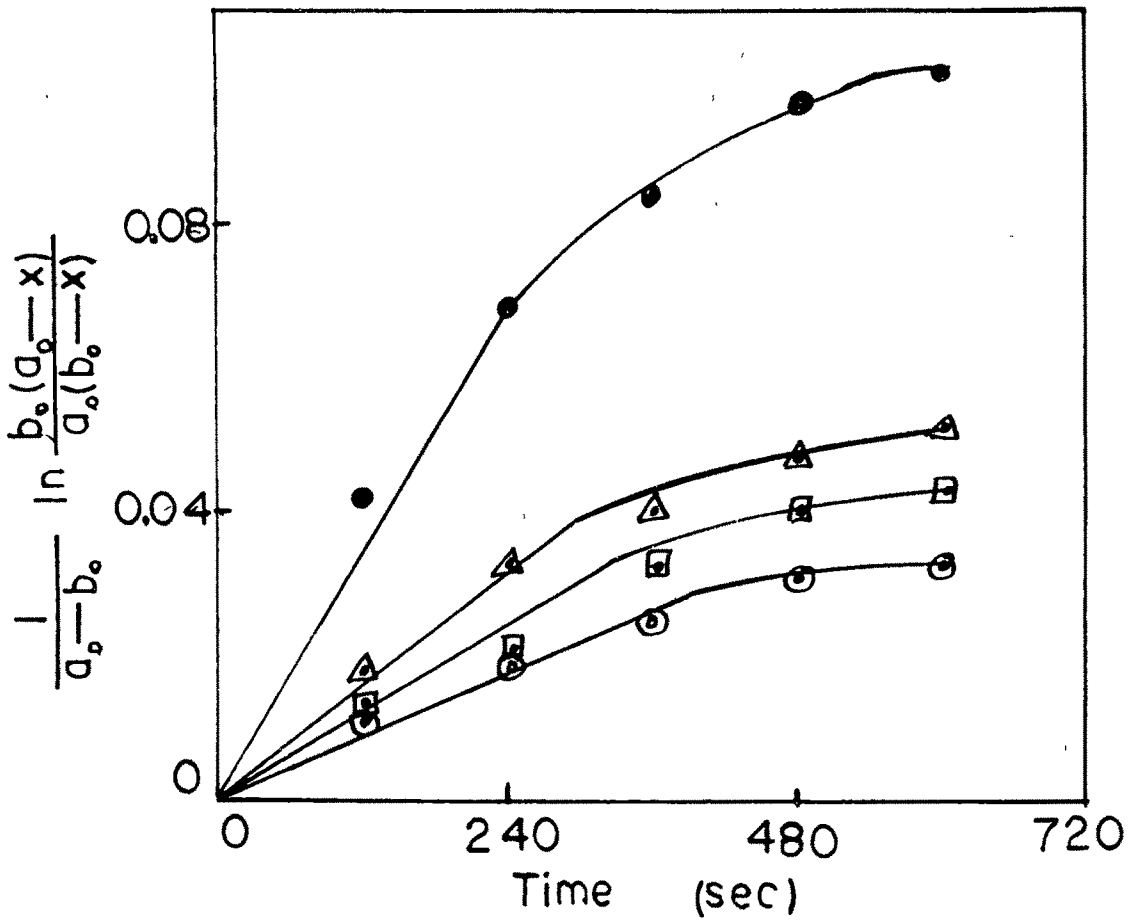

Fig.4.18h Plot of $\frac{1}{a_o-b_o} \ln \frac{b_o(a_o-x)}{a_o(b_o-x)}$ vs time for the iodination of acetone in TX100 microemulsion system with o/w=35/10. Symbols are the same as in Fig.4.18a.

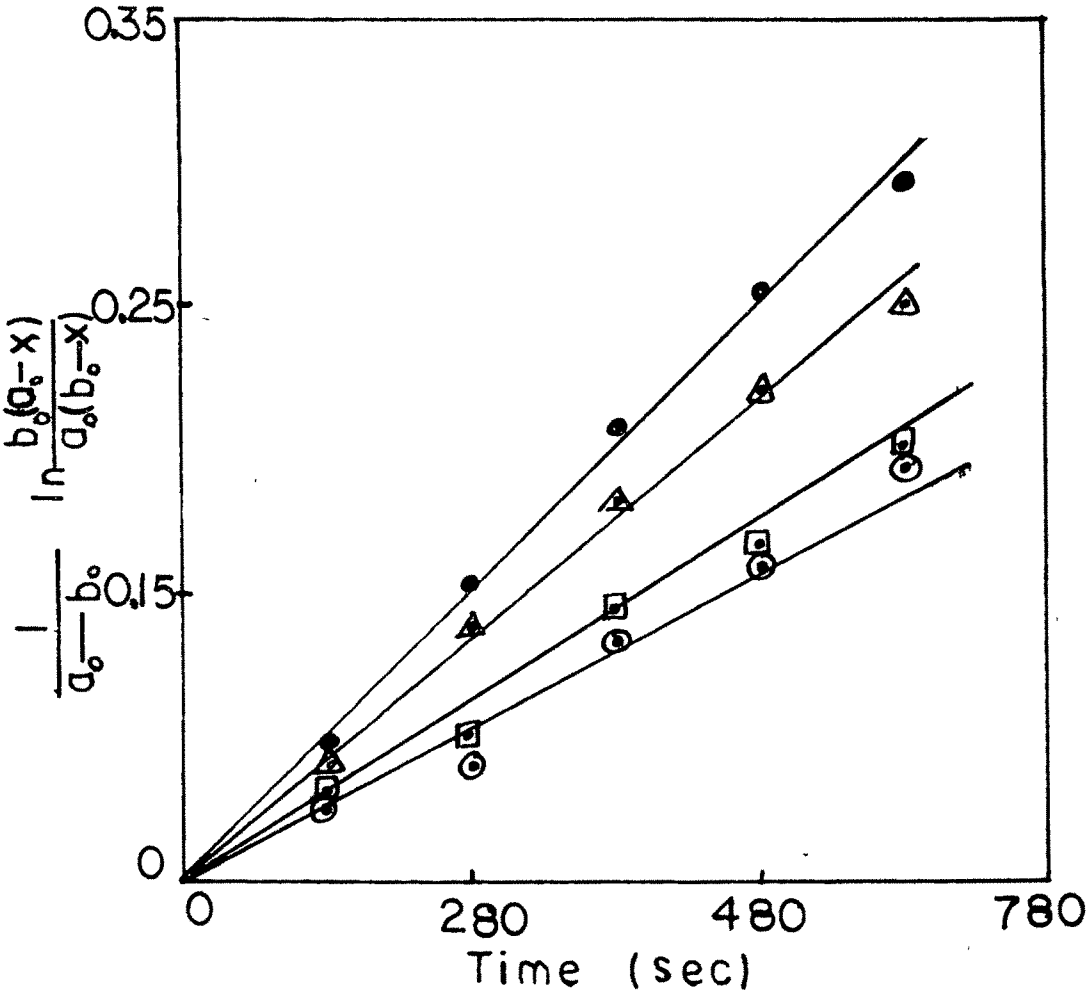

Fig.4.18i Plot of $\frac{1}{a_o-b_o} \ln \frac{b_o(a_o-x)}{a_o(b_o-x)}$ vs time for the iodination of acetone in TX100 microemulsion system with o/w=40/5. Symbols are the same as in Fig.4.18a.

Table 4.11 **Second order rate constant k in l mol^{-1} sec^{-1} for the iodination of acetone in TX100 microemulsion. TX100 concentration = 55%.**

	Temperature ^0C			
O/W	30	35	40	45
1/44	5.22×10^{-5}	1.39×10^{-4}	1.85×10^{-4}	2.38×10^{-4}
5/40	7.93×10^{-5}	1.52×10^{-4}	1.85×10^{-4}	2.78×10^{-4}
10/35	9.27×10^{-5}	1.67×10^{-4}	1.85×10^{-4}	3.33×10^{-4}
15/30	4.17×10^{-5}	6.95×10^{-5}	1.04×10^{-4}	1.19×10^{-4}
20/25	3.57×10^{-5}	6.17×10^{-5}	9.2×10^{-5}	1.19×10^{-4}
25/30	4.17×10^{-5}	5.0×10^{-5}	1.0×10^{-4}	1.18×10^{-4}
30/15	4.92×10^{-5}	6.33×10^{-5}	6.7×10^{-5}	1.175×10^{-4}
35/10	4.67×10^{-5}	6.7×10^{-5}	1.03×10^{-4}	1.35×10^{-4}
40/5	2.85×10^{-4}	3.17×10^{-4}	3.52×10^{-4}	3.93×10^{-4}
S/W = 55/45	4.65×10^{-4}	4.9×10^{-4}	5.28×10^{-4}	6.42×10^{-4}

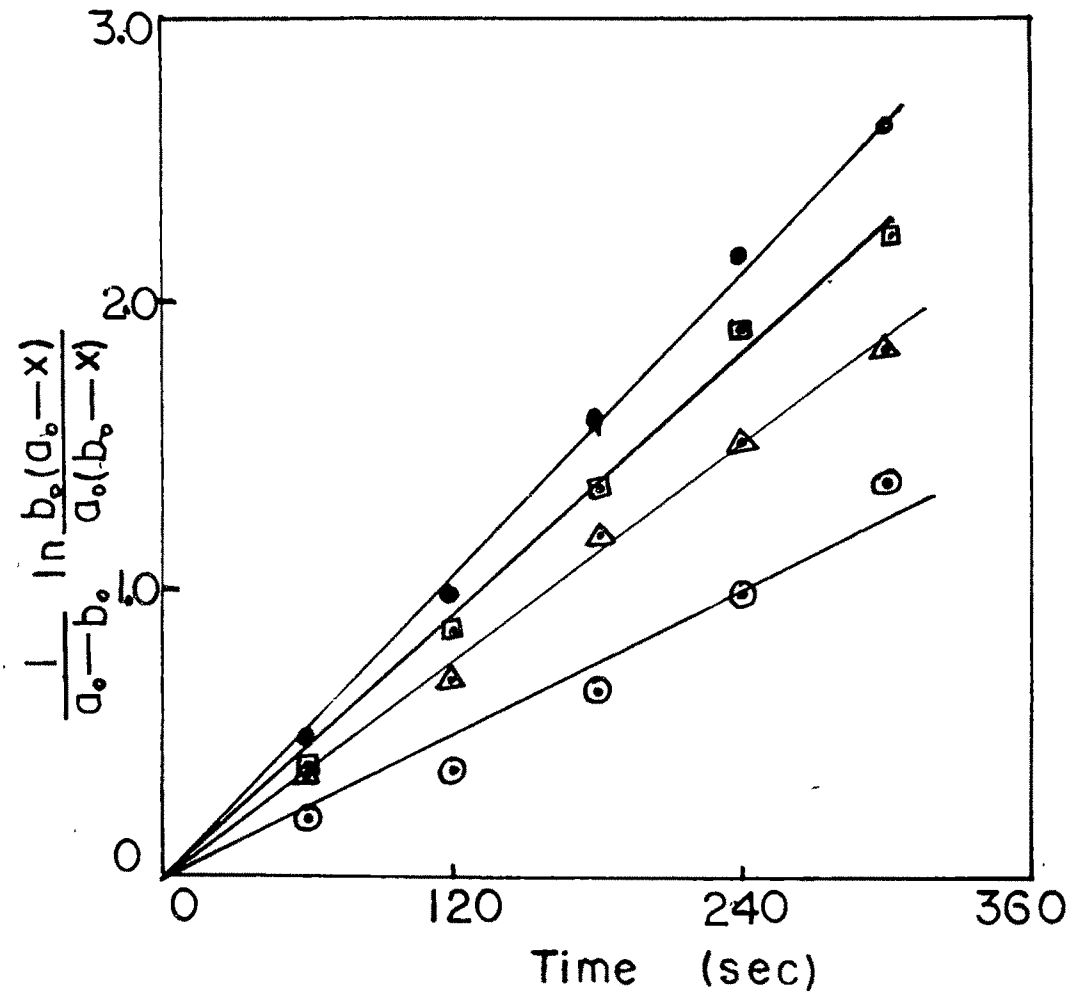

Fig.4.19a Plot of $\frac{1}{a_o-b_o} \ln \frac{b_o(a_o-x)}{a_o(b_o-x)}$ vs time for the iodination of acetone in SDS microemulsion system with o/w=5/52.5 by applying the correction factor for partition coefficient. ⊙ 30°C; △ 35°C; ⊡ 40°C; ● 45°C

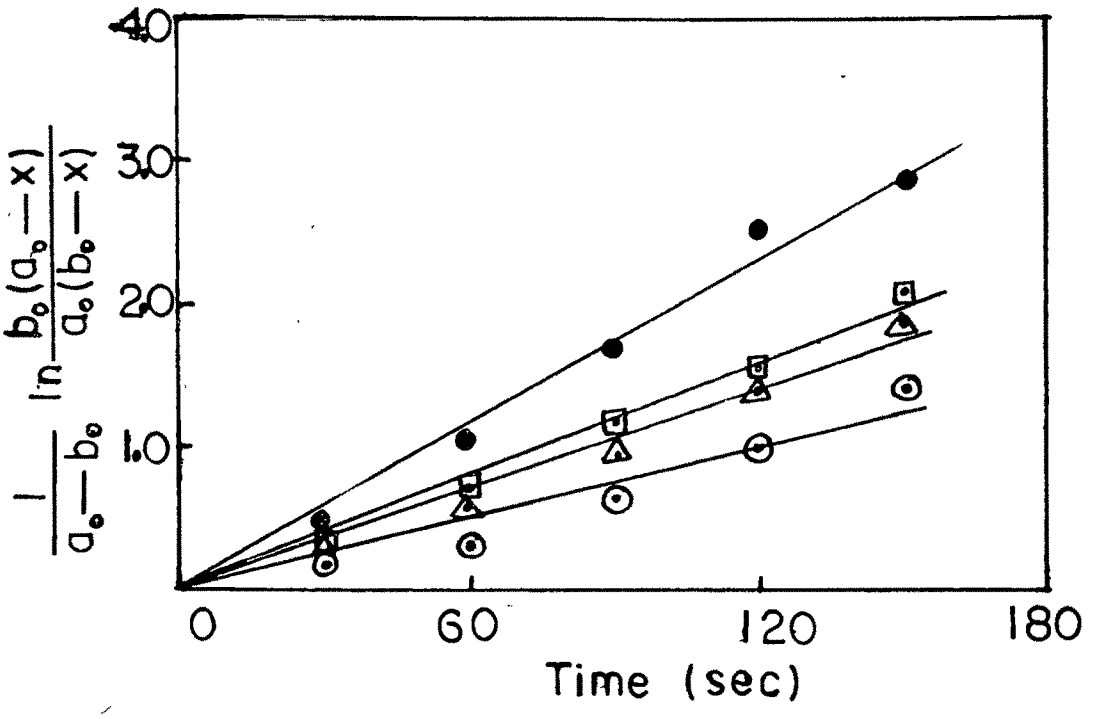

Fig.4.19b Plot of $\frac{1}{a_o-b_o}\ln\frac{b_o(a_o-x)}{a_o(b_o-x)}$ vs time for the iodination of acetone in SDS microemulsion system with o/w=10/47.5 by applying the correction factor for partition coefficient. Symbols are the same as in Fig.4.19a.

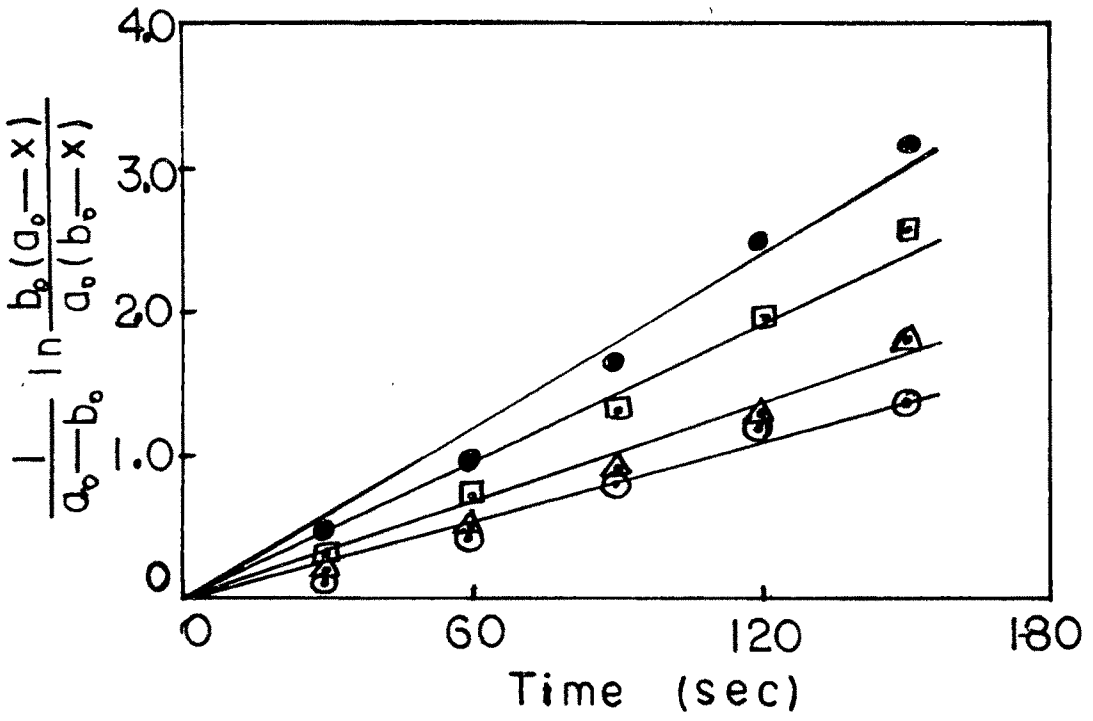

Fig.4.19c Plot of $\frac{1}{a_o-b_o} \ln \frac{b_o(a_o-x)}{a_o(b_o-x)}$ vs time for the iodination of acetone in SDS microemulsion system with o/w=15/42.5 by applying the correction factor for partition coefficient. Symbols are the same as in Fig.4.19a.

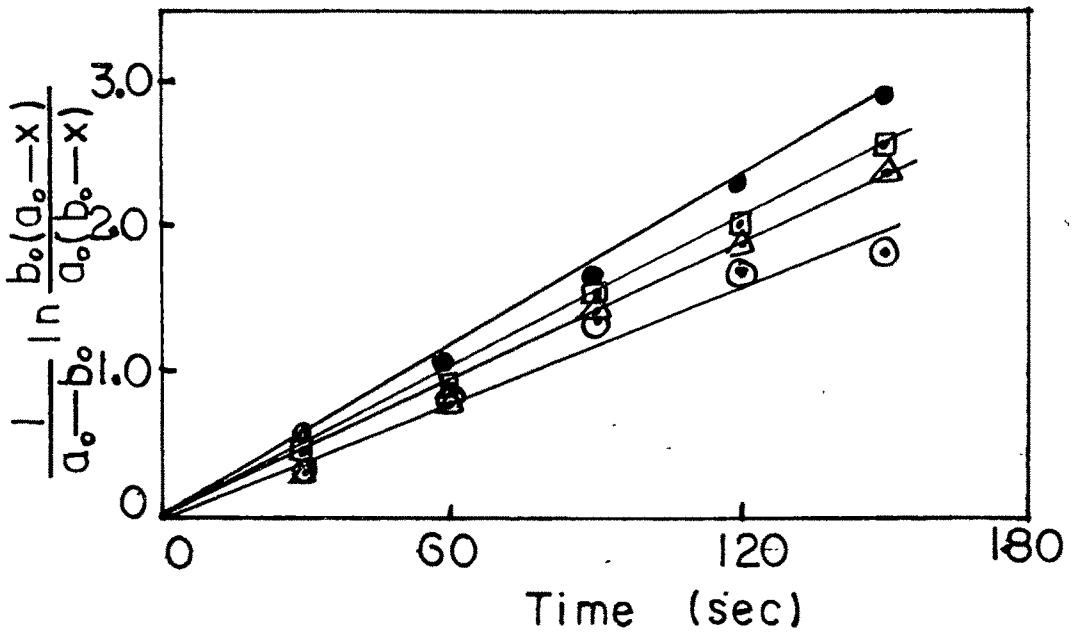

Fig.4.19d Plot of $\frac{1}{a_o-b_o} \ln \frac{b_o(a_o-x)}{a_o(b_o-x)}$ vs time for the iodination of acetone in SDS microemulsion system with o/w=20/37.5 by applying the correction factor for partition coefficient. Symbols are the same as in Fig.4.19a.

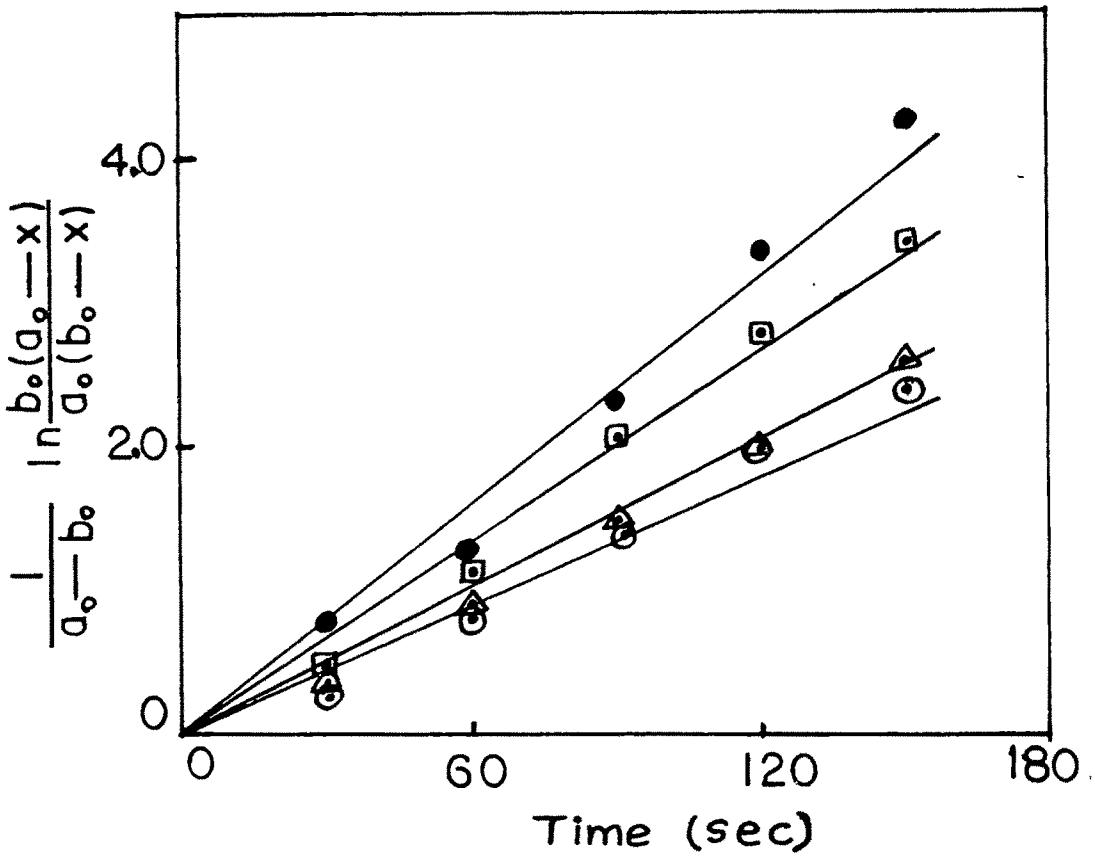

Fig.4.19e Plot of $\frac{1}{a_o - b_o} \ln \frac{b_o(a_o - x)}{a_o(b_o - x)}$ vs time for the iodination of acetone in SDS microemulsion system with o/w=25/32.5 by applying the correction factor for partition coefficient. Symbols are the same as in Fig.4.19a.

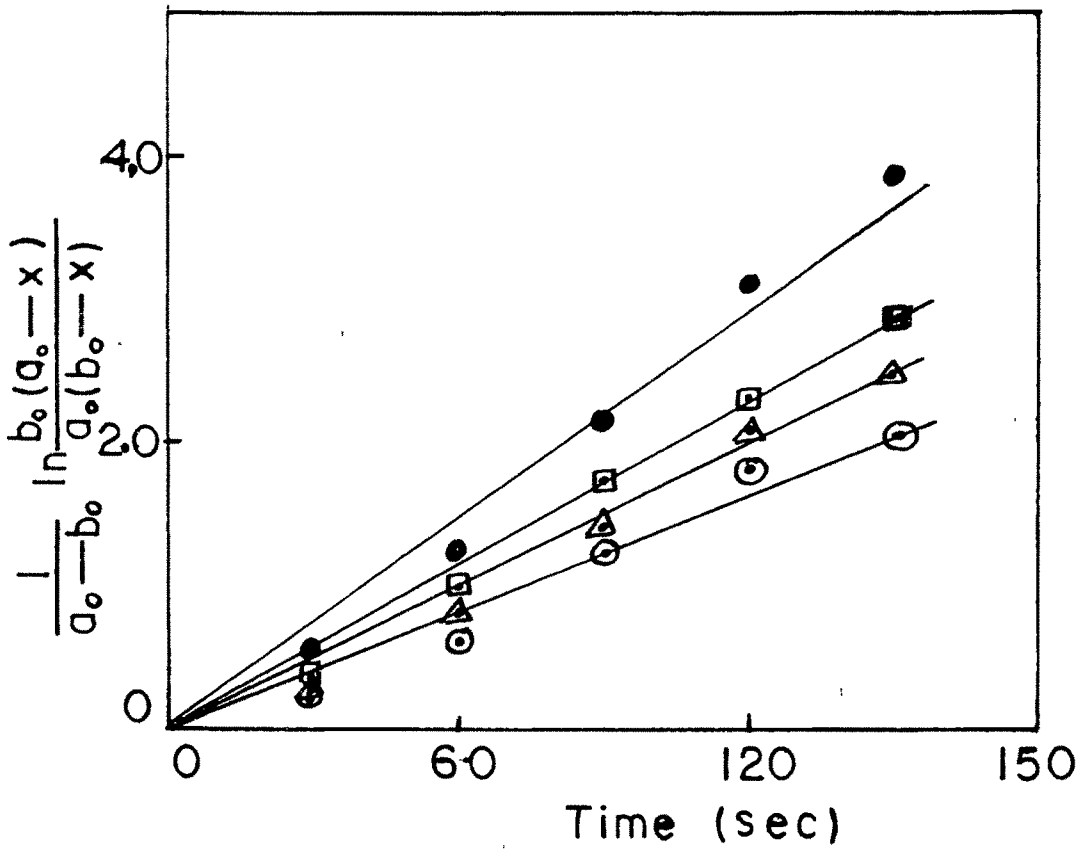

Fig.4.19f Plot of $\frac{1}{a_o-b_o}\ln\frac{b_o(a_o-x)}{a_o(b_o-x)}$ vs time for the iodination of acetone in SDS microemulsion system with o/w=30/27.5 by applying the correction factor for partition coefficient. Symbols are the same as in Fig.4.19a.

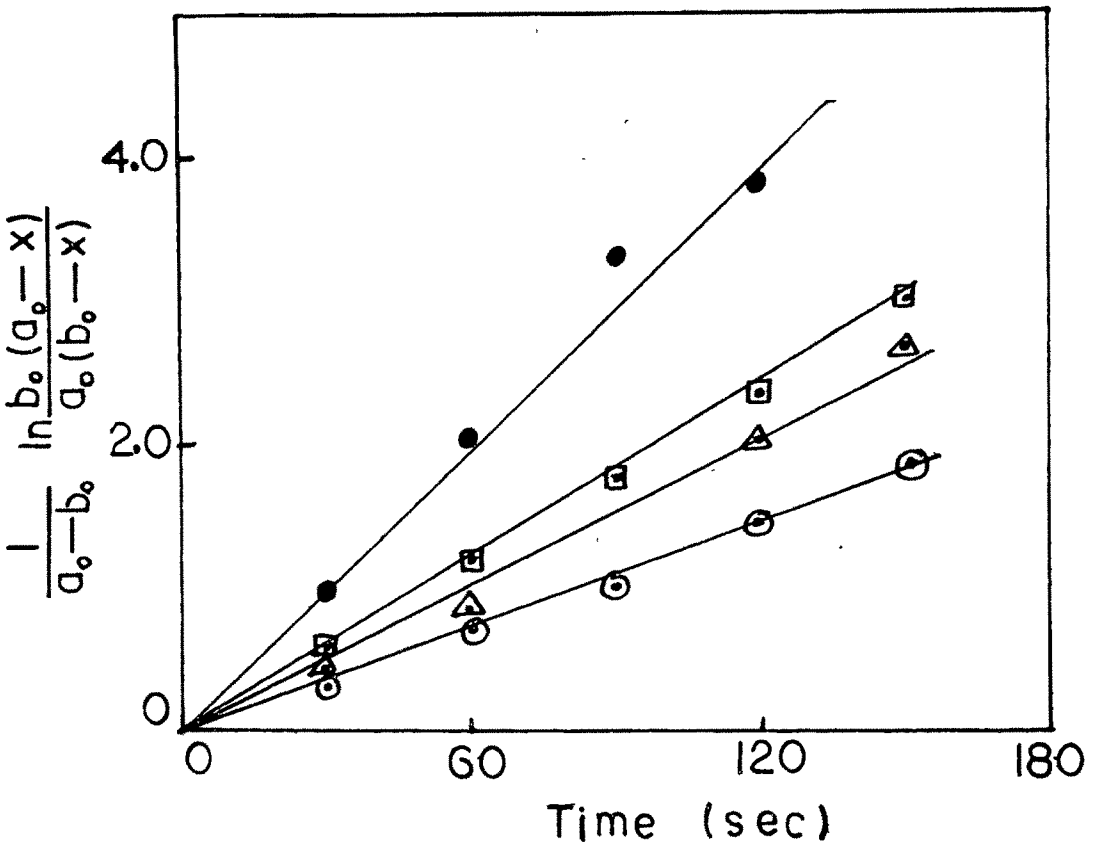

Fig.4.19g Plot of $\frac{1}{a_o-b_o} \ln \frac{b_o(a_o-x)}{a_o(b_o-x)}$ vs time for the iodination of acetone in SDS microemulsion system with o/w=35/22.5 by applying the correction factor for partition coefficient. Symbols are the same as in Fig.4.19a.

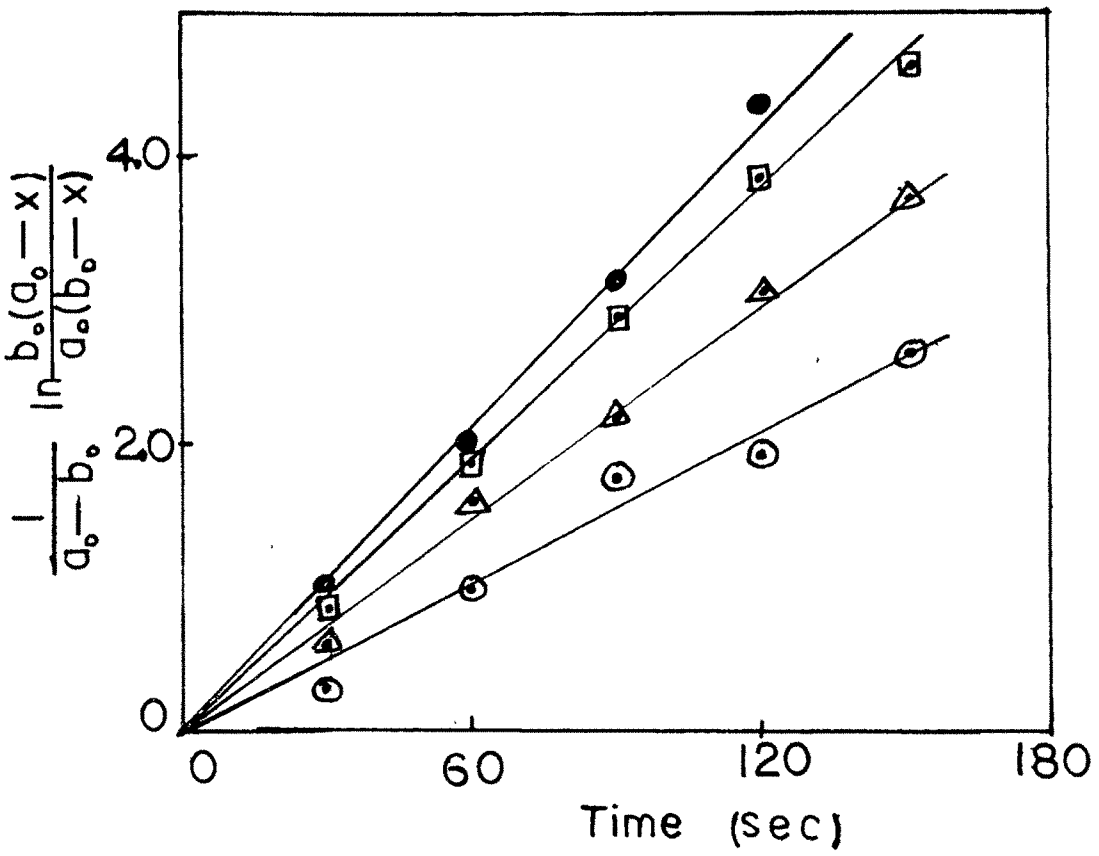

Fig.4.19h Plot of $\frac{1}{a_0-b_0}\ln\frac{b_0(a_0-x)}{a_0(b_0-x)}$ vs time for the iodination of acetone in SDS microemulsion system with o/w=40/17.5 by applying the correction factor for partition coefficient. Symbols are the same as in Fig.4.19a.

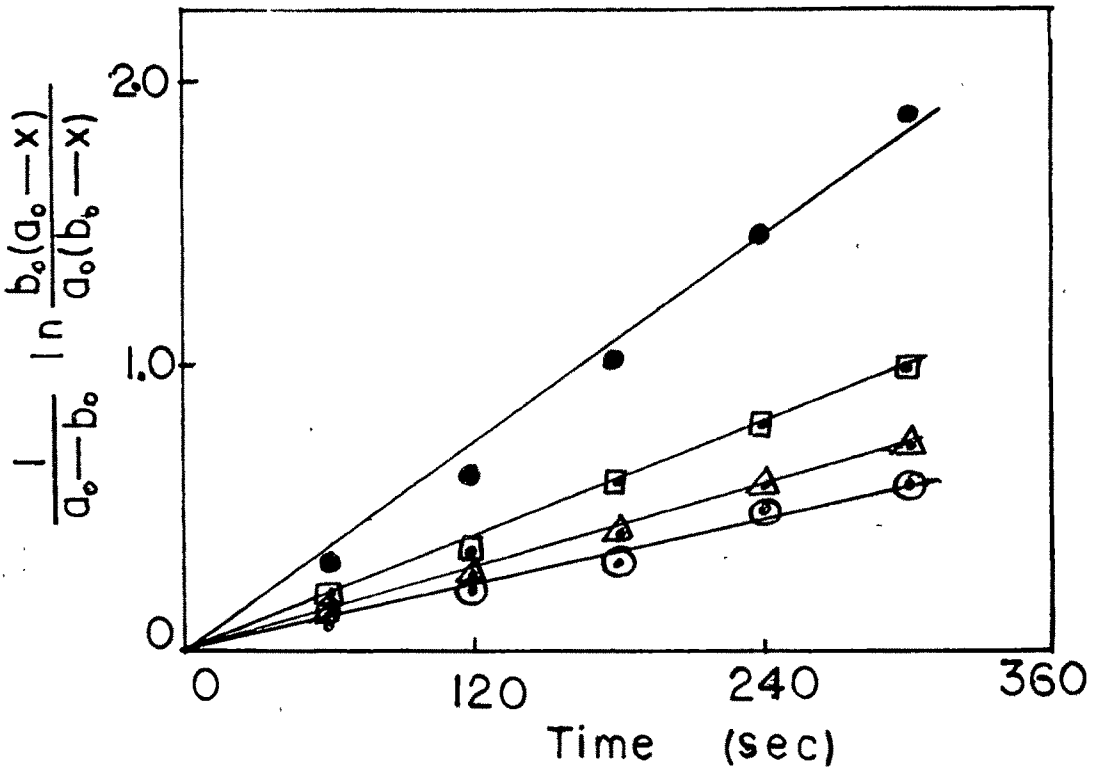

Fig.4.19i Plot of $\frac{1}{a_o-b_o} \ln \frac{b_o(a_o-x)}{a_o(b_o-x)}$ vs time for the iodination of acetone in SDS microemulsion system with no oil s/w=47.5/52.5 by applying the correction factor for partition coefficient. Symbols are the same as in Fig.4.19a.

Table 4.12 **Rate constant k ($lmol^{-1}$ sec^{-1}) for the iodination of acetone in SDS microemulsion by applying the correction factor for partition coefficient. (see text)**

O/W	Temperature ^0C			
	30	35	40	45
5/52.5	8.33×10^{-3}	1.19×10^{-2}	1.39×10^{-2}	1.39×10^{-2}
10/47.5	8.33×10^{-3}	1.04×10^{-2}	1.28×10^{-2}	1.85×10^{-2}
15/42.5	8.77×10^{-3}	1.11×10^{-2}	1.52×10^{-2}	1.85×10^{-2}
20/37.5	1.19×10^{-2}	1.52×10^{-2}	1.85×10^{-2}	2.08×10^{-2}
25/32.5	1.52×10^{-2}	1.67×10^{-2}	2.08×10^{-2}	2.83×10^{-2}
30/27.5	1.28×10^{-2}	1.67×10^{-2}	2.08×10^{-2}	2.83×10^{-2}
35/22.5	1.28×10^{-2}	1.67×10^{-2}	2.08×10^{-2}	2.78×10^{-2}
40/17.5	1.67×10^{-2}	2.08×10^{-2}	2.78×10^{-2}	3.33×10^{-2}
S/W= 42.5/57.5	3.97×10^{-3}	4.38×10^{-3}	6.41×10^{-3}	1.19×10^{-2}

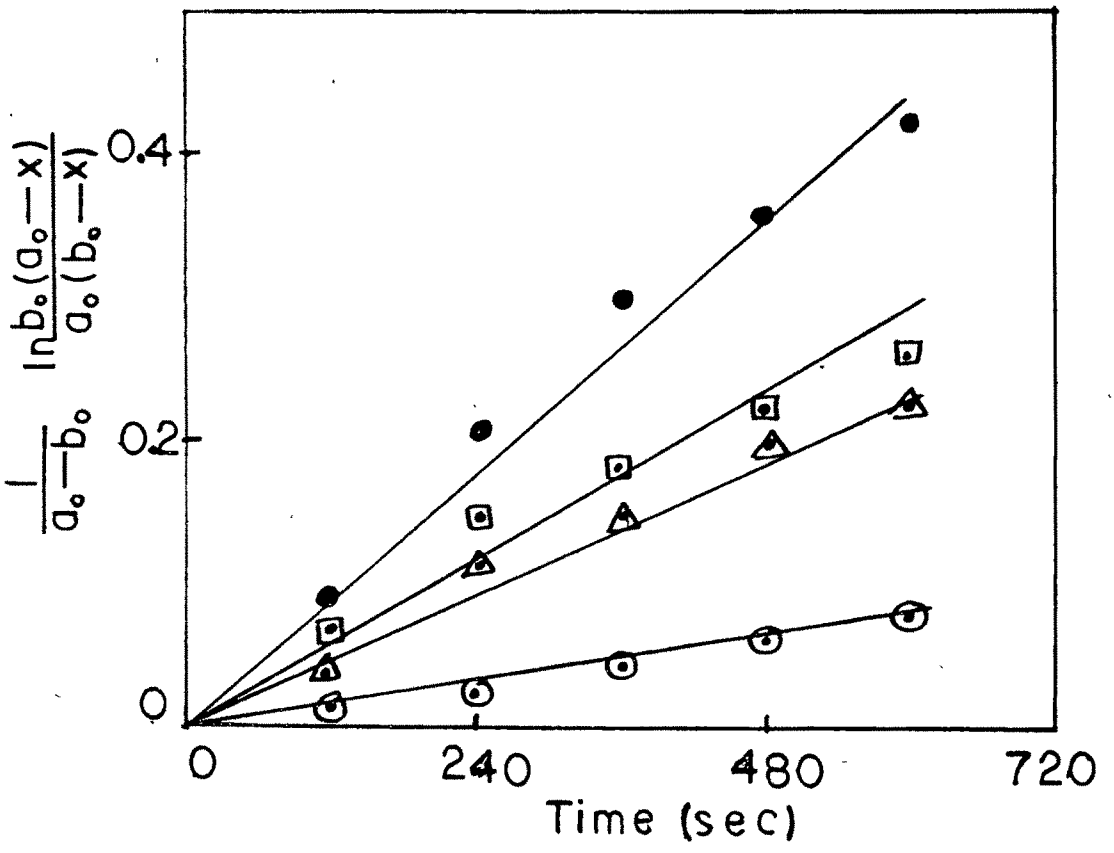

Fig.4.20a Plot of $\frac{1}{a_o-b_o}\ln\frac{b_o(a_o-x)}{a_o(b_o-x)}$ vs time for the iodination of acetone in TX100 microemulsion system with o/w=1/44 by applying the correction factor. ⊙ 30°C; ◬ 35°C; ⊡ 40°C; ● 45°C

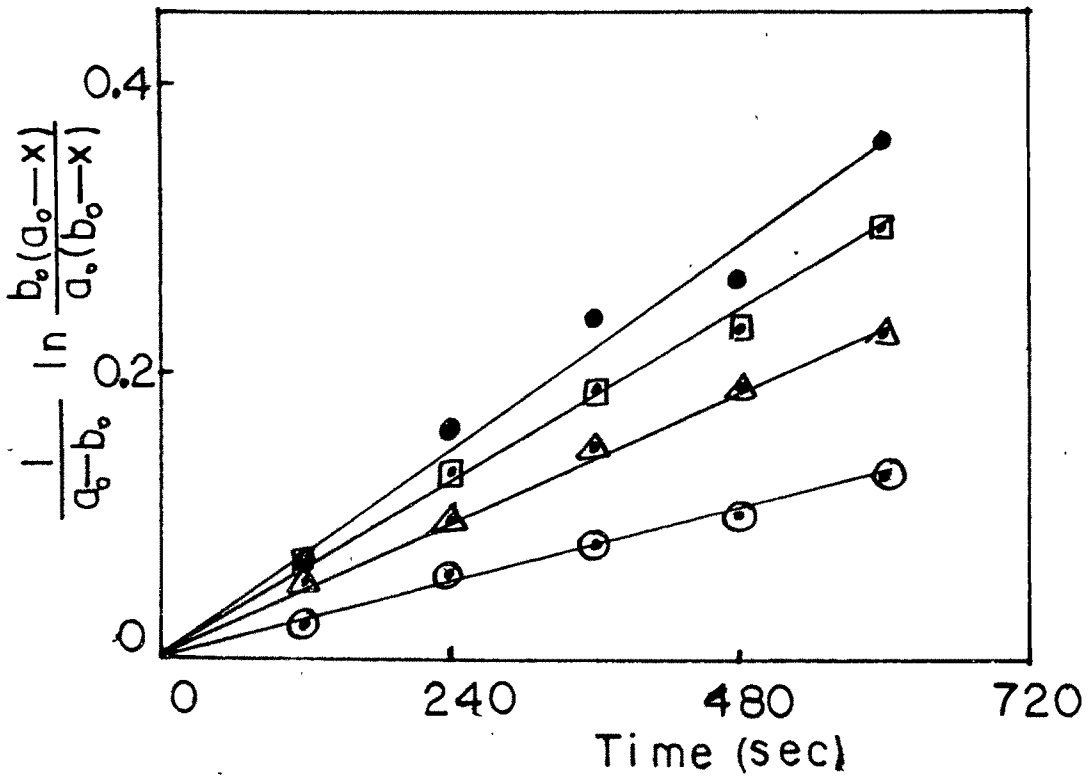

Fig.4.20b Plot of $\frac{1}{a_o-b_o} \ln \frac{b_o(a_o-x)}{a_o(b_o-x)}$ vs time for the iodination of acetone in TX100 microemulsion system with o/w=5/40 by applying the correction factor. Symbols are the same as in Fig.4.20a.

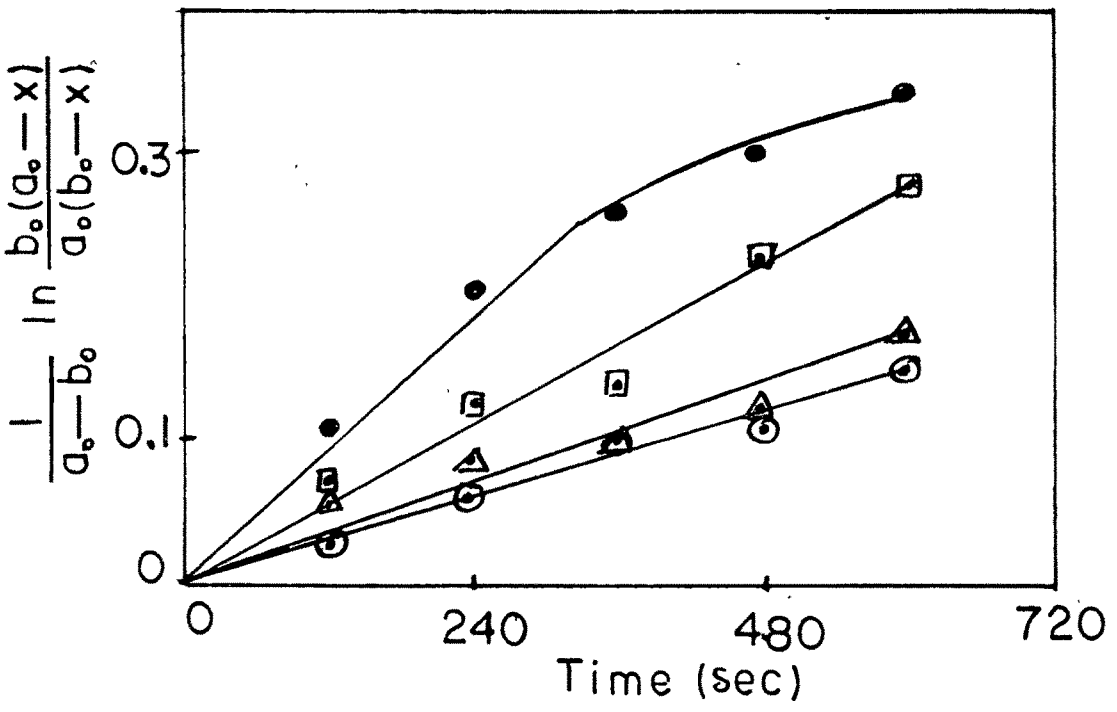

Fig.4.20c Plot of $\frac{1}{a_o - b_o} \ln \frac{b_o(a_o - x)}{a_o(b_o - x)}$ vs time for the iodination of acetone in TX100 microemulsion system with o/w=10/35 by applying the correction factor. Symbols are the same as in Fig.4.20a.

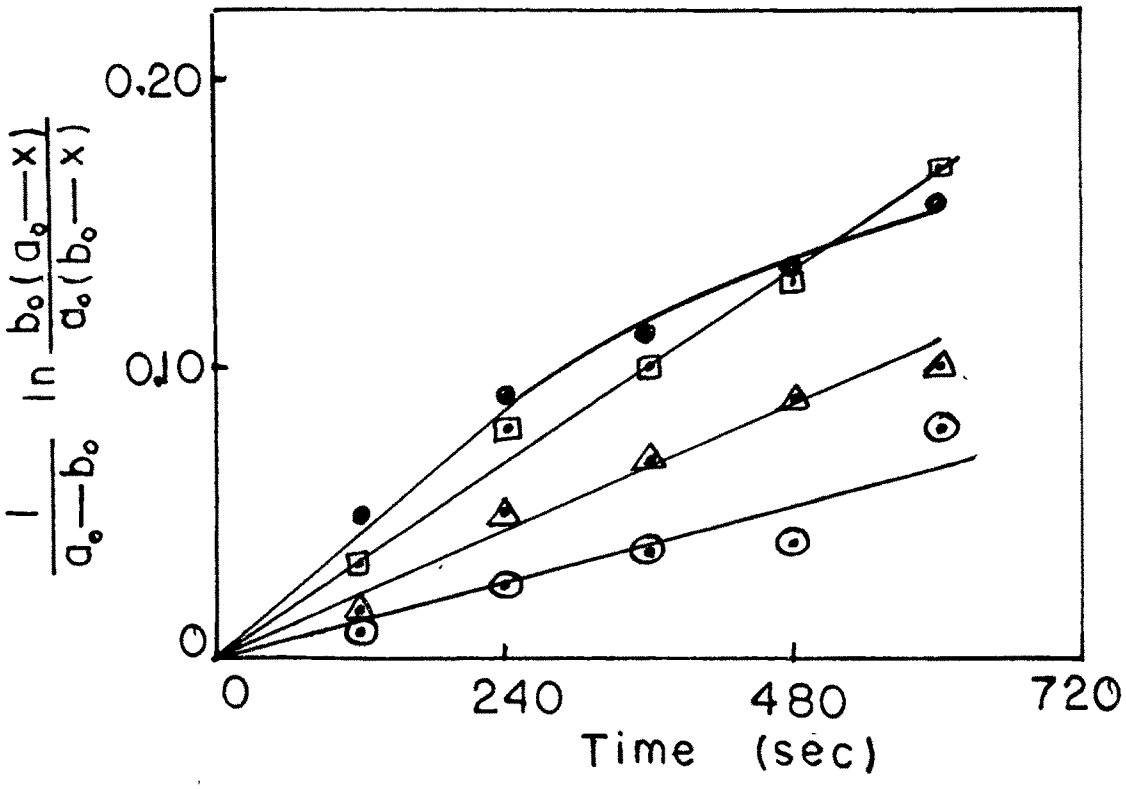

Fig.4.20d Plot of $\frac{1}{a_o-b_o} \ln \frac{b_o(a_o-x)}{a_o(b_o-x)}$ vs time for the iodination of acetone in TX100 microemulsion system with o/w=15/30 by applying the correction factor. Symbols are the same as in Fig.4.20a.

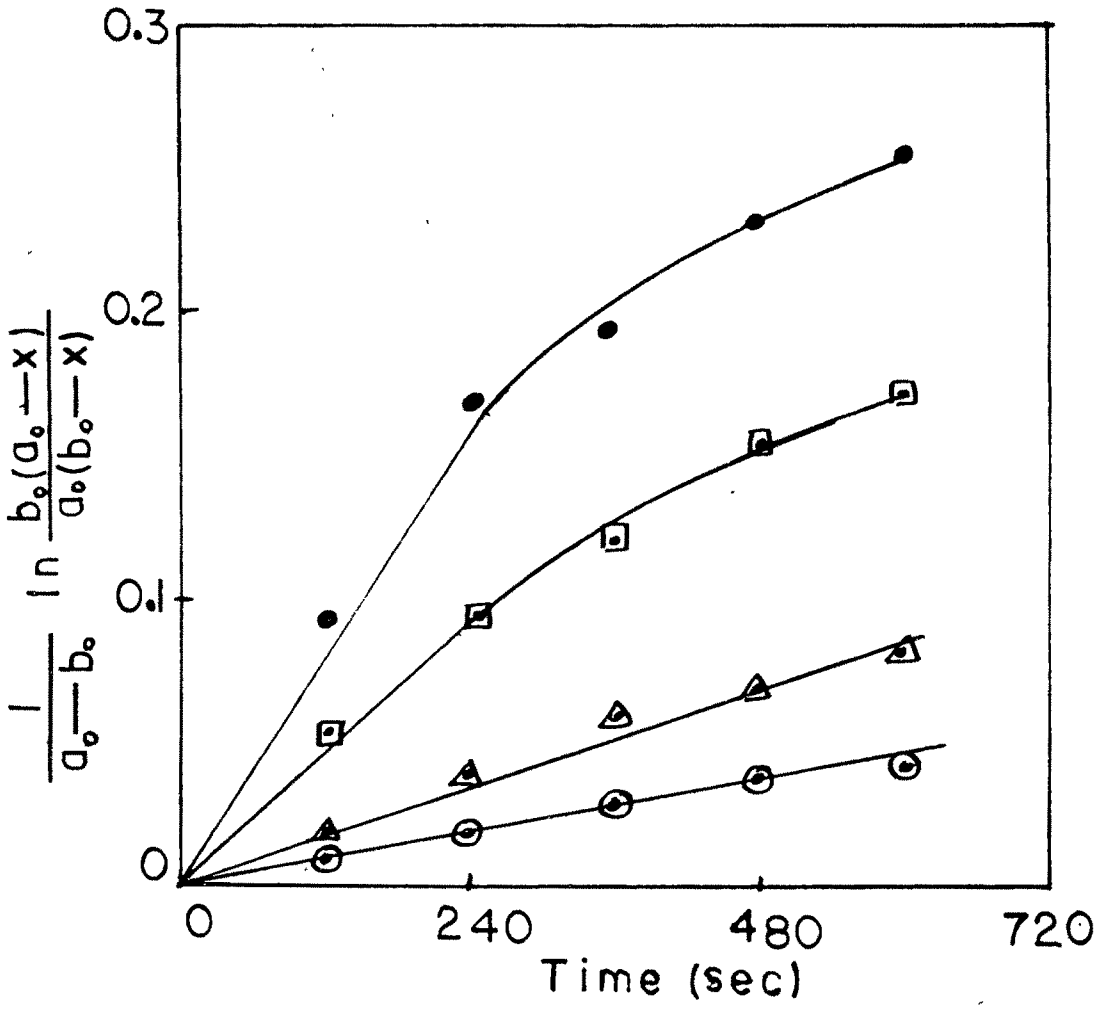

Fig.4.20e Plot of $\frac{1}{a_o - b_o} \ln \frac{b_o(a_o - x)}{a_o(b_o - x)}$ vs time for the iodination of acetone in TX100 microemulsion system with o/w=20/25 by applying the correction factor. Symbols are the same as in Fig.4.20a.

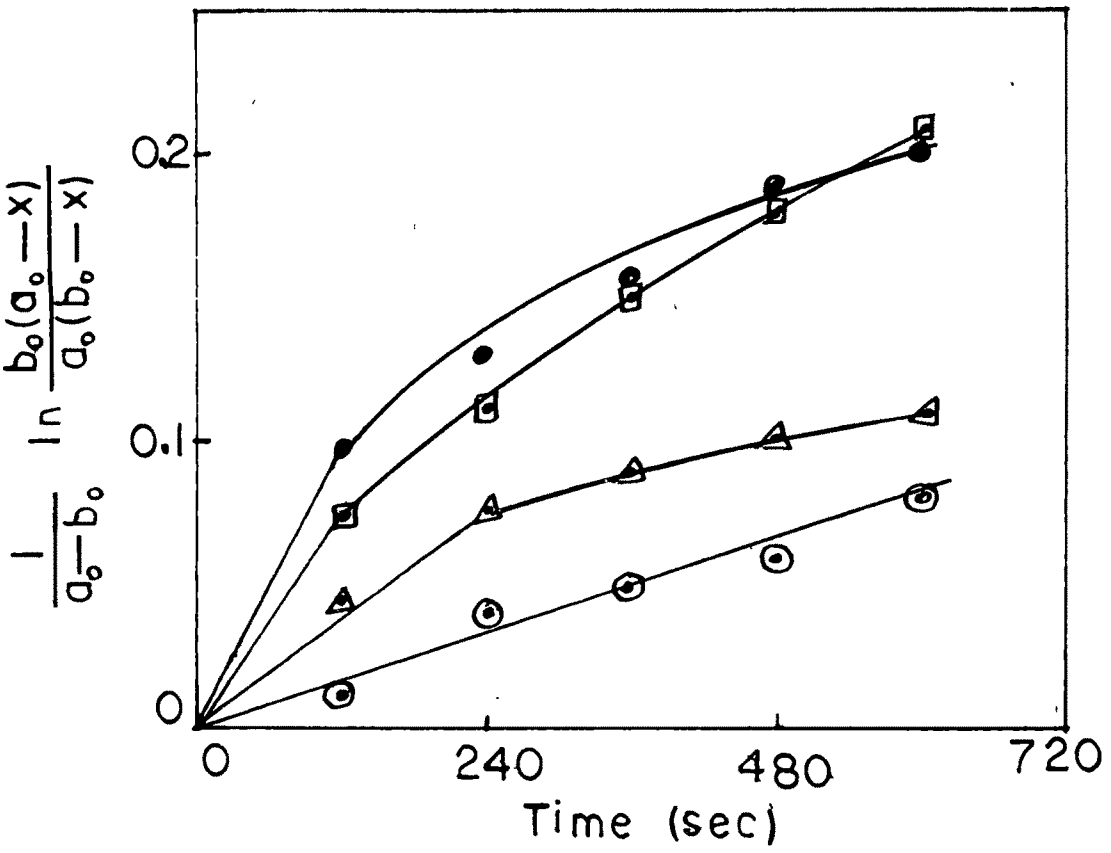

Fig.4.20f Plot of $\frac{1}{a_o-b_o} \ln \frac{b_o(a_o-x)}{a_o(b_o-x)}$ vs time for the iodination of acetone in TX100 microemulsion system with o/w=25/20 by applying the correction factor. Symbols are the same as in Fig.4.20a.

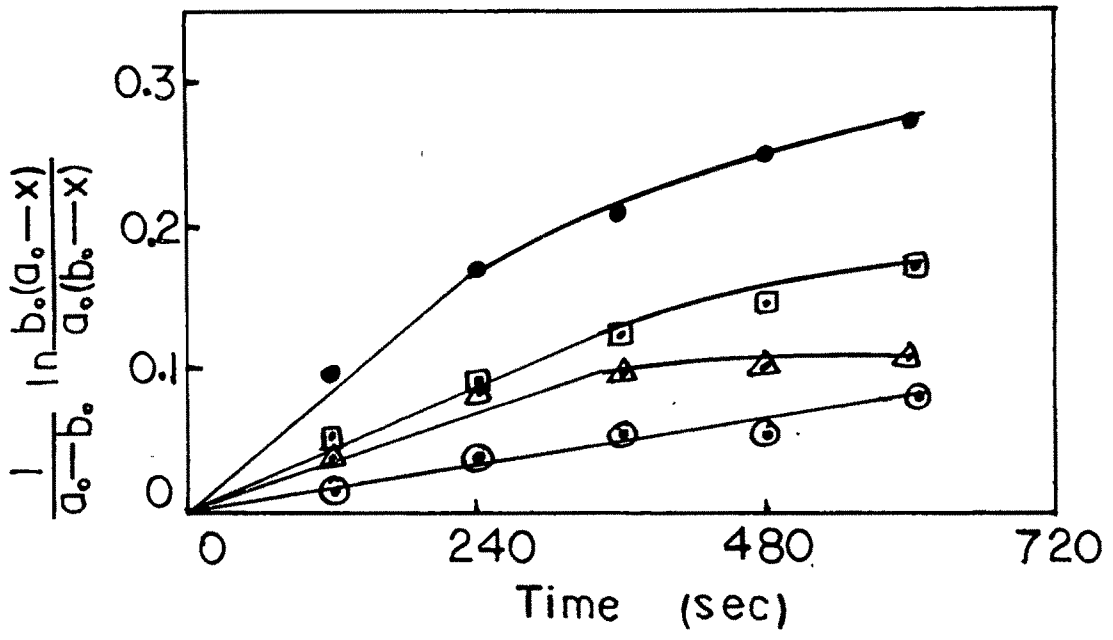

Fig.4.20g Plot of $\frac{1}{a_o-b_o}\ln\frac{b_o(a_o-x)}{a_o(b_o-x)}$ vs time for the iodination of acetone in TX100 microemulsion system with o/w=30/15 by applying the correction factor. Symbols are the same as in Fig.4.20a.

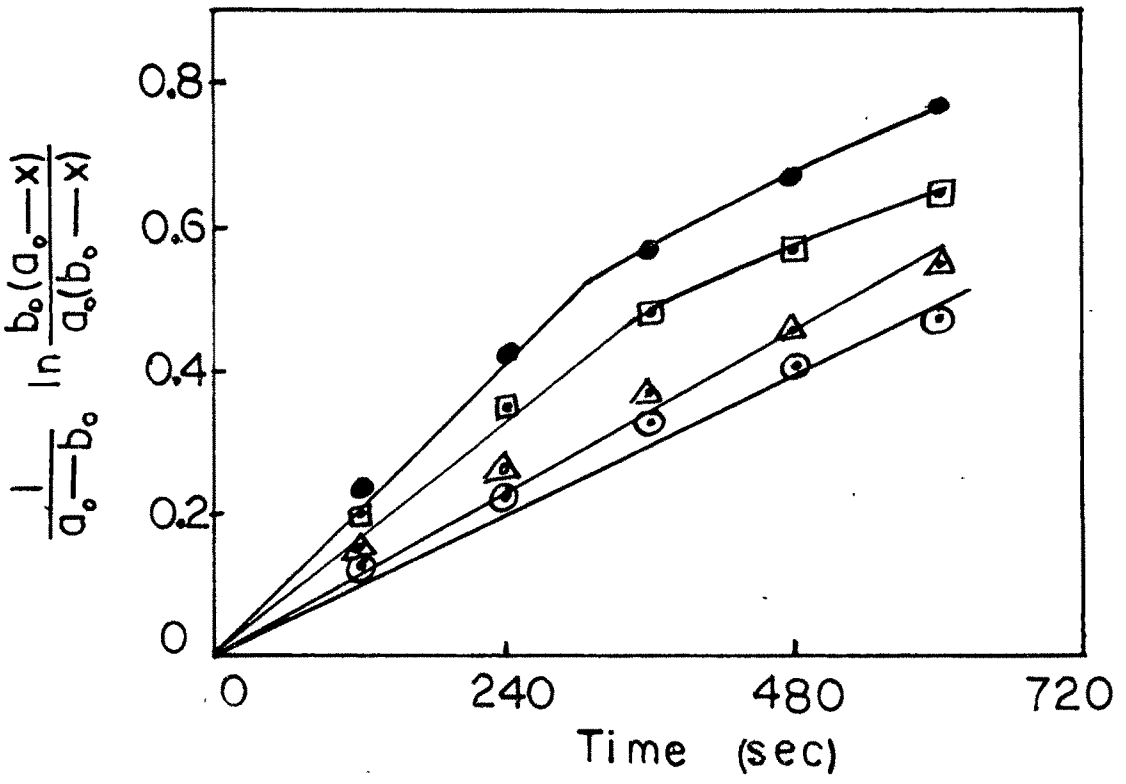

Fig.4.20h Plot of $\frac{1}{a_o - b_o} \ln \frac{b_o(a_o - x)}{a_o(b_o - x)}$ vs time for the iodination of acetone in TX100 microemulsion system with o/w=35/10 by applying the correction factor. Symbols are the same as in Fig.4.20a.

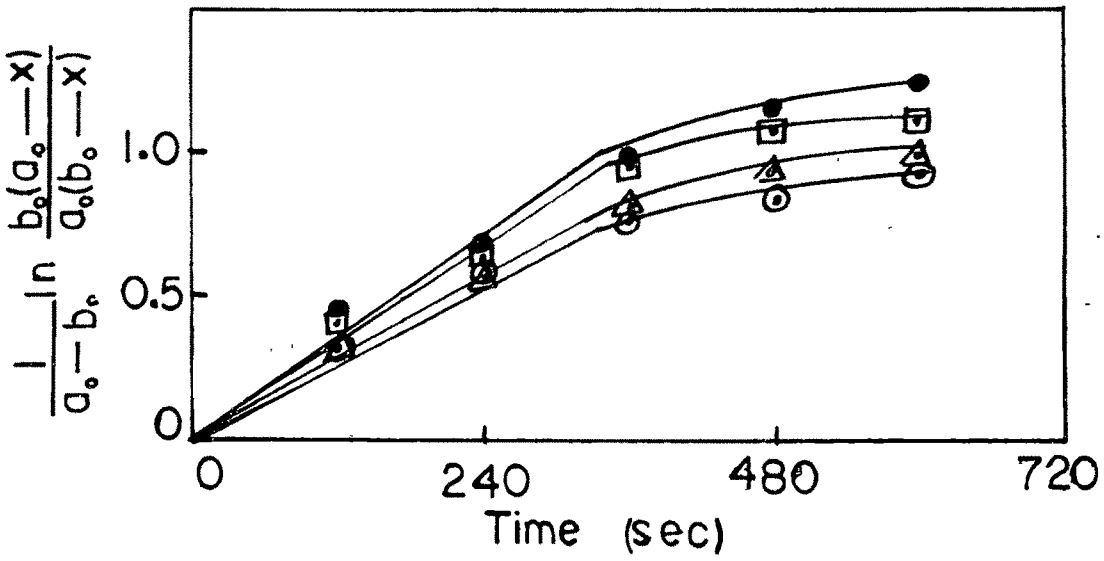

Fig.4.20i Plot of $\frac{1}{a_o-b_o} \ln \frac{b_o(a_o-x)}{a_o(b_o-x)}$ vs time for the iodination of acetone in TX100 microemulsion system with o/w=40/5 by applying the correction factor. Symbols are the same as in Fig.4.20a.

Table 4.13 **Rate constant k (l mol^{-1} sec^{-1}) for the iodination of acetone in TX100 microemulsion by applying the correction factor for partition coefficient. (see text)**

O/W	Temperature ^0C			
	30	35	40	45
1/44	1.39×10^{-4}	3.21×10^{-4}	4.63×10^{-4}	6.94×10^{-4}
5/40	2.32×10^{-4}	3.79×10^{-4}	4.63×10^{-4}	5.95×10^{-4}
10/35	2.45×10^{-4}	3.21×10^{-4}	4.17×10^{-4}	6.94×10^{-4}
15/30	1.16×10^{-4}	1.74×10^{-4}	2.98×10^{-4}	2.98×10^{-4}
20/25	8.01×10^{-5}	1.49×10^{-4}	4.17×10^{-4}	6.94×10^{-4}
25/20	1.39×10^{-4}	2.98×10^{-4}	6.94×10^{-4}	1.04×10^{-3}
30/15	1.43×10^{-4}	3.20×10^{-4}	3.79×10^{-4}	6.94×10^{-4}
35/10	1.49×10^{-4}	2.78×10^{-4}	5.95×10^{-4}	6.94×10^{-4}
40/5	7.58×10^{-4}	8.33×10^{-3}	1.39×10^{-3}	1.67×10^{-3}
S/W=55/45	2.08×10^{-3}	2.08×10^{-3}	2.60×10^{-3}	2.60×10^{-3}

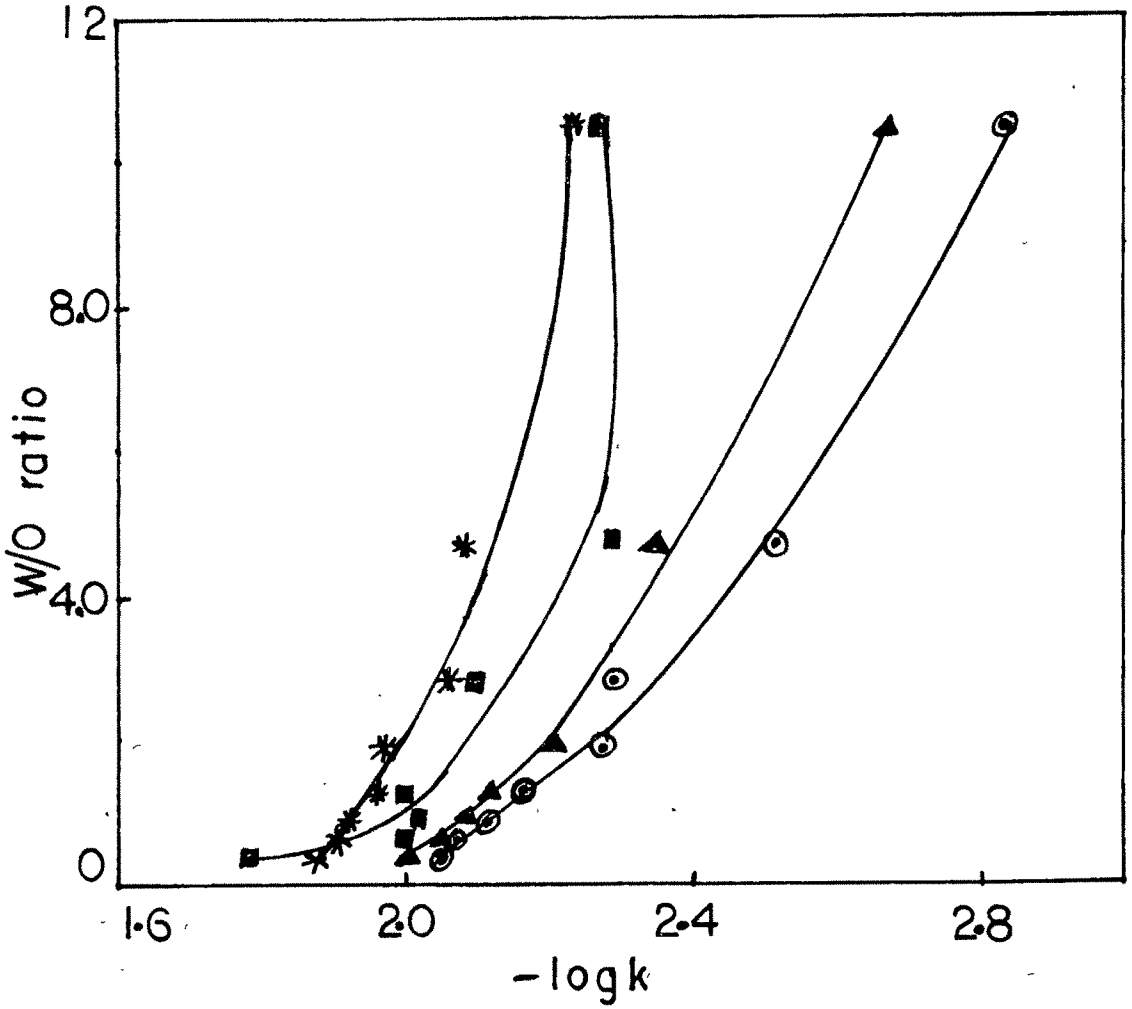

Fig.4.21a Plot of w/o ratio vs log k for the iodination of acetone in SDS microemulsion system. ⊙ 30°C; ▲ 35°C; ■ 40°C; ✳ 45°C

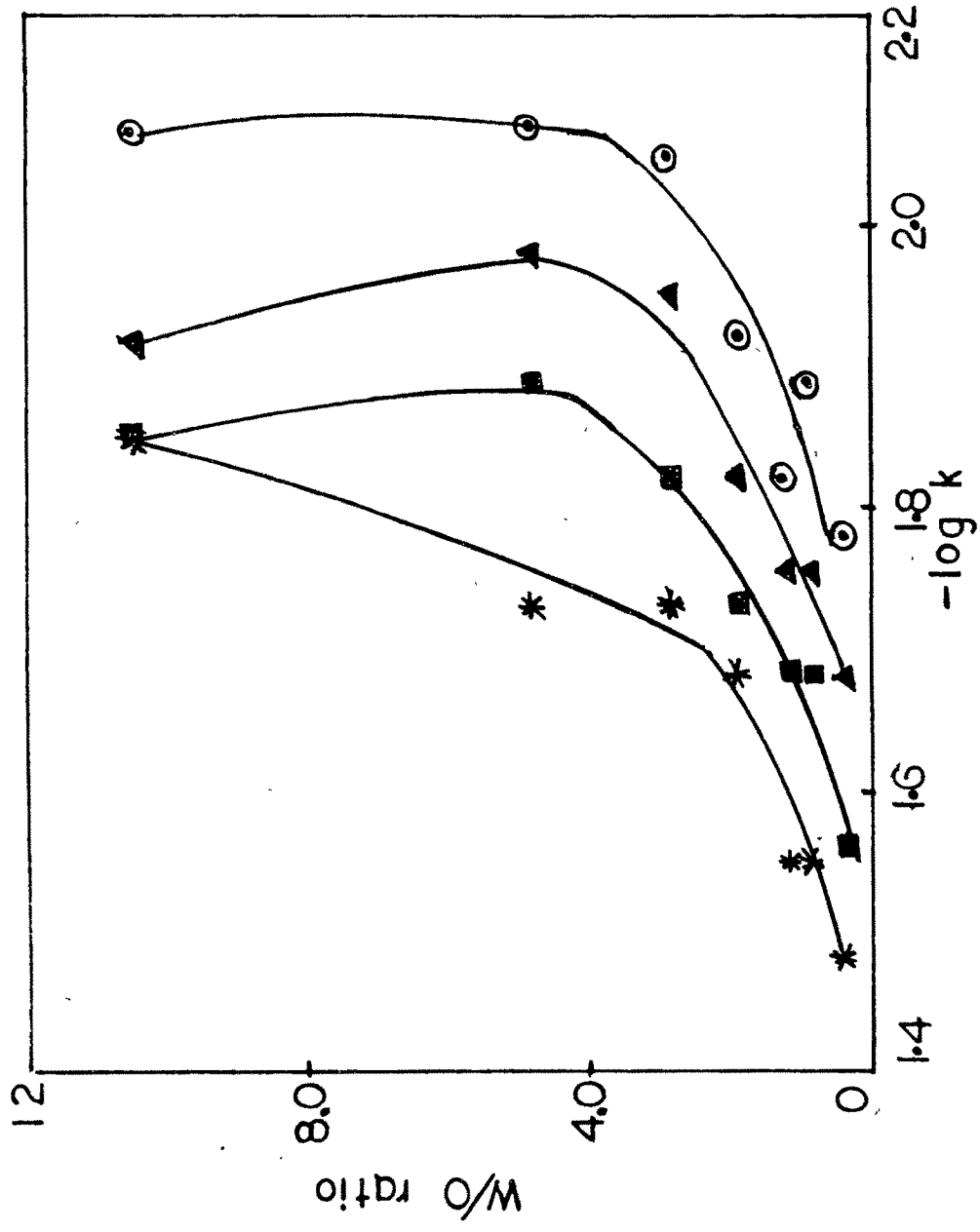

Fig.4.21b Plot of w/o ratio versus log k for the iodination of acetone in SDS microemulsion system by applying the correction factor.
⊙ 30°C; ▲ 35°C; ■ 40°C; ✱ 45°C

Table 4.14 Activation energy (Ea) in kJ mol^{-1} for the second order iodination of acetone in SDS (Ea_{11})

O/W	Ea_{13}
5/52.5	63.8
10/47.5	54.7
15/42.5	40.3
20/37.5	42.6
25/32.5	40.3
30/27.5	42.6
35/22.5	30.6
40/17.5	30.6
S/W = 42.5/57.5	63.8

Table 4.15 **Activation energy (Ea) in kJ mol^{-1} for the second order iodination of acetone in SDS (Ea_{12}) microemulsion by applying the correction factor for partition coefficient.**

O/W	Ea_{12}
5/52.5	42.6
10/47.5	42.6
15/42.5	38.3
20/37.5	36.5
25/32.5	34.8
30/27.5	33.3
35/22.5	30.6
40/17.5	29.5
S/W = 42.5/57.5	47.9

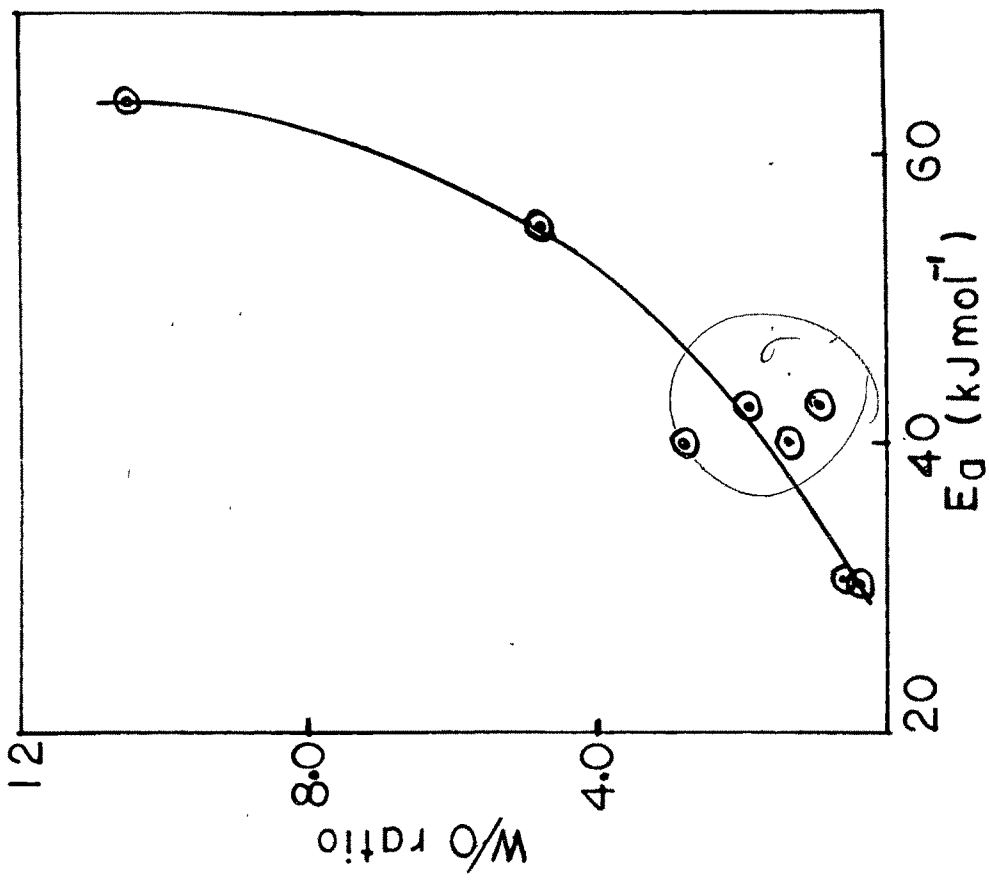

Fig.4.22a Plot of w/o ratio vs Ea for iodination of acetone in SDS system.

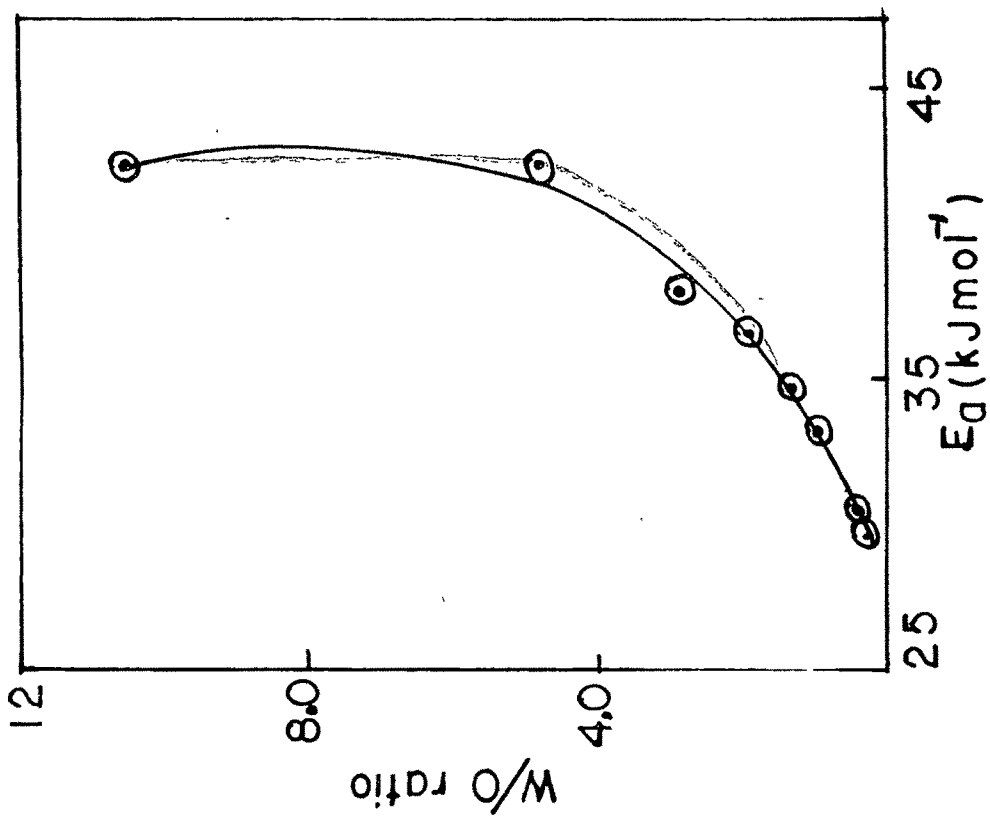

Fig.4.22b Plot of w/o ratio vs Ea for the iodination of acetone in SDS system by applying the correction factor.

We have studied the temperature effect on rate constant. The rate constant shows a linear relationship with temperature; it increases with increasing temperature. With increasing temperature, the interfacial tension is reduced and hence more tiny microdroplets are formed with large water/oil interface. This offers a large reaction area and the rate of reaction is increased.

Higher temperature also induces higher thermal instability to the transition state and the reaction rate can be accelerated. From the Table 4.10 & 4.12 it is clear that the rate of reaction increases with decreasing water content also.

The reaction in TX100 microemulsion is also enhanced to some extent as it provides large interfacial area compared to the conventional aqueous phase. The rate of reaction increases with increasing temperature due to increase in interfacial area and the higher thermal instability of the transition state. With changing oil-water ratios, the rate constant does not show a linear relationship probably due to the microstructural change the microemulsion.

W/O ratio plot against log k value (Fig 4.21 (a-b)) shows that log k value decreases with decreasing W/O ratio for SDS system. This is probably due to the higher approachability between with lower concentration of water.

Table 4.14 & 4.15 summarize the kinetic activation energy obtained from the temperature dependence of the rate constant obtained from the Arrhenius plots. Fig 4.22 shows the W/O versus activation energy plots. In SDS system, the activation energy decreases as the W/O ratio decreases and the rate of reaction is increased.

It was not possible to study the iodination of acetone in CTAB microemulsion. Iodine interacts with CTAB and it was not possible to follow the reaction.

Conclusion

The kinetics of the anion-anion reaction between iodide and persulphate have been studied in ionic (both anionic and cationic) and nonionic surfactants stabilized microemulsion. The reaction was followed spectrophotometrically by recording the absorbance due to iodine formation at regular intervals of time. Both

pseudofirst order and second order reaction rate constants were enhanced in SDS microemulsion compared with the pure aqueous system. The magnitude of second order rate constant was higher than the pseudofirst order rate constants. The reaction was inhibited in CTAB and TX100 microemulsions when compared with the results in the aqueous system. The rate enhancement and inhibition were explained in terms of the electrostatic interaction between the reactant and the hydrophilic head group of the surfactant. In all systems reaction was faster with increasing temperature as is generally the expected trend. The reaction rate increases with decreasing water content i.e., as the system changes from water rich to the oil rich phase due to the increase in the local concentration of the reactants due to the decrease in water activity.

Methyl acetate hydrolysis in SDS, CTAB and TX100 stabilized microemulsions was studied kinetically using aqueous HCl medium. All these systems enhance the reaction rate compared to pure aqueous system. The decreasing order of magnitude of rate constant in these systems can be written as SDS > CTAB > TX100. Rate constant increases with increasing temperature and increases also with decreasing water content.

Kinetic studies of iodination of acetone in SDS & TX100 microemulsion show that the reaction is faster than in the aqueous system. The reaction is supposed to take place in the aqueous phase as NaOH does dissolve in the polar phase. The magnitude of rate constant computed by applying the correction factor for partition coefficient was found to be higher than the condition where it is not taken into consideration as local concentration of the reactant is found to be higher when we consider the partition of the reactants between the oil phase and water phase.